

**Development of Biotin Protein Ligase
inhibitors as new antibiotics to treat
*Staphylococcus aureus***

By

Ashleigh Susan Paparella

B.Sc. (Honours)



**A thesis submitted to the University of Adelaide, South Australia
in fulfilment of the requirements for the degree of Doctor of
Philosophy**

Department of Molecular and Cellular Biology

School of Biological Sciences

University of Adelaide

South Australia

November 2016

Table of Contents

Abbreviations.....	vi
Abstract.....	x
Declaration for thesis containing published work.....	xiv
Publication listing.....	xvi
Communications and presentations.....	xviii
Acknowledgements.....	xxi
Chapter 1: Introduction.....	1
1.1 Need for new antibiotics.....	2
1.2 Approaches to antibacterial discovery.....	4
1.3 Approaches used to develop inhibitors of <i>S. aureus</i> biotin protein ligase.....	7
1.4 Research described in this thesis.....	10
1.5 References.....	12
Chapter 2: Structure guided design of Biotin Protein Ligase Inhibitors for Antibiotic Discovery.....	15
Statement of authorship.....	16
Published manuscript.....	18
Chapter 3: General materials and methods.....	35
3.1 Materials.....	36
3.1.1 General materials.....	36
3.1.2 Chemical reagents.....	37
3.1.3 Bacterial strains.....	38
3.1.4 Bacterial media.....	38
3.1.5 Commercial kits.....	39
3.1.6 Buffers and solutions.....	39
3.1.7 Tracers.....	41

3.1.8 Oligonucleotides.....	41
3.1.9 Plasmids.....	41
3.1.10 Computer software.....	42
3.1.11 Web resources.....	42
3.2 Methods.....	43
3.2.1 Protein techniques.....	43
3.2.2.1 Preparation of cell lysates.....	43
3.2.1.2 Determination of protein concentration.....	43
3.2.1.3 SDS PAGE electrophoresis and gel staining.....	44
3.2.1.4 Concentration of proteins.....	44
3.2.2 Molecular Biology techniques.....	45
3.2.2.1 Agarose gel electrophoresis.....	45
3.2.2.2 Preparation of competent <i>E. coli</i> BL21(DE3) and BL21 (DE3)-RIPL cells...45	45
3.2.2.3 Transformation of plasmids into competent cells.....	46
3.2.2.4 Preparation of glycerol stocks.....	46
3.2.2.5 Plasmid purification.....	46
3.2.2.6 DNA sequencing.....	47
Chapter 4: Assay development.....	48
4.1 Introduction.....	49
4.2 Specific methods.....	51
4.2.1 Recombinant <i>SaBPL</i> and <i>KpBPL</i> expression in <i>E. coli</i> BL21-CodonPlus (DE3)-RIPL strain.....	51
4.2.2 Recombinant <i>MtBPL</i> and <i>AcBPL</i> expression in <i>E. coli</i> BL21(DE3) strain.....	51
4.2.3 Purification of recombinantly expressed <i>SaBPL</i> , <i>MtBPL</i> , <i>KpBPL</i> , <i>AcBPL</i>	52

4.2.4 Expression and purification of apo GST- <i>Sa</i> PC90.....	53
4.2.5 Streptavidin-blot analysis of GST- <i>Sa</i> PC90.....	54
4.2.6 <i>In vitro</i> ³ H-biotin incorporation assay.....	54
4.2.7 SPR binding assay.....	56
4.3 Results and discussion.....	58
4.3.1 Purification of recombinantly expressed BPL protein.....	58
4.3.2 Purification and streptavidin-western analysis of apo-GST- <i>Sa</i> PC90.....	59
4.3.3 Development of high-throughput <i>in vitro</i> ³ H-biotin incorporation assay using HTS multiscreen immobilon-P plates.....	61
4.3.4 Surface plasmon resonance binding assay.....	67
4.4 Conclusions.....	71
4.5 References.....	72
Chapter 5: Improved synthesis of Biotinol-5'-AMP: Implications for antibacterial development.....	74
Statement of authorship.....	75
Published manuscript.....	78
Chapter 6: A new series of BPL inhibitors to probe the ribose-binding pocket of <i>Staphylococcus aureus</i> biotin protein ligase.....	83
Statement of authorship.....	84
Published manuscript.....	86
Chapter 7: Heterocyclic acyl-phosphate bioisostere-based inhibitors of <i>Staphylococcus aureus</i> biotin protein ligase.....	91
Statement of authorship.....	92
Published manuscript.....	94

Chapter 8: Halogenation of biotin protein ligase inhibitors improves antibacterial activity against <i>Staphylococcus aureus</i>	99
Statement of authorship.....	100
Manuscript.....	102
Chapter 9: A template guided approach to generating cell permeable inhibitors of <i>Staphylococcus aureus</i> biotin protein ligase	130
Statement of authorship.....	131
Manuscript.....	134
Chapter 10: Final discussions and future directions	166
10.1 Final discussions and future directions.....	167
10.1.1 Key findings.....	167
10.1.2 Investigating mechanism of uptake of BPL inhibitors.....	170
10.1.3 Investigating the mechanism of action of BPL inhibitors.....	171
10.1.4 Pharmacological properties of BPL inhibitors in pre-clinical candidates.....	174
10.1.5 Addressing the problems of antibacterial discovery.....	175
10.2 Conclusions.....	179
10.3 References.....	180

Abbreviations

AcBPL	<i>Acinetobacter calcoaceticus</i> biotin protein ligase
ACC	Acetyl-CoA carboxylase
AMP	Adenosine monophosphate
Apo	Unliganded enzyme
ATP	Adenosine triphosphate
BC	Biotin carboxylase
BCCP	Biotin carboxyl carrier protein
BirA	Biotin inducible repressor
BME	β -mercaptethanol
bp	Base pair
BPL	Biotin protein ligase
BSA	Bovine serum albumin
$^{\circ}\text{C}$	Degrees Celsius
C-	carboxyl-
CA-MRSA	Community acquired methicillin resistant <i>Staphylococcus aureus</i>
CT	Carboxyl transferase
Da	Dalton
DMSO	Dimethyl sulfoxide
DNA	Deoxyribonucleic acid

DTT	Dithiothreitol
<i>Ec</i> BPL	<i>Escherchia coli</i> biotin protein ligase
EDTA	Ethylenediaminetetraacetic acid
FDA	Food and Drug Administration
g	gram
HA-MRSA	Hospital acquired methicillin resistant <i>Staphylococcus aureus</i>
HCS	Holocarboxylase synthetase
Holo	Ligand bound enzyme
HPLC	High-performance liquid chromatography
<i>Hs</i> BPL	<i>Homo sapiens</i> BPL
HTS	High-throughput screening
IC_{50}	Inhibition concentration at 50% enzyme activity
k_a	Association rate constant
KCl	potassium chloride
k_d	Dissociation rate constant
K_D	Dissociation constant
kDa	kilo Dalton
K_m	Michaelis-Menten constant
K_i	Inhibition constant
<i>Kp</i> BPL	<i>Klebsiella pneumoniae</i> biotin protein ligase

LB	luria broth
m	milli-
MW	Molecular weight
min	Minute
M	Molar
Mg	Magnesium
MgCl ₂	Magnesium chloride
MIC	Minimal inhibitory concentration
MRSA	Methicillin resistant <i>Staphylococcus aureus</i>
MSSA	Methicillin sensitive <i>Staphylococcus aureus</i>
<i>MtBPL</i>	<i>Mycobacterium tuberculosis</i> biotin protein ligase
n	nano-
N-	amino-
NMR	Nuclear magnetic resonance
OD _{xnm}	optical density at x nm wavelength
PAGE	Polyacrylamide gel electrophoresis
PC	Pyruvate carboxylase
PCR	Polymerase chain reaction
PDB	Protein data bank
PBS	Phosphate buffered saline

PMSF	phenylmethanesulfonyl fluoride
rpm	Revolutions per minute
RNA	Ribonucleic acid
RU	Resonance units
s	Seconds
<i>SaBPL</i>	<i>Staphylococcus aureus</i> biotin protein ligase
<i>SaPC</i>	<i>Staphylococcus aureus</i> pyruvate carboxylase
SAR	Structure-activity relationship
SDS	Sodium dodecyl sulphate
SEM	standard error of the mean
SPR	Surface plasmon resonance
TBS	Tris buffered saline
Tris	2-amino-2-hydroxymethylpropane-1,3-diol
μ	micro-
V	Voltage
WT	Wild-type

Abstract

There is an urgent need to discover new antibiotics to combat the rise of antibiotic resistant bacteria, such as methicillin resistant *Staphylococcus aureus* (MRSA). Many of the antibiotics currently in clinical use are synthetic derivatives of chemical scaffolds identified over 50 years ago in the golden era of antibiotic drug discovery. These antibiotics are often subject to existing resistance mechanisms and, as such, represent a short term solution to the antibiotic resistance crisis. Therefore it is imperative that new classes of antibiotics are developed that exhibit new modes of action and that are not subject to existing resistance mechanisms. Most antibacterial discovery efforts are focussed on drug targets with no mammalian equivalent. These targets have been well explored and therefore new antibacterial targets need to be identified. One strategy to identify new antibiotics is to explore targets that have a closely related human homologue. However, it is important that such inhibitors exhibit extremely high selectivity for the bacterial target over the human equivalent. One example of such a target is the essential enzyme biotin protein ligase (BPL) which catalyses the attachment of the micronutrient biotin onto biotin-dependent enzymes. In bacteria biotin-dependent enzymes play important roles in fatty acid synthesis and the tricarboxylic acid cycle. Without protein biotinylation these enzymes are devoid of activity and unable to perform their essential metabolic functions. Hence, inhibitors of BPL with selectivity over the human homologue represent a potential new class of antibiotic to combat MRSA.

Our group has previously reported the X-ray crystal structure of *S. aureus* BPL (*Sa*BPL) that provides the essential information necessary for structure guided design of new inhibitors. Of particular importance are two adjacent binding sites for the ligands biotin and ATP which, when bound, conjugate to form the adenylated reaction intermediate, biotinyl-5'AMP. Whilst amino acid residues in the biotin-binding pocket are highly conserved, residues in the ATP binding pocket are more variable and can be exploited to create species selective inhibitors. Our laboratory has previously reported analogues of biotinyl-5'AMP as BPL inhibitors where

the labile phosphoanhydride linker present in the native reaction intermediate has been replaced with a non-hydrolysable 1,4-disubstituted-1,2,3-triazole linker. The triazole linker can be readily synthesised by the Huisgen cycloaddition reaction that occurs between an acetylene and azide. This cycloaddition reaction can proceed in two ways. Firstly, copper or ruthenium catalysts can be used to produce the 1,4 or 1,5 regio-isomers respectively. Alternatively, in special cases, this reaction can be catalysed by an enzyme. This is known as *in situ* click chemistry. Our laboratory has identified a biotin triazole pharmacophore, containing the biotinyl moiety and a 1,4-disubstituted triazole. Various groups that can probe available binding sites on *Sa*BPL can be conjugated to the triazole through click chemistry. The most potent triazole inhibitor of *Sa*BPL, BPL068, had an inhibition constant of 90 nM and, importantly exhibited >1000-fold selectivity over the human homologue (Soares da Costa *et al*, *Journal of Biological Chemistry*, vol. 287, p 17823-17832). Here, the biotin triazole was conjugated to a 2-benzoxalone moiety that was designed to bind in the ATP binding pocket. This compound inhibited growth of *S. aureus* and did not show any *in vivo* cytotoxicity against cultured mammalian cells. Although BPL068 exhibited antibacterial activity, the effect was not strong enough to determine a minimal inhibitory concentration (MIC), which is required for a pre-clinical candidate.

The first aim of this project was to characterize new *Sa*BPL inhibitors with the goal of improving the antibacterial activity of the parent compound. Here I have employed structure guided drug design and protein biochemistry techniques to design new *Sa*BPL inhibitors with desirable properties for pre-clinical candidates. To facilitate the characterization of *Sa*BPL inhibitors I developed a high-throughput enzyme assay to measure protein biotinylation, and a surface plasmon resonance assay to determine the kinetics of ligand binding (Chapter 4). With these techniques in hand I have characterised 40 rationally designed *Sa*BPL inhibitors. Biotinol-5'AMP, a literature compound that has previously been developed as a research tool to characterize BPL function, was first characterized. Here the inhibition of BPLs from a

panel of clinically important bacteria was measured using an *in vitro* protein biotinylation assay. The spectrum of whole cell antibacterial activity was also addressed, with *S. aureus* and *Mycobacterium tuberculosis* being most susceptible to this compound (Chapter 5). A series of triazole inhibitors of *SaBPL*, designed to probe the ribose binding pocket was also investigated. Here 25, 1,4-triazole based compounds with 1-benzyl substituents were synthesized and tested for inhibition of *SaBPL*. These compounds are smaller in molecular weight compared to the parent molecule, BPL068, allowing further optimization by extending into the ATP binding pocket. The most potent compound from this series had an inhibition constant of 280 nM and exhibited antibacterial activity against *S. aureus*. Furthermore, all compounds did not inhibit the human homologue or cultured mammalian cells (Chapter 6).

A further series of compounds were next synthesized to optimise the triazole linker in BPL068. Firstly, compounds were synthesized in which the triazole linker has been replaced with alternative heterocycles with a view to improving its biological activity. A 1,2,4-oxadiazole linker was found to inhibit *SaBPL* with an inhibition constant of 1.2 μ M, with no inhibition of the human homologue (Chapter 7). A separate series of 1,4,5-trisubstituted-1,2,3 triazole analogues were also investigated (Chapter 8). Here, the hydrogen of the C5 atom in the triazole heterocycle was replaced with halogenated substituents to investigate whether halogenation of BPL068 could improve antibacterial activity. A 5-fluoro-1,2,3 triazole was found to inhibit *SaBPL* with an inhibition constant of 420 nM. Importantly, the fluorinated analogue exhibited an MIC of 8 μ g/mL against a clinical isolate of *S. aureus*. This compound is the first example of a triazole based BPL inhibitor in which an MIC could be determined.

Following the identification of BPL antibacterials, the mechanism of action needed to be addressed. Therefore the second aim of my project was to develop probes that could facilitate mechanism of action and uptake studies. Here a fragment based approach was employed using *in situ* click chemistry. *In situ* click chemistry relies on the ability of the target enzyme to select out and synthesize its own inhibitors from a series of small molecule building block

precursors. This technique exploits the Huisgen cycloaddition reaction that proceeds between an acetylene and an azide to produce the 1,2,3-triazole heterocycle. Here, I have demonstrated that the *in situ* click chemistry approach could be adopted to identify inhibitors of a panel of 4 BPLs from clinically important bacteria. Next, azide-functionalized analogues of 2 fluorophores were synthesized and tested for chemical ligation to biotin acetylene using BPL as a catalyst. The ‘clicked’ compounds were confirmed for inhibition of SaBPL and entry into *S. aureus*. This newly developed probe will be used in solution based and con-focal microscopy studies to probe the mechanism of entry and action in *S. aureus* (Chapter 9).

In summary, I have characterized a new series of SaBPL inhibitors that have improved antibacterial activity and still maintain the selectivity required for a pre-clinical candidate. Using *in situ* click chemistry, I also developed a new inhibitor that will be used to probe the mechanism of entry and action of BPL inhibitors in *S. aureus*. The work demonstrated in this thesis will be used to help optimize BPL inhibitors, ultimately leading to the development of a pre-clinical candidate.

Thesis layout:

The thesis will be presented as a series of manuscripts either published, submitted or to be submitted for publication. Each manuscript will be a chapter with its own references. A general introduction and discussion will also be included to link together all the research conducted during candidature. A publishing agreement with all co-authors involved with the work is also included.



Declaration for thesis containing published work and/or work prepared for publication

I certify that this work contains no material which has been accepted for the award of any other degree or diploma in any university or other tertiary institution and, to the best of my knowledge and belief, contains no material previously published or written by another person, except where due reference has been made in the text, In addition, I certify that no part of this work will, in the future, be used in a submission for any other degree or diploma in any university or other tertiary institution without the prior approval of the University of Adelaide and where applicable, any partner institution responsible for the joint-award of this degree.

I give consent to this copy of my thesis when deposited in the University library, being made available for loan and photocopying, subject to the provisions of the Copyright Act 1968. I acknowledge that copyright of published works contained within this thesis resides with the copyright holder(s) of those works.

I also give permission for the digital version of my thesis to be made available on the web, via the University's digital research repository, the Library catalogue and also through web search engines, unless permission has been granted by the University to restrict access for a period of time.

.....

.....

.....16/11/16.....

Ashleigh Susan Paparella

Date

I acknowledge the copyright of published works contained within this thesis including:

Chapter 2:

Ashleigh S. Paparella, Tatiana P. Soares da Costa, Min Y. Yap, William Tieu, Matthew C. J. Wilce, Grant W. Booker, Andrew D. Abell, Steven W. Polyak (2014) Structure Guided Design of Biotin Protein Ligase Inhibitors for Antibiotic Discovery. *Current Topics in Medicinal Chemistry*. 14, 4-20.

Chapter 5:

William Tieu, Steven W. Polyak, **Ashleigh S. Paparella**, Min Y. Yap, Tatiana P. Soares da Costa, Belinda Ng, Geqing Wang, Richard Lumb, Jan M. Bell, John D. Turnidge, Matthew C. J. Wilce, Grant W. Booker, Andrew D. Abell (2015) Improved Synthesis of Biotinol-5'-AMP: Implications for Antibacterial Discovery. *ACS Medicinal Chemistry Letters*. 6, 216-220.

Chapter 6:

Jiage Feng, **Ashleigh S. Paparella**, William Tieu, David Heim, Sarah Clark, Andrew Hayes, Grant W. Booker, Steven W. Polyak, Andrew D. Abell (2016) A new series of BPL inhibitors to probe the ribose-binding pocket of *Staphylococcus aureus* biotin protein ligase. Accepted for publication in *ACS Medicinal Chemistry Letters*, Manuscript ID: ml-2016-00248v.R1.

Chapter 7:

William Tieu, Angie M. Jarrad, **Ashleigh S. Paparella**, Kelley A. Keeling, Tatiana P. Soares da Costa, John C. Wallace, Grant W. Booker, Steven W. Polyak, Andrew D. Abell (2014) Heterocyclic acyl-phosphate bioisotere-based inhibitors of *Staphylococcus aureus* biotin protein ligase. *Bioorganic & Medicinal Chemistry Letters*. 24, 4689-4693.

Chapter 8:

Ashleigh S. Paparella, Jiage Feng, Andrew Hayes, David Heim, Grant W. Booker, Andrew D. Abell, Steven W. Polyak (2016) Halogenation of biotin protein ligase inhibitors improve antibacterial activity against *Staphylococcus aureus*. Manuscript in preparation

Chapter 9:

Ashleigh S. Paparella, Jiage Feng, Beatriz Blanco-Rodriguez, Zikai Feng, Andrew Hayes, Wanida Phetsang, Mark Blaskovich, Matthew A. Cooper, Grant W. Booker, Andrew D. Abell, Steven W. Polyak (2016) A template guided approach to generating cell permeable inhibitors of biotin *Staphylococcus aureus* biotin protein ligase. Manuscript in preparation.

Authorization to publish each paper has been given and provided in print for each chapter containing copyright and co-authored work, including acknowledgement of contribution to the work from each author

All supplementary material can be found online using the citation information as described above for each published article.

Communications and Presentations

Paparella AS, Feng J, Blanco-Rodriguez B, Heim DJ, Hayes AJ, Tieu W, Clark SN, Booker GW, Abell AD, Polyak SW. Biotin triazoles represent a new class of antibiotics to treat *Staphylococcus aureus* infections. *Adelaide Protein Group Meeting, Adelaide, Australia, May 2016* Poster Presentation.

Paparella AS, Feng J, Blanco-Rodriguez B, Sternicki LM, Cooper MA, Booker GW, Abell AD, Polyak SW. Template guided synthesis provides a route to new antibacterials and antifungals. *Gordon Research Seminar on Enabling New Antibiotic Discovery and Development, Tuscany, Italy, March 2016*, Oral Presentation. **Awarded** student travel award \$2000 from ATA scientific to put towards travel expenses.

Paparella AS, Feng J, Blanco-Rodriguez B, Heim DJ, Hayes AJ, Tieu W, Clark SN, Booker GW, Abell AD, Polyak SW. Biotin triazoles represent a new class of antibiotics to treat *Staphylococcus aureus* infections. *Gordon Research Conference on Enabling New Antibiotic Discovery and Development, Tuscany, Italy, March 2016*, Poster Presentation. **Awarded** student travel award \$2000 from ATA scientific to put towards travel expenses.

Paparella AS, Feng J, Blanco-Rodriguez B, Sternicki LM, Cooper MA, Booker GW, Abell AD, Polyak SW. Template guided synthesis provides a route to new antibacterials and antifungals. *41st Lorne Conference on Protein Structure and Function, Lorne, Victoria, Australia, February 2016*, Poster Presentation.

Paparella AS, Feng J, Blanco-Rodriguez B, Yap MY, Hayes A, Heim DJ, Sternicki LM, Cooper MA, Wilce MC, Booker GW, Abell AD, Polyak SW. Structure Guided Design of small molecule inhibitors of biotin protein ligase for antibiotic drug discovery. *Adelaide Pharmacology Group Student Meeting, Adelaide, Australia, November 2015*, Oral Presentation.

Paparella AS, Feng J, Blanco-Rodriguez B, Sternicki LM, Cooper MA, Booker GW, Abell AD, Polyak SW. Template guided synthesis provides a new route to antibacterials and antifungals. *Combio Conference, Melbourne, Australia, 2015 October 2015*. Oral Presentation, **Awarded** Student registration bursary \$380

Paparella AS, Feng J, Heim DJ, Tieu W, Clark S, Booker GW, Abell AD, Polyak SW., Optimisation of Biotin Triazoles as new antibiotics targeting Biotin Protein Ligase from *Staphylococcus aureus*. *Melbourne Protein Group, student symposium, Melbourne, Australia*. Poster Presentation, July 2015. **Winner** Best Student Poster Prize, awarded \$100.

Paparella AS, Feng J, Heim DJ, Tieu W, Clark S, Booker GW, Abell AD, Polyak SW., Optimisation of Biotin Triazoles as new antibiotics targeting Biotin Protein Ligase from *Staphylococcus aureus*. *Adelaide Protein Group student symposium, Adelaide, Australia*. Poster Presentation, June 2015

Paparella AS, Feng J, Heim DJ, Tieu W, Clark S, Booker GW, Abell AD, Polyak SW., Optimisation of Biotin Triazoles as new antibiotics targeting Biotin Protein Ligase from *Staphylococcus aureus*. *40th Lorne Conference on Protein Structure and Function, Lorne, Victoria, Australia, February 2015*. Poster Presentation

Paparella AS, Tieu W, Feng J, Soares da Costa TP, Abell AD, Beckham S, Wilce MC, Polyak SW, Booker GW, Wegener KL., Probing enzymatic plasticity with nuclear magnetic resonance spectroscopy. *School of Biological Sciences Research Symposia, University of Adelaide, Adelaide, Australia*. Poster Presentation, November 2014. **Winner** Best Student Poster Prize, awarded \$100.

Paparella AS, Biotin Protein Ligase: A novel antibiotic drug target. *Three minute thesis competition, Faculty of Sciences, University of Adelaide, Adelaide, Australia*. Finalist, August 2014, Oral Presentation.

Paparella AS, Tieu W, Feng J, Soares da Costa TP, Abell AD, Beckham S, Wilce MC, Polyak SW, Booker GW, Wegener KL., Probing enzymatic plasticity with nuclear magnetic resonance spectroscopy. *Melbourne Protein Group, student symposium, Melbourne, Australia*. Poster Presentation, July 2014.

Paparella AS, Tieu W, Lumb R, Soares da Costa TP, Abell AD, Bastian I, Polyak SW, Booker GW., Biotin Protein Ligase: a novel antibiotic drug target. *39th Lorne Conference on Protein structure and Function, Lorne, Victoria, Australia, February 2014*. Poster Presentation.

Paparella AS, Tieu W, Soares da Costa TP, Abell AD, Polyak SW, Booker GW. Biotin triazoles represent a new class of antibiotics for tuberculosis. *School of Biological Sciences Research Symposium, University of Adelaide, Adelaide, Australia*. Poster Presentation, November 2013.

Paparella AS, Tieu W, Lumb R, Soares da Costa TP, Abell AD, Bastian I, Polyak SW, Booker GW., Biotin protein ligase: a novel anti-TB drug target. *ComBio conference, Perth, Australia*. Poster Presentation, September 2013.

Paparella AS, Tieu W, Soares da Costa, Abell AD, Polyak SW, Booker GW., Biotin triazoles represent a new class of antibiotics for tuberculosis. *Adelaide Protein Group student symposium, Adelaide, Australia*. Poster Presentation, June 2013.

Paparella AS, Tieu W, Soares da Costa TP, Abell AD, Polyak SW, Booker GW., Biotin triazoles represent a new class of antibiotics for tuberculosis. *ASMR SA annual scientific meeting, Adelaide, Australia*. June 2013. **Winner** best PhD student poster prize, awarded \$200.

Acknowledgements

Firstly I would like to express my sincere gratitude to my supervisors Professor Grant Booker, Dr. Steven Polyak and Professor Andrew Abell for their continual support, guidance and motivation throughout my research candidature.

Grant, thank you for giving me the opportunity to pursue both my honours and PhD studies in your laboratory and for all your helpful advice, I'm sure it will be very valuable in my future research endeavours. Steven, thank you for all the advice you have given me, for being there whenever I have had troubles with my project and for helping me grow as a future scientist. Andrew, thank you for your help with all the chemistry aspects of my project, and for your encouragement.

Thank you to Professor John Wallace, for sharing your knowledge with me in all aspects of my project. Thank you for your support and helpful comments and for reading manuscripts.

I would also like to acknowledge all the members of the BPL team in the Department of Chemistry for synthesizing all the compounds I was able to work with, namely, Jacko Feng, Dr. William Tieu, Dr. Beatriz Blanco-Rodriguez and Sarah Clark. Special thanks to Jacko, for your help in all chemistry-related things, it has been a pleasure to work with you over the past 4 years.

Thank you to all past members of the Booker lab, Lungisa, Karen, Martin, Al, Wanisa, Wei Wei, Jorinda, David and Okki. A special thanks to Tatiana for all the advice that you have given to me over the years, I truly appreciate it 😊. Thank you to all the summer research students, Natasha, Sarah and Jordan, for your involvement in the BPL project. Thank you to all the present students of the Booker lab, Andrew Thompson, Andrew Hayes ('The Andrews' 😊) and Zikai. Thank you to the members of the Brunning lab, Andrew and Alice for your friendly chats across the corridor. Thank you to Kate for all the helpful advice you have given me over the years. Thank you to Julia and Lousie, I will always remember all the Friday

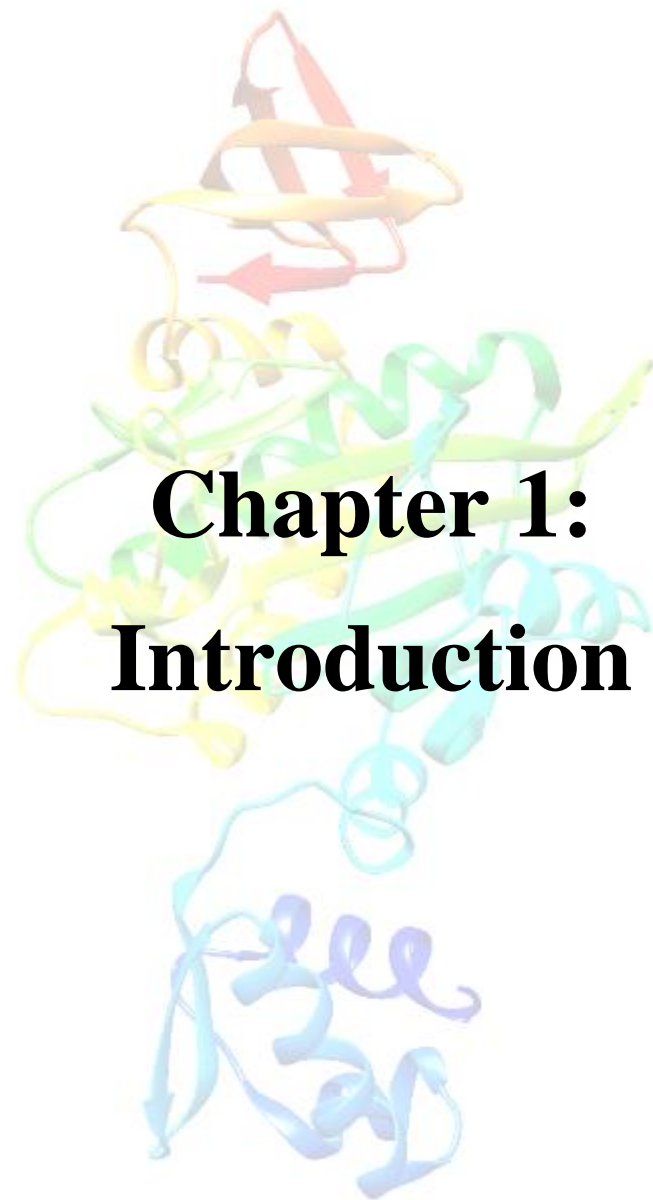
night dinners, I think we have just about covered all the Dessert bars in Adelaide ☺. A special thanks to Jiulia, I'm so glad I got to share this experience with you, it has certainly being memorable (Although I don't think I will miss the scary movies! ☺). Thank you for all the advice you have given me and for being there for me, especially during the last year.

Thank you to our collaborators To Professor Matthew Wilce, Dr. Simone Beckham, Dr. Min Yap and Danielle Cini at Monash University for providing us with X-ray crystal structures.

Thank you to Dr. Keith Shearwin in the School of Biological Sciences for giving me the opportunity to be involved in undergraduate teaching during my studies, I truly appreciate it. Thank you to all the CSU and professional staff in the School of Biological sciences, especially Jennifer Peters and Imelda Levy, you were always very friendly and helpful whenever I needed anything.

I'm very grateful for all the support from my family and friends during my studies at university. Thank you to Ben, Emma, Erin, Nanna and Poppa and Grandma and Grandpa for all the encouragement you have given me.

Lastly I would like to thank my Mum and Dad for all their support during my university studies. A special thanks to my mum for all the support and motivation you have given me over the last year, I couldn't have done it without you.



Chapter 1: Introduction

1.1 Need for new antibiotics

Antibiotic resistance is a major threat to human health worldwide. Many of the antibiotics in clinical use are synthetic derivatives of chemical scaffolds identified over 50 years ago. These next generation analogues are often subject to existing resistance mechanisms and only represent a short term solution to the antibiotic crisis [1]. New antibiotics are required that have novel modes of action and are not subject to existing resistance mechanisms [1]. Despite this desperate need for new antibiotics, there has been a decline in the introduction of new drugs into the clinic [2]. Most large pharmaceutical companies have terminated their antibiotic discovery programs due to low return on investment, strict regulatory requirements and the time and difficulty involved in developing a novel antibiotic [3]. Therefore much of the early stage antibiotic research is carried out by academic and government laboratories [3]. Many of the obvious drug targets present in bacteria with no mammalian homologue have been well explored. One strategy to develop new antibiotics is to investigate targets that have a closely related human homologue. However, inhibitors of these targets must have extremely high selectivity for the bacterial target. One such example is the essential enzyme biotin protein ligase (BPL).

BPL catalyses the attachment of the micronutrient biotin onto biotin-dependent enzymes. In bacteria, biotin-dependent enzymes play important roles in fatty acid synthesis and the tricarboxylic acid cycle. Without the attached co-factor these enzymes are devoid of activity and are unable to perform their essential metabolic roles [4]. BPL catalyses protein biotinylation through the formation of an adenylated reaction intermediate, biotinyl-5'AMP, from its substrates biotin and ATP [4]. Multiple approaches by our group [5-9] and others [10-12] to design BPL inhibitors have been investigated, including analogues of biotin and non-hydrolysable analogues of the reaction intermediate. Of particular importance to this project are the biotin triazoles, which are not only potent inhibitors of *Staphylococcus aureus*

BPL (*Sa*BPL), but importantly, demonstrate excellent selectivity over the human homologue [5].

In this thesis I have characterized rationally designed *Sa*BPL inhibitors in order to optimize the biotin triazole pharmacophore (figure 1.1) and identify favourable drug-like properties that are required for a pre-clinical development candidate (Chapters 5-8). I have also used a fragment based drug discovery approach, called *in situ* click chemistry, to generate BPL inhibitors that can be used as fluorescent probes to investigate the mechanism of uptake and action of BPL inhibitors in *S. aureus* (Chapter 9).

In this chapter I will provide a brief discussion on the various approaches to antibacterial discovery. This section focusses on the development process from a newly identified enzyme inhibitor to a pre-clinical candidate. I have also provided a brief overview of the current status of BPL inhibitors. Finally, I will provide a description of the research presented in this thesis. A comprehensive literature review on the structure and function of BPL and the development of BPL inhibitors is provided in chapter 2 which is a published article entitled ‘Structure Guided Design of Biotin Protein Ligase Inhibitors for Antibiotic Discovery’ [4].

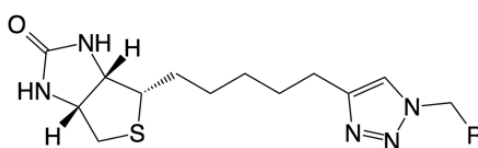


Figure 1.1: Pharmacophore representing the biotin-triazole moiety

1.2 Approaches to antibacterial discovery:

Two common screening platforms used to discover antibiotics are phenotypic and target based screening [13]. Phenotypic screening involves testing compound collections for whole cell antibacterial activity against bacteria. This widely used approach has been responsible for the discovery of many of the antibiotics in clinical use today [13]. Following the birth of high-throughput screening technologies and advances in DNA sequencing in the 1990's, target based screening approaches took over and were thought to be the solution to replenishing the antibiotic pipeline [3]. Target based approaches involve screening chemical compound collections against a biological target to identify hit molecules that have the potential to be developed into lead compounds with whole cell activity. However, target based approaches have under-delivered [3]. One of the reasons is possibly due to the limited chemical diversity found in corporate compound collections [3, 14]. Corporate libraries are heavily biased towards compounds that follow Lipinski's rule of 5. In Lipinski's landmark study the ideal properties for orally available drug candidates were described [15]. Here, a drug candidate should have no more than 5 hydrogen bond donors, no more than 10 hydrogen bond acceptors, a molecular weight of no more than 500 and a calculated Log P, the partition coefficient that is a measure of lipophilicity greater than 5 [15]. However, antibacterials do not generally follow these rules [16, 17]. BPL was recognized as a potential antibiotic target by both GlaxoSmith Kline [3] and Astrazeneca [18] and was the subject of high-throughput screening campaigns. However, no hits were identified by either large company. These studies highlight that an alternative approach to identify BPL inhibitors was required. Structure based drug design (SBDD), is another approach that is employed by many small academic and government laboratories to develop new antibiotics [19]. Approaches to the design of BPL inhibitors using structural biology is detailed further in chapter 2.

Once inhibitors have been discovered it is important to characterize the kinetics of inhibitor binding. The kinetics of binding can be measured using label free detection technologies, such

as surface plasmon resonance (SPR) (Chapter 4 and Chapter 8). SPR allows real time monitoring of protein: small molecule interactions and has been shown to be a powerful tool for early stage drug discovery [20, 21]. In this approach, the protein target is covalently attached to the surface of a sensor chip and small molecules are injected in solution across the surface. If a small molecule binds to the protein target the refractive index at the surface alters in proportion to a change in mass, resulting in a change in surface resonance [22]. SPR can be used to measure both the association and dissociation rates of inhibitors, the latter of which can be used to calculate the drug's residence time, a measure of the lifetime of the drug-target complex [23]. SPR studies have been used to investigate the reaction mechanism of *Sa*BPL. Here, *Sa*BPL was found to bind its substrates biotin and ATP in an ordered manner with biotin binding first [5]. SPR studies have also shown that biotin binds to *Sa*BPL with fast association and dissociation rates, but the reaction intermediate, biotinyl-5'AMP forms a stable complex with *Sa*BPL on the surface of the sensor chip. This technology has been used to identify *Sa*BPL inhibitors that exhibit slow dissociation kinetics and remain tightly associated with the BPL active site [5, 6, 9].

One of the limitations associated with target based and SBDD approaches to antibacterial discovery is the identification of small molecule inhibitors that also exhibit whole cell antibacterial activity [18]. Hence, small molecule inhibitors should be tested early for whole cell activity against clinically important bacteria [13]. An important consideration here is to determine whether the compounds have broad or narrow spectrum antibacterial activity. Broad spectrum antibacterial agents, typically have bioactivity against both Gram-positive and Gram-negative bacteria. An example is the fluoroquinolones, which act by inhibiting two DNA topoisomerases [24, 25]. Such agents are highly sought after by industry but have been difficult to find [18]. Alternatively, compounds may have a narrow spectrum of activity. Examples include the macrolides, protein synthesis inhibitors and vancomycin, a glycopeptide antibiotic that is a cell wall synthesis inhibitor. Both of these antibiotics are only active

against Gram-positive bacteria [13]. It is also useful to determine whether the inhibitor has a bactericidal or bacteriostatic mode of action. Bactericidal antibiotics, for example penicillin, kill bacteria directly, whereas bacteriostatic antibiotics like tetracycline slow the growth of bacteria, allowing the host immune system to clear the infection [26].

It is necessary in the development of a new antibacterial to investigate whether the compounds will exhibit any host cytotoxicity, either through inhibition of an equivalent target in mammalian cells or through an unrelated mechanism [13]. As BPL is a ubiquitous enzyme, all BPL inhibitors are tested for inhibitory activity against the human homologue. Only those inhibitors that do not inhibit the human isozyme are selected for further development. In addition to testing for activity against the human isozyme, compounds are also tested for any cytotoxic effects against cultured mammalian liver and kidney cells. It is important to identify potentially toxic compounds as early as possible so they can be eliminated before more pre-clinical tests are performed.

Once a small molecule has been identified that exhibits good potency against the biological target and whole cell activity against clinically relevant bacteria, the next step is to ascertain that the antibacterial activity is consistent with the inhibition of the biological target [13]. A number of methods have been developed to verify the mechanism of action of an antibacterial *in vivo*. Macromolecular synthesis assays are a relatively simple way to gain insight into the mechanism of action of an antibacterial. These assays use radiolabelled precursors to determine if a compound specifically inhibits protein, RNA, DNA, lipid or peptidoglycan synthesis [27]. An alternative approach is to use genetically modified strains of bacteria that are engineered to under-express or over-express the expected biological target. These methods can be used to either sensitize or increase the resistance of the organism to the compound, respectively [13]. This approach has been used to confirm the *in vivo* mechanism of action of inhibitors targeting *Mycobacterium tuberculosis* BPL [11]. A third method that can be used to help elucidate the *in vivo* mechanism of action is the use of fluorescent probes. Fluorescent

analogues of linezolid [28], vancomycin [29] and daptomycin [30] have all been used to support the mechanism of action of these antibiotics. In this thesis I developed a fluorescent BPL inhibitor that can be employed to investigate the mechanism of uptake in *S. aureus* (Chapter 9).

1.3 Approaches used to develop inhibitors of *S. aureus* biotin protein ligase

Three different series of compounds have been developed by our laboratory as inhibitors of BPL from *Staphylococcus aureus* [5, 6, 8]. Here, each of these are briefly discussed alongside a more detailed description in chapter 2. Firstly, analogues of the substrate biotin **1** (figure 1.2a) were tested for their potential as leads for BPL inhibitor development [6]. The biotin analogues were potent inhibitors of *Sa*BPL with one example, biotin acetylene **2** (figure 1.2b), exhibiting an inhibition constant of 0.3 μ M. However, this series of compounds exhibited minimal selectivity over the human enzyme (<20-fold). The biotin binding pocket is small and highly conserved and therefore chemical modifications to the biotin scaffold to improve upon selectivity are difficult [4, 6, 31]. Hence, biotin analogues are not suitable as pre-clinical candidates.

Analogues of the native reaction intermediate, biotinyl-5'AMP **3** (figure 1.2c), have also been pursued as potential inhibitors. The first example is biotinol-5'AMP **4** (figure 1.2d), a non-hydrolysable analogue where the labile phosphoanhydride present in **3** has been replaced by an ester linkage [8, 32]. Literature compound **4** was initially designed to characterize the dimerization and repressor activities of *Escherichia coli* BPL [33]. Chapter 5 is a published manuscript entitled 'Improved synthesis of biotinol-5'AMP: Implications for antibacterial discovery' [8]. In this study **4** was tested for inhibition of BPL from clinically relevant bacteria and was also tested for whole cell antibacterial activity against *S. aureus*, *M. tuberculosis*, *E. coli* and *Enterococci* species. Compound **4** was a potent inhibitor of both *Sa*BPL and *M. tuberculosis* BPL. Compound **4** only exhibited 10-fold selectivity over the human homologue and therefore is an inappropriate pre-clinical development candidate.

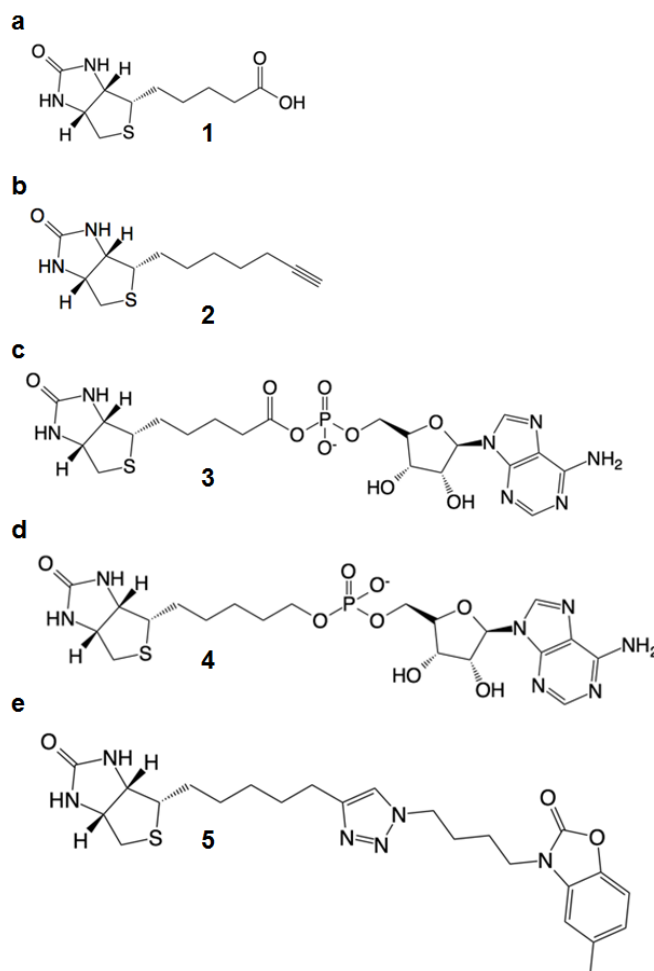


Figure 1.2: Rationally designed BPL inhibitors: a). BPL substrate biotin. b). Biotin acetylene, a biotin analogue. c). Native reaction intermediate employed by BPLs, biotinyl-5'AMP. d). Biotinol-5'-AMP, a reaction intermediate analogue and a first generation BPL inhibitor. e). BPL068, parent molecule for this study.

Soares da Costa and co-workers also reported the development of the biotin triazoles, as inhibitors of *Sa*BPL [5, 9]. Here, the phosphoanhydride present in the reaction intermediate has been replaced with a 1,4-disubstituted-1,2,3-triazole heterocycle [5]. The triazole can be readily synthesized by the Huisgen cycloaddition reaction that occurs between acetylene and azide containing molecules. This reaction proceeds using either a copper or ruthenium catalyst or in special cases, this reaction can be catalysed by an enzyme (Chapters 2 and 9). The most potent biotin triazole exemplar, BPL068 **5** in figure 1.2e, has an inhibition constant of 0.09 μM against *Sa*BPL [5]. By varying the length of the alkyl chain joining the thiophane

ring of biotin with the triazole linker, an alkyl chain length of 5 carbon atoms was shown to be optimal. A 1,4-disubstituted 1,2,3-triazole linker was also preferred over a 1,5-disubstituted 1,2,3-triazole linker. The ribose ring present in the native reaction intermediate was also shown to be dispensable for inhibitor binding and has been replaced by an alkyl chain, with an optimum length of 4 carbon atoms. Finally, the adenine moiety was replaced with a structurally related bicyclic ring system, in this case a 2-benzoxalone scaffold designed to occupy the ATP binding pocket. Compound **5** showed no inhibition of the human homologue (selectivity > 1000-fold) and had no cytotoxic activity against cultured mammalian liver cells. Finally, compound **5** was also able to inhibit the growth of *S. aureus* by 80% when 8 µg/mL was included in the growth medium [5].

BPL068 **5** exhibits many favourable properties that makes it an appropriate candidate for pre-clinical development, including good potency against the enzyme target, excellent selectivity over the human homologue (>1000-fold), no cytotoxicity against cultured mammalian liver cells and exhibits antibacterial activity against *S.aureus*. However, one of the major limitations for compound **5** is that the antibacterial activity was not potent enough to determine a minimal inhibitory concentration (MIC). An MIC is the lowest inhibitor concentration that prevents visible micro-organism growth after overnight incubation or reduces the viable cell count by 3-log units [18]. Therefore, compound **5** requires chemical optimization to improve upon the antibacterial activity. In this project I have characterized a series of analogues of **5** with the aim of discovering compounds with improved antibacterial activity (Chapters 6-8).

1.4 Research described in this thesis:

In this project my aim was to characterize rationally designed BPL inhibitors in order to identify compounds with improved properties that are required for a pre-clinical candidate. In addition to the characterization of BPL inhibitors I have also used an *in situ* click chemistry approach to develop a BPL inhibitor with fluorescent properties that will be used to confirm the mechanism of entry of BPL inhibitors in *S. aureus*.

In order to characterize rationally designed BPL inhibitors it is important to develop biochemical assays to measure enzyme activity and ligand binding to facilitate compound development. Chapter 4 is focussed upon the development of such assays. Here, an enzyme assay with improved throughput compared to published methods has been developed using radiolabelled biotin to measure protein biotinylation. An SPR binding assay was also employed to characterize the kinetics of inhibitor binding. Chapter 5 is a published paper in *ACS Medicinal Chemistry Letters* entitled ‘Improved synthesis of biotinol-5'-AMP: Implications for antibacterial discovery’ [8]. Here, literature compound **4**, was tested for enzymatic inhibition of a panel of BPLs from bacteria and the spectrum of antibacterial activity was determined against strains of *S. aureus* and *M. tuberculosis*. My contribution to this work involved biochemical characterization of biotinol-5'-AMP. Chapter 6 is a manuscript that has been accepted for publication in *ACS Medicinal Chemistry Letters* entitled ‘A new series of BPL inhibitors to probe the ribose-binding pocket of *Staphylococcus aureus* biotin protein ligase.’ In this work 25 biotin triazole inhibitors with 1-benzyl substituents were synthesized and tested for inhibition against SaBPL. These compounds are smaller in molecular weight compared to parent compound **5**, but still maintain good potency and selectivity against the biological target making them promising candidates for further optimization. Chapter 7 is a published paper in *Bioorganic & Medicinal Chemistry Letters* entitled ‘Heterocyclic acyl-phosphate bioisostere-based inhibitors of *Staphylococcus aureus* biotin protein ligase [7].’ In this work two series of compounds were synthesized, that are

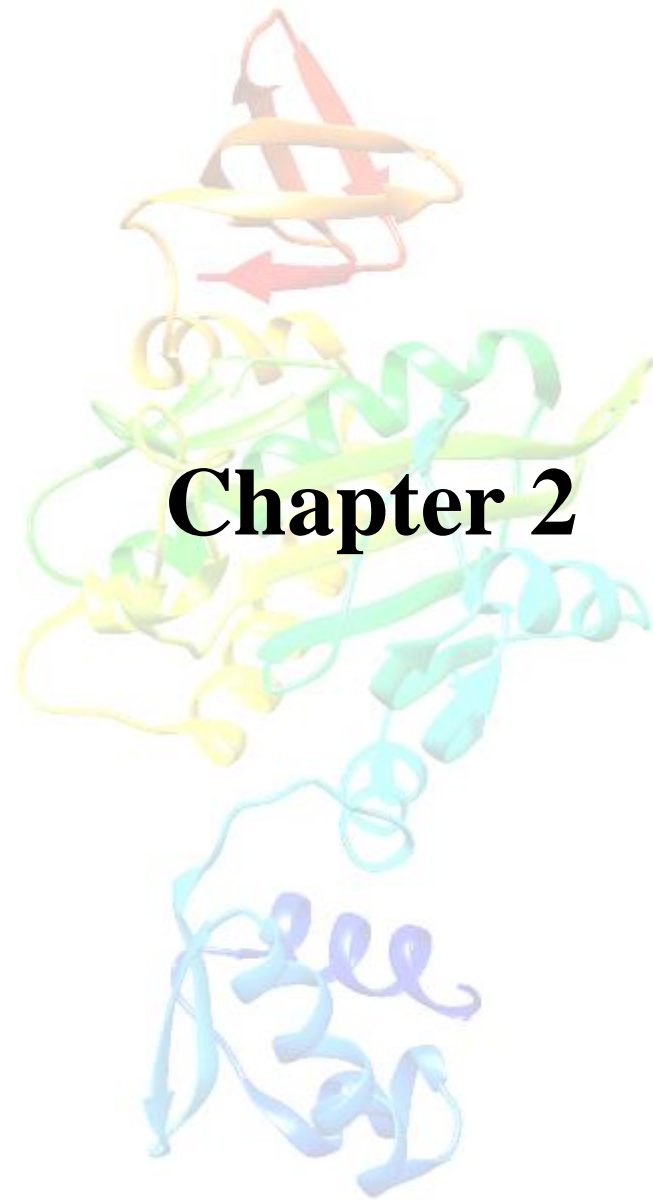
analogues of **5**. My contribution to this work involved biochemical characterization of a series of compounds for inhibition against SaBPL in which the 1,2,3-triazole has been replaced with alternative heterocycles. Chapter 8 is a draft of a manuscript entitled ‘Halogenation of biotin protein ligase inhibitors improves antibacterial activity against *Staphylococcus aureus*.’ In this work halogenated analogues of **5** were synthesized in order to investigate whether halogenation improves the antibacterial activity against *S. aureus*. Chapter 9 is a draft of a manuscript entitled ‘A template guided approach to generating cell permeable inhibitors of *Staphylococcus aureus* biotin protein ligase.’ In this work high resolution mass spectrometry was adapted to detect BPL-catalysed *in situ* click chemistry reactions. Here we showed that the reaction of biotin acetylene **1** with an azide can be catalysed by recombinant BPLs from clinically relevant bacteria, demonstrating that this approach could be used to identify biotin triazole inhibitors of other BPLs. In this work we also synthesized azide-functionalized analogues of two fluorophores and tested them for chemical ligation to biotin acetylene **1** in the presence of BPL. The fluorescent probes identified in this study will be used to help elucidate the mechanism of uptake and action of in *S. aureus*. All the work that presented in this thesis will be used to identify BPL inhibitors with favourable drug-like properties in order to develop new pre-clinical candidates.

1.5 References:

1. Fischbach, M.A. and C.T. Walsh, *Antibiotics for Emerging Pathogens*. Science, 2009. **325**(5944): p. 1089-1093.
2. Cooper, M.A. and D. Shlaes, *Fix the antibiotics pipeline*. Nature, 2011. **472**(7341): p. 32-32.
3. Payne, D.J., et al., *Drugs for bad bugs: confronting the challenges of antibacterial discovery*. Nat Rev Drug Discov, 2007. **6**(1): p. 29-40.
4. Paparella, A.S., et al., *Structure guided design of biotin protein ligase inhibitors for antibiotic discovery*. Curr top med chem, 2014. **14**(1): p. 4-20.
5. Soares da Costa, T.P., et al., *Selective inhibition of Biotin Protein Ligase from Staphylococcus aureus*. J Biol Chem, 2012. **287**(21): p. 17823-17832.
6. Soares da Costa, T.P., et al., *Biotin Analogues with Antibacterial Activity Are Potent Inhibitors of Biotin Protein Ligase*. ACS Med Chem Lett, 2012. **3**(6): p. 509-514.
7. Tieu, W., et al., *Heterocyclic acyl-phosphate bioisostere-based inhibitors of Staphylococcus aureus biotin protein ligase*. Bioorg Med Chem Lett, 2014. **24**(19): p. 4689-4693.
8. Tieu, W., et al., *Improved Synthesis of Biotinol-5'-AMP: Implications for Antibacterial Discovery*. ACS Med Chem Lett, 2015. **6**(2): p. 216-220.
9. Tieu, W., et al., *Optimising in situ click chemistry: the screening and identification of biotin protein ligase inhibitors*. Chem Sci, 2013.
10. Bockman, M.R., et al., *Targeting Mycobacterium tuberculosis Biotin Protein Ligase (MtBPL) with Nucleoside-Based Bisubstrate Adenylation Inhibitors*. J Med Chem, 2015. **58**(18): p. 7349-7369.
11. Duckworth, Benjamin P., et al., *Bisubstrate Adenylation Inhibitors of Biotin Protein Ligase from Mycobacterium tuberculosis*. Chem & Biol, 2011. **18**(11): p. 1432-1441.
12. Shi, C., et al., *Bisubstrate Inhibitors of Biotin Protein Ligase in Mycobacterium tuberculosis Resistant to Cyclonucleoside Formation*. ACS Med Chem Lett, 2013. **4**(12): p. 1213-1217.
13. Silver, L.L., *Challenges of Antibacterial Discovery*. Clin Microbiol Rev, 2011. **24**(1): p. 71-109.
14. Gwynn, M.N., et al., *Challenges of antibacterial discovery revisited*. Annals of the New York Academy of Sciences, 2010. **1213**(1): p. 5-19.
15. Lipinski, C.A., et al., *Experimental and computational approaches to estimate solubility and permeability in drug discovery and development settings1*. Adv Drug Del Rev, 2001. **46**(1-3): p. 3-26.

16. O'Shea, R. and H.E. Moser, *Physicochemical Properties of Antibacterial Compounds: Implications for Drug Discovery*. J Med Chem, 2008. **51**(10): p. 2871-2878.
17. Brown, D.G., et al., *Trends and Exceptions of Physical Properties on Antibacterial Activity for Gram-Positive and Gram-Negative Pathogens*. J Med Chem, 2014. **57**(23): p. 10144-10161.
18. Tommasi, R., et al., *ESKAPEing the labyrinth of antibacterial discovery*. Nat Rev Drug Discov, 2015. **14**(8): p. 529-542.
19. Simmons, K.J., I. Chopra, and C.W.G. Fishwick, *Structure-based discovery of antibacterial drugs*. Nat Rev Micro, 2010. **8**(7): p. 501-510.
20. Myszka, D.G. and R.L. Rich, *Implementing surface plasmon resonance biosensors in drug discovery*. Pharm Sci Tech Today, 2000. **3**(9): p. 310-317.
21. GE Healthcare, *Biacore: Sensor surface handbook*. 2007, Sweeden: General Electric company.
22. GE Healthcare, *Biacore assay Handbook*, 2012, GE Healthcare: GE Healthcare Bio-Sciences AB, Uppsala, Sweden.
23. Copeland, R.A., D.L. Pompliano, and T.D. Meek, *Drug-target residence time and its implications for lead optimization*. Nat Rev Drug Discov, 2006. **5**(9): p. 730-739.
24. Kocsis, B., J. Domokos, and D. Szabo, *Chemical structure and pharmacokinetics of novel quinolone agents represented by avarofloxacin, delafloxacin, finafloxacin, zabofloxacin and nemonoxacin*. Annals Clin Microbiol Antimicrob, 2016. **15**(1): p. 1-8.
25. Blondeau, J.M., *Fluoroquinolones: mechanism of action, classification, and development of resistance*. Survey of Ophthalmology, 2004. **49**(2, Supplement 2): p. S73-S78.
26. Nemeth, J., G. Oesch, and S.P. Kuster, *Bacteriostatic versus bactericidal antibiotics for patients with serious bacterial infections: systematic review and meta-analysis*. J Antimicrob Chemother, 2015. **70**(2): p. 382-395.
27. Cotsonas King, A. and L. Wu, *Macromolecular Synthesis and Membrane Perturbation Assays for Mechanisms of Action Studies of Antimicrobial Agents*, in *Curr Prot Pharm*. 2001, John Wiley & Sons, Inc.
28. Phetsang, W., et al., *An azido-oxazolidinone antibiotic for live bacterial cell imaging and generation of antibiotic variants*. Bioorg Med Chem, 2014. **22**(16): p. 4490-4498.
29. Jefferson, K.K., D.A. Goldmann, and G.B. Pier, *Use of Confocal Microscopy To Analyze the Rate of Vancomycin Penetration through Staphylococcus aureus Biofilms*. Antimicrob Agents Chemother, 2005. **49**(6): p. 2467-2473.

30. Tran, T.T., et al., *Daptomycin-Resistant Enterococcus faecalis Diverts the Antibiotic Molecule from the Division Septum and Remodels Cell Membrane Phospholipids*. *mBio*, 2013. **4**(4).
31. Slavoff, S.A., et al., *Expanding the Substrate Tolerance of Biotin Ligase through Exploration of Enzymes from Diverse Species*. *J Am Chem Soc*, 2008. **130**(4): p. 1160-1162.
32. Brown, P.H. and D. Beckett, *Use of Binding Enthalpy To Drive an Allosteric Transition*. *Biochemistry*, 2005. **44**(8): p. 3112-3121.
33. Brown, P.H., et al., *The Biotin Repressor: Modulation of Allostery by Corepressor Analogs*. *J Mol Biol*, 2004. **337**(4): p. 857-869.



Statement of Authorship

Title of Paper	Structure Guided Design of Biotin Protein Ligase Inhibitors for Antibiotic Discovery
Publication Status	<input checked="" type="checkbox"/> Published <input type="checkbox"/> Accepted for Publication <input type="checkbox"/> Submitted for Publication <input type="checkbox"/> Unpublished and Unsubmitted work written in manuscript style
Publication Details	Ashleigh S. Paparella, Tatiana P. Soares da Costa, Min Y. Yap, William Tieu, Matthew C. J. Wilce, Grant W. Booker, Andrew D. Abell and Steven W. Polyak (2014). Structure Guided Design of Biotin Protein Ligase Inhibitors for Antibiotic Discovery. <i>Current Topics in Medicinal Chemistry</i> , 14, 4-20.

Principal Author

Name of Principal Author (Candidate)	Ashleigh S. Paparella
Contribution to the Paper	Contributed approximately 1/3 of the written text primarily on section 4 entitled 'BPL inhibitors'. Prepared figures 4-9, 11 and 14-17
Overall percentage (%)	25%
Certification:	This paper reports on original research I conducted during the period of my Higher Degree by Research candidature and is not subject to any obligations or contractual agreements with a third party that would constrain its inclusion in this thesis. I am the primary author of this paper.
Signature	Date 25/10/2016

Co-Author Contributions

By signing the Statement of Authorship, each author certifies that:

- the candidate's stated contribution to the publication is accurate (as detailed above);
- permission is granted for the candidate to include the publication in the thesis; and
- the sum of all co-author contributions is equal to 100% less the candidate's stated contribution.

Name of Co-Author	Tatiana P. Soares da Costa
Contribution to the Paper	Contributed approximately 1/3 of the written text Overall contribution: 15%
Signature	Date 10/10/2016

Name of Co-Author	Min Y. Yap
Contribution to the Paper	Contributed approximately 1/3 of the written text Overall contribution: 15%
Signature	Date 18/10/2016

Name of Co-Author	William Tieu		
Contribution to the Paper	Assisted in proof reading and editing of manuscript Overall contribution: 5%		
Signature		Date	24/10/16

Name of Co-Author	Matthew C. J. Wilce		
Contribution to the Paper	Assisted in proof reading and editing of manuscript Overall contribution: 5%		
Signature		Date	11/10/2016

Name of Co-Author	Grant W. Booker		
Contribution to the Paper	Assisted in Proof reading and editing of manuscript Overall contribution: 5%		
Signature		Date	19/10/2016

Name of Co-Author	Andrew D. Abell		
Contribution to the Paper	Assisted in proof reading and editing of manuscript Overall contribution: 5%		
Signature		Date	19/10/2016

Name of Co-Author	Steven W. Polyak		
Contribution to the Paper	Primary role in preparing Manuscript sections 1-3 Primary role in proof reading and editing of manuscript Corresponding author Overall contribution: 25%		
Signature		Date	30/9/2016

Structure Guided Design of Biotin Protein Ligase Inhibitors for Antibiotic Discovery

Ashleigh S. Paparella¹, Tatiana P. Soares da Costa^{1,#}, Min Y. Yap^{2,^}, William Tieu³,
Matthew C. J. Wilce², Grant W. Booker¹, Andrew D. Abell³ and Steven W. Polyak^{1,*}

¹School of Molecular and Biomedical Science, University of Adelaide, South Australia 5005, Australia;

²School of Biomedical Science, Monash University, Victoria 3800, Australia; ³School of Chemistry and Physics, University of Adelaide, South Australia 5005, Australia

Abstract: Biotin protein ligase (BPL) represents a promising target for the discovery of new antibacterial chemotherapeutics. Here we review the central role of BPL for the survival and virulence of clinically important *Staphylococcus aureus* in support of this claim. X-ray crystallography structures of BPLs in complex with ligands and small molecule inhibitors provide new insights into the mechanism of protein biotinylation, and a template for structure guided approaches to the design of inhibitors for antibacterial discovery. Most BPLs employ an ordered ligand binding mechanism for the synthesis of the reaction intermediate biotinyl-5'-AMP from substrates biotin and ATP. Recent studies reporting chemical analogs of biotin and biotinyl-5'-AMP as BPL inhibitors that represent new classes of anti-*S. aureus* agents are reviewed. We highlight strategies to selectively inhibit bacterial BPL over the mammalian equivalent using a 1,2,3-triazole isostere to replace the labile phosphoanhydride naturally present in biotinyl-5'-AMP. A novel *in situ* approach to improve the detection of triazole-based inhibitors is also presented that could potentially be widely applied to other protein targets.

Keywords: Antibiotic, biotin, biotin protein ligase, *Staphylococcus aureus*, structure guided drug design, inhibitor design, X-ray crystallography.

1. INTRODUCTION

1.1. Need for New Antibiotics

New classes of antibiotic are urgently required to overcome the growing problem of antibiotic resistance [1, 2]. Despite this clear need, there has been a decline in the rate of submission and introduction of new drug candidates [3]. The problem is exacerbated by the fact that most new antibiotics introduced over the last 30 years are derivatives of existing classes and are thus subjected to the same resistance mechanisms [4-6]. Efforts to identify novel classes of antibacterial chemotherapies must be renewed [7]. Much of this early stage antibiotic research is now carried out by academic and government laboratories as most large pharmaceutical companies that previously occupied this space have terminated their antibiotic research programmes due to a perceived low return on investment, strict drug regulatory requirements and technical difficulty of developing a novel drug [2, 3, 8].

Staphylococcus aureus is a clinically important Gram-positive pathogen that commonly colonizes the anterior nares, respiratory system and urinary tract of the host [9-11].

It is implicated in a wide range of diseases including skin infections, pneumonia, meningitis and bacteraemia [12, 13]. *S. aureus* is the most common cause of nosocomial infections and a leading cause of death in hospitalized patients. Antibiotic resistant *S. aureus* first appeared in the 1940s after mass production of penicillin. Methicillin-resistant *S. aureus* (MRSA) is particularly problematic as it has developed antibiotic resistance to most penicillin-based antibiotics, including methicillin [14]. Two major variants of MRSA have been described, hospital acquired and community acquired MRSA. Both are becoming increasingly difficult and costly to treat with many available β -lactam antibiotics ineffective against both strains [15-21]. MRSA infections have also surfaced in recent years that are resistant to vancomycin, once considered the drug of last resort [19, 22]. Overall these factors have contributed to an increase in the mortality rate by MRSA infections worldwide [23]. An important strategy to combat drug resistance in *S. aureus* is to develop new chemical entities against novel targets that are known to be essential for cell survival and that have no pre-existing target-based resistance [6]. Here we review biotin protein ligase (BPL) as one such target. Its critical role in bacterial physiology is discussed, as are recent successes in designing small molecule inhibitors of BPL for antibacterial discovery.

1.2. BPL as a Novel Antibacterial Target

BPL is the enzyme responsible for the post-translational attachment of biotin onto biotin-dependent enzymes that are known to catalyze key reactions in important metabolic pathways. *S. aureus* expresses two such enzymes, namely

*Address correspondence to this author at the Department of Biochemistry, School of Molecular and Biomedical Sciences, University of Adelaide, Adelaide, SA 5005, Australia; Tel: 61-8-8303-5289; Fax: 61-8-8303-4362; E-mail: steven.polyak@adelaide.edu.au

[#]Present address: Charles Sturt University, Wagga Wagga, New South Wales 2650, Australia;

[^]Present address: CSL Limited, 45 Poplar Road, Parkville, Victoria 3052, Australia

acetyl CoA carboxylase (ACC) and pyruvate carboxylase (PC), that are intimately involved in fatty acid biosynthesis and anaplerosis (ie topping up) of the tricarboxylic acid cycle respectively. The significance of these pathways on *S. aureus* survival and virulence is discussed below. BPL has been identified as a potential new antibacterial drug target due to its pivotal role in the activation of ACC and PC via protein biotinylation. Without protein biotinylation, these enzymes are devoid of activity and are unable to fulfill their key metabolic functions. Multiple lines of evidence support the approach of targeting BPL to generate a new class of antibiotic. For example, genetic knockout studies have demonstrated the essential roles played by BPL and ACC in a number of important bacterial pathogens including *S. aureus* [8, 24], *Escherichia coli* [25-27], *Mycobacterium tuberculosis* [28] and *Streptococcus pneumoniae* [29] amongst others. These studies highlight that no alternative pathway for protein biotinylation exists in bacteria. Recent studies have shown BPL to be a druggable antibiotic target, with the identification of inhibitors that are effective anti *S. aureus* agents (see below).

2. BIOTIN DEPENDENT ENZYMES

Biotin functions as an indispensable enzyme cofactor required for certain carboxylation, decarboxylation and transcarboxylation reactions (reviewed [30, 31]). The common feature of these reactions is the transfer of a carboxyl group between metabolites utilizing biotin as a carboxyl carrier. Here our discussion is focused on the biotin-dependent carboxylases as *S. aureus* expresses two examples from this enzyme family. The reactions catalyzed by the biotin-dependent carboxylases take place as two distinct partial reactions shown in Eq 1 and Eq 2.

Eq 1. Enzyme-biotin + HCO_3^- + MgATP \rightarrow Enzyme-biotin- CO_2 + MgADP + Pi

Eq. 2. Enzyme-biotin- CO_2 + acceptor \rightarrow acceptor- CO_2 + enzyme-biotin

These two partial reactions are performed at two discrete sites in the biotin-dependent enzyme, and as such the cova-

lently-bound biotin moiety must translocate between these two active sites (Fig. 1) [32-34]. Thus, the reactions catalyzed by the biotin-dependent enzymes can only be performed when biotin is attached to the enzyme. Accordingly, inhibiting the attachment of the biotin cofactor onto the target enzymes provides a route to new antibiotics. Here we provide an overview of the role of biotin in bacterial metabolism and its function as a cofactor for ACC and PC in order to establish their importance in *S. aureus* physiology and pathogenicity.

2.1. Acetyl CoA Carboxylase

ACC [E.C. 6.4.1.2] catalyzes the first committed step in the fatty acid biosynthetic pathway, the carboxylation of acetyl-CoA into malonyl-CoA, that is essential for cell membrane maintenance and biogenesis (reviewed [35, 36]). It is well documented that bacterial enzymes belonging to the type II fatty acid synthetic pathway provide an exciting source of new drug targets due to the essential role played by fatty acids in membrane biogenesis and maintenance [8, 37, 38]. Clinical validation for this approach comes from chemotherapeutic intervention of key enzymes in the fatty acid synthesis pathway including the anti-tuberculosis drug isoniazid and antiseptics such as triclosan (reviewed [37, 39]). However, recent studies have identified key differences between Gram-positive and Gram-negative bacteria regarding the incorporation of exogenous fatty acids from human serum into membrane, thereby bypassing the need for *de novo* synthesis. These studies suggest that the inhibition of fatty acid synthesis will not be efficacious for all species of bacteria. It is clear that fatty acid synthesis is essential in Gram-negative bacteria as there is no mechanism to allow fatty acid supplementation to form the lipid A core structure of outer membrane polysaccharides [40]. Supplementation of exogenous β -hydroxy-fatty acids is ineffective in replacing *de novo* fatty acid synthesis, thus highlighting the essential function performed by this metabolic pathway [41]. The story for Gram-positive bacteria is more controversial [40, 42-44] in that *S. aureus* can incorporate exogenous fatty acids into its membrane to overcome any antibacterial activity

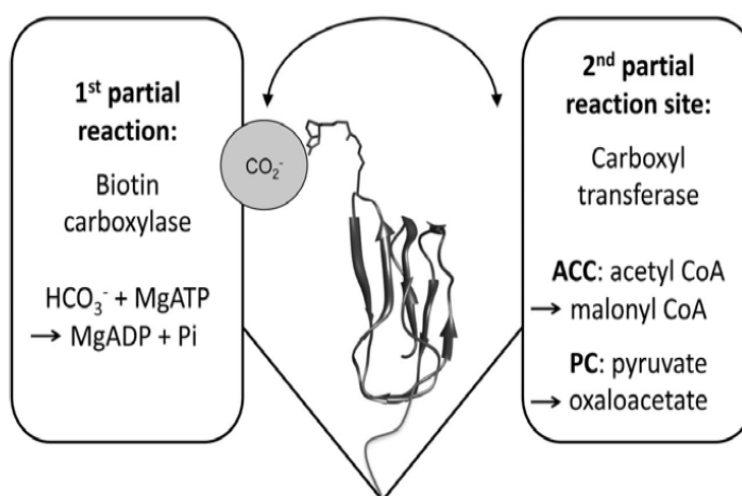


Fig. (1). Mechanism of biotin-dependent carboxylases. Schematic diagram depicting biotin, attached to the biotin domain, that carries an CO_2 anion between two partial reaction sites.

of fatty acid synthesis inhibition [44]. However, Balemans *et al.* showed that serum fatty acids can not totally overcome the antibacterial activity of fatty acid synthesis inhibitors in *S. aureus* [43]. Recently, Parsons *et al.* demonstrated that *S. aureus* and *Streptococcus pneumoniae* utilize exogenous material to different extents. Whilst *S. pneumoniae* can produce all its membrane phospholipids using exogenous fatty acids, *S. aureus* only generates 50% of its phospholipids using exogenous material [45]. In a mechanism that is not yet understood, exogenous fatty acids can completely inhibit ACC activity in *S. pneumoniae*, thereby creating a blockage of the fatty acid synthesis pathway and bypassing the need for *de novo* synthesis. In contrast, ACC activity is reduced only by 50% when *S. aureus* is grown in serum-containing media. Additionally, *S. aureus* synthesizes branched chain, saturated fatty acids that are vital for bacterial membrane function but are not present in mammals and, therefore, unlikely to circumvent *de novo* synthesis [40]. Inhibition of the fatty acid synthesis pathway is thus a valid approach for antibacterial therapy in *S. aureus*, where *de novo* fatty acid synthesis is required. This observation is further supported by several reports demonstrating the efficacy of fatty acid synthesis inhibitors for antibacterial therapy in murine models of *S. aureus* bacteraemia [46-49]. For example, the FabF inhibitor platensimycin, a secondary metabolite isolated from *Streptomyces platensis*, has been reported with *in vivo* efficacy in a murine infection model [50]. Together the evidence supports the hypothesis that targeting fatty acid synthesis is a promising approach to combat Gram-negative pathogens and certain Gram-positive species such as *S. aureus*.

2.2. Pyruvate Carboxylase

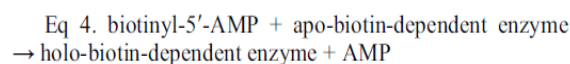
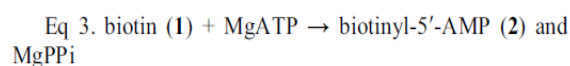
PC [EC 6.4.1.1] catalyzes the synthesis of oxaloacetate through the carboxylation of pyruvate. Oxaloacetate is one of several intermediates in the tricarboxylic acid cycle that is diverted for use in alternative biosynthetic pathways, namely the synthesis of amino acids lysine, aspartate, asparagine, methionine, threonine and isoleucine [51]. Therefore, PC performs an anaplerotic (“filling up”) role to replenish the tricarboxylic acid cycle. Certain prokaryotes contain PC, such as *Staphylococcus*, *Bacillus*, *Rhizobium*, *Mycobacterium* and *Pseudomonas* [52]. Enteric bacteria do not possess a gene for PC, but instead synthesize oxaloacetate from phosphoenolpyruvate using phosphoenolpyruvate carboxylase. There are a number of comprehensive reviews on metabolism in PC containing bacteria including *Staphylococci* [53], *Bacillus subtilis* [54], *Rhizobium etli* [55] and *Corynebacterium glutamicum* [56].

The fact that PC has not appeared in various genome-wide screens for essential genes suggests that it is dispensable for the growth of *S. aureus* in the laboratory [24, 57]. However, PC was identified in a transposon-mediated, gene disruption screen to identify virulence factors required in a nematode killing assay [58]. The molecular basis for this is unclear, but various studies suggest a possible link between PC, the composition of the bacterial membrane, and avoidance of the host immune system. Early work demonstrated that the addition of biotin into media improves growth rates of *S. aureus* [59, 60], protein synthesis [61] and coagulase production [62]. Exogenous biotin can also influence the

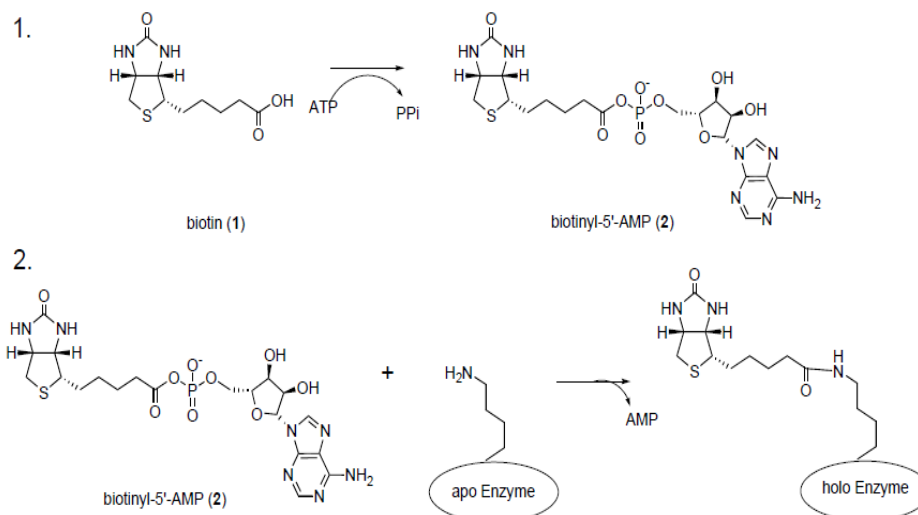
composition of the bacterial cell membrane. Biotin supplementation in the growth media is reported to increase the proportion of lysine-containing phosphatidyl glycerol in *S. aureus* membranes [61], thus altering the electrostatic charge on the membrane. Modification of membrane lipids provides bacteria with a resistance mechanism against cationic lipopeptide antibiotics, such as daptomycin [63]. Daptomycin's mode of action is similar to that employed by cationic antimicrobial peptides produced by the host's innate immune response; to integrate into the bacterial membranes causing its disruption. Due to their cationic properties, the antimicrobial peptides can readily bind to the highly negatively charged bacterial cell envelope. As lysyl-phosphatidylglycerol is less acidic than non-modified phosphatidylglycerol, the antibacterial activity of the cationic peptides can be overcome *via* electrostatic repulsion (reviewed [64, 65]). Growth of *S. aureus* in biotin deficient media results in increased sensitivity of *S. aureus* to a range of antibiotics that function through distinct drug targets, such as cell wall synthesis (i.e. bacitracin, methicillin, penicillin and ampicillin) and protein synthesis (i.e. erythromycin, tetracycline, chloramphenicol, streptomycin and kanamycin) [62]. Hence, an adequate supply of lysine to incorporate into phosphatidylglycerol is required. Genetic and metabolic studies have shown that PC is one of several key enzymes involved in lysine biosynthesis [66], and its co-ordinated expression in *C. glutamicum* improves lysine production used as a food additive for livestock [67]. Together these studies suggest that inactivation of PC *via* inhibition of BPL is likely to disrupt *S. aureus* virulence and may function as a useful co-therapy with other antibacterial agents.

3. STRUCTURAL BASIS OF PROTEIN BIOTINYLA-TION

BPL catalyzed protein biotinylation is a post-translational modification of exquisite specificity that occurs at a single lysine residue present within a “biotin domain” in the biotin-dependent enzymes. Structural biology has provided powerful new insights into the conserved reaction mechanism performed by all BPLs, and shown in Eq 3 and Eq 4 and Scheme 1:



In the first partial reaction, biotin **1** and ATP bind within their respective sites in a fixed confirmation that places the ligands spatially close to each other to facilitate the nucleophilic attack of the biotin carboxylate group with the α -phosphate group of ATP to form the reaction intermediate biotinyl-5'-AMP (**2**) with the concomitant release of pyrophosphate (Eq 3, and Scheme 1) [68]. The BPL-2 complex then forms a protein: protein complex with the biotin-dependent enzyme to allow the second partial reaction (Eq 4). Structural studies, performed with mutants of BPL from *Pyrococcus horikoshii* unable to release the biotin domain substrate following biotinylation, provide a possible scenario for the transfer mechanism of biotin onto the protein substrate [68, 69]. During the first “formation stage”, the side



Scheme (1). BPL catalyzed protein biotinylation.

chain of the target lysine on the biotin domain enters the BPL active site. Correct positioning of the biotin domain, and hence the target lysine, is essential for the biotinylation reaction. X-ray crystallographic studies revealed two alternative BPL biotin domain complexes, indicating a degree of flexibility in how the protein substrate can dock with BPL [69]. In the second stage, once the biotin domain is appropriately bound, the ϵ -amino of the substrate lysine provides a positive charge that facilitates the nucleophilic attack on the carbonyl group of **2**, resulting in the transfer of biotin onto the biotin domain with the release of AMP (Eq. 4 and Scheme 1). This second catalytic step is known as the “reaction stage”. The third and final stage is the “product stage”, where the biotinylated protein is released from BPL [68]. The sum of these events ensures that biotin is reliably transferred only onto the appropriate protein substrate *in vivo*.

3.1. BPL Structure

BPLs can be divided into 3 distinct structural classes (Fig. 2). The BPLs from Archaea, prokaryotes and plants belong to either class I or class II, whilst BPLs from yeast, insects and mammals fall into class III. All BPLs contain a conserved catalytic domain and a C-terminal cap domain both of which are required for protein biotinylation. BPLs that consist solely of these two domains are classified as class I BPLs. Class II BPLs are bifunctional proteins that possess both biotin ligase and DNA binding activities. Apart from catalyzing the biotinylation reaction, the class II members contain a winged helix-turn-helix on their N-terminus to facilitate binding to DNA. Biotin and/or **2** induce the dimerization of BPL, which is a prerequisite for DNA binding. Here the dimeric BPL-biotin complex serves as transcriptional repressor of the biotin biosynthetic operon thereby providing an elegant feedback mechanism to control the synthesis of cellular biotin (reviewed [70]). In contrast, class III BPLs have a large N-terminal extension that is distinct from the DNA-binding domain of class II enzymes. Domain mapping studies, using engineered truncations and limited proteolysis, have revealed a structured domain housed within this extension in human and yeast BPLs [71-74]. Biochemical data supports a role for this domain in stabilizing the pro-

tein:protein interaction between BPL and its protein substrate during catalysis thereby ensuring the fidelity of protein biotinylation [72, 75, 76]. An X-ray crystal structure of a class III enzyme has not yet been reported. This would be a useful tool to aid the design of BPL inhibitors that are inactive against the human homolog.

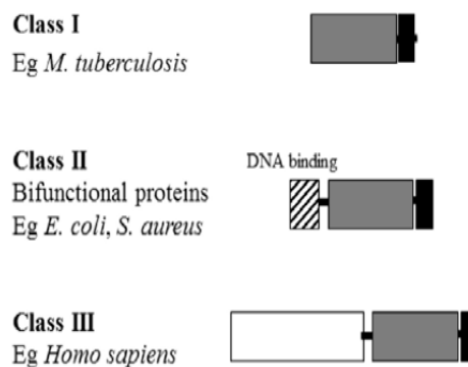


Fig. (2). Schematic diagram of the 3 classes of BPL. The conserved catalytic (grey) and C-terminal (black box) domains are shown. The relative sizes of the N-terminal extensions on class II and class III enzymes are represented.

Much of our understanding of the mechanism and structure of BPLs has been provided through biochemical, mutational and structural studies performed on class I and class II BPLs, due to the relative ease of performing genetic manipulation, recombinant expression, purification and crystallization. The most highly characterized BPL is the class II example from the prototypical bacteria *Escherichia coli*, also known as the biotin retention protein BirA. The crystal structure of the non-liganded (ie apo) BirA was first determined in 1992 [77]. Complexes with biotin and a non-hydrolyzable analog of **2**, biotinol-5'-AMP (see **3** in Fig. 3), were subsequently reported thereby revealing molecular details about the binding pockets for biotin and ATP [78, 79]. These structural features will be described in further detail below with a view to designing inhibitors that can occupy these sites. The complex of BirA with **3** revealed that the compound adopts a tight V-shaped geometry necessary for occupying the adja-

cent biotin and ATP pockets (Fig. 4). X-ray crystal structures of class I BPLs from, *Aquifex aeolicus*, *M. tuberculosis* and *P. horikoshii* [28, 29, 68, 69, 80] and the class II BPL from *S. aureus* [81, 82] have subsequently been determined. These data demonstrate that all BPLs adopt a highly conserved protein fold. Additionally, the native reaction intermediate **2** adopts the same mode of binding as **3** in all available structures.

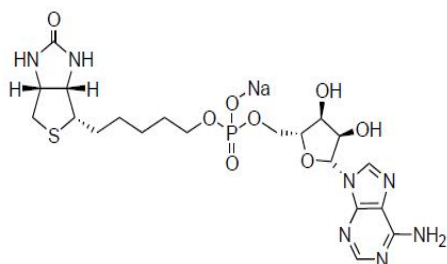


Fig. (3). Chemical structure of biotinyl-5'-AMP (**3**).

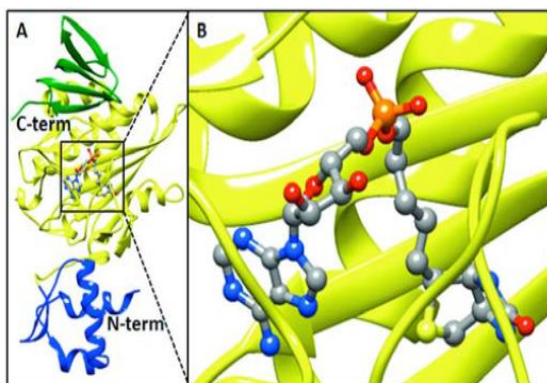


Fig. (4). Structure of *E. coli* BirA in complex with biotinyl-5'-AMP (**3**). (A) The N-terminal (blue), central catalytic (yellow) and C-terminal domains (green) of BirA are shown, as is **3** in ball and stick representation. (B) V-shaped binding geometry adopted by **3** in the active site of BirA. PDB 2EWN [79].

3.2. Catalytic Domain

The C-terminal cap and catalytic domains of BPLs across organisms are highly conserved, with between 20 – 25 % identity in their primary structures. Mutational studies have identified conserved sequences located in the catalytic domain of BPLs that are involved in biotin and ATP binding, the formation of **2** and binding to biotin domain substrates [69, 80, 83-86]. Available X-ray crystal structures of the catalytic domain of different BPLs show conservation of several key features: a mixed β -sheet packed between several α -helices, as well as solvent exposed surface loops [68, 77, 80] (Fig. 5). The greatest differences observed between the crystallographic structures of class I and class II BPLs is the mobility of these surface loops. In unliganded BirA (ie the apo enzyme), four of the surface loops (residues 116-124, 140-146, 193-199 and 212-223) were not visualized in the electron density map, consistent with the notion that these segments are highly mobile or unstructured. When crystallized in complex with **3**, all segments of BirA become ordered indicative of a disordered-to-ordered transition accompanying ligand binding. Chemical proteolysis studies per-

formed in solution with BirA showed the same surface loops were protected from cleavage by hydroxyl radicals in the presence of **2** [87], thereby highlighting these conformational changes are genuine and not merely artifacts of protein crystallography. In the case of apo-BPL from the thermophilic archaea *P. horikoshii* and *A. aeolicus*, only one of the surface loops is disordered. Furthermore, the same loops are pre-ordered in the archaeal structures. This is consistent with studies on other proteins isolated from hyperthermophiles that often adopt more ordered structures at higher temperatures, usually stabilized *via* an increased number of hydrophobic interactions [88].

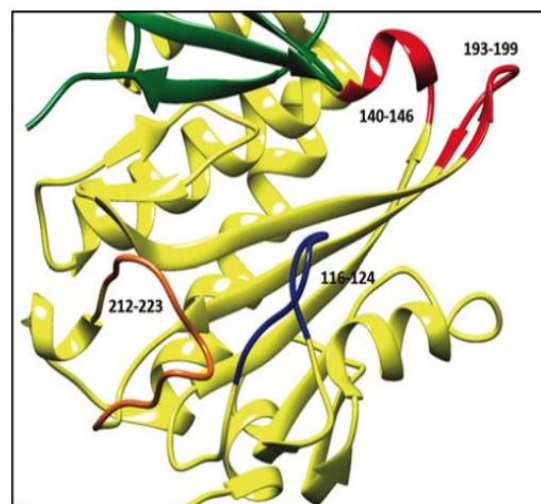


Fig. (5). Conformational changes in *E. coli* BirA. Surface loops that undergo a disordered-to-ordered transition upon ligand binding are depicted. Highlighted are the biotin-binding (blue, 116-124) and adenylylate-binding loops (orange, 212-223). PDB 2EWN [79].

The catalytic domain of BPL contains binding sites for biotin and ATP that facilitate the reaction to give **2**. The biotin-binding site, located on the surface of the mixed β -sheet in the catalytic domain (Fig. 6), consists of a hydrophobic wall and a glycine rich hydrophilic bottom. The oxygen on the ureido heterocycle of biotin forms hydrogen bonds to a backbone amide at Arg116 and the side chain of Ser89 at the base of the pocket. The 1' and 2' nitrogens also form hydrogen bonds with the backbone oxygen of Arg116 and side chain of Thr90, respectively (Fig. 6A). A hydrophobic interaction occurs between the sulphur atom on biotin and Trp123. Additional hydrophobic interactions are apparent between carbon atoms in the heterocycles and Gly204 and Ala205. The carbon chain on the valeric acid moiety is encased in a hydrophobic tunnel consisting of Gly117, Gly206, Gly186, Leu188 and Ile187 [78]. Biotin binding results in an ordering of the biotin-binding loop (residues 116-124), which then folds over the ligand shielding it from solvent (Fig. 6B). A hydrogen bond between the biotin hydroxyl group and the backbone amide at Arg118 helps stabilize the biotin-binding loop. A defining feature on the loop is a highly conserved "Gly-Arg-Gly-Arg-X" motif present in all BPLs. Noteworthy is Arg118 (ie Gly-Arg-Gly-Arg-Arg¹¹⁸-X) that plays a key role in stabilizing the biotin-binding loop *via* an intra-molecular salt bridge with the side chain of Asp176 (Fig. 6B). Substitution of Arg118 with glycine resulted in

dissociation rates that were enhanced by 100- and 400-fold for biotin and **2**, respectively, over wildtype BirA implying that the salt bridge is required for anchoring these ligands in the active site [83]. The consequence of **2** readily diffusing out from the protected environment of the BPL active site is the promiscuous biotinylation of non-target proteins, such as BirA itself, bovine serum albumin and RNase A [85]. The “leaky phenotype” of the BirA Arg118-Gly mutant has been exploited to identify inhibitors of *S. aureus* BPL (see the section on *in situ* click chemistry later in this review).

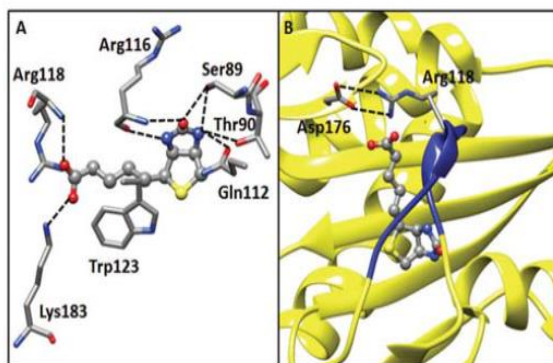


Fig. (6). The biotin-binding pocket of *E. coli* BirA. (A) Hydrogen bonds between the protein and biotin (ball and stick representation) are shown with black dashed lines. (B) The salt bridge, involving Arg118 and Asp176, that helps stabilize the biotin-binding loop (blue). PDB 1HXD [78].

This structural data provides a molecular explanation for the ordered ligand binding mechanism employed by BirA. The before mentioned ordering of the biotin-binding loop positions the side chain of Trp123 such that it creates the binding surface necessary for nucleotide binding in the ATP binding pocket (Fig. 7). Nucleotide triphosphate binding is stabilized by a π - π stacking interaction between the adenyl moiety and the indole ring of Trp123 [79]. Trp123 is not appropriately positioned for this key binding interaction to occur in the absence of biotin. The purine also hydrogen bonds with Asn208 and the main chain atoms of Phe124. Following ATP binding, the synthesis of **2** can proceed. An adenylate-binding loop (residues 212-223) also undergoes a disordered-to-ordered transition to further stabilize the interaction with the reaction intermediate [79] (Fig. 7). Here the loop folds over the adenylate base of **2** and forms hydrophobic interactions with the ligand through Val214, Val219 and Trp223 [86]. Unlike BirA, the BPLs from *A. aeolicus* and *P. horikoshii* have pre-ordered biotin-binding and adenylate-binding loops, thereby allowing these enzymes to bind to biotin and ATP in a random manner [68, 80]. This ordered binding mechanism is central to the design of inhibitors. The structural biology highlights potential sites for inhibitor binding that may be absent at certain times of the enzyme’s reaction cycle.

3.3. C-terminal Cap Domain

The C-terminal cap domain evident in available BPL structures is formed by 5 – 6 strands of mixed β - sheets and structurally resemble SH3 domains [77, 80, 89]. Structural studies performed on *P. horikoshii* BPL show that the C-terminal domain undergoes large structural changes when

ligands are bound in the active site [69]. A point mutation of residue Arg317, located in the C-terminal domain of BirA, resulted in a decrease in ATP-binding despite a lack of any contacts with residues located in the catalytic active site [90]. Tron *et al.* reported that long range hydrogen bonds are formed between the oxygen atoms of the ATP γ -phosphate bound within the ATP-binding site and residues Ser229, Leu230 and Arg231 located on the C-terminal domain of *A. aeolicus* BPL [80]. These structural data, together with mutational studies performed on BirA, suggest that the C-terminal domain plays a role in priming the enzyme: **2** complex such that the BPL is ready for the interaction with the protein substrate and facilitating the second partial reaction [78, 90].

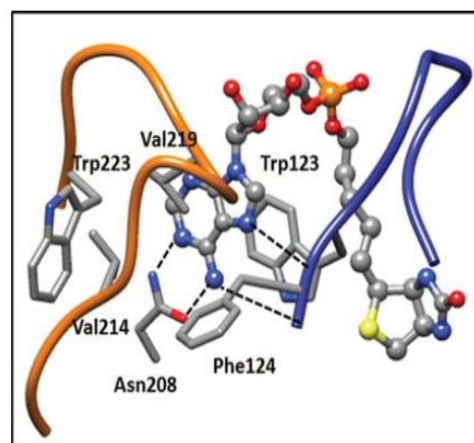


Fig. (7). The ATP-binding pocket of *E. coli* BirA. Hydrogen bonds between the protein and the adenosine moiety on **3** (ball and stick representation) are shown with black dashed lines. Highlighted are the biotin-binding (blue) and the adenylate-binding (red) loops. PDB 2EWN [79].

3.4. Protein: Protein Interaction with Biotin Domain Substrate

An important feature common to all biotin-dependent enzymes is the biotin domain that houses the target lysine residue to which biotin is covalently attached. A comparison of the biotin domains from a diverse selection of species from all three kingdoms shows that these domains are highly conserved in both amino acid composition and structure [91, 92]. A number of biotin domain structures have now been solved with the first example being that of *E. coli* biotin carboxyl carrier protein that was determined using both X-ray crystallography [93] and NMR [94]. Both techniques gave rise to essentially identical structures that have a flattened β -barrel containing two sets of four anti-parallel β -strands forming a β -sandwich (Fig. 8). These proteins are structurally analogous to the lipoyl domains of 2-oxo acid dehydrogenase complexes that are also subject to post-translational modification. In recent years, more biotin-accepting domain structures have become available with all adopting the same, highly conserved conformation (reviewed in [92]). The tertiary structure of the biotin-accepting domain has remained highly conserved, as adopting the appropriate fold is a key requirement for an interaction with BPL and subsequent protein biotinylation.

Biotin is covalently attached to a single lysine residue present in a highly conserved Ala-Met-Lys-Met motif, which

is located at the surface of a hairpin turn between β -strands 4 and 5 [95]. Correct positioning of the lysine residue in the biotin domain is absolutely critical for protein biotinylation as moving it by just one position to the N- or C-terminal side results in the abolishment of biotinylation *in vitro* and *in vivo* [95, 96]. Mutagenesis studies show that while the flanking methionine residues are not essential for biotinylation [95, 97-100], they do affect the binding of the carboxyl anion during carboxyl transfer reactions [100, 101]. A recent X-ray crystallographic structure of a mutant variant of *P. horikoshii* BPL in complex with a biotin domain of ACC provides clues about the molecular mechanisms governing substrate recognition (Fig. 9) [69]. The complex crystallized as a heterotetramer containing a BPL dimer associated with two separate biotin domain substrates. The complex formed an extended intermolecular β -sheet involving a β -strand of BPL and the β 2 strand of the biotin domain with the intermolecular surface stabilized through hydrophobic and hydrogen bonding interactions [69]. Small molecule inhibitors that bind in the interface and block this protein:protein interaction have not been reported, but this approach could be pursued as a route to the inhibition of BPL.

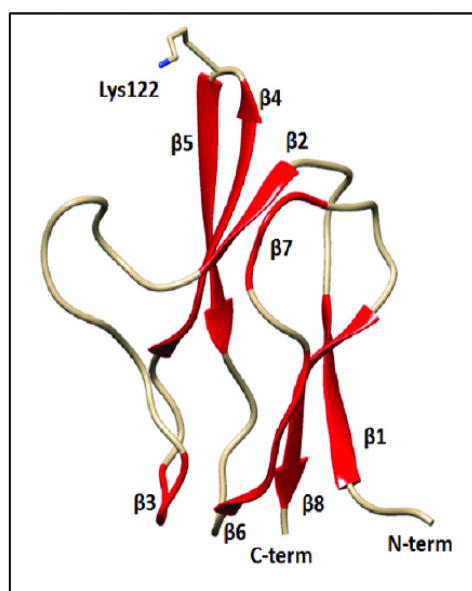


Fig. (8). Structure of the biotin domain from *E. coli* ACC. β -sheets 1-8 are shown, as is the side-chain of Lys122 that is targeted for biotinylation. PDB 1BDO [93].

4. BPL INHIBITORS

BPL was identified by GlaxoSmith Kline as an essential gene in *S. aureus* that could be a potential target for new antibiotics [8]. High-throughput screens were carried out against random compound libraries containing 260,000 to 530,000 compounds but no hits were identified. A more recent structure-guided approach to the design of small molecule inhibitors against *S. aureus* BPL (SaBPL) has led to the discovery of BPL inhibitors that bind selectively to bacterial BPL but not the human homolog. This consideration is critical for antibacterial development as compromised activity of human BPL can be lethal, as observed with patients with congenital defects that cause inactivation of the enzyme (reviewed in [92]).

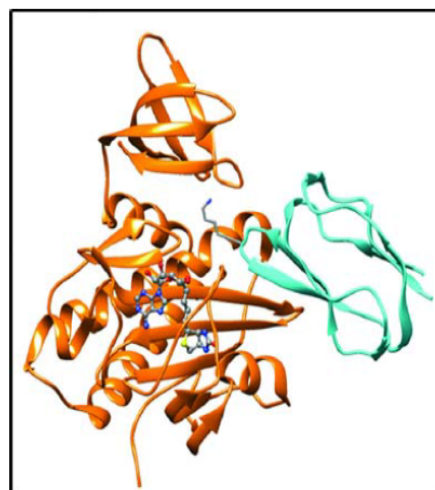


Fig. (9). Co-crystal structure of BPL and biotin domain from ACC from *P. horikoshii*. The class I BPL (orange) is shown in complex with the biotin domain (cyan). Biotin and adenosine are shown in ball and stick representation, as is the side-chain of Lys122 targeted for biotinylation. PDB 2EJF[69].

4.1. Biotin Analogs as Antibacterial Agents

Naturally occurring analogs of biotin with antibacterial activity have been identified. For example, α -dehydrobiotin (see 4 in Fig. 10) isolated as a secondary metabolite from *Streptomyces lydicus*, has antibacterial activity against *E. coli*, *B. subtilis* and several strains of *M. tuberculosis* in defined media, but not media supplemented with biotin [102]. Anti-tubular activity was also observed for the secondary metabolites α -methylbiotin (5 in Fig. 10, MIC 12.5 μ g/ml) and α -methyldehydrobiotin (see 6 in Fig. 10, MIC 0.2 μ g/ml) [103]. These analogs share the carboxyl group on biotin 1 that is required for the attachment of the ligand onto biotin-dependent enzymes. Thus, their mechanism of action is to be incorporated into a biotin-dependent enzyme thereby inhibiting the enzyme's biotin carboxylation activity (Eq 1 and 2) [104]. Similar synthetic variants of biotin that "cripple" biotin-dependent enzymes have been explored as enzyme inhibitors. As biotin accepts the carboxyl anion at the 1' nitrogen, modification of biotin's structure at this site inactivates biotin-dependent enzymes. For example, a biotin analog with phosphonacetic acid coupled to biotin at the 1' N (see 7 in Fig. 10), designed to be a stable mimic of the naturally occurring carboxyphosphate intermediate produced in biotin-mediated carbon dioxide transfer, was shown to inhibit *E. coli* biotin carboxylase activity *in vitro* [105, 106]. Whilst these biotin analogs have proved to be useful research tools they are unlikely to have utility as anti-microbial agents.

The strategy of crippling biotin-dependent enzymes described above requires the biotin analogs to be ligated onto the protein substrates. Thus, the antibacterial activity of these analogs has not been linked directly to the inhibition of BPL. However, this approach has a serious limitation. The biotin analogs only occupy the BPL active site in a transient manner, providing an opportunity for biotin to bind BPL and be incorporated into a biotin-dependent enzyme. This would allow the bacteria an opportunity to bypass the antibacterial effects of the compound. A more effective approach to

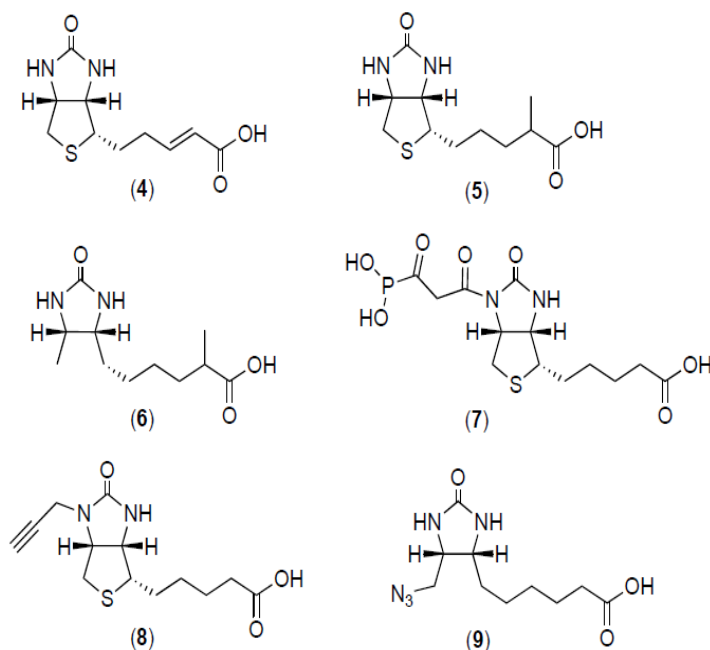


Fig. (10). Chemical structures of biotin analogues.

prevent protein biotinylation is to design small molecule inhibitors that bind tightly and specifically to the ligand binding site of bacterial BPL, thereby blocking all protein biotinylation. Towards this goal, our understanding of molecular architecture of the biotin-binding site from X-ray crystallography studies has assisted in the design of new BPL inhibitors. In one study, biotin analogs with chemical modifications to the ureido and thiophane rings were designed and synthesized with a view to defining what substitutions could be tolerated by the BPLs from a wide variety of species [107]. Nine biotin analogs were each assayed with eight different BPLs. Overall, the BPLs displayed high selectivity towards the natural structure of **1**. BPLs from *P. horikoshii* and *S. cerevisiae* could both accommodate a propargyl group attached at the 3' nitrogen (see **8** in Fig. 10), and *P. horikoshii* could also incorporate dethiobiotin azide into a protein substrate (see **9** in Fig. 10). All the other BPLs studied did not utilize the biotin analogs as substrates [107]. This finding, together with the available X-ray crystallographic data and primary sequence analysis [81, 91, 108], highlights that the biotin-binding pocket is highly conserved amongst all BPLs – including human BPL. This is not favorable for the design of an inhibitor with high selectivity for bacterial BPLs over the human counterpart. Additionally, the available X-ray crystallography data from BPLs from different species show that the biotin-binding pocket itself is relatively small, which restricts the opportunity to extend upon the heterocycles of the biotin structure. Likewise, the hydrophobic tunnel that encases the valeric acid moiety is very narrow, thereby limiting the modifications that can be made to this feature on the biotin structure. In contrast, the carboxyl group is relatively solvent exposed making it a more attractive target for chemical modification.

The approach of targeting the carboxyl group of biotin yielded a series of BPL inhibitors with antibacterial activity against *S. aureus* in a recent study [109]. Of particular note

were alcohol, alkane and alkyne analogs (see pharmacophore **10** in Table 1). All analogs were assayed for inhibitory activity against BPLs from *S. aureus*, *E. coli* (BirA) and *Homo sapiens* to address potency and species selectivity. The alcohol derivative biotinol (**11**) was identified as a pan inhibitor of BPLs from all three species with a $K_i \approx 4 \mu\text{M}$ in each case (Table 1). X-ray structures of *SaBPL* in complex with **11** revealed a similar mode of binding to **1** using a conserved hydrogen bonding interaction between the ligand's hydroxyl group and the backbone amide at residue Arg122. Interestingly, increasing the length of the carbon chain from five to six carbons as in **12** abolished inhibitory activity, presumably through the disruption of this key bonding interaction. Analogs with the carboxyl group replaced with more hydrophobic alkane and alkyne substituents (see **13** – **17** in Table 1) displayed up to 70-fold greater *in vitro* potency against *SaBPL* over the alcohol derivative. Furthermore, the selectivity was improved for *SaBPL* by up to 25-fold over BirA and human BPL with biotin alkyne **16**. Again, the X-ray crystal structure of *SaBPL* in complex with biotin alkyne (**16**) showed the mode of binding was in the biotin-binding pocket and that the complex was stabilized through a hydrophobic interaction between the alkyne functional group and the sidechain of Trp127 in the biotin-binding loop (Fig. 11) [109]. This highly conserved tryptophan is the same residue required for the π - π stacking interaction with the adenine ring of ATP.

Surface plasmon resonance analysis has been employed to define the kinetics of inhibitor binding and extrapolate rates of ligand occupancy on the BPL target. The binding of biotin to *SaBPL* displays fast on and off rates. This is consistent with a two-step binding mechanism that has been reported for BirA [110] and shown in Eq 5:

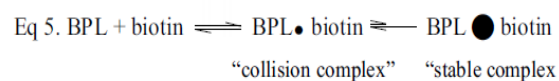
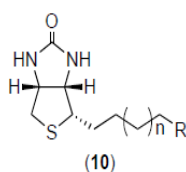


Table 1. Biotin Analog Series.



ID	N	R	K _i (μM)
11	2	OH	<i>Sa</i> 3.4 <i>Ec</i> 4.0 <i>Hs</i> 9.0
12	3	OH	<i>Sa</i> >20 <i>Ec</i> >20 <i>Hs</i> >20
13	1	CH ₃	<i>Sa</i> 0.05 <i>Ec</i> 1.1 <i>Hs</i> 0.1
14	2	CH ₃	<i>Sa</i> 0.5 <i>Ec</i> 7.3 <i>Hs</i> 6.4
15	1	C=C	<i>Sa</i> 0.08 <i>Ec</i> 0.9 <i>Hs</i> 0.2
16	2	C=C	<i>Sa</i> 0.3 <i>Ec</i> 7.3 <i>Hs</i> 3.5
17	3	C=C	<i>Sa</i> 2.4 <i>Ec</i> 20 <i>Hs</i> 12

A SAR series was investigated based upon pharmacophore **10**. Compounds were assayed for inhibitory activity against BPLs from *S. aureus* (*Sa*), *E. coli* (*Ec*) and *Homo sapiens* (*Hs*). Data from [109].

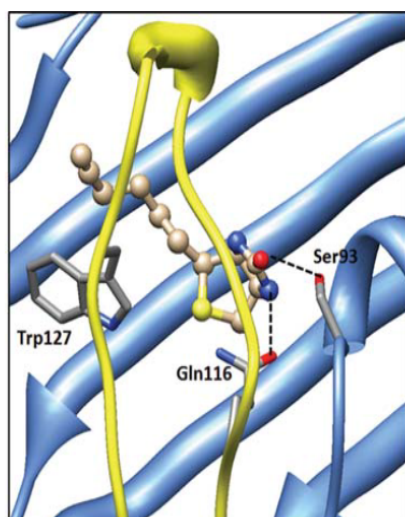


Fig. (11). Crystal structure of *S. aureus* BPL in complex with biotin alkyne (**16**). The catalytic domain of BPL (blue) and the biotin-binding loop (yellow) is shown with the ligand in ball and stick representation [109].

Initially BPL forms a “collision complex” with biotin, and this is followed by a slower conformational change that is both rate limiting and necessary to stabilize the enzyme-biotin complex. The alcohol derivative **11** showed similar binding kinetics to **1** consistent with a dynamic equilibrium between the free enzyme and collision complex, but unable to form a stable complex [109]. However, the alkane **13** and alkyne **15** analogs exhibited significantly slower association and dissociation kinetics which is in agreement with the proposal that these inhibitors are effective in inducing the slow conformational change necessary to stabilize the enzyme-ligand complex [109]. This work highlighted the key role of conformational change in anchoring inhibitors within the BPL active site. Often compounds that form a long-lived complex with their biological target are considered ideal for antibacterial discovery [111]. Consistently, the most potent inhibitors that display slow dissociation kinetics from the *Sa*BPL active site, biotin alkane **13** and alkyne **15**, also displayed bacteriostatic activity against *S. aureus*. Methicillin-sensitive ($n = 8$) and resistant strains ($n = 8$) had MIC₅₀ values of 8 μg/ml for both **13** and **15**, and greater potency against coagulase negative *Staphylococci* ($n = 7$; MIC 2 μg/ml for **13**, 4 μg/ml for **15**) [109]. Compound **15** was also an inhibitor of *E. coli* K12 (MIC 32 μg/ml). Recombinant overexpression of BPL in *E. coli* induced resistance to **15**, thereby establishing that the mechanism of action was indeed *via* inhibition of BPL [109]. Importantly the metabolic activity of mammalian HepG2 cells grown in culture was unaffected when grown in the presence of 64 μg/ml of compounds **13** - **17**, suggesting a lack of general toxicity. This study highlights that biotin analogs represent one route for the design of new BPL inhibitors.

4.2. BPL Reaction Intermediate Analogs as Antibacterial Agents

The first step of the BPL reaction is to catalyze the formation of the acyl-adenylate intermediate **2**. The reaction is related to that of aminoacyl-tRNA synthetases and lipoyl ligases, where an adenylated intermediate is also employed. A comparison of available X-ray crystallographic structures, together with the conserved reaction mechanism, suggests these enzymes share a common ancestor [112, 113]. Studies targeting aminoacyl-tRNA synthetases provided initial proof of concept that replacement of the labile phosphoanhydride linker shared in **2** can be substituted with more stable bioisosteres. This approach provides a route to the design of small molecule inhibitors targeting enzymes that employ an acyl-adenylate intermediate [114-120]. Several recent studies have applied this strategy to the design of novel BPL inhibitors.

Brown *et al* synthesized two stable analogs of the BPL reaction intermediate, biotinol-5'-AMP (**3**) and a sulfamoyl analog (see **18** in Fig. 12) [121]. BirA was crystallized in complex with **3**, thereby providing the first molecular details of both the biotin and nucleotide-binding sites [121]. The sulfamoyl analog was chemically unstable and readily decomposed [28]. Recently, a sulfamide analog **19** (Fig. 12), with greater stability than **18**, was prepared to target the BPL from *M. tuberculosis* [28]. *M. tuberculosis* BPL is an example of a class I BPL in that it only catalyzes post-translational protein biotinylation [122]. Importantly, **19** was

a competitive inhibitor against biotin and bound *M. tuberculosis* BPL with 1700-fold higher affinity than biotin, **19** also displayed anti-mycobacterial activity against the laboratory virulent strain *M. tuberculosis* H37Rv as well as a number of multi-drug resistant and extensively-drug resistant *M. tuberculosis* strains (MIC 0.625 – 0.16 $\mu\text{g/ml}$). **19** was inactive against Gram-negative *Acinetobacter baumannii*, *Klebsiella pneumoniae*, *E. coli* and *Pseudomonas aeruginosa*, Gram-positive *Enterococcus faecalis* and *S. aureus* and fungi *Candida albicans* and *Cryptococcus neoformans*. Treatment of *M. tuberculosis* H37Rv with **19** resulted in decreased levels of protein biotinylation consistent with reduced BPL activity. Furthermore, the mechanism of action *via* the BPL target was demonstrated by the construction of *M. smegmatis* strains that over-expressed BPL to varying extents resulting in increased resistance to **19**. Although the *in vitro* activity of **19** against human BPL was not assessed in this study, cytotoxicity was observed in Vero cells suggesting potential issues with selectivity for the bacterial BPL over the human homolog.

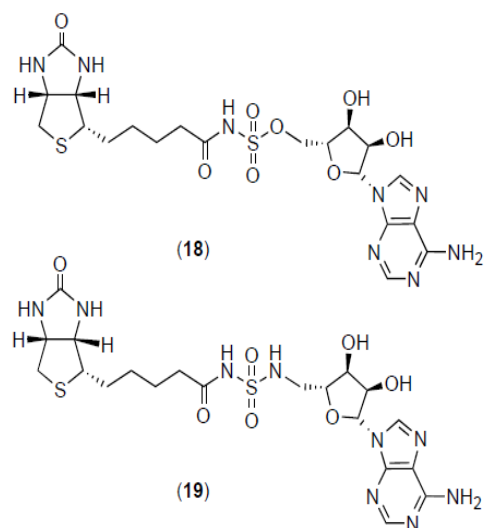
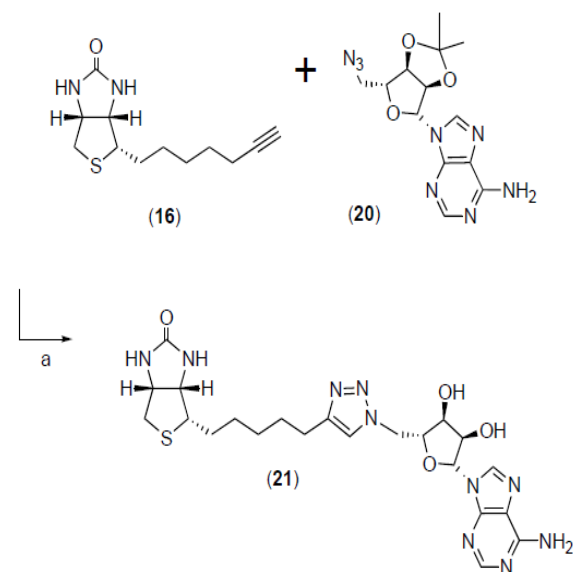


Fig. (12). Chemical structures of BPL reaction intermediate analogues.

In an attempt to improve selectivity, Soares da Costa *et al.* selected a 1,2,3-triazole as an alternative bioisostere for the labile phosphoanhydride in **2** [108]. The 1,2,3-triazole linker can be readily synthesized from an azide and alkyne using the Huisgen cycloaddition reaction under chemically benign conditions [123, 124]. Other desirable properties of the 1,2,3-triazole motif include three potential hydrogen bond acceptor sites and the ability to participate in π - π stacking interactions. The triazole linker is also stable to acid/base hydrolysis as well as severe oxidative/reductive conditions, making it resistant to metabolic degradation [125]. In the study by Soares da Costa *et al.*, a series of the biotin triazoles was synthesized and tested for inhibitory activity against *S. aureus* and human BPLs [108]. The reaction of biotin alkyne **16** and adenosine azide **20** in the presence of copper nanopowder followed by acid removal of the isopropylidene diol-protecting group gave the 1,4-disubstituted triazole **21** (Scheme 2). Triazole **21** exhibited inhibitory activity against *Sa*BPL ($K_i = 1.2 \mu\text{M}$) but was devoid of activity against the human BPL *in vitro*, thereby providing the first example of a

selective BPL inhibitor. Furthermore, **21** showed no toxicity against mammalian HepG2 cells in culture when the compound was included in the growth media at 64 $\mu\text{g/ml}$.



Scheme (2). Synthesis of biotin 1,4-triazole **21** from biotin alkyne **16** and azide **20**. Conditions and reagents: a, (i) copper nanopowder, 2:1 MeCN/H₂O, 35 °C; (ii) 90% TFA (aq), dichloromethane (CH₂Cl₂).

A library of biotin triazole derivatives was synthesized and assayed to further define the chemical features necessary for inhibitory activity. The presence of the isopropylidene diol protecting group had no significant effect on inhibition (see **22** in Fig. 13, $K_i = 1.8 \mu\text{M}$) suggesting the 2',3' diol was not required for binding. In fact, biotin triazole **23** (Fig. 13) that lacks the ribose group was a more potent inhibitor with a K_i of 0.7 μM [126]. The 1,5 triazole isomer **24**, prepared *via* an alternative route using a ruthenium catalyst in place of copper(I) [127], was devoid of inhibitory activity. This finding demonstrated that the 1,4 triazole bioisostere is optimal for mimicking the appropriate V-shaped geometry that is imparted by the phosphoanhydride linker in the native reaction intermediate **2**. Furthermore, removal (**25**) or addition (**26**) of a single methyl group in the hydrocarbon chain connecting biotin to the triazole in **22** abolished inhibitory activity. X-ray crystal structures of *Sa*BPL in complex with biotin triazole **22** confirmed the inhibitor's mode of binding and highlighted the importance of precisely positioning the bioisostere in the inhibitor [108]. As expected, the 1,4-disubstituted biotin triazoles adopted the same V-shaped geometry in the enzyme's active site as the native intermediate **2** [81]. The 1,2,3-triazole ring contributes to binding *via* an edge-tilted-T shape interaction with Trp127. The interaction is further stabilized by hydrogen bonding interactions involving the 2' nitrogen with the guanidinium side-chain of Arg125, the 3' nitrogen with the backbone amide of Arg122 and the C5 proton with the carboxylate side chain of Asp180 (Fig. 14). Mutagenesis studies performed upon *Sa*BPL addressed the mechanism of selective inhibition towards the bacterial enzyme over the human equivalent [108]. Arg125 was substituted with asparagine, the equivalent residue in the human BPL. The inhibitory activity of biotin triazole **22** was

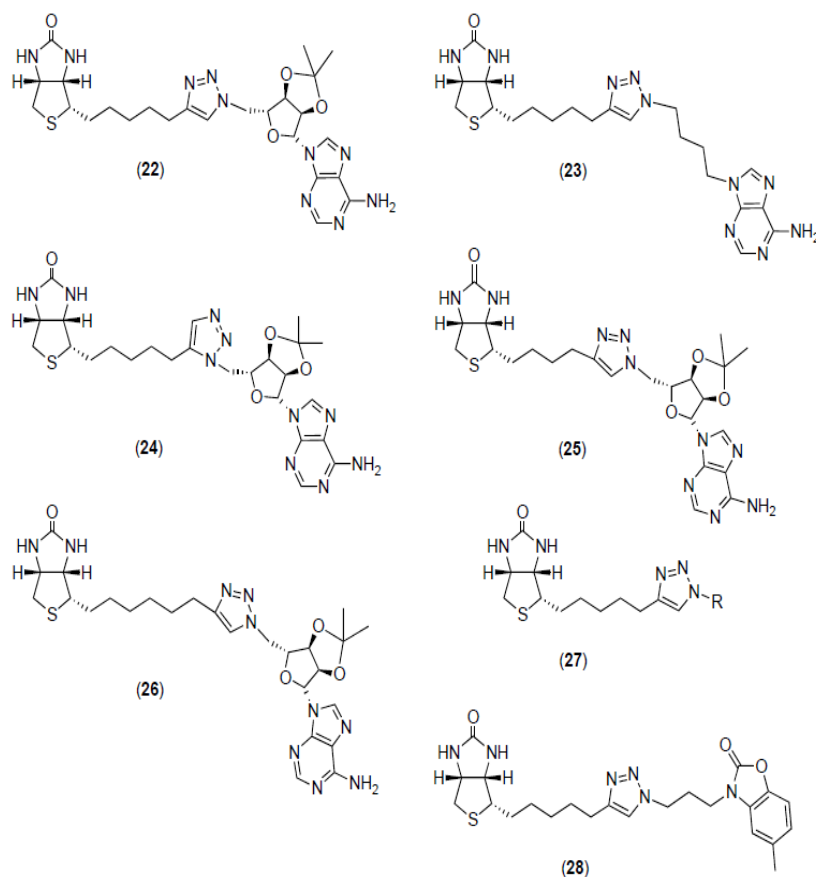


Fig. (13). Chemical structures of biotin triazoles.

abolished in the mutant *Sa*BPL, highlighting that Arg125 plays a key role in the selective binding of the biotin triazoles. The findings from this study provided the first proof of concept that the BPL from *S. aureus* can be selectively inhibited over the human BPL.

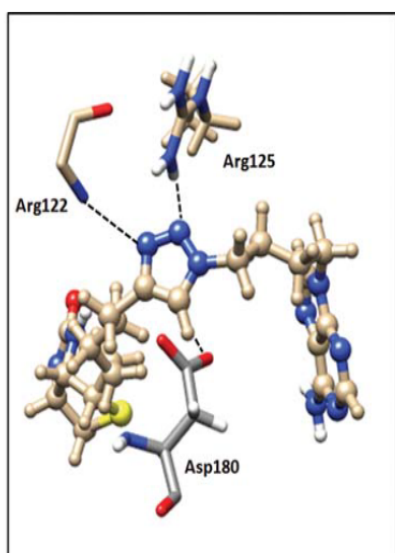


Fig. (14). Hydrogen bonding interactions with biotin triazole. Crystal structure of *S.aureus* BPL in complex with biotin triazole 23. Amino acid residues involved in hydrogen bonds with the 1,2,3, triazole heterocycle are shown (black dashed lines). Biotin triazole 23 is shown in ball and stick representation. PDB 3V7R [108].

4.3. Targeting the ATP Binding Site

The conserved nature of the biotin-binding pocket limits the opportunity to design selective inhibitors that occupy this site. However, a comparison of the *Sa*BPL crystal structure with other available BPL structures, as well as a model for the human BPL [92], revealed that the amino acid residues within the ATP binding pocket show greater divergence between species. For example, there are five amino acid residues encompassing the ATP binding pocket of *Sa*BPL that are not conserved in the human BPL, namely His126, Ser128, Glu215 and Arg227, as well as Phe220 in the hydrophobic adenylate-binding loop (Fig. 15) [108]. Hence, targeting the ATP binding pocket was anticipated to provide opportunities for greater selective inhibition and increased potency. Surface plasmon resonance experiments confirmed that *Sa*BPL undergoes catalysis using an ordered reaction mechanism [108]. Therefore the enzyme must bind biotin, or a biotin analog, in order to induce the conformational change necessary to form the ATP-binding pocket. Hence, a number of adenosine analogs were incorporated into the inhibitor design as represented by the biotin triazole pharmacophore 27 (Fig. 13). A series of azides was prepared and reacted with biotin alkyne 15 under the Huisgen cycloaddition conditions to generate a library of biotin triazoles to explore the ATP binding pocket. Based on these studies, biotin triazole 28 (Fig. 13) with a 2-benzoxazolone moiety was identified as the most potent compound with a K_i of $0.09 \pm 0.02 \mu\text{M}$ against *Sa*BPL [108]. Again, none of biotin triazoles showed inhibitory activity against human BPL in the *in vitro* biotin-

lation assay. Noteworthy is that **28** exhibited >1100-fold selectivity over the human isoform and represents the most selective inhibitor identified to date. As the concentration of inhibitor that could be included in the aqueous BPL reaction mixture was solubility-limited at $\approx 200 \mu\text{M}$, at which point no inhibitory activity was measured against human BPL, we expect the actual difference in affinity to be much larger than three orders of magnitude reported. Bacteriostatic activity was observed against *S. aureus* ATCC strain 49775 for **28** at $8 \mu\text{g/mL}$ where it reduced bacterial growth by 80% [108]. None of the biotin triazoles showed any toxicity in a cell culture model using HepG2 cells, making them useful hits for further antibacterial discovery.

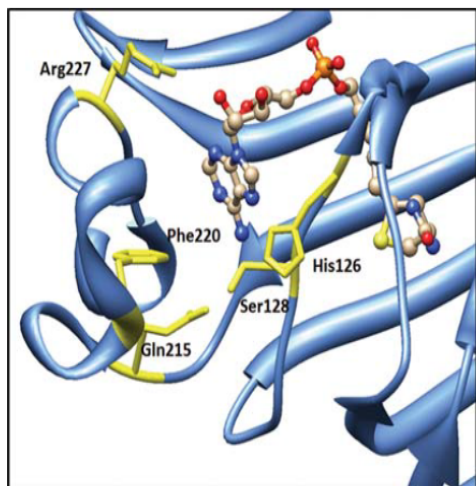


Fig. (15). Divergence in the ATP-binding site. Amino acid residues that are not conserved between *S. aureus* and human BPL are shown in yellow. Biotinol-5'-AMP 3 is in ball and stick representation. PDB 4DQ2 [108].

4.4. *In Situ* Click Chemistry as an Alternative Approach to Discover BPL Inhibitors

An *in situ* click approach has also been investigated as a means to optimize the biotin triazole series. Here the BPL is used as a template to identify and bind the optimum azide and alkyne partners from a library of such structures. Once bound in the appropriate pockets a cycloaddition reaction occurs in the absence of copper to give the triazole inhibitor. The Huisgen cycloaddition reaction is ideal for this target guided *in situ* synthesis as the reactants are inert to biological molecules and the 'click chemistry' reaction is compatible in biological buffers [128-130]. Furthermore, as the biological target is capable of selecting its most potent inhibitor from a library of precursors, this approach circumvents the need to individually synthesize and assay all possible triazole combinations thus greatly facilitating the discovery of new hits.

Soares da Costa *et al.* previously demonstrated that *SaBPL* can be selectively inhibited by the biotin triazoles [108]. Furthermore, the biotin and ATP binding pockets are juxtaposed in the X-ray crystal structure making BPL an appropriate candidate for *in situ* click chemistry [81]. In the first instance, biotin alkyne **16** and adenosine azide **20** were reacted with wild type *SaBPL* to give 1.07 ± 0.1 mol of triazole formed per mol of enzyme [126]. Next alkyne **16** and a small library of azides were screened against wildtype *SaBPL* in order to detect the most potent inhibitors synthe-

sized by the enzyme. However, triazole products could not be detected above the background level by standard HPLC or mass spectrometry techniques. One of the limitations of *in situ* click chemistry is that it can be difficult to detect the formation of tightly bound inhibitors due to the resulting compound having high affinity for the target enzyme, thereby occupying the active site and preventing multiple rounds of catalysis (Fig. 16A). In order to overcome this limitation, improving the catalytic efficiency of *SaBPL* was investigated.

As described earlier, the biotin-binding loop folds over the active site to prevent diffusion of **2** from the active site. In *SaBPL*, the loop is stabilized through key interactions involving the side-chain of Arg122 in the Gly-Arg-Gly-Arg¹²²-X motif (*SaBPL* numbering). The guanidinium sidechain of Arg122 forms a network of hydrogen bonding interactions with amino acid residues in the *SaBPL* dimer interface, including the backbone hydroxyl at Asp320 on the same subunit and the side-chain of Asp200 on the opposing subunit (Fig. 17). Therefore, in the study by Tieu *et al.*, Arg122 was targeted for mutagenesis studies in order to encourage diffusion of the triazole inhibitors from the enzyme, and enhance the enzyme's turnover rate (Fig. 16B) [126]. Binding studies by surface plasmon resonance and enzyme kinetic analysis performed upon wildtype and mutant *SaBPL* revealed that the affinities for both biotin and MgATP were unaffected by the amino acid substitution Arg122-Gly. Circular dichroism analysis also indicated that the amino acid substitution did not impose any significant structural changes to the secondary structure of the enzyme. Furthermore, the Arg122-Gly mutant was also able to promiscuously biotinylate non-target bacterial proteins when recombinantly expressed in *E. coli* implying that the Arg122-Gly mutant did indeed exhibit the desirable 'leaky' phenotype observed previously with the BirA Arg118-Gly mutant [83, 85]. Hence, the mutant protein possessed all the properties to be a good surrogate template for the wildtype enzyme.

The *in situ* click reaction of alkyne **16** and azide **20** (Scheme 2) with *SaBPL* Arg122-Gly gave significantly improved formation of the triazole product than the wildtype enzyme, yielding 11.9 ± 0.7 moles of triazole per mol of enzyme [126]. This experiment demonstrated that the Arg122-Gly mutant performed multiple rounds of catalysis, thereby enhancing the sensitivity of detection of the triazole product by both HPLC and mass spectrometry. The library screening experiment involving alkyne **16** and a series of azides was repeated using the Arg122-Gly mutant. Analysis of the product mixture indicated efficient formation of the 1,4 triazole **23** as well as lesser quantities of **22**. The 10 possible biotin triazole products were independently synthesized and assayed against *SaBPL* to confirm that the *SaBPL* Arg122-Gly mutant had indeed selected and assembled the most potent inhibitors. Each compound was tested using an *in vitro* biotinylation assay with triazole **23** being identified as the most potent ($K_i = 0.7 \mu\text{M}$), consistent with previous studies [108]. A second *in situ* click chemistry reaction was performed with either wildtype or mutant *SaBPL* with alkyne **16** and the 2-benzoxazolone azide precursor required to synthesize potent inhibitor **28**, described earlier. Again, the *SaBPL* Arg122-Gly mutant was effective in catalyzing the

formation of biotin triazole **28** while the wildtype enzyme was not. This study highlights that *Sa*BPL is an appropriate candidate for *in situ* click chemistry as it was able to select the appropriate azide and alkyne and catalyze the synthesis of its most potent inhibitor. The *in situ* click chemistry technology can be used as an alternative approach to discover BPL inhibitors, where a library of azides and alkynes can be screened and assembled by the BPL itself, followed by subsequent testing for inhibitor potency.

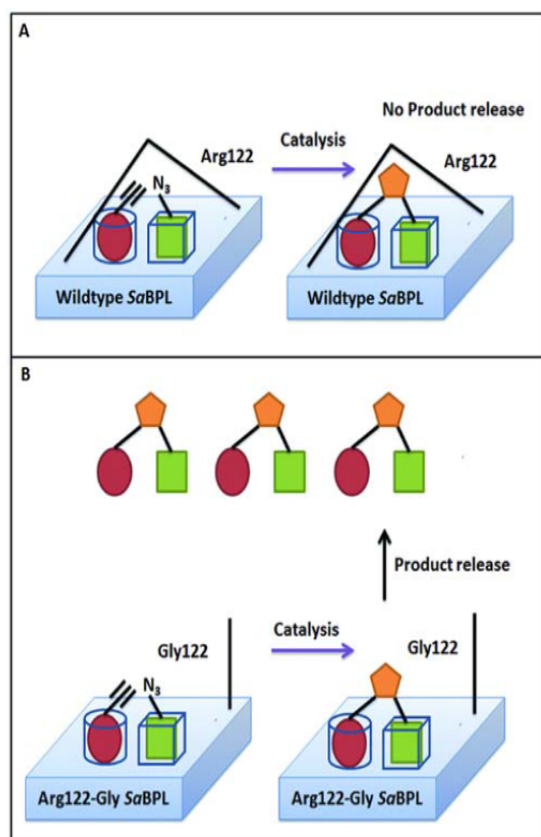


Fig. (16). Schematic diagram of *in situ* click reaction performed by *S.aureus* BPL. (A) Wildtype *Sa*BPL. Biotin acetylene (**16**, red circle) and an azide partner (green square) bind to the target and induce the biotin-binding loop over the active site. Following synthesis of the 1,2,3 triazole (orange pentagon) the product is not released. (B) Arg122-Gly mutant *Sa*BPL. The biotin-binding loop is not stabilized over the active site, allowing products to diffuse from the enzyme and facilitating multiple rounds of catalysis and increased product synthesis.

CONCLUSION

The constant threat to human health posed by antibiotic resistance is the driver that demands that we must continue to develop new chemotherapeutic agents. The discovery of novel classes of antibacterials with new modes of action provides one strategy to combat drug resistance. Many of the obvious drug targets without a human equivalent have now been extensively investigated. Essential metabolic enzymes that have a close human homolog need to be considered. This approach requires that small molecule inhibitors bind with exquisite specificity to their bacterial target. BPL repre-

sents one such promising example that is not the target of any current drugs in clinical use. Through the discovery of the biotin triazole series, we provide proof of principle that *Sa*BPL can be selectively inhibited with >1100-fold difference in affinity over human BPL. In this example, the labile phosphoanhydride linker in the BPL reaction intermediate was replaced with a 1,2,3-triazole. Whilst alternative bios-teres have been reported, the number is relatively low and further exemplars should be considered. Here the X-ray crystal structure of BPL from *S. aureus* will aid in the design of new derivative with greater potency and selectivity. The biotin triazole **27** provides a pharmacophore for further chemical optimization. Through the addition of functional groups at position R on the pharmacophore, the compound can be grown such that it can occupy the nucleotide-binding pocket. Here the divergence observed in the amino acids that contribute to this pocket between bacteria and human BPLs can be exploited for greater selectivity. Currently, an X-ray crystal structure of the human enzyme to aid in inhibitor design has not been reported. This would be a valuable tool to aid in the development of new inhibitors against the BPL from *S. aureus*, as well as the BPLs of other clinically important bacteria and fungi.

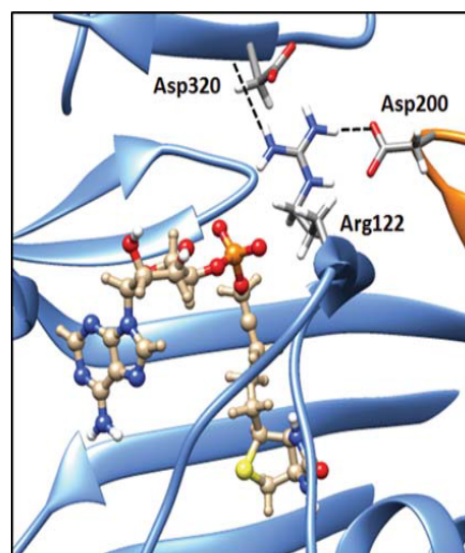


Fig. (17). Hydrogen-bonding interactions involving Arg122. *S.aureus* BPL in complex with **3** (shown in ball and stick representation) and hydrogen bonding interactions involving Arg122 are shown. One subunit of the protein dimer is blue, whilst the second subunit is orange. PDB 4DQ2 [108].

CONFLICT OF INTEREST

The author(s) confirm that this article content has no conflicts of interest.

ACKNOWLEDGEMENTS

This work was supported by the National Health and Medical Research Council of Australia (application 1011806), the Centre for Molecular Pathology, University of Adelaide, and Adelaide Research and Innovation's Commercial Accelerator Scheme. MCJW is an Australian NHMRC Senior Research Fellow.

LIST OF ABBREVIATIONS

ACC	=	Acetyl CoA carboxylase
BirA	=	Biotin retention protein A from <i>Escherichia coli</i>
BPL	=	Biotin protein ligase
MIC	=	Minimal inhibitory constant
MRSA	=	Methicillin resistant <i>S. aureus</i>
PC	=	Pyruvate carboxylase
SaBPL	=	Biotin protein ligase from <i>S. aureus</i>

REFERENCES

- [1] Boucher, H. W.; Talbot, G. H.; Bradley, J. S.; Edwards, J. E.; Gilbert, D.; Rice, L. B.; Scheld, M.; Spellberg, B.; Bartlett, J. Bad bugs, no drugs: no ESKAPE! An update from the Infectious Diseases Society of America. *Clin. Infect. Dis.*, **2009**, *48*(1), 1-12.
- [2] Lewis, K. Antibiotics: Recover the lost art of drug discovery. *Nature*, **2012**, *485*(7399), 439-40.
- [3] Cooper, M. A.; Shlaes, D. Fix the antibiotics pipeline. *Nature*, **2011**, *472*(7341), 32.
- [4] Butler, M. S.; Cooper, M. A. Antibiotics in the clinical pipeline in 2011. *J. Antibiot. (Tokyo)*, **2011**, *64*(6), 413-25.
- [5] Coates, A. R.; Halls, G. Antibiotics in phase II and III clinical trials. *Handb. Exp. Pharmacol.*, **2012**, *211*, 167-83.
- [6] Fischbach, M. A.; Walsh, C. T. Antibiotics for emerging pathogens. *Science*, **2009**, *325*(5944), 1089-93.
- [7] Lewis, K. Platforms for antibiotic discovery. *Nat. Rev. Drug Discov.*, **2013**, *12*(5), 371-87.
- [8] Payne, D. J.; Gwynn, M. N.; Holmes, D. J.; Pompliano, D. L. Drugs for bad bugs: confronting the challenges of antibacterial discovery. *Nat. Rev. Drug Discov.*, **2007**, *6*(1), 29-40.
- [9] Archer, G. L. *Staphylococcus aureus*: a well-armed pathogen. *Clin. Infect. Dis.*, **1998**, *26*(5), 1179-81.
- [10] Grundmann, H.; Aires-de-Sousa, M.; Boyce, J.; Tiemersma, E. Emergence and resurgence of methicillin-resistant *Staphylococcus aureus* as a public-health threat. *Lancet*, **2006**, *368*(9538), 874-85.
- [11] Weidenmaier, C.; Goerke, C.; Wolz, C. *Staphylococcus aureus* determinants for nasal colonization. *Trends Microbiol.*, **2012**, *20*(5), 243-50.
- [12] Lowy, F. D. *Staphylococcus aureus* infections. *N. Engl. J. Med.*, **1998**, *339*(8), 520-32.
- [13] Tong, S. Y.; Chen, L. F.; Fowler, V. G., Jr. Colonization, pathogenicity, host susceptibility, and therapeutics for *Staphylococcus aureus*: what is the clinical relevance? *Semin. Immunopathol.*, **2012**, *34*(2), 185-200.
- [14] Chambers, H. F. Methicillin-resistant staphylococci. *Clin. Microbiol. Rev.*, **1988**, *1*(2), 173-86.
- [15] Otto, M. Community-associated MRSA: What makes them special? *Int. J. Med. Microbiol.*, **2013**, *303*(6-7), 324-330.
- [16] Sievert, D. M.; Ricks, P.; Edwards, J. R.; Schneider, A.; Patel, J.; Srinivasan, A.; Kallen, A.; Limbago, B.; Fridkin, S. Antimicrobial-resistant pathogens associated with healthcare-associated infections: summary of data reported to the National Healthcare Safety Network at the Centers for Disease Control and Prevention, 2009-2010. *Infect. Control Hosp. Epidemiol.*, **2013**, *34*(1), 1-14.
- [17] de Kraker, M. E.; Davey, P. G.; Grundmann, H. Mortality and hospital stay associated with resistant *Staphylococcus aureus* and *Escherichia coli* bacteremia: estimating the burden of antibiotic resistance in Europe. *PLoS Med.*, **2011**, *8*(10), e1001104.
- [18] de Kraker, M. E.; Wolkewitz, M.; Davey, P. G.; Koller, W.; Berger, J.; Nagler, J.; Ickert, C.; Kalenic, S.; Horvatic, J.; Seifert, H.; Kaasch, A. J.; Paniara, O.; Argyropoulou, A.; Bompola, M.; Smyth, E.; Skally, M.; Raglio, A.; Dumpis, U.; Kelmere, A. M.; Borg, M.; Xuereb, D.; Ghita, M. C.; Noble, M.; Kolman, J.; Grabljevec, S.; Tumer, D.; Lansbury, L.; Grundmann, H. Clinical impact of antimicrobial resistance in European hospitals: excess mortality and length of hospital stay related to methicillin-resistant *Staphylococcus aureus* bloodstream infections. *Antimicrob. Agents Chemother.*, **2011**, *55*(4), 1598-605.
- [19] Holmes, N. E.; Turnidge, J. D.; Munchhof, W. J.; Robinson, J. O.; Komman, T. M.; O'Sullivan, M. V.; Anderson, T. L.; Roberts, S. A.; Gao, W.; Christiansen, K. J.; Coombs, G. W.; Johnson, P. D.; Howden, B. P. Antibiotic choice may not explain poorer outcomes in patients with *Staphylococcus aureus* bacteremia and high vancomycin minimum inhibitory concentrations. *J. Infect. Dis.*, **2011**, *204*(3), 340-7.
- [20] Tumidge, J. D.; Kotsanas, D.; Munchhof, W.; Roberts, S.; Bennett, C. M.; Nimmo, G. R.; Coombs, G. W.; Murray, R. J.; Howden, B.; Johnson, P. D.; Dowling, K. *Staphylococcus aureus* bacteraemia: a major cause of mortality in Australia and New Zealand. *Med. J. Aust.*, **2009**, *191*(7), 368-73.
- [21] Nimmo, G. R.; Coombs, G. W.; Pearson, J. C.; O'Brien, F. G.; Christiansen, K. J.; Tumidge, J. D.; Gosbell, I. B.; Collignon, P.; McLaws, M. L. Methicillin-resistant *Staphylococcus aureus* in the Australian community: an evolving epidemic. *Med. J. Aust.*, **2006**, *184*(8), 384-8.
- [22] Weigel, L. M.; Clewell, D. B.; Gill, S. R.; Clark, N. C.; McDougal, L. K.; Flannagan, S. E.; Kolonay, J. F.; Shetty, J.; Killgore, G. E.; Tenover, F. C. Genetic analysis of a high-level vancomycin-resistant isolate of *Staphylococcus aureus*. *Science*, **2003**, *302*(5650), 1569-71.
- [23] Klein, E.; Smith, D. L.; Laxminarayan, R. Hospitalizations and deaths caused by methicillin-resistant *Staphylococcus aureus*, United States, 1999-2005. *Emerg. Infect. Dis.*, **2007**, *13*(12), 1840-6.
- [24] Forsyth, R. A.; Haselbeck, R. J.; Ohlsen, K. L.; Yamamoto, R. T.; Xu, H.; Trawick, J. D.; Wall, D.; Wang, L.; Brown-Driver, V.; Froelich, J. M.; Keder, G. C.; King, P.; McCarthy, M.; Malone, C.; Misiner, B.; Robbins, D.; Tan, Z.; Zhu Zy, Z. Y.; Carr, G.; Mosca, D. A.; Zamudio, C.; Foulkes, J. G.; Zyskind, J. W. A genome-wide strategy for the identification of essential genes in *Staphylococcus aureus*. *Mol. Microbiol.*, **2002**, *43*(6), 1387-400.
- [25] Barker, D. F.; Campbell, A. M. Genetic and biochemical characterisation of the birA gene and its product: Evidence for a direct role of biotin holoenzyme synthetase in repression of the biotin operon in *Escherichia coli*. *J. Mol. Biol.*, **1981**, *146*, 469-492.
- [26] Chapman-Smith, A.; Turner, D. L.; Cronan, J. E.; Morris, T. W.; Wallace, J. C. Expression, biotinylation and purification of a biotin-domain peptide from the biotin carboxy carrier protein of *Escherichia coli* acetyl-CoA carboxylase. *Biochem. J.*, **1994**, *302*(3), 881-887.
- [27] Gerdes, S. Y.; Scholle, M. D.; Campbell, J. W.; Balazsi, G.; Ravasz, E.; Daugherty, M. D.; Somera, A. L.; Kyrpidis, N. C.; Anderson, I.; Gelfand, M. S.; Bhattacharya, A.; Kapatal, V.; D'Souza, M.; Baev, M. V.; Grechkin, Y.; Mseeh, F.; Fonstein, M. Y.; Overbeek, R.; Barabasi, A. L.; Oltvai, Z. N.; Osterman, A. L. Experimental determination and system level analysis of essential genes in *Escherichia coli* MG1655. *J. Bacteriol.*, **2003**, *185*(19), 5673-84.
- [28] Duckworth, B. P.; Geders, T. W.; Tiwari, D.; Boshoff, H. I.; Sibbald, P. A.; Barry, C. E., 3rd; Schnappinger, D.; Finzel, B. C.; Aldrich, C. C. Bisubstrate adenylation inhibitors of biotin protein ligase from *Mycobacterium tuberculosis*. *Chem. Biol.*, **2011**, *18*(11), 1432-41.
- [29] Thanassi, J. A.; Hartman-Neumann, S. L.; Dougherty, T. J.; Dougherty, B. A.; Pucci, M. J. Identification of 113 conserved essential genes using a high-throughput gene disruption system in *Streptococcus pneumoniae*. *Nucleic Acids Res.*, **2002**, *30*(14), 3152-62.
- [30] Polyak, S. W.; Bailey, L. M.; Azhar, A.; Booker, G. W. Biotin (Vitamin H or B7). In *Micronutrients: Sources, properties and health benefits*. Eds Betancourt, A. I.; Gaitan, H. F. Nova Science Publishers: New York, USA., **2012**; pp 65 - 94.
- [31] Waldrop, G. L.; Holden, H. M.; St Maurice, M. The enzymes of biotin dependent CO(2) metabolism: what structures reveal about their reaction mechanisms. *Protein Sci.*, **2012**, *21*(11), 1597-619.
- [32] St Maurice, M.; Reinhardt, L.; Surinya, K. H.; Attwood, P. V.; Wallace, J. C.; Cleland, W. W.; Rayment, I. Domain architecture of pyruvate carboxylase, a biotin-dependent multifunctional enzyme. *Science*, **2007**, *317*(5841), 1076-9.
- [33] Tong, L. Structure and function of biotin-dependent carboxylases. *Cell. Mol. Life Sci.*, **2013**, *70*(5), 863-91.
- [34] Attwood, P. V. The structure and mechanism of action of pyruvate carboxylase. *Int. J. Biochem. Cell Biol.*, **1995**, *27*, 231-249.
- [35] Cronan, J. E., Jr.; Waldrop, G. L. Multi-subunit acetyl-CoA carboxylases. *Prog. Lipid Res.*, **2002**, *41*(5), 407-35.

- [36] White, S. W.; Zheng, J.; Zhang, Y. M.; Rock The structural biology of type II fatty acid biosynthesis. *Annu. Rev. Biochem.*, **2005**, *74*, 791-831.
- [37] Campbell, J. W.; Cronan, J. E., Jr. Bacterial fatty acid biosynthesis: targets for antibacterial drug discovery. *Annu. Rev. Microbiol.*, **2001**, *55*, 305-32.
- [38] Polyak, S. W.; Abell, A. D.; Wilce, M. C.; Zhang, L.; Booker, G. W. Structure, function and selective inhibition of bacterial acetyl-CoA carboxylase. *Appl. Microbiol. Biotechnol.*, **2012**, *93*(3), 983-92.
- [39] Wright, H. T.; Reynolds, K. A. Antibacterial targets in fatty acid biosynthesis. *Curr. Opin. Microbiol.*, **2007**, *10*(5), 447-53.
- [40] Parsons, J. B.; Rock, C. O. Is bacterial fatty acid synthesis a valid target for antibacterial drug discovery? *Curr. Opin. Microbiol.*, **2011**, *14*(5), 544-9.
- [41] Raetz, C. R.; Reynolds, C. M.; Trent, M. S.; Bishop, R. E. Lipid A modification systems in Gram-negative bacteria. *Annu. Rev. Biochem.*, **2007**, *76*, 295-329.
- [42] Brinster, S.; Lamberet, G.; Staels, B.; Trieu-Cuot, P.; Gruss, A.; Poyart, C. Type II fatty acid synthesis is not a suitable antibiotic target for Gram-positive pathogens. *Nature*, **2009**, *458*(7234), 83-6.
- [43] Balemans, W.; Lounis, N.; Gilissen, R.; Guillemont, J.; Simmen, K.; Andries, K.; Koul, A. Essentiality of FASII pathway for *Staphylococcus aureus*. *Nature*, **2010**, *463*(7279), E3-4.
- [44] Brinster, S.; Lamberet, G.; Staels, B.; Trieu-Cuot, P.; Gruss, A.; Poyart, C. Brinster et al. reply. *Nature*, **2010**, *463*(E4-E4).
- [45] Parsons, J. B.; Frank, M. W.; Subramanian, C.; Saenkham, P.; Rock, C. O. Metabolic basis for the differential susceptibility of Gram-positive pathogens to fatty acid synthesis inhibitors. *Proc. Natl. Acad. Sci. U S A*, **2011**, *108*(37), 15378-83.
- [46] Payne, D. J.; Miller, W. H.; Berry, V.; Brosky, J.; Burgess, W. J.; Chen, E.; DeWolf Jr, W. E., Jr.; Fosberry, A. P.; Greenwood, R.; Head, M. S.; Heering, D. A.; Janson, C. A.; Jaworski, D. D.; Keller, P. M.; Manley, P. J.; Moore, T. D.; Newlander, K. A.; Pearson, S.; Polizzi, B. J.; Qiu, X.; Rittenhouse, S. F.; Slater-Radosti, C.; Salyers, K. L.; Seefeld, M. A.; Smyth, M. G.; Takata, D. T.; Uzinskas, I. N.; Vaidya, K.; Wallis, N. G.; Winram, S. B.; Yuan, C. C.; Huffman, W. F. Discovery of a novel and potent class of FabI-directed antibacterial agents. *Antimicrob. Agents Chemother.*, **2002**, *46*(10), 3118-24.
- [47] Freiberg, C.; Brunner, N. A.; Schiffer, G.; Lampe, T.; Pohlmann, J.; Brands, M.; Raabe, M.; Habich, D.; Ziegelbauer, K. Identification and characterization of the first class of potent bacterial acetyl-CoA carboxylase inhibitors with antibacterial activity. *J. Biol. Chem.*, **2004**, *279*(25), 26066-73.
- [48] Miller, W. H.; Seefeld, M. A.; Newlander, K. A.; Uzinskas, I. N.; Burgess, W. J.; Heering, D. A.; Yuan, C. C.; Head, M. S.; Payne, D. J.; Rittenhouse, S. F.; Moore, T. D.; Pearson, S. C.; Berry, V.; DeWolf, W. E., Jr.; Keller, P. M.; Polizzi, B. J.; Qiu, X.; Janson, C. A.; Huffman, W. F. Discovery of aminopyridine-based inhibitors of bacterial enoyl-ACP reductase (FabI). *J. Med. Chem.*, **2002**, *45*(15), 3246-56.
- [49] Miller, J. R.; Dunham, S.; Mochalkin, I.; Banotai, C.; Bowman, M.; Buist, S.; Dunkle, B.; Hanna, D.; Harwood, H. J.; Huband, M. D.; Karnovsky, A.; Kuhn, M.; Limberakis, C.; Liu, J. Y.; Mehrens, S.; Mueller, W. T.; Narasimhan, L.; Ogen, A.; Ohren, J.; Prasad, J. V.; Shelly, J. A.; Skerlos, L.; Sulavik, M.; Thomas, V. H.; VanderRoest, S.; Wang, L.; Wang, Z.; Whitton, A.; Zhu, T.; Stover, C. K. A class of selective antibacterials derived from a protein kinase inhibitor pharmacophore. *Proc. Natl. Acad. Sci. U S A*, **2009**, *106*(6), 1737-42.
- [50] Wang, J.; Soisson, S. M.; Young, K.; Shoop, W.; Kodali, S.; Galgoci, A.; Painter, R.; Parthasarathy, G.; Tang, Y. S.; Cummings, R.; Ha, S.; Dorso, K.; Motyl, M.; Jayasuriya, H.; Ondeyka, J.; Herath, K.; Zhang, C.; Hernandez, L.; Alloco, J.; Basilio, A.; Tomo, J. R.; Genilloud, O.; Vicente, F.; Pelaez, F.; Colwell, L.; Lee, S. H.; Michael, B.; Felcetto, T.; Gill, C.; Silver, L. L.; Hermes, J. D.; Baritzal, K.; Barrett, J.; Schmatz, D.; Becker, J. W.; Cully, D.; Singh, S. B. Platensimycin is a selective FabF inhibitor with potent antibiotic properties. *Nature*, **2006**, *441*(7091), 358-61.
- [51] Jitrapakdee, S.; St Maurice, M.; Rayment, I.; Cleland, W. W.; Wallace, J. C.; Attwood, P. V. Structure, mechanism and regulation of pyruvate carboxylase. *Biochem. J.*, **2008**, *413*(3), 369-87.
- [52] Jitrapakdee, S.; Wallace, J. C. Structure, function and regulation of pyruvate carboxylase. *Biochem. J.*, **1999**, *340*(1), 1-16.
- [53] Somerville, G. A.; Proctor, R. A. At the crossroads of bacterial metabolism and virulence factor synthesis in *Staphylococci*. *Microbiol. Mol. Biol. Rev.*, **2009**, *73*(2), 233-48.
- [54] Sonenshein, A. L. Control of key metabolic intersections in *Bacillus subtilis*. *Nat. Rev. Microbiol.*, **2007**, *5*(12), 917-27.
- [55] Dunn, M. F. Tricarboxylic acid cycle and anaplerotic enzymes in rhizobia. *FEMS Microbiol. Rev.*, **1998**, *22*(2), 105-23.
- [56] Petersen, S.; de Graaf, A. A.; Eggeling, L.; Mollney, M.; Wiechert, W.; Sahm, H. In vivo quantification of parallel and bidirectional fluxes in the anaplerosis of *Corynebacterium glutamicum*. *J. Biol. Chem.*, **2000**, *275*(46), 35932-41.
- [57] Chaudhuri, R. R.; Allen, A. G.; Owen, P. J.; Shalom, G.; Stone, K.; Harrison, M.; Burgis, T. A.; Lockyer, M.; Garcia-Lara, J.; Foster, S. J.; Pleasance, S. J.; Peters, S. E.; Maskell, D. J.; Charles, I. G. Comprehensive identification of essential *Staphylococcus aureus* genes using Transposon-Mediated Differential Hybridisation (TMDH). *BMC Genomics*, **2009**, *10*, 291.
- [58] Bae, T.; Banger, A. K.; Wallace, A.; Glass, E. M.; Aslund, F.; Schneewind, O.; Missiakas, D. M. *Staphylococcus aureus* virulence genes identified by *Bursa aurealis* mutagenesis and nematode killing. *Proc. Natl. Acad. Sci. U S A*, **2004**, *101*(33), 12312-7.
- [59] Gretler, A. C.; Mucciolo, P.; Evans, J. B.; Niven, C. F. Vitamin nutrition of the *Staphylococci* with special reference to their biotin requirements. *J. Bacteriol.*, **1955**, *70*, 44-49.
- [60] Porter, J. R.; Pelczar, M. J., Jr. Biotin (Bios lib, Vitamin H)—an essential growth factor for certain staphylococci. *Science*, **1940**, *91*(2372), 576-577.
- [61] Hugo, W. B.; Davidson, J. R. Effect of cell lipid depletion in *Staphylococcus aureus* upon its resistance to antimicrobial agents I. Lipid depletion induced by biotin deficiency. *Microbios*, **1973**, *8*, 43-51.
- [62] Adekeye, J. D.; Coles, E. H. Effect of biotin deficiency on some properties of *Staphylococcus aureus* isolates from humans and other animals. *Infect. Immun.*, **1976**, *13*(2), 475-479.
- [63] Baltz, R. H. Daptomycin: mechanisms of action and resistance, and biosynthetic engineering. *Curr. Opin. Chem. Biol.*, **2009**, *13*(2), 144-51.
- [64] Fedtke, I.; Gotz, F.; Peschel, A. Bacterial evasion of innate host defenses—the *Staphylococcus aureus* lesson. *Int. J. Med. Microbiol.*, **2004**, *294*(2-3), 189-94.
- [65] Kraus, D.; Peschel, A. *Staphylococcus aureus* evasion of innate antimicrobial defense. *Future Microbiol.*, **2008**, *3*, 437-51.
- [66] Sahm, H.; Eggeling, L.; de Graaf, A. A. Pathway analysis and metabolic engineering in *Corynebacterium glutamicum*. *Biol. Chem.*, **2000**, *381*(9-10), 899-910.
- [67] Pfeifferle, W.; Mockel, B.; Bathe, B.; Marx, A. Biotechnological manufacture of lysine. *Adv. Biochem. Eng. Biotechnol.*, **2003**, *79*, 59-112.
- [68] Bagautdinov, B.; Kuroishi, C.; Sugahara, M.; Kunishima, N. Crystal structures of biotin protein ligase from *Pyrococcus horikoshii* OT3 and its complexes: structural basis of biotin activation. *J. Mol. Biol.*, **2005**, *353*(2), 322-33.
- [69] Bagautdinov, B.; Matsuura, Y.; Bagautdinova, S.; Kunishima, N. Protein biotinylation visualized by a complex structure of biotin protein ligase with a substrate. *J. Biol. Chem.*, **2008**, *283*(21), 14739-50.
- [70] Beckett, D. Biotin sensing at the molecular level. *J. Nutr.*, **2009**, *139*(1), 167-70.
- [71] Campeau, E.; Gravel, R. A. Expression in *Escherichia coli* of N- and C-terminally deleted human holocarboxylase synthetase. Influence of the N-terminus on biotinylation and identification of a minimum functional protein. *J. Biol. Chem.*, **2001**, *276*(15), 12310-6.
- [72] Mayende, L.; Swift, R. D.; Bailey, L. M.; Soares da Costa, T. P.; Wallace, J. C.; Booker, G. W.; Polyak, S. W. A novel molecular mechanism to explain biotin-unresponsive holocarboxylase synthetase deficiency. *J. Mol. Med.*, **2012**, *90*(1), 81-8.
- [73] Pendini, N. R.; Bailey, L. M.; Booker, G. W.; Wilce, M. C.; Wallace, J. C.; Polyak, S. W. Biotin protein ligase from *Candida albicans*: expression, purification and development of a novel assay. *Arch. Biochem. Biophys.*, **2008**, *479*(2), 163-9.
- [74] Polyak, S. W.; Chapman-Smith, A.; Brautigan, P. J.; Wallace, J. C. Biotin protein ligase from *Saccharomyces cerevisiae*. The N-terminal domain is required for complete activity. *J. Biol. Chem.*, **1999**, *274*(46), 32847-54.

- [75] Hassan, Y. I.; Moriyama, H.; Olsen, L. J.; Bi, X.; Zemleni, J. N. and C-terminal domains in human holocarboxylase synthetase participate in substrate recognition. *Mol. Genet. Metab.*, **2009**, *96*(4), 183-8.
- [76] Lee, C. K.; Cheong, C.; Jeon, Y. H. The N-terminal domain of human holocarboxylase synthetase facilitates biotinylation via direct interaction with the substrate protein. *FEBS Lett.*, **2010**, *584*(4), 675-80.
- [77] Wilson, K. P.; Shewchuk, L. M.; Brennan, R. G.; Otsuka, A. J.; Matthews, B. W. *Escherichia coli* biotin holoenzyme synthetase/bio repressor crystal structure delineates the biotin- and DNA-binding domains. *Proc. Natl. Acad. Sci. U S A*, **1992**, *89*, 9257-9261.
- [78] Weaver, L. H.; Kwon, K.; Beckett, D.; Matthews, B. W. Corepressor-induced organization and assembly of the biotin repressor: a model for allosteric activation of a transcriptional regulator. *Proc. Natl. Acad. Sci. U S A*, **2001**, *98*(11), 6045-50.
- [79] Wood, Z. A.; Weaver, L. H.; Brown, P. H.; Beckett, D.; Matthews, B. W. Co-repressor induced order and biotin repressor dimerization: a case for divergent followed by convergent evolution. *J. Mol. Biol.*, **2006**, *357*(2), 509-23.
- [80] Tron, C. M.; McNae, I. W.; Nutley, M.; Clarke, D. J.; Cooper, A.; Walkinshaw, M. D.; Baxter, R. L.; Campopiano, D. J. Structural and functional studies of the biotin protein ligase from *Aquifex aeolicus* reveal a critical role for a conserved residue in target specificity. *J. Mol. Biol.*, **2009**, *387*(1), 129-46.
- [81] Pardini, N. R.; Yap, M. Y.; Polyak, S. W.; Cowieson, N. P.; Abell, A.; Booker, G. W.; Wallace, J. C.; Wilce, J. A.; Wilce, M. C. Structural characterization of *Staphylococcus aureus* biotin protein ligase and interaction partners: An antibiotic target. *Protein Sci.*, **2013**, *22*(6), 762-73.
- [82] Pardini, N. R.; Polyak, S. W.; Booker, G. W.; Wallace, J. C.; Wilce, M. C. Purification, crystallization and preliminary crystallographic analysis of biotin protein ligase from *Staphylococcus aureus*. *Acta Crystallogr. Sect. F. Struct. Biol. Cryst. Commun.*, **2008**, *64*(Pt 6), 520-3.
- [83] Kwon, K.; Beckett, D. Function of a conserved sequence motif in biotin holoenzyme synthetases. *Protein Sci.*, **2000**, *9*(8), 1530-9.
- [84] Xu, Y.; Beckett, D. Kinetics of biotinyl-5'-adenylate synthesis catalyzed by the *Escherichia coli* repressor of biotin biosynthesis and the stability of the enzyme-product complex. *Biochemistry*, **1994**, *33*(23), 7354-7360.
- [85] Choi-Rhee, E.; Schulman, H.; Cronan, J. E. Promiscuous protein biotinylation by *Escherichia coli* biotin protein ligase. *Protein Sci.*, **2004**, *13*(11), 3043-50.
- [86] Naganathan, S.; Beckett, D. Nucleation of an allosteric response via ligand-induced loop folding. *J. Mol. Biol.*, **2007**, *373*(1), 96-111.
- [87] Streaker, E. D.; Beckett, D. Ligand-linked structural changes in the *Escherichia coli* biotin repressor: the significance of surface loops for binding and allostery. *J. Mol. Biol.*, **1999**, *292*(3), 619-32.
- [88] Kumar, N.; Shukla, S.; Kumar, S.; Suryawanshi, A.; Chaudhry, U.; Ramachandran, S.; Maiti, S. Intrinsically disordered protein from a pathogenic mesophile *Mycobacterium tuberculosis* adopts structured conformation at high temperature. *Proteins*, **2008**, *71*(3), 1123-33.
- [89] Noble, M. E. M.; Musacchio, A.; Saraste, M.; Courtneidge, S. A.; Wierenga, R. K. Crystal structure of the SH3 domain in human Fyn - Comparison of the 3-dimensional structures of SH3 domains in tyrosine kinases and spectrin. *EMBO J.*, **1993**, *12*(7), 2617-2624.
- [90] Chapman-Smith, A.; Mulhern, T. D.; Whelan, F.; Cronan, J. E., Jr.; Wallace, J. C. The C-terminal domain of biotin protein ligase from *E. coli* is required for catalytic activity. *Protein Sci.*, **2001**, *10*(12), 2608-17.
- [91] Chapman-Smith, A.; Cronan, J. E. J. The enzymatic biotinylation of proteins: a post-translational modification of exceptional specificity. *Trends Biochem. Sci.*, **1999**, *24*, 359-363.
- [92] Pardini, N. R.; Bailey, L. M.; Booker, G. W.; Wilce, M. C.; Wallace, J. C.; Polyak, S. W. Microbial biotin protein ligases aid in understanding holocarboxylase synthetase deficiency. *Biochim. Biophys. Acta*, **2008**, *1784*(7-8), 973-82.
- [93] Athappilly, F. K.; Hendrickson, W. A. Structure of the biotinyl domain of acetyl-coenzyme A carboxylase determined by MAD phasing. *Structure*, **1995**, *3*(12), 1407-1419.
- [94] Roberts, E. L.; Shu, N. C.; Howard, M. J.; Broadhurst, R. W.; Chapman-Smith, A.; Wallace, J. C.; Morris, T.; Cronan, J. E.; Perham, R. N. Solution structures of apo and holo biotinyl domains from acetyl coenzyme A carboxylase of *Escherichia coli* determined by triple-resonance nuclear magnetic resonance spectroscopy. *Biochemistry*, **1999**, *38*(16), 5045-5053.
- [95] Reche, P.; Li, Y. L.; Fuller, C.; Eichhorn, K.; Perham, R. N. Selectivity of post-translational modification in biotinylated proteins - the carboxy carrier protein of the acetyl-CoA carboxylase of *Escherichia coli*. *Biochem. J.*, **1998**, *329*(3), 589-596.
- [96] Reche, P.; Perham, R. N. Structure and selectivity in post-translational modification: attaching the biotinyl-lysine and lipoyl-lysine swinging arms in multifunctional enzymes. *EMBO J.*, **1999**, *18*, 2673-2682.
- [97] Leon-Del-Rio, A.; Gravel, R. A. Sequence requirements for the biotinylation of carboxyl-terminal fragments of human propionyl-CoA carboxylase alpha subunit expressed in *Escherichia coli*. *J. Biol. Chem.*, **1994**, *269*(37), 22964-22968.
- [98] Polyak, S. W.; Chapman-Smith, A.; Mulhern, T. D.; Cronan, J. E., Jr.; Wallace, J. C. Mutational analysis of protein substrate presentation in the post-translational attachment of biotin to biotin domains. *J. Biol. Chem.*, **2001**, *276*(5), 3037-45.
- [99] Shenoy, B. C.; Wood, H. G. Effect of mutations at Met-88 and Met-90 on the biotinylation of Lys-89 of the apo 1.3S subunit of transcarboxylase. *FASEB J.*, **1988**, *2*, 2396-2401.
- [100] Shenoy, B. C.; Xie, Y.; Park, V. L.; Kumar, G. K.; Beegan, H.; Wood, H. G.; Samols, D. The importance of methionine residues for the catalysis of the biotin enzyme, transcarboxylase. *J. Biol. Chem.*, **1992**, *267*(26), 18407-18412.
- [101] Kondo, H.; Uno, S.; Komizo, Y. Y.; Sunamoto, J. Importance of methionine residues in the enzymatic carboxylation of biotin containing peptides representing the local bindyl site of *E. coli* acyl CoA carboxylase. *Int. J. Peptide Protein Res.*, **1984**, *23*, 559-564.
- [102] Hanka, L. J.; Bergy, M. E.; Kelly, R. B. Naturally occurring antimetabolite antibiotic related to biotin. *Science*, **1966**, *154*(757), 1667-8.
- [103] Hanka, L. J.; Martin, D. G.; Reineke, L. M. Two new antimetabolites of biotin: alpha-methyldeithiobiotin and alpha-methylbiotin. *Antimicrob. Agents Chemother.*, **1972**, *1*(2), 135-8.
- [104] Piffeteau, A.; Dufour, M. N.; Zamboni, M.; Gaudry, M.; Marquet, A. Mechanism of the antibiotic action of alpha-dehydrobiotin. *Biochemistry*, **1980**, *19*(13), 3069-73.
- [105] Ampacher, D. R.; Blanchard, C. Z.; Fronczek, F. R.; Saraiva, M. C.; Waldrop, G. L.; Strongin, R. M. Synthesis of a reaction intermediate analogue of biotin-dependent carboxylases via a selective derivatization of biotin. *Org. Lett.*, **1999**, *1*(1), 99-102.
- [106] Blanchard, C. Z.; Ampacher, D.; Strongin, R.; Waldrop, G. L. Inhibition of biotin carboxylase by a reaction intermediate analog: implications for the kinetic mechanism. *Biochem. Biophys. Res. Commun.*, **1999**, *266*(2), 466-71.
- [107] Slavoff, S. A.; Chen, I.; Choi, Y. A.; Ting, A. Y. Expanding the substrate tolerance of biotin ligase through exploration of enzymes from diverse species. *J. Am. Chem. Soc.*, **2008**, *130*(4), 1160-2.
- [108] Soares da Costa, T. P.; Tieu, W.; Yap, M. Y.; Pardini, N. R.; Polyak, S. W.; Sejer Pedersen, D.; Morona, R.; Tumidge, J. D.; Wallace, J. C.; Wilce, M. C.; Booker, G. W.; Abell, A. D. Selective inhibition of Biotin protein ligase from *Staphylococcus aureus*. *J. Biol. Chem.*, **2012**, *287*(21), 17823-32.
- [109] Soares da Costa, T. P.; Tieu, W.; Yap, M. Y.; Zvarec, O.; Bell, J.; Tumidge, J. D.; Wallace, J. C.; Booker, G. W.; Wilce, M. C. J.; Abell, A. D.; Polyak, S. W. Biotin analogues with antibacterial activity are potent inhibitors of Biotin protein ligase. *ACS Med. Chem. Lett.*, **2012**, *3*, 509-514.
- [110] Xu, Y.; Nenortas, E.; Beckett, D. Evidence for distinct ligand-bound conformational states of the multifunctional *Escherichia coli* repressor of biotin biosynthesis. *Biochemistry*, **1995**, *34*(51), 16624-16631.
- [111] Lu, H.; England, K.; am Ende, C.; Truglio, J. J.; Luckner, S.; Reddy, B. G.; Marlenee, N. L.; Knudson, S. E.; Knudson, D. L.; Bowen, R. A.; Kisker, C.; Slayden, R. A.; Tonge, P. J. Slow-onset inhibition of the FabI enoyl reductase from *Francisella tularensis*: residence time and *in vivo* activity. *ACS Chem. Biol.*, **2009**, *4*(3), 221-31.
- [112] Artymiuk, P. J.; Rice, D. W.; Poirrette, A. R.; Willet, P. A tale of two synthetases. *Nat. Struct. Biol.*, **1994**, *1*(11), 758-760.
- [113] Reche, P. A. Lipoylating and biotinylating enzymes contain a homologous catalytic module. *Protein Sci.*, **2000**, *9*(10), 1922-9.

- [114] Bernier, S.; Akochy, P. M.; Lapointe, J.; Chenevert, R. Synthesis and aminoacyl-tRNA synthetase inhibitory activity of aspartyl adenylate analogs. *Bioorg. Med. Chem.*, **2005**, *13*(1), 69-75.
- [115] Bottcher, C.; Dennis, E. G.; Booker, G. W.; Polyak, S. W.; Boss, P. K.; Davies, C. A novel tool for studying auxin-metabolism: the inhibition of grapevine indole-3-acetic Acid-amido synthetases by a reaction intermediate analogue. *PLoS One*, **2012**, *7*(5), e37632.
- [116] Forrest, A. K.; Jarvest, R. L.; Mensah, L. M.; O'Hanlon, P. J.; Pope, A. J.; Sheppard, R. J. Aminoalkyl adenylate and aminoacyl sulfamate intermediate analogues differing greatly in affinity for their cognate *Staphylococcus aureus* aminoacyl tRNA synthetases. *Bioorg. Med. Chem. Lett.*, **2000**, *10*(16), 1871-4.
- [117] Lee, J.; Kang, S. U.; Kang, M. K.; Chun, M. W.; Jo, Y. J.; Kwak, J. H.; Kim, S. Methionyl adenylate analogues as inhibitors of methionyl-tRNA synthetase. *Bioorg. Med. Chem. Lett.*, **1999**, *9*(10), 1365-70.
- [118] Patrone, J. D.; Yao, J.; Scott, N. E.; Dotson, G. D. Selective inhibitors of bacterial phosphantiotheneoylcysteine synthetase. *J. Am. Chem. Soc.*, **2009**, *131*(45), 16340-1.
- [119] Tian, Y.; Suk, D. H.; Cai, F.; Crich, D.; Mesecar, A. D. *Bacillus anthracis* o-succinylbenzoyl-CoA synthetase: reaction kinetics and a novel inhibitor mimicking its reaction intermediate. *Biochemistry*, **2008**, *47*(47), 12434-47.
- [120] Yu, X. Y.; Hill, J. M.; Yu, G.; Wang, W.; Kluge, A. F.; Wendler, P.; Gallant, P. Synthesis and structure-activity relationships of a series of novel thiazoles as inhibitors of aminoacyl-tRNA synthetases. *Bioorg. Med. Chem. Lett.*, **1999**, *9*(3), 375-80.
- [121] Brown, P. H.; Cronan, J. E.; Grotli, M.; Beckett, D. The biotin repressor: modulation of allostery by corepressor analogs. *J. Mol. Biol.*, **2004**, *337*(4), 857-69.
- [122] Purushothaman, S.; Gupta, G.; Srivastava, R.; Ramu, V. G.; Surolia, A. Ligand specificity of group I biotin protein ligase of *Mycobacterium tuberculosis*. *PLoS One*, **2008**, *3*(5), e2320.
- [123] Meldal, M.; Tornøe, C. W. Cu-catalyzed azide-alkyne cycloaddition. *Chem. Rev.*, **2008**, *108*(8), 2952-3015.
- [124] Rostovtsev, V. V.; Green, L. G.; Fokin, V. V.; Sharpless, K. B. A stepwise Huisgen cycloaddition process: copper(I)-catalyzed regioselective "ligation" of azides and terminal alkynes. *Angew. Chem. Int. Ed. Engl.*, **2002**, *41*(14), 2596-9.
- [125] Whiting, M.; Muldoon, J.; Lin, Y. C.; Silverman, S. M.; Lindstrom, W.; Olson, A. J.; Kolb, H. C.; Finn, M. G.; Sharpless, K. B.; Elder, J. H.; Fokin, V. V. Inhibitors of HIV-1 protease by using *in situ* click chemistry. *Angew. Chem. Int. Ed. Engl.*, **2006**, *45*(9), 1435-9.
- [126] Tieu, W.; Soares da Costa, T. P.; Yap, M. Y.; Keeling, K. L.; Wilce, M. C. J.; Wallace, J. C.; Booker, G. W.; Polyak, S. W.; Abell, A. D. Optimising *in situ* click chemistry: the screening and identification of biotin protein ligase inhibitors. *Chem. Sci.*, **2013**, *4*, 3533-3537.
- [127] Zhang, L.; Chen, X.; Xue, P.; Sun, H. H.; Williams, I. D.; Sharpless, K. B.; Fokin, V. V.; Jia, G. Ruthenium-catalyzed cycloaddition of alkynes and organic azides. *J. Am. Chem. Soc.*, **2005**, *127*(46), 15998-9.
- [128] Sharpless, K. B.; Manetsch, R. *In situ* click chemistry: a powerful means for lead discovery. *Expert. Opin. Drug. Discov.*, **2006**, *1*(6), 525-38.
- [129] Thirumurugan, P.; Matusiuk, D.; Jozwiak, K. Click chemistry for drug development and diverse chemical-biology applications. *Chem. Rev.*, **2013**, *113*(7), 4905-4979.
- [130] Manetsch, R.; Krasinski, A.; Radic, Z.; Raushel, J.; Taylor, P.; Sharpless, K. B.; Kolb, H. C. *In situ* click chemistry: enzyme inhibitors made to their own specifications. *J. Am. Chem. Soc.*, **2004**, *126*(40), 12809-18.



Chapter 3:
Materials & Methods

3.1 MATERIALS

3.1.1 General Materials

Materials	Suppliers
CoStar 96 well round bottom clear plate	Corning Life Sciences, USA
Amicon® centrifugal devices	Millipore, MA, USA
Sartorius VIVASPIN20, 10000 MWCO	Sartorius, Goettingen, Germany
Cellu.SepT ₂ MWCO 6000-8000 dialysis tubing	Membrane Filtration Products Inc., Seguin, TX, USA
Ministart syringe filter 0.2µM, 0.45µM and 0.8µM	Sartorius, Goettingen, Germany
NuPage® 4-12% Bis-Tris polyacrylamide gels	Invitrogen, CA, USA
5 mL Profinia® IMAC cartridge	Bio-Rad Laboratories Inc., CA, USA
40 mL glutathione agarose column	Scientifix, Australia
PD-10 Desalting column	GE Healthcare, Buckinghamshire, England
epT.I.P.S.® Standard 50-1250µL	Eppendorf, Hamburg, Germany
epT.I.P.S.® Standard 20-300µL	Eppendorf, Hamburg, Germany
Eclipse Pipette Tip refill System	Labcon, North America
SealPlate® Plate seals	Excel Scientific Inc., Victorville, USA
96 well LUMITRAC 600 white plate	Greiner Bio One, Germany
96 well Multiscreen-IP FilterPlate, 0.45µM	Merck Millipore, MA, USA
Clear 96 well flexible pet microplate, round bottom	Perkin Elmer, Boston, MA, USA
Biacore Series S Sensor chip CM5	GE Healthcare Bio-sciences AB, Uppsala, Sweden
PVDF membrane (Hybond™-C extra)	Amersham Pharmacia Biotech, CA, USA
Gel blotting paper	Schleicher & Schuell Bioscience GmbH, Germany
pH indicator strips	Merck, Darmstadt, Germany

3.1.2 Chemical Reagents

All chemicals and reagents were of analytical grade or higher. Most common laboratory chemicals were purchased from Sigma Aldrich Inc (St Louis, MO, USA) or BDH chemicals Ltd. (Victoria, Australia). Specialized reagents and their suppliers are listed below.

Reagents	Supplier
2-log DNA ladder	New England Biolabs, MA, USA
Agarose, DNA grade	Probiogen Biochemicals, Australia
Biotin	Sigma-Aldrich inc., CA, USA
Bradford protein reagent concentrate	Bio-Rad Laboratories Inc., CA, USA
Phenylmethanesulfonyl fluoride (PMSF)	Sigma-Aldrich, MO, USA
Dithiothreitol (DTT)	Sigma-Aldrich, MO, USA
Isopropyl β -D-1-thiogalactopyranoside (IPTG)	BioVectra, PE, USA
MOPS/MES SDS running buffer	Invitrogen Life Technologies Inc., NY, USA
Precision Plus Protein Kaleidoscope standards	Bio-Rad Laboratories Inc., CA, USA
GelRED TM Nucleic acid gel stain	Biotium Inc., CA, USA
BigDye (version 3) reaction mix	Perkin Elmer, CA, USA
Ampicillin	Sigma-Aldrich, MO, USA
Bovine Serum Albumin	Roche Diagnostics, IN, USA
Chloramphenicol	Sigma-Aldrich, MO, USA
Erythromycin	Sigma-Aldrich, MO, USA
Streptomycin sulfate salt	Sigma-Aldrich, MO, USA
DELFI A Enhancement Solution	Perkin Elmer, Boston, MA, USA
Eu-Streptavidin	Perkin Elmer, Boston, MA, USA
Optiphase Supermix Scintillation Fluid	Perkin Elmer, Boston, MA, USA

3.1.3 Bacterial strains

***E. coli* BL21 (hsdS gal (λcIts857) ind Sam7 nin5 lacUV5T7gene1):** *E. coli* BL21 carrying (λDE3) insertion for expression of recombinant proteins using pET expression vector (Stratagene, La Jolla, CA, USA)

***E. coli* DH5α (supEΔlac169 (p80lacZΔM15) hsdR17 recA1 end AA1 gyrA96 thi-1 relA1):**
For routine molecular cloning (New England Biolabs, MA, USA)

***E. coli* BL21-CodonPlus(DE3)-RIPL strain (B F⁻ ompT hsdS(r_B⁻ m_B⁻) dcm⁺ Tet^r gal λ(DE3) endA The [argU proL Cam^r] [argU ileY leuW Sterp/Spec^r]:** *E. coli* BL21 carrying (λDE3) insertion and contains plasmids encoding extra copies of genes for rare tRNAs in *E. coli*. This strain was used for recombinant expression of pET expression vector encoding the gene for *Staphylococcus aureus* and *Klebsiella pneumoniae* biotin protein ligases (Aglient Technologies, CA, USA).

Methicillin Sensitive *Staphylococcus aureus* ATCC 49775: Purchased from the American Tissue Culture Collection. This strain was used for antimicrobial susceptibility assays.

3.1.4 Bacterial Media

Luria Broth (LB): 1% (w/v) tryptone, 0.5% (w/v) yeast extract, 1% (w/v) NaCl, adjusted to pH 7.0 with NaOH.

LB agar: LB supplemented with 1.5% (w/v) bacto-agar

Cation-adjusted Mueller Hinton Broth (CAMHB): 3 % (w/v) beef extract, 17.5 % (w/v) acid hydrolysate of casein, 1.5 % (w/v) starch, supplemented to contain 20-25 mg/L calcium and 10-12.5 mg/L magnesium.

Bacterial selection: Selection of bacteria bearing plasmid was achieved through addition of appropriate antibiotics to both liquid and solid media. Ampicillin was used at 100 µg/mL. For expression of *S. aureus* BPL in *E.coli* BL21 CodonPlus(DE3)-RIPL strain, chloramphenicol (34 µg/mL) and streptomycin (25 µg/mL) were used in addition to ampicillin (100 µg/mL).

3.1.5 Commercial kits

Kit	Suppliers
QIAprep Miniprep Kit	QIAGEN, GmbH, Germany

3.1.6 Buffers and Solutions

Blocking Buffer (For Western analysis): 1% (w/v) BSA in PBS

Cell Lysis Buffer: 10% (v/v) β-mercaptoethanol, 2% (w/v) SDS

Cleaning solution 1 (2x): 100 mM NaCl, 100 mM Tris, at pH 8.0

Cleaning solution 2 (4x): 2M NaCl, 0.4 M sodium acetate, at pH 4.5

Coomassie blue stain: 0.2% (w/v) coomassie brilliant blue, 10% (v/v) ethanol, 10% (v/v) acetic acid

Coomassie de-stain: 10% (v/v) methanol, 10% (v/v) acetic acid

DNA loading buffer (6X): 0.5x Tris-borate-EDTA (TBE) buffer, 40% (v/v) glycerol, 1mg/ml bromophenol blue

HBS running buffer 1: 10 mM HEPES at pH 7.4, 150 mM NaCl, 3 mM EDTA 0.005% surfactant p20

HBS running buffer 2: 10 mM HEPES at pH 7.4, 150 mM NaCl, 5 % DMSO, 0.005% surfactant p20

Immobilization buffer: 10 mM sodium acetate at pH 5.8

Native IMAC lysis buffer/wash buffer 1: 300 mM KCl, 50 mM Tris at pH 8.0, 5 mM imidazole

Native IMAC wash buffer 2 : 300 mM KCl, 50 mM Tris at pH 8.0, 10 mM imidazole

Native elution buffer : 300 mM KCl, 50 mM Tris at pH 8.0, 250 mM imidazole

SDS-PAGE loading buffer: 0.1 M Tris (pH 7), 4% (w/v) SDS, 0.2% (w/v) bromophenol blue

SDS-PAGE Coomassie Blue staining solution: 0.2% (w/v) Coomassie brilliant blue, 10% (v/v) Methanol, 10% (v/v) Acetic acid

SDS-PAGE de-staining solution: 10% (v/v) Methanol, 10% (v/v) Acetic acid

PBS: 0.136 M NaCl, 2.7 mM KCl, 1.46 mM KH_2PO_4 at pH 7.4

PBS-Tween: PBS, 0.1% (v/v) Tween 20

TAE: 40mM tris pH 8.2, 20 mM sodium acetate, 1 mM EDTA

TBS: 25 mM Tris pH 7.5, 150 mM NaCl

TE: 10 mM Tris pH 7.5, 1 mM EDTA

Transfer Buffer: 39 mM glycine, 48 mM Tris, 0.037% (w/v) SDS, 20% (v/v) methanol

Transformation buffer 1: 30 mM potassium acetate, 100 mM RbCl, 10 mM CaCl_2 , 50 mM MnCl_2 , 15% glycerol

Transformation buffer 2: 10 mM MOPS, 10 mM RbCl, 75 mM CaCl_2 , 15% glycerol

BPL storage buffer: 50 mM Tris pH 8.0, 100 mM KCl, 5% glycerol, 0.1 mM EDTA pH 8.0, 1mM DTT

3.1.7 Tracers

d-[8,9-³H]-biotin were purchased from Amersham Australia, North Ryde, NSW, Australia and Perkin-Elmer, Boston, MA, USA.

3.1.8 Oligonucleotides

All oligonucleotides were purchased from Geneworks Pty Ltd., Hindmarsh, South Australia.

All primers were of sequencing grade.

Oligo Name	Sequence 5' → 3'
T7-26mer Forward	5' CGA AAT TAA TAC GAC TCA CTA TAG GG 3'
T7-23mer Reverse	5' CAA GAA TTC TCA TGT TTG ACA GC 3'

3.1.9 Plasmids

pET-TEV-H₆: a derivative of pET16b, obtained from Dr Steven Polyak (School of molecular and Biomedical Science, University of Adelaide).

pET-TEV-H₆-*Mt*BPL: a derivative of pET16b, used for recombinant expression of *M.tuberculosis* BPL.

pET-*Sa*BPL-H₆: For recombinant expression of *S. aureus* BPL in *E. coli* BL21 CodonPlus(DE3) RIPL strain

pET-*Ac*BPL-H₆: A derivative of pET22b, used for recombinant expression of *A. calcoaceticus* BPL, obtained from Dr. Simone Beckham (School of Biological Sciences, Monash University)

pET- *Kp*BPL-H₆: A derivative of pET22b, used for recombinant expression of *K. pneumoniae* BPL, obtained from Dr. Simone Beckham (School of Biological Sciences, Monash University)

3.1.10 Computer Software

Data were analysed using GraphPad Prism 6 (GraphPad Software, Inc., CA, USA). UCSF Chimera version 1.8.1 (UCSF, CA, USA) was used for viewing and analysis of PDB files. AutoDock-Vina version 1.5.4 (UCSF, CA, USA) was used for *in silico* docking. ChemDraw[®] version 10.0 (Perkin Elmer, Inc., MA, USA) was used for preparing chemical structures

3.1.11 Web resources

NCBI (<http://www.ncbi.nlm.nih.gov/>) was used to access protein, nucleotide, and PubMed databases. An Online SMILES Translator and Structure File Generator Software (<http://cactus.nci.nih.gov/services/translate/>) was used for generating 3D structures of compounds.

3.2 METHODS

3.2.1 Protein Techniques

3.2.1.1 Preparation of cell lysate

For the preparation of whole cell lysates for SDS-PAGE analysis, 1 mL of culture was centrifuged at 2600 x g for 1 minute. The supernatant was discarded and the cell pellet was resuspended with 40 μ L of cell lysis buffer per unit OD. Cell suspension was vortexed, spun and boiled at 95 °C for 5 minutes, this process was repeated.

3.2.1.2 Determination of protein concentration

Protein concentration was assayed using the Bradford Reagent (Bio-Rad Laboratories Inc., CA, USA). A standard curve of bovine serum albumin (BSA) was generated using stock concentrations from 0 to 1 mg/mL and a linear regression was used to calculate protein concentration. For the Bradford assay 10 μ L of sample was mixed with 200 μ L of 1x Bradford Reagent in a 96 well plate (Corning Life Sciences, USA). Absorbance at 620 nm wavelength was measured on a microplate reader (Molecular Devices, CA, USA).

3.2.1.3 SDS PAGE electrophoresis and gel staining

Protein samples were diluted in protein sample buffer to a final concentration of 1X. Samples were then boiled for 5 min, and centrifuged briefly to collect condensation from the top of the tube. The proteins samples were fractioned on NuPage[®] 4-12% Bis-Tris polyacrylamide precast gel (Invitrogen) using 1X NuPAGE[®] MES running buffer (Invitrogen) at 200 V for approximately 40 min or until the dye front reached the bottom of the gel. The protein bands were visualized using SDS-PAGE Coomassie Blue staining solution. The gel was first soaked in staining solution (0.2% Coomassie Blue, 50% ethanol and 10% acetic acid) at room temperature for at least 1 hour, before soaking in SDS-PAGE destaining solution (10% acetic acid and 5% methanol) overnight.

3.2.1.4 Concentration of proteins

Concentration of protein solutions was performed using Amicon[®] centrifugal filter devices (10000 MWCO) (Millipore, MA, USA) following manufacturer's instruction manual. The columns were rinsed with MilliQ water and then equilibrated in the appropriate buffer by centrifugation at 5000 x g at 4 °C for 20 minutes or until reaching a required retentate volume. The buffer was discarded prior to adding protein sample into the spin column. Likewise, protein was concentrated by centrifugation at 5000 x g at 4 °C until reaching a required retentate volume. For retentate recovery, the concentrate was collected using a pipette with 200 microliter tip to new pre-cold microcentrifuge tube. The protein was kept at -80 °C until needed. For storage of using Amicon[®] centrifugal filter devices, the centrifuge tube was washed with distilled water to remove residual buffer components and kept in MilliQ water at 4 °C.

3.2.2 Molecular Biology Techniques

3.2.2.1 Agarose Gel Electrophoresis

Analysis of DNA and separation of DNA fragments was performed using Agarose gel electrophoresis. Gel slabs were poured by melting 1-2% (w/v) Agarose in TAE buffer. Prior to loading into wells, DNA samples were mixed with an appropriate volume of 6x DNA loading buffer. Samples were electrophoresed in TAE buffer at 100V and then stained in 1x GelRedTM nucleic acid gel stain solution for at least 10 minutes. DNA was visualized on a UV transilluminator and photographed using a Mitsubishi video processor.

3.2.2.2 Preparation of competent *E. coli* BL21 (DE3) and *E. coli* BL21 CodonPlus(DE3)-RIPL competent cells

Overnight cultures of cells in LB media were prepared and subcultured the next day into LB medium (330 μ L of overnight culture into 10 mL of LB). The cell cultures were grown at 37 °C for 1.5 – 2 hours until they reached an OD₆₀₀ measurement of 0.6. 5 mL of culture was then subcultured into 100 mL of pre-warmed LB media in a 1 L flask and was grown at 37 °C for 1.5 hours. The cells were then pelleted by centrifugation at 5000 x g for 5 minutes at 4 °C and resuspended in 10 mL/pellet of transformation buffer 1 and incubated on ice for 5 minutes. The cells were then pelleted by centrifugation at 5000 x g for 5 minutes at 4 °C and resuspended in 1 mL/ pellet of transformation buffer 2 and incubated on ice for 5 minutes. The cells were then aliquoted and stored in pre-chilled 1.5 mL microcentrifuge tubes at -80 °C.

3.2.2.3 Transformation of plasmids into competent cells

3.2.2.3.1 Transformation of *E. coli* DH5 α and *E. coli* BL21(DE3) competent cells

1-5 μ L of plasmid was added to 200 μ L of competent cells and incubated on ice for at least 30 minutes. This was followed by heat shock treatment at 42 °C for 3 minutes followed by further 5 minutes incubation on ice. Cells were immediately plated onto pre-warmed LB agar plates with Ampicilin selection.

3.2.2.3.2 Transformation of *E. coli* BL21 CodonPlus(DE3)-RIPL competent cells

50 μ L of competent cells were treated with 1 μ L of β -mercaptoethanol that had been diluted 1:10 in MilliQ water. The competent cells were incubated on ice for 10 min. The contents were mixed gently every 2 min. 1 -5 μ L of plasmid was added to 50 μ L of β -mercaptoethanol treated competent cells and incubated on ice for at least 30 min. This was followed by heat shock treatment at 42 °C for 20 seconds, followed by further 2 min incubation on ice. 900 μ L of pre-warmed SOC media was added to each transformation and the cells were incubated for 1 hour at 37 °C with shaking. Cells were then pelleted by centrifugation at 2600 x g for 1 min and the pellet was resuspended in 100 – 200 μ L of supernatant. Cells were immediately plated onto pre-warmed LB plates containing Ampicillin, chloramphenicol and streptomycin selection.

3.2.2.4 Preparation of glycerol stocks

For long term storage of *E. coli* strains, equal volumes of an overnight culture and 80% (v/v) glycerol were mixed and stored at -80 °C.

3.2.2.5 Plasmid Purification

For purification of plasmid DNA, the QIAGEN QIAprep Miniprep Kit was employed according to manufacturer's instructions.

3.2.2.6 DNA Sequencing

Plasmid DNA or PCR products were used as templates for DNA sequencing. A 20 μL reaction containing 200 ng DNA, 100 ng of appropriate primer, 1 μL of BigDye version 3 reaction mix (Perkin Elmer, Applied Biosystems, CA, USA) and 4 μL of 5x sequencing buffer for PCR. The PCR profile consisted of 30 cycles of denaturation at 96 °C for 30 seconds, annealing at 50 °C for 15 seconds and extension at 60°C for 4 minutes. After thermocycling 80 μL of 75% (v/v) isopropanol was added to the PCR products, vortexed and incubated at room temperature for 30 minutes. Precipitated DNA was isolated by centrifugation at 17500 x g for 20 minutes. The pellet was washed in 250 μL of 75% (v/v) isopropanol followed by centrifugation at 17500 x g for 5 minutes and dried in a 37 °C heating block. Sequencing was performed by the molecular pathology sequencing service at the institute of Medical and Veterinary Science, Adelaide using 3730 Analyser (Perkin Elmer, Applied Biosystems, CA, USA).



Chapter 4:
Assay Development

4.1 Introduction

In order to characterize rationally designed BPL inhibitors, there is a need to develop a BPL enzyme assay that is potentially amenable to high-throughput screening applications. Our well established assay for BPL enzymatic activity is to measure the incorporation of ^3H -biotin into an acid precipitable biotin domain substrate that is captured and then washed on filter paper [1]. This assay involves a number of manual handling steps, and is not suited to high-throughput applications. One of the considerations for an *in vitro* biotinylation assay is the need to separate unincorporated radiolabel from protein bound ^3H -biotin. These separation techniques are not easily automated, and so the first aim of this project was to develop an alternative BPL enzyme assay that removes the cumbersome washing step. Firstly, a scintillation proximity assay was investigated to measure protein biotinylation. This technology removes the need for a separation step, allowing the entire assay to be performed in a single 96-well plate [2]. However, there were difficulties in achieving an appropriate level of signal above the background. Therefore this was abandoned for an alternative approach. Following this, commercially available HTS-multiscreen filter plates were investigated. This system allows the rapid separation of ^3H -biotinylated protein from unincorporated ^3H -biotin through the use of an immobilonTM PVDF membrane in the well of a 96-well plate [3]. This new BPL assay will be used to characterize rationally designed BPL inhibitors in chapters 5, 6, 7, 8 and 9. A surface plasmon resonance (SPR) binding assay was also developed to monitor the binding of BPL inhibitors. SPR has many advantages including label-free detection and real-time monitoring [4].

In this chapter I will describe the production of tools required throughout this thesis. The production of highly pure BPL for enzyme assays is discussed. Here, I have optimized the expression and purification of BPLs from *S. aureus*, *M. tuberculosis*, *Klebsiella pneumoniae* and *Acinetobacter calcoaceticus*. To measure BPL activity a suitable protein substrate is also required. Here I have optimized the expression and purification of apo (non-biotinylated)

protein substrate to be used in enzyme assays in order to measure protein biotinylation. The combined use of the ^3H -biotin incorporation assay and the SPR binding assay, will be employed to characterize the inhibition and binding of rationally designed BPL inhibitors. Both assays will be used to identify promising compounds that exhibit good inhibitory activity and binding affinity to direct further medicinal chemistry efforts, to help optimize the biotin triazole pharmacophore

4.2 Specific Methods

4.2.1 Recombinant *SaBPL* and *KpBPL* expression in *E. coli* BL21-CodonPlus(DE3)-RIPL strain

Overnight cultures of *E. coli* BL21-CodonPlus(DE3)-RIPL cells harbouring either pET-*SaBPL*-H₆ or pET-*KpBPL*-H₆ expression plasmids were grown at 30 °C in LB for *SaBPL* or 2YT medium for *KpBPL* supplemented with 200 µg/mL ampicillin, 34 µg/mL chloramphenicol and 75 µg/mL streptomycin. This was followed by subculturing at 1:50 dilution into fresh media supplemented with 200 µg/mL ampicillin, 34 µg/mL chloramphenicol and 75 µg/mL streptomycin, 10 µM biotin and 2 % glucose. The cells were grown at 30 °C to an OD₆₀₀ of approximately 0.6-0.8. Recombinant protein expression was induced with 1 mM IPTG for 3 hours at 30 °C. The cells were harvested by centrifugation at 4500 x g for 5 minutes at 4 °C. The cell pellets were washed with 100 mL of 1 x TBS and pelleted by centrifugation at 4500 x g for 5 minutes at 4 °C and stored at -80 °C.

4.2.2 Recombinant *MtBPL* and *AcBPL* expression in *E. coli* BL21 (DE3) strain

Overnight cultures of *E. coli* BL21 (DE3) cells harbouring pET-TEV-H₆-*MtBPL* or pET-*AcBPL*-H₆ were grown in LB medium supplemented with 200 µg/mL ampicillin at 30 °C. This was followed by subculturing at 1:50 dilution into fresh media supplemented with 200 µg/mL ampicillin, 10 µM biotin and 2 % glucose. The cells were grown at 30 °C to an OD₆₀₀ of approximately 0.6-0.8. Recombinant protein expression was induced with 1 mM IPTG for 3 hours at 30 °C. The cells were harvested by centrifugation at 4500 x g for 5 minutes at 4 °C. The cell pellets were washed with 100 mL of 1 x TBS and pelleted by centrifugation at 4500 x g for 5 minutes at 4 °C and stored at -80 °C.

4.2.3 Purification of recombinantly expressed *Sa*BPL, *Mt*BPL, *Kp*BPL and *Ac*BPL

Cell pellets were resuspended in 30 mL ice cold native IMAC lysis buffer containing 1 mM PMSF. Cells were disrupted by at least 5 passages through a M110L homogenizer (Microfluidics, USA) until the solution became clear and homogenous. Cellular debris was removed by two centrifugation steps each at 45 000 x g for 10 minutes at 4 °C and then the solution was passed through 0.8 µm and 0.45 µm filters.

His-tagged BPL proteins were purified by immobilized nickel affinity chromatography (IMAC). The filtered lysate was applied at 5 mL/min onto a 5 mL Profinia IMAC cartridge that was pre-equilibrated with 10 column volumes of milliQ water then 10 column volumes of native IMAC lysis buffer. The column was washed with 6 column volumes of native IMAC lysis buffer (300 mM KCl, 50 mM Tris pH 8.0, 5 mM imidazole) followed by 6 column volumes of native IMAC wash buffer 2 (300 mM, 50 mM Tris pH 8.0, 10 mM imidazole). His-tagged BPL was eluted with native elution buffer (300 mM KCl, 50 mM Tris pH 8.0, 250 mM imidazole). Material eluting from the column was detected by UV absorbance at 280 nm and pooled and subsequently exchanged into storage buffer (50 mM tris pH 8.0, 100 mM KCl, 5% glycerol, 1 mM EDTA, 1mM DTT) using overnight dialysis at 4 °C. For SPR experiments *Sa*BPL was dialysed into storage buffer containing 1X PBS, 100 mM KCl, 5 % glycerol, 1 mM EDTA and 1 mM DTT. Protein concentrations were determined using a Bradford protein assay (BioRad) using bovine serum albumin (Sigma Aldrich®) as a standard (section 3.2.1.2). The fractions containing BPL were confirmed using SDS-PAGE gel electrophoresis and the *in vitro* ³H-biotin incorporation assay. The purified enzyme was aliquoted and stored at -80 °C.

4.2.4 Expression and purification of apo GST-*SaPC90*

Expression of apo (non-biotinylated) *SaPC90* domain was performed in the temperature sensitive *birA85⁻* *E. coli* strain BM4062 [5]. The *SaPC90* biotin domain was expressed as a GST fusion protein permitting high-level expression and rapid purification by affinity chromatography. Cells were grown in LB Media supplemented with 200 µg/mL ampicillin and 10 µM biotin at 30 °C to OD₆₀₀ ~0.8. The cultures were then moved to 42 °C for 30 minutes to heat inactivate endogenous BirA before a 3 hour incubation with 0.2 mM IPTG. The cells were harvested by centrifugation at 4600 x g for 5 minutes at 4 °C. The cell pellets were washed with 100 mL of 1 x TBS and pelleted by centrifugation at 4600 x g for 5 minutes at 4 °C and stored at -80 °C. Cell pellets were resuspended in 30 mL ice cold TBS pH 8.5 containing 1 mM PMSF. Cells were disrupted by at least 5 passages through a M110L homogenizer (Microfluidics, USA) until the solution became clear and homogenous. Cellular debris was removed by two centrifugation steps each at 45 000 x g for 10 minutes at 4 °C and then the solution was passed through 0.8 µm and 0.45 µm filters. The filtered lysate was passed over a 40 mL glutathione agarose column (Scientifix, Australia) that had been equilibrated with 5 column volumes of milliQ water and 5 column volumes of TBS pH 8.5 at a flow rate of 2 mL/min. Unbound material was removed by washing with 3 column volumes of TBS pH 8.5. The GST fusion was eluted with 10 mM reduced glutathione in TBS pH 8.5. Protein concentrations were determined using a Bradford protein assay (BioRad) using bovine serum albumin (Sigma Aldrich®) as a standard (section 3.2.1.2). The fractions containing GST-*SaPC90* were confirmed using SDS-PAGE and tested for activity using the *in vitro* ³H-biotin incorporation assay. The purified biotin domain was aliquoted and stored at -80 °C.

4.2.5 Streptavidin – blot analysis of GST-SaPC90 domain

To test whether purified GST-SaPC90 domain was indeed apo (non-biotinylated) a streptavidin-blot analysis was performed. Briefly, biotin incorporation assays were set up as described in section 4.2.6, except each reaction contained 5 μ M unlabelled biotin (ie, no 3 H-biotin was added). At completion of the assay, an appropriate volume of 2X SDS loading dye was added to each reaction. The samples were then boiled at 100 °C for 5 min and centrifuged briefly before being loaded and fractioned on a NuPage[®] 4-12% Bis-Tris polyacrylamide precast gel (Invitrogen) using 1X NuPAGE[®] MES running buffer (Invitrogen) at 200 V for approximately 40 min or until the dye front reached the bottom of the gel. The proteins fractionated by SDS-PAGE were transferred onto a PVDF membrane (Hybond[™]-LFP) using a semi dry transfer unit (Hoefer Semiphor, Amersham Pharmacia Biotech, CA, USA). The PVDF membrane was pre-soaked briefly in methanol, then milliQ water, followed by transfer buffer. The transfer was run for 1 hour at 80 mA per gel. The membrane was then soaked with blocking buffer (1% (w/v) BSA in PBS) for at least 1 hour at room temperature and washed 3 times with PBS-Tween before being probed with streptavidin conjugated - Alexa-488 (Life Technologies, 1:1000 dilution, PBS-Tween) for another hour at room temperature. The membrane was washed another 3 times with PBS-Tween then analysed using the ChemiDoc[™] MP imaging system (BioRad).

4.2.6 *In vitro* 3 H-biotin incorporation assays

In vitro biotinylation assays were carried out as described previously [1]. Briefly, an *in vitro* biotinylation reaction was performed for at least 10 minutes at 37 °C in a 20 μ L reaction mix containing 50 mM Tris pH 8.0, 3 mM ATP, 5.5 mM MgCl₂, 10 μ M apo SaPC90, 0.1 μ M DTT, 0.5 μ M 3 H-biotin, 4.5 μ M biotin and purified BPL enzyme at an appropriate concentration to detect the completed reaction in the linear phase (typically 6 – 150 nM).

4.2.6.1 *In vitro* ^3H -biotin incorporation assays: ^3H -biotin incorporated domain captured using filter paper

In vitro biotinylation assays were set up as described in section 4.2.6 with the addition of BSA at 0.1 mg/mL. At completion of the assay 4 μL aliquots were spotted onto gel blotting paper pre-treated with 10% trichloroacetic acid and 0.2 mM biotin. Blotting papers were washed twice in ice cold 10% trichloroacetic acid and once in ice cold absolute ethanol and dried. The blotting papers were placed in glass vials and added with the appropriate volume of Ultima Gold F scintillation fluid. Radioactivity measurements were obtained using a Rackbeta Liquid Scintillation Counter (Perkin Elmer, MA, USA).

4.2.6.2 *In vitro* ^3H -biotin incorporation assays: ^3H -biotin incorporated domain captured using HTS immobilon-P treated multiscreen Plates

In vitro biotinylation assays were carried out as described in section 4.2.6. At the completion of the assay, BPL catalysed reactions were stopped with the addition of 90 μL stopping buffer (110 mM EDTA, 50 mM tris pH 8.0) and 100 μL of each reaction was added to the wells of 96-well HTS multiscreen plate with a PVDF membrane (Merck Millipore) that had been pre-treated with 50 μL of 70% ethanol and 400 μL of MilliQ water under vacuum at 5 mmHg. The wells were washed by the addition of 1 X TBS under vacuum at 5 mmHg. 25 μL of Optiphase Supermix Scintillation fluid was added to each well and quantitation of protein-bound radiolabelled biotin was determined by liquid scintillation counting using a MicroBeta²® scintillation counter (Perkin Elmer, MA, USA).

4.2.6.3 *In vitro* ^3H -biotin incorporation assays with BPL inhibitors

Quantitation of BPL catalysed ^3H -biotin into SaPC90 was performed as described in section 4.2.6.2 The IC_{50} value of each compound was determined from a dose-response curve by varying the concentration of the inhibitor under the same enzyme concentration. The data was analysed with GraphPad Prism Software using a non-linear fit of \log_{10} (inhibitor) vs.

normalized response. The K_i , the absolute inhibition constant for a compound, was determined using Eq1 [6]:

$$K_i = \frac{IC_{50}}{1 + \frac{[S]}{K_M}}$$

Where K_M is the affinity of the substrate for the enzyme ([biotin] = 1.0 μ M for *SaBPL*) and [S] is the substrate concentration ([biotin] = 5 μ M).

4.2.7 SPR – binding Assay

The kinetics of the interaction between *SaBPL* and biotin was analysed using a BIAcore S200. *SaBPL* was immobilized onto the surface of a CM5 sensor chip using amide coupling chemistry. After activating the surface with 1-ethyl-3(3-dimethylaminopropyl)-carbodiimide (EDC) and N-hydroxysuccinimide (NHS), *SaBPL* solution at a concentration of 0.12 mg/mL in 10 mM sodium acetate buffer (pH 5.8) was applied at a constant flow rate of 5 μ L/min for 1200 seconds. Approximately 7,500 resonance units (RU) of *SaBPL* were immobilized. A control lacking immobilized ligand was performed alongside immobilized *SaBPL* in order to correct for bulk refractive index changes with buffer and distinguish non-specific binding events. Biotin was diluted in running buffer (10 mM HEPES pH 7.4, 150 mM NaCl, 0.005 % surfactant P20). As analytes bind to immobilized *SaBPL*, the refractive index at the surface alters in proportion to the change in mass, resulting in a change of RU (resonance units) value. The binding capacity of the surface depends on the level and activity of immobilized ligand. The maximum binding capacity (Rmax) of the immobilized ligand was calculated using Equation 2 where MW is the molecular weight of either the ligand or analyte, RL is the amount of immobilized ligand in RU and, Sm is the stoichiometry as defined by the number of binding sites on the ligand. The percent activity of the immobilized ligand was determined using Equation 3.

$$\text{Equation 2: } R_{\max} = (MW_{\text{analyte}} / MW_{\text{ligand}}) \times RL \times S_m$$

Equation 3: $\% \text{ ligand activity} = (\text{Rmax}_{\text{experiment}} / \text{Rmax}_{\text{theory}}) \times 100$

The binding affinity (K_D) was determined by transforming the time-dependent binding curves into an affinity-steady state 1:1 model using BIAcore S200 evaluation software (GE Healthcare).

4.3 Results and discussion

4.3.1 Purification of recombinantly expressed BPL proteins

Bacterial BPL proteins were recombinantly produced in *E. coli* using the pET-16b expression system containing a hexa-histidine tag at the C-terminus of the protein, except for *MtBPL* where the tag was at the N-terminus. *MtBPL* and *AcBPL* were expressed as soluble proteins in *E. coli* BL21(DE3) cells. For optimal expression *SaBPL* and *KpBPL* were expressed as soluble proteins in *E. coli* BL21(DE3)CodonPlus RIPL cells. These cells contain extra copies of the *argU*, *ileY*, *leuW* and *proL* tRNA genes to help facilitate expression of recombinant proteins in *E. coli* [7]. The His₆-tag facilitated protein purification using immobilized nickel affinity chromatography (IMAC) which produced highly pure protein in a single purification step. SDS-PAGE analysis of the IMAC purified material showed the expected molecular mass of 38 kDa for *SaBPL*, 28.9 kDa for *MtBPL*, 28.7 kDa for *AcBPL* and 36.3 kDa for *KpBPL* (Figure 4.1 lanes 2, 3, 4 and 5 respectively). The yields for each recombinantly produced BPL varied between 60 mg of *SaBPL*, 25 mg of *MtBPL* and 100 mg of *AcBPL* eluted from the column in a single step. It was difficult to over express *KpBPL* and, therefore, only 4 mg of material was obtained. All BPLs were found to be enzymatically active using the ³H-biotin incorporation assay with specific activities calculated to be 88 μM/min/mg, 69.4 μM/min/mg, 33.3 μM/min/mg and 125 μM/min/mg for *SaBPL*, *MtBPL*, *AcBPL* and *KpBPL* respectively.

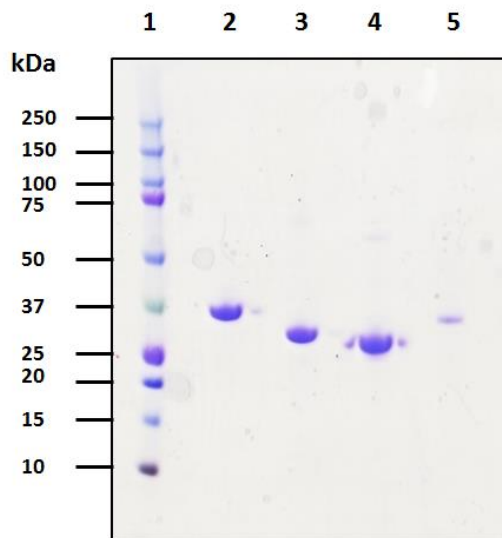


Figure 4.1 SDS-PAGE analysis of bacterially produced BPLs. IMAC purification of recombinantly expressed bacterial BPLs; lane 1, Precision Plus Protein Kaleidoscope Prestained Standards; lane 2, *Sa*BPL (250 mM imidazole); lane 3, *Mt*BPL (250 mM imidazole); lane 4, *Ac*BPL (250 mM imidazole); lane 5, *Kp*BPL (250 mM imidazole).

4.3.2 Purification and streptavidin-western analysis of apo GST-*Sa*PC90

The 90 C-terminal amino acids of the *S. aureus* biotin domain from pyruvate carboxylase (*Sa*PC90) was used as the biotin-accepting protein substrate in the BPL assays. Fusion of a GST tag at the N-terminus of the protein facilitated high level recombinant expression in *E. coli* and rapid protein purification using a glutathione agarose column and a thrombin cleavage site to facilitate the removal of the GST-tag if required. The attachment of biotin onto a conserved lysine residue within the biotin domain of biotin-dependent enzymes catalysed by BPL is a highly specific modification. Consequently, the overall fold of the biotin domain is highly conserved amongst species permitting biotinylation by non-native BPLs [1, 8-10]. To avoid biotinylation of the *Sa*PC90 domain by the endogenous *E. coli* BPL, the *Sa*PC90 biotin domain was expressed in the *E. coli* BM4062 strain [5]. This *E. coli* strain contains the *birA85* allele which encodes a temperature sensitive BPL that cannot catalyse protein biotinylation at 43 °C. *Sa*PC90 was expressed as a soluble protein at 43 °C for 3 hours and purification was performed using a glutathione agarose column. SDS-PAGE analysis of

the purified material revealed highly pure (>90%) material in the glutathione eluted fraction with the expected molecular mass of 36 kDa (figure 4.2 lane 2). Furthermore the BPL enzyme was found to attach biotin to the purified biotin domain using the ^3H biotin incorporation assay.

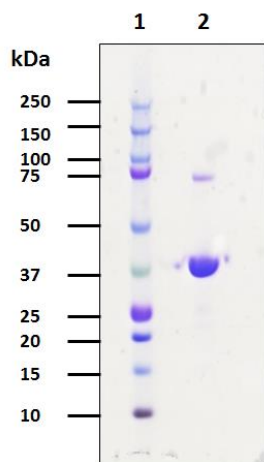


Figure 4.2 SDS-PAGE analysis of GST-*SaPC90*. GST affinity purification of GST-*SaPC90*; lane 1, Precision Plus Protein Kaleidoscope Prestained Standards; lane 2, eluted GST-*SaPC90* (10 mM reduced glutathione).

To confirm that the purified GST-*SaPC90* was indeed expressed in its apo (non-biotinylated) form, streptavidin blot analysis using a streptavidin-conjugated Alexa488 probe was performed. Purified GST-*SaPC90* was added to a mixture of biotin and MgATP in 2 parallel reactions. *AcBPL* was added to the first tube to allow the biotinylation reaction to take place. An equivalent volume of buffer was added to a second reaction, to serve as the non-biotinylated control. *AcBPL* was chosen here as it has a molecular weight different to GST-*SaPC90* allowing the two proteins to be resolved by SDS-PAGE. The reaction components were separated by SDS-PAGE and Western analysis was performed to compare biotinylated and non-biotinylated reactions (figure 4.3). As shown in figure 4.3a, in the absence of BPL, there is minimal signal corresponding to biotinylated domain, indicating that the GST tagged *SaPC90* domain was expressed and predominantly in its apo form.

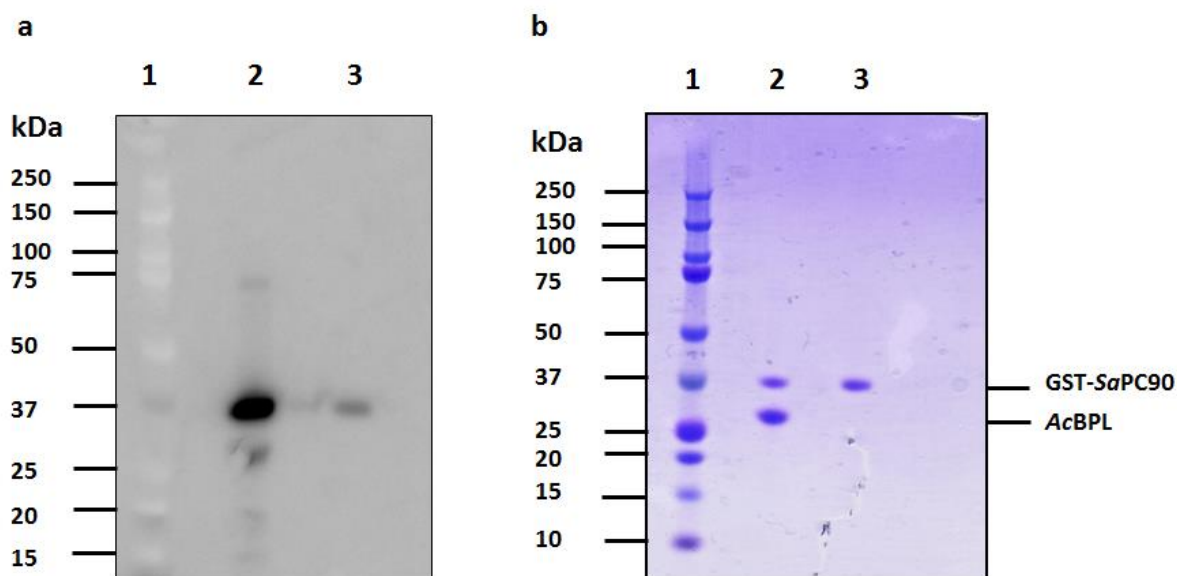


Figure 4.3 Streptavidin Western analysis of Purified GST-SaPC90. a). Biotin incorporation was set up as discussed in 3.2.6 using *AcBPL* and analysed using a western blot with streptavidin-Alexa488. b). SDS-PAGE analysis of reaction; lane 1, Precision Plus Protein Kaleidoscope Prestained Standards; lane 2, Biotinylation of GST-SaPC90 (36 kDa) by *AcBPL* (27.5 kDa); lane 3, negative control reaction (no *AcBPL* added). Panel B served as the loading control.

4.3.3 Development of high-throughput *In vitro* ^3H -biotin incorporation assay using HTS multiscreen immobilon-P plates

The current *in vitro* biotinylation assay that has been employed in our laboratory involves measuring the incorporation of ^3H -biotin into an acid precipitable substrate biotin carboxyl carrier protein (BCCP) (section 4.2.6.1) [1]. Following the BPL catalysed reaction, protein is precipitated onto Whatman paper using trichloroacetic acid, and washed with cold ethanol to remove unincorporated radiolabel. This facilitated the quantitation of ^3H -biotin-BCCP on filters using a scintillation counter. Whilst this filter-based assay is robust and yields reliable quantitative data, it does have limitations that impede its use in high-throughput applications, such as numerous pipetting and manual handling steps that introduce the potential for errors and assay to assay variation. Therefore, a more robust BPL assay was required to measure the bioactivity of compounds planned for this study. One of the hurdles that must be addressed when performing this radiolabel ligand binding assay is the need to remove the

unincorporated radiolabel after the biotinylation reaction. This has been performed through the use of filter paper and protein precipitation (as described above) or gel-filtration [11]. However, these steps are not easily automated [11]. To overcome this, an approach using the HTS-Multiscreen system was employed. The Multiscreen assay system is a rapid, multi-sample filter based system that has a number of applications including ligand binding and cell based assays [3, 12]. Here, multiscreen plates were used to capture the *SaPC90* domain via a vacuum manifold and then quantitate the amount of incorporated ^3H -biotin by liquid scintillation counting. Multiscreen plates that contain an immobilonTM PVDF membrane were used for protein capture. The PVDF membrane allows for high protein binding to capture the biotinylated domain, but not the low molecular weight ^3H -biotin which passes through the membrane under vacuum. Scintillation fluid can then be added directly to each well of the 96-well plate to quantitate the amount of ^3H -biotinylated *SaPC90*.

The first experiment performed was to investigate whether the HTS-multiscreen plates could be used to capture ^3H -biotinylated *SaPC90* with sufficiently strong signal above the background. The accepted signal to background ratio for enzyme assays should be greater than 10 [13]. An *in vitro* biotinylation reaction was set up using *M. tuberculosis* BPL (*MtBPL*) and 125 nM of ^3H -biotin. This reaction was performed for 4 hours when it was assumed that all of the available biotin was incorporated into protein. The captured protein substrate was quantified with one of three commercially available scintillation fluids: Ultima Gold F, Microscint PS and Optiphase Supermix (Perkin Elmer). All three scintillation fluids have high counting efficiency for ^3H containing samples, and all contain the same solvent Diisopropylnaphthaline [14]. As shown in figure 4.4, the HTS-multiscreen plates were able to capture appropriate amounts of ^3H -biotinylated *SaPC90*. The use of either Ultima Gold F, Microscint PS or Optiphase supermix scintillation fluids gave average ‘counts per minute’ (CPM) of 1066, 3169 and 25236 and calculated signal to background ratios of 25.8, 15.5 and 47.2 respectively. All three scintillation fluids had signal to background ratios that were

higher than the minimal signal to background ratio for enzyme assays [13]. Optiphase supermix scintillation fluid gave the highest CPM, presumably because it is optimized for liquid scintillation counting in microplates. As Optiphase scintillation fluid gave the highest signal, it was chosen for all further *in vitro* biotinylation assays.

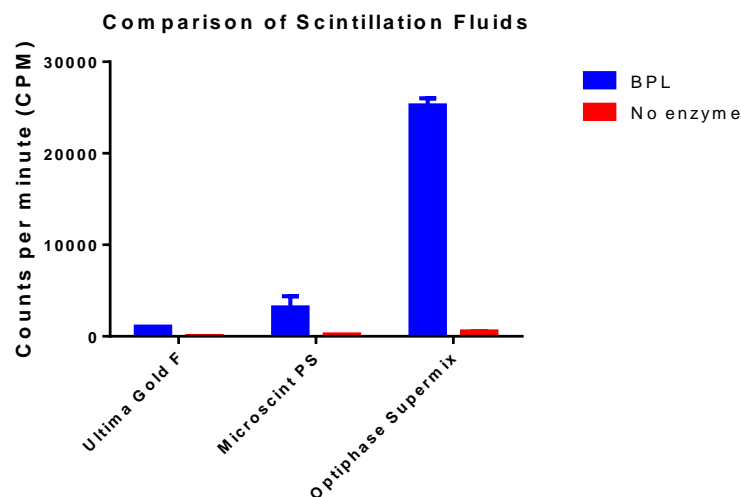


Figure 4.4 *In vitro* ^3H -biotin incorporation assays measured with different scintillation fluids. *In vitro* ^3H -biotin incorporation assays with *Mt*BPL were set up using $0.125\ \mu\text{M}$ ^3H -biotin. $25\ \mu\text{L}$ of each scintillation fluid was added to either BPL catalysed samples (blue) or non-catalysed reactions (red). Liquid Scintillation counting was performed on a MicroBeta2 scintillation counter using normal counting mode. Data is plotted as the average of 3 readings from 1 well of the 96-well plate. Error bars represent standard error of the means (SEM) of data. All experiments were conducted in triplicate at three different occasions.

The next experiment determined the optimum concentration of ^3H -biotin to include in each reaction. *In vitro* biotinylation reactions were set up with *Mt*BPL using 2-fold serial dilutions of ^3H -biotin. The total counts for each reaction ranged from 143,000 CPM at $500\ \text{nM}$ ^3H -biotin to 3175 CPM at $3.9\ \text{nM}$ ^3H -biotin (Figure 4.5). The results with a concentration of $62.5\ \text{nM}$ ^3H -biotin were 10172 CPM with a signal to background ratio of 44.3 (figure 3.5). To characterize BPL inhibitors biotinylation assays must be performed under steady state conditions, where the reaction is measured within the first 10% of the reaction [13]. As $62.5\ \text{nM}$ of ^3H -biotin in a reaction that was at completion was $\sim 10,000$ CPM. Capturing the

reaction at 10% would yield ~1000 CPM, and still have a signal to background ratio ≥ 10 . Therefore 62.5 nM ^3H -biotin was determined to be the most suitable for the BPL enzyme assay.

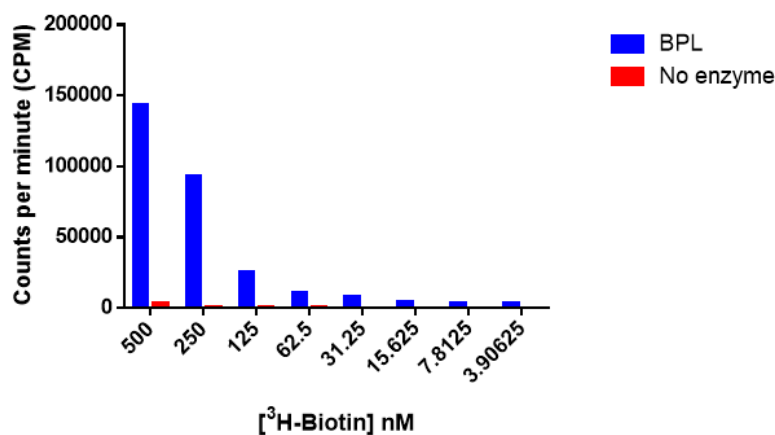


Figure 4.5 *In vitro* ^3H -biotin incorporation assays with varying concentrations of ^3H -biotin. ^3H -biotin incorporated assays were set with a 2-fold serial dilution series of ^3H -biotin. The total biotin concentration was 5 μM in each reaction. *MtBPL* catalysed reactions are shown in blue, while corresponding non-catalysed reactions are shown in red. The data represents 1 is plotted as the average of 3 readings from 1 well of the 96-well plate. Error bars represent standard error of the means (SEM) of data. All experiments were conducted in triplicate at 3 different occasions.

To show that the *in vitro* ^3H -biotinylation assay can be measured under steady state conditions (i.e in the linear phase), a series of biotinylation reactions were set up using *MtBPL* and terminated at different time points (figure 4.6). After 30 minutes ~1200 CPM of ^3H -biotinylated *SaPC90* could be detected, which was the equivalent of ~10% of the reaction. This result demonstrates that this alternative biotinylation assay can be used to characterize BPL inhibitors.

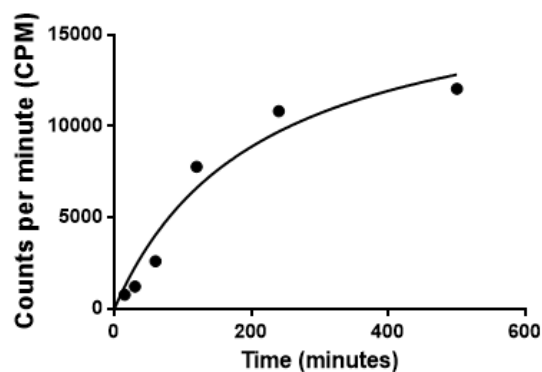


Figure 4.6 Time course ^3H -biotinylation assay with *MtBPL*. ^3H -biotinylation assays were set up and started with the addition of *MtBPL* (50 nM). Each reaction was stopped after either 15, 30, 60, 120, 240 or 480 minutes after the addition of *MtBPL*. The samples were prepared using the multiscreen filtration system and counted using liquid scintillation on a MicroBeta2 scintillation counter. The data is plotted as the average of 3 readings from 1 sample.

To validate the use of this ^3H -biotin incorporation assay to characterize the inhibition of rationally designed BPL inhibitors, two known *SaBPL* inhibitors (BPL068 and biotinol-5'AMP) were characterized. BPL068 inhibited *SaBPL* with an IC_{50} of 1.3 μM and had a calculated K_i value of 0.23 μM . (figure 4.7) This was in good agreement with the previously published K_i value of BPL068 (K_i *SaBPL* = 0.09 μM) [15]. Biotinol-5'AMP, was also characterized (figure 4.8). Biotinol-5'AMP inhibited *SaBPL* with a K_i of 16 nM, which was in good agreement with the reported K_i value (20 nM) determined in our laboratory [16]. This new ^3H -biotin incorporation assay with the multiscreen filtration system is now placed to measure BPL enzyme activity and to characterize rationally designed BPL inhibitors. This assay has been used in chapters 5-9 to measure the inhibition constants of rationally designed BPL inhibitors.

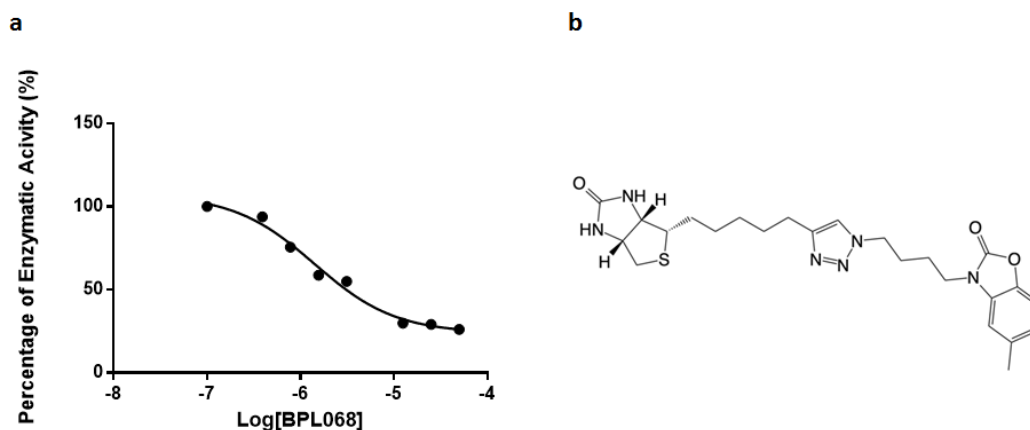


Figure 4.7 Inhibition of SaBPL activity by BPL068. a). An *in vitro* ^3H -biotin incorporation assay was setup as described in section (4.2.6). The IC_{50} of BPL068 was determined by fitting the non-linear regression of the data in GraphPad Prism 6.0 and expressed as the mean of the data. The inhibition was calculated as the percentage of enzyme activity correlated to 100% of total enzyme activity without BPL068 in the reaction containing a saturating concentration of 5 μM biotin and 3 mM ATP. Determined IC_{50} value of BPL068 was $1.4 \pm 0.06 \mu\text{M}$. The K_i value was calculated to be $0.23 \pm 0.01 \mu\text{M}$ with respect to the biotin substrate. The data is plotted as the average of 3 readings from 1 well of the 96-well plate. Error bars represent standard error of the means (SEM) of data. All experiments were conducted in triplicate at three different occasions b). Structure of BPL068.

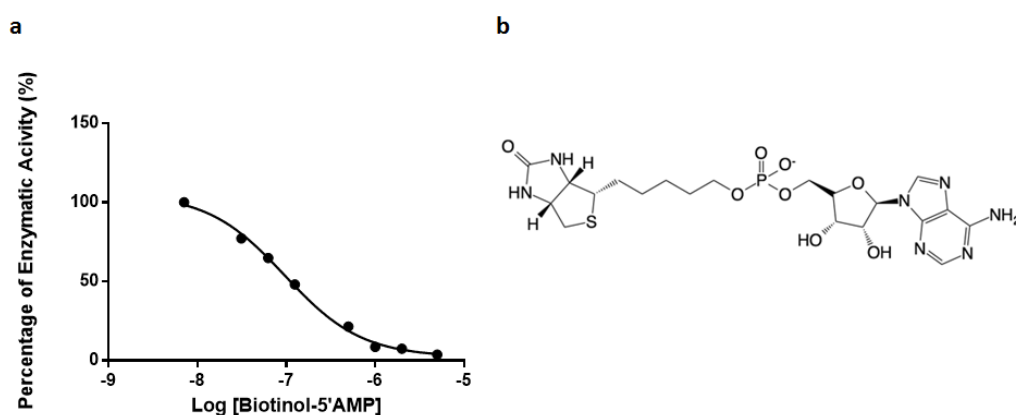


Figure 4.8 Inhibition of SaBPL activity by biotinol-5'AMP. a). An *in vitro* ^3H -biotin incorporation assay was set up as described in section (4.2.6). The IC_{50} of biotinol-5'AMP was determined by fitting the non-linear regression of the data in GraphPad Prism 6.0 and expressed as the mean of the data. The inhibition was calculated as the percentage of enzyme activity correlated to 100% of total enzyme activity without biotinol-5'AMP in the reaction containing a saturating concentration of 5 μM biotin and 3 mM ATP. Determined IC_{50} value of biotinol-5'AMP was $96.8 \pm 5.5 \text{ nM}$. The K_i value was calculated to be $16.1 \pm 0.9 \text{ nM}$ with respect to the biotin substrate. The data is plotted as the average of 3 readings from 1 well of the 96-well plate. Error bars represent standard error of the means (SEM) of data. All experiments were conducted in triplicate at three different occasions b). Structure of biotinol-5'AMP.

4.3.4 Surface Plasmon Resonance Binding assay

Surface plasmon resonance (SPR) is a powerful tool for early drug discovery applications as it can monitor the kinetics of biomolecular interactions in real time, providing association rates, dissociation rates and affinity measurements [17]. Here, one molecule is immobilized onto the surface of a sensor chip (the ligand). An interacting partner, referred to as the analyte, is then injected into solution across the sensor surface. As the analyte binds to the ligand, the refractive index at the surfaces alters in proportion to a change in mass. This results in an SPR signal (measured as Resonance units, RU), and is detected in real time [17]. There are several approaches for immobilizing the ligand to the sensor chip surface, including, covalent immobilization, high affinity capture and hydrophobic adsorption [17]. In this project, covalent immobilization of BPL was performed through the use of amine coupling onto CM5 sensor chips. This has a matrix of carboxymethylated dextran that is attached to a gold surface. In amine coupling, the carboxymethylated dextran surface is activated with a mixture of 1-ethyl-3(3-dimethylaminopropyl)-carbodiimide (EDC) and N-hydroxysuccinimide (NHS), to give reactive succinimide esters. Ligands were then covalently linked with the dextran matrix through the reaction of amine groups with the esters on the activated surface (figure 4.9).

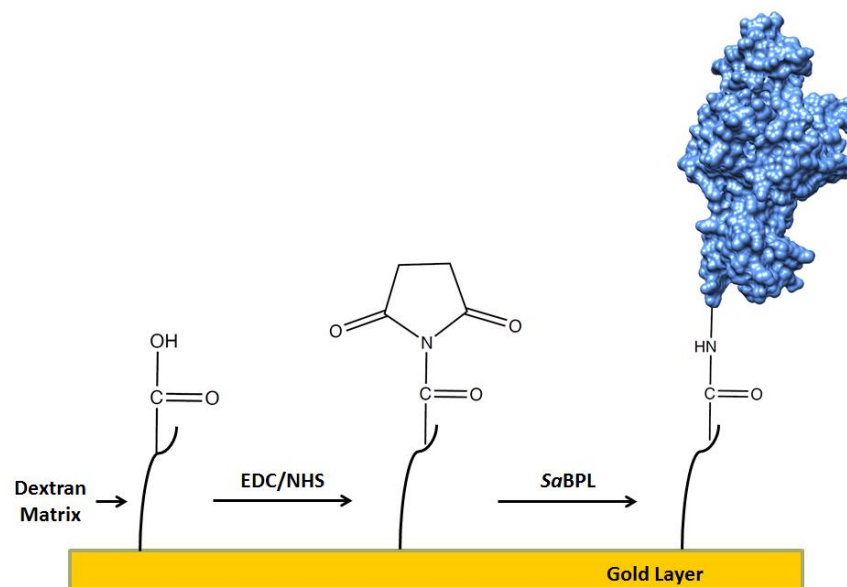


Figure 4.9 Amide coupling of *SaBPL* to the CM5 sensor chip surface. The carboxylmethylated dextran on the surface of the gold layer on the sensor chip was activated with the mixture of EDC/NHS to give succinimide esters. *SaBPL* was then immobilized randomly on the surface by the reaction that occurs between its amide groups and the esters on the surface of the sensor chip.

The binding affinity of an analyte is represented by the dissociation constant (K_D). The K_D is equal to the dissociation rate over the association rate (K_d/K_a). As mentioned in chapter 2 *SaBPL* exhibits an ordered binding mechanism for its two substrates with biotin binding first followed by ATP. Therefore, biotin represents an appropriate control analyte to establish an SPR binding assay that can be used to characterize the binding of rationally designed BPL inhibitors. *SaBPL* was immobilized to the surface of a CM5 sensor chip using amine coupling. To establish whether the immobilized *SaBPL* retained biological activity, the native substrate biotin was injected over the sensor chip surface. Figure 4.10 shows that increase in resonance units was observed with increasing concentrations of biotin from 2 μM to 500 μM . Biotin bound with fast on and off rates as indicated by the rapid response at the start and end of the injection. The association and dissociation rates were outside of the range of quantification of the Biacore analysis software. Therefore, the K_D was calculated using steady state analysis. In steady state analysis, the response obtained at different concentrations of biotin was fitted to a steady state model by the Biacore analysis software. The K_D obtained

from two independent experiments were $25.9 \pm 2.7 \mu\text{M}$ and $21.1 \pm 4.3 \mu\text{M}$ respectively. The binding affinities obtained from these experiments are in good agreement with the published K_D for biotin ($10 \mu\text{M}$) [15]. The experimental R_{max} obtained from biotin binding was then used to assess the percent activity of the immobilized ligand. Typically around 7500 resonance units of *Sa*BPL was immobilized onto the sensor chip surface, leading to a theoretical R_{max} of ~ 48.2 . As a result 93% of immobilized ligand on the sensor chip was considered active. This SPR binding assay will be used to characterize the binding of rationally designed BPL inhibitors as discussed in chapter 8.

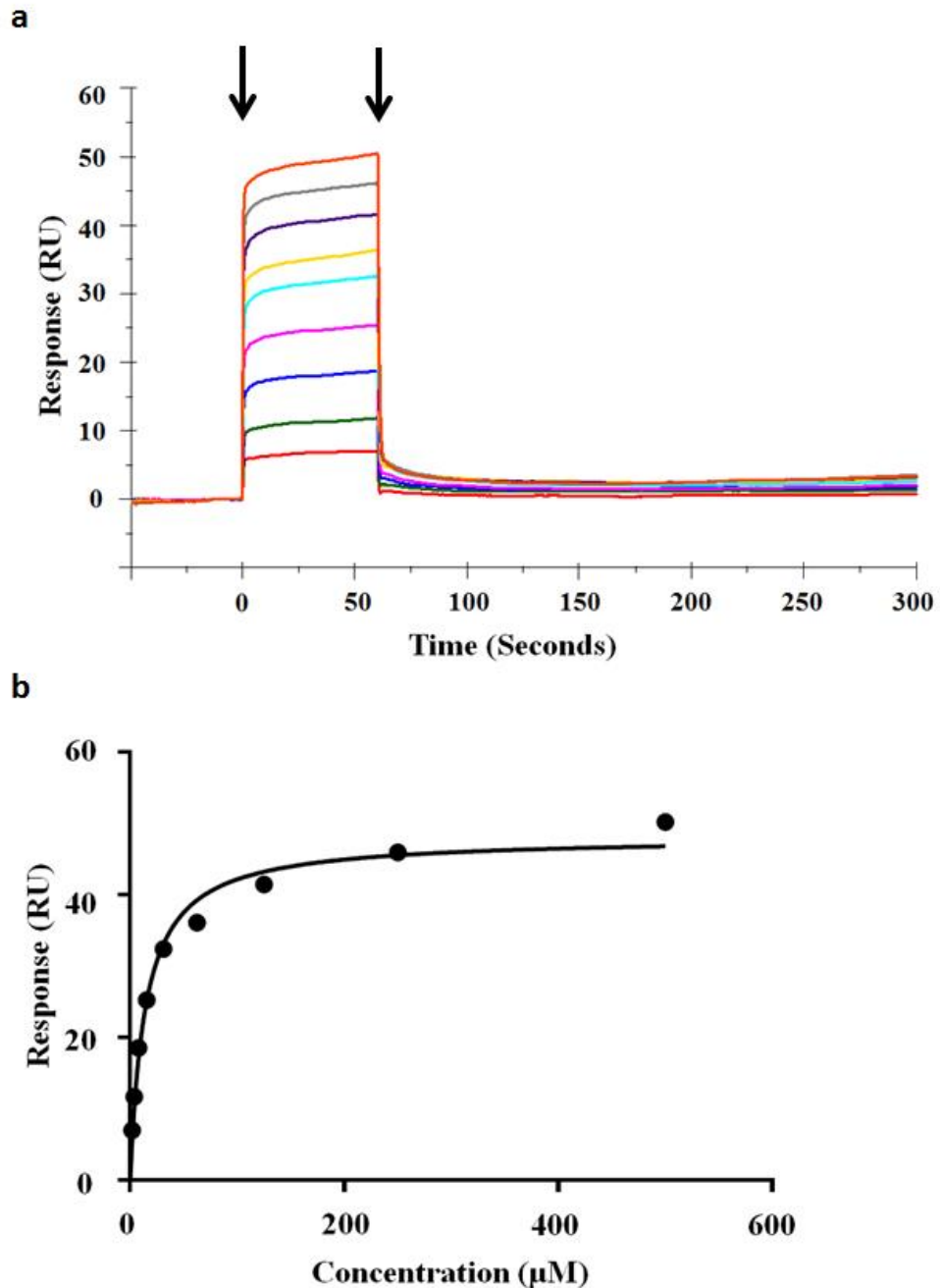


Figure 4.10 Dose-response SPR-binding analysis. a). Time-dependent binding curves of biotin correlated to dose-response. Arrows represent the start and the end of injection of biotin. Concentrations of biotin used were: 2 μM (red), 3.9 μM (green), 7.8 μM (blue), 15.6 μM (magenta), 31.25 μM (cyan), 62.5 μM (yellow), 125 μM (purple), 250 μM (grey) and 500 μM (orange). b). Concentration vs response plot of biotin binding. Binding analysis based on affinity-steady state 1:1 model. The binding affinity (K_D) of biotin to SaBPL was calculated to be $21.1 \pm 4.3 \mu\text{M}$

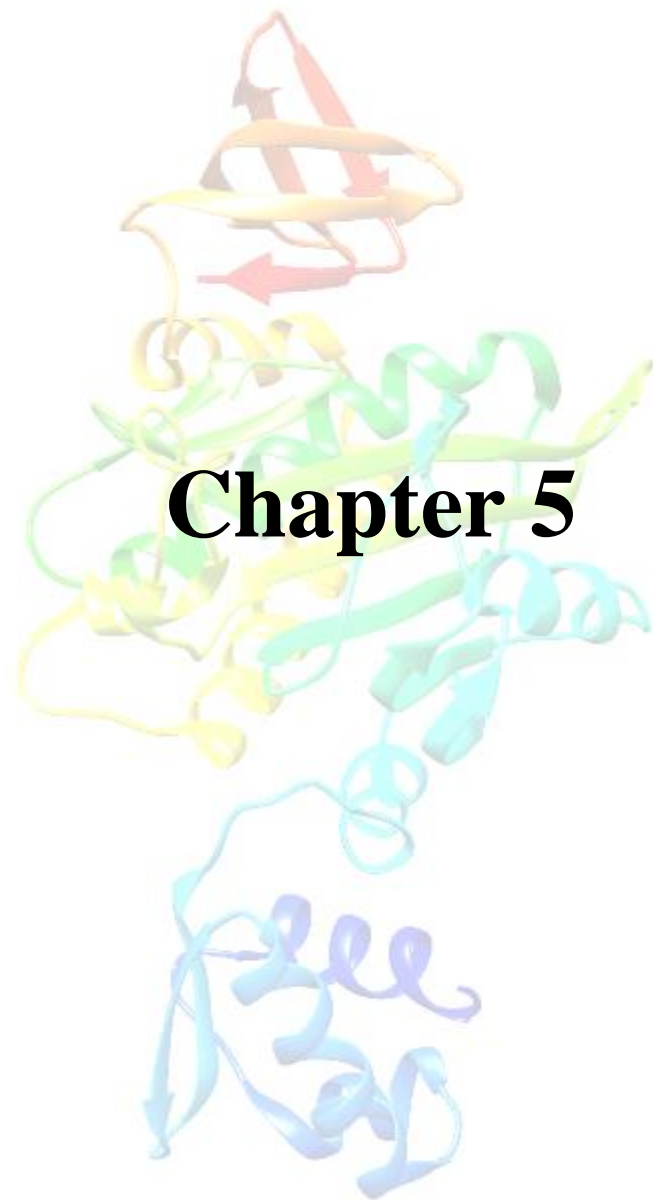
4.4 Conclusions

In this chapter I have developed a number of protein biochemistry techniques that are necessary to characterize BPL inhibitors. Firstly, I optimized the expression and purification of His-tagged BPLs from clinically relevant bacteria. I obtained highly pure material in a single step, that was active in BPL enzyme assays. I also demonstrated the expression and purification of apo (non-biotinylated) SaPC90 required for the enzyme assays. In the second part of this chapter I developed an alternative *in vitro* biotinylation assay with improved throughput, where the biotinylated protein substrate was captured through the use of HTS-multiscreen plates. This assay was used in later chapters to characterize rationally designed BPL inhibitors. Finally I developed a SPR binding assay, that was characterized using the native substrate biotin. This SPR binding assay was used to monitor the kinetics of inhibitor binding in real time. All of the techniques developed in this chapter were used to help identify favourable inhibitor properties, ultimately leading to the development of a pre-clinical candidate.

4.5 References

1. Chapman-Smith, A., et al., *Molecular recognition in a post-translational modification of exceptional specificity. Mutants of the biotinylated domain of acetyl-CoA carboxylase defective in recognition by biotin protein ligase*. J. Biol Chem, 1999. **274**(3): p. 1449-1457.
2. Udenfriend, S., L. Gerber, and N. Nelson, *Scintillation proximity assay: a sensitive and continuous isotopic method for monitoring ligand/receptor and antigen/antibody interactions*. Anal Biochem, 1987. **161**(2): p. 494-500.
3. Millipore, M. *MultiScreen Methods: Efficient Low-energy Radioisotope Detection in Vial-based Liquid Scintillation Counting Using the MultiScreen Assay System*. [cited 2014 20/1/14]; Technical note/Brochure]. Available from: http://www.merckmillipore.com/AU/en/product/MultiScreen-Plate-Overview,MM_NF-C7781#documentation.
4. Myszka, D.G. and R.L. Rich, *Implementing surface plasmon resonance biosensors in drug discovery*. Pharm Sci Technolo Today, 2000. **3**(9): p. 310-317.
5. Barker, D.F. and A.M. Campbell, *Use of bio-lac fusion strains to study regulation of biotin biosynthesis in Escherichia coli*. J. Bacteriol, 1980. **143**(2): p. 789-800.
6. Yung-Chi, C. and W.H. Prusoff, *Relationship between the inhibition constant (KI) and the concentration of inhibitor which causes 50 per cent inhibition (I50) of an enzymatic reaction*. Biochem Pharmacol, 1973. **22**(23): p. 3099-3108.
7. Stratagene, *BL21-CodonPlus Competent Cells - instruction manual*, Stratagene: LaJolla, California.
8. Chapman-Smith, A. and J.E. Cronan Jr, *The enzymatic biotinylation of proteins: a post-translational modification of exceptional specificity*. Trends Biochem Sci, 1999. **24**(9): p. 359-363.
9. Chapman-Smith, A. and J.E. Cronan Jr, *Molecular Biology of Biotin Attachment to Proteins*. J. Nutr, 1999. **129**(2): p. 477S-484S.
10. Chapman-Smith, A., et al., *Molecular Recognition in a Post-translational Modification of Exceptional Specificity*. J. Biol Chem, 1999. **274**(3): p. 1449-1457.
11. Glickman, J., A. Schmid, and S. Ferrand, *Scintillation proximity assays in high-throughput screening*. Assay drug dev technol, 2008. **6**(3): p. 433-455.
12. Millipore, M. *Multiscreen Methods: Guidelines for Bioassays on MultiScreen Filter Plates*.
13. *Assay Guidance Manual*, G.S. Sittampalam, Editor 2016, Eli Lilly & Company and the National Center for Advancing Translation Sciences: Bethesda, Maryland.

14. Edler, R. *Application Note: Cocktails for Liquid Scintillation Counting*. 2015.
15. Soares da Costa, T.P., et al., *Selective inhibition of Biotin Protein Ligase from Staphylococcus aureus*. *J. Biol Chem*, 2012. **287**(21): p. 17823-17832.
16. Costa, T.P.S.d., *Exploring the structure-function relationship of Biotin Protein Ligase from Staphylococcus aureus: Implications for selective inhibitor design in Discipline of Biochemistry*2012, University of Adelaide: Adelaide, South Australia.
17. Healthcare, G., *Biacore assay Handbook*, 2012, GE Healthcare: GE Healthcare Bio-Sciences AB, Uppsala, Sweden.



Statement of Authorship

Title of Paper	Improved Synthesis of Biotinol-5'-AMP: Implications for Antibacterial Discovery
Publication Status	<input checked="" type="checkbox"/> Published <input type="checkbox"/> Accepted for Publication <input type="checkbox"/> Submitted for Publication <input type="checkbox"/> Unpublished and Unsubmitted work written in manuscript style
Publication Details	William Tieu, Steven W. Polyak, Ashleigh S. Paparella, Min Y. Yap, Tatiana P. Soares da Costa, Belinda Ng, Geqing Wang, Richard Lumb, Jan M. Bell, John D. Turnidge, Matthew C. J. Wilce, Grant W. Booker, and Andrew D. Abell, 2015, <i>ACS Medicinal Chemistry Letters</i> , 6, 216-220

Candidate Author

Name of Principal Author (Candidate)	Ashleigh S. Paparella
Contribution to the Paper	<i>In vitro</i> Biotinylation assay of biotinol-5'-AMP against SαBPL. Analysis of Inhibition data
Overall percentage (%)	5%
Certification:	This paper reports on original research I conducted during the period of my Higher Degree by Research candidature and is not subject to any obligations or contractual agreements with a third party that would constrain its inclusion in this thesis..
Signature	Date 11/11/2016

Co-Author Contributions

By signing the Statement of Authorship, each author certifies that:

- the candidate's stated contribution to the publication is accurate (as detailed above);
- permission is granted for the candidate to include the publication in the thesis; and
- the sum of all co-author contributions is equal to 100% less the candidate's stated contribution.

Name of Co-Author	William Tieu
Contribution to the Paper	Primary role in manuscript preparation Synthesis and characterization of biotinol-5'AMP Overall Contribution: 20%
Signature	Date 25/10/16

Name of Co-Author	Steven W. Polyak
Contribution to the Paper	Performed cell culture assays Provided project direction and supervised biological aspects of the project and is corresponding author on manuscript. Overall Contribution: 15%
Signature	Date 24/10/2016

Name of Co-Author	Min Y. Yap		
Contribution to the Paper	Performed biochemical assays and analysis of data Overall Contribution: 5%		
Signature		Date	18/10/16

Name of Co-Author	Tatiana P. Soares da Costa		
Contribution to the Paper	Performed biochemical assays and analysis of data Overall Contribution: 5%		
Signature		Date	10/10/16

Name of Co-Author	Belinda Ng		
Contribution to the Paper	Performed biochemical assays and analysis of data Overall Contribution: 5% Author was not contactable.		
Signature		Date	

Name of Co-Author	Geging Wang		
Contribution to the Paper	Performed biochemical assays and analysis of data Overall Contribution: 5%		
Signature		Date	25/10/2016

Name of Co-Author	Richard Lumb		
Contribution to the Paper	Performed antibacterial susceptibility assays Overall Contribution: 5%		
Signature		Date	26/10/2016

Name of Co-Author	Jan M. Bell		
Contribution to the Paper	Performed antibacterial susceptibility assays Overall Contribution: 5%		
Signature		Date	26/10/2016

Name of Co-Author	John D. Tumidge		
Contribution to the Paper	Provided direction for antibacterial susceptibility assays Overall Contribution: 5%		
Signature		Date	26/10/2016

Name of Co-Author	Matthew C. J. Wiice		
Contribution to the Paper	Provided direction in protein chemistry Overall Contribution: 5%		
Signature		Date	11/10/2016

Name of Co-Author	Grant W. Booker		
Contribution to the Paper	Provided direction in all aspects of protein chemistry and supervised biological aspects of the project. Overall Contribution: 5%		
Signature		Date	19/10/2016

Name of Co-Author	Andrew D. Abell		
Contribution to the Paper	Provided direction in all aspects of synthetic chemistry and is corresponding author Overall Contribution: 15%		
Signature		Date	19/10/2016

Improved Synthesis of Biotinol-5'-AMP: Implications for Antibacterial Discovery

William Tieu,^{†,‡,¶} Steven W. Polyak,^{*,‡,‡,‡} Ashleigh S. Paparella,[‡] Min Y. Yap,^{§,∇} Tatiana P. Soares da Costa,^{‡,○} Belinda Ng,[‡] Geqing Wang,^{‡,◆} Richard Lumb,^{||} Jan M. Bell,^{||} John D. Turnidge,^{‡,||} Matthew C. J. Wilce,[§] Grant W. Booker,^{‡,‡} and Andrew D. Abell^{*,†,‡}

[†]School of Chemistry and Physics, University of Adelaide, Adelaide, South Australia 5005, Australia

[‡]School of Molecular and Biomedical Science, University of Adelaide, Adelaide, South Australia 5005, Australia

[§]School of Biomedical Science, Monash University, Victoria 3800, Australia

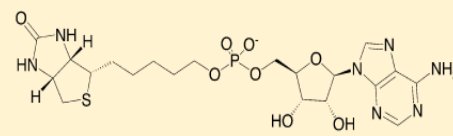
^{||}Microbiology and Infectious Diseases Directorate, SA Pathology, Women's and Children's Hospital, Adelaide, South Australia 5006, Australia

[∇]Centre for Molecular Pathology, The University of Adelaide, Adelaide, South Australia 5005, Australia

Supporting Information

ABSTRACT: An improved synthesis of biotinol-5'-AMP, an acyl-AMP mimic of the natural reaction intermediate of biotin protein ligase (BPL), is reported. This compound was shown to be a pan inhibitor of BPLs from a series of clinically important bacteria, particularly *Staphylococcus aureus* and *Mycobacterium tuberculosis*, and kinetic analysis revealed it to be competitive against the substrate biotin. Biotinol-5'-AMP also exhibits antibacterial activity against a panel of clinical isolates of *S. aureus* and *M. tuberculosis* with MIC values of 1–8 and 0.5–2.5 $\mu\text{g}/\text{mL}$, respectively, while being devoid of cytotoxicity to human HepG2 cells.

KEYWORDS: Antibiotics, enzyme inhibitors, biotin protein ligase, chemical synthesis, drug design



<i>Staphylococcus aureus</i>	K_i 18 nM	MIC 1 - 4 $\mu\text{g}/\text{ml}$
<i>Mycobacteria tuberculosis</i>	K_i 52 nM	MIC 0.5 - 2.5 $\mu\text{g}/\text{ml}$

Adenylate-forming enzymes play a central role in many key metabolic pathways such as ribosomal and nonribosomal peptide synthesis, fatty acid synthesis, and enzyme regulation. As such they are of significant interest as potential drug targets.^{1,2} These enzymes function by activating a carboxylate metabolite on reaction with ATP to form an acyl-AMP intermediate, which then reacts with a nucleophile to generate the desired product (Figure 1). The acyl-AMP reaction intermediates possess a high binding affinity for the enzyme, often 2–3 orders of magnitude greater than the carboxylic acid or ATP substrates.^{3,4}

The inhibition of biotinol-5'-AMP 1, one such intermediate produced by the biotin protein ligase (BPL) catalyzed reaction of biotin and ATP, has attracted recent interest as a potential new class of antibiotic.^{5,6} An important approach to these inhibitors involves replacing the hydrolytically unstable acyl phosphate linker of 1 with a more stable bioisostere, as in biotinol-5'-AMP 2.^{6,7} This phosphodiester mimic is a potent inhibitor of BPLs from *S. aureus*, *Escherichia coli*, and *Homo sapiens*.^{6,8} However, its antibacterial properties have not been investigated. Other acyl phosphate bioisosteres used in this context include, sulfonyl and 1,2,3-triazole groups, among others.^{5,6,9–25} Importantly, acyl-AMP mimics (containing sulfonyl and 1,2,3-triazole isosteres, see 3 and 4 in Figure 1) have been shown to be potent agents against *M. tuberculosis* and *S. aureus*, respectively.²⁶ Given the central importance of

biotinol-5'-AMP 2 as a BPL inhibitor, we now report an expedient method for its synthesis and an investigation of its activity profile against clinically significant bacteria.

Biotinol-5'-AMP 2 is reportedly prepared according to a modified "phosphodiester" procedure as shown in Scheme 1.⁷ However, in our hands this procedure gave an unsatisfactory overall yield of 9% from adenosine 5. The key limitation with this procedure was a DCC mediated coupling of 6 and 8 to give phosphodiester 9, with subsequent *in situ* deprotection of the acetonide group to give 2. An overall yield of 15% was obtained over these two steps. Attempts to optimize the DCC coupling step using other solvents, particularly pyridine or DMF, or longer reaction times (up to 48 h) failed to improve the yield. The use of other acids for the deprotection (20–60% acetic acid instead of TFA) similarly failed to improve the efficiency of this sequence. Thus, an alternative approach to biotinol-5'-AMP 2 was investigated that would avoid the problematic DCC coupling and hemiacetal deprotection steps, see Scheme 2. This methodology was then used to prepare sufficient quantities of 2 for antimicrobial studies. A very recent report, investigating biotinol-5'-AMP 2 and its phosphite analogues as human BPL

Received: November 20, 2014

Accepted: December 11, 2014

Published: December 11, 2014

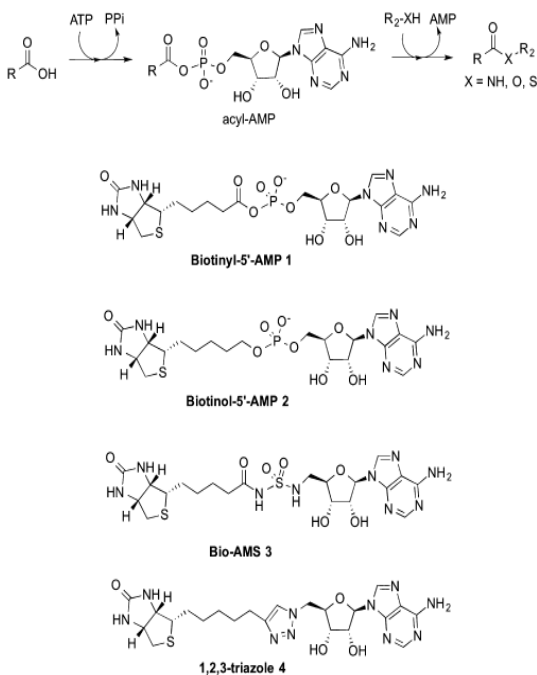
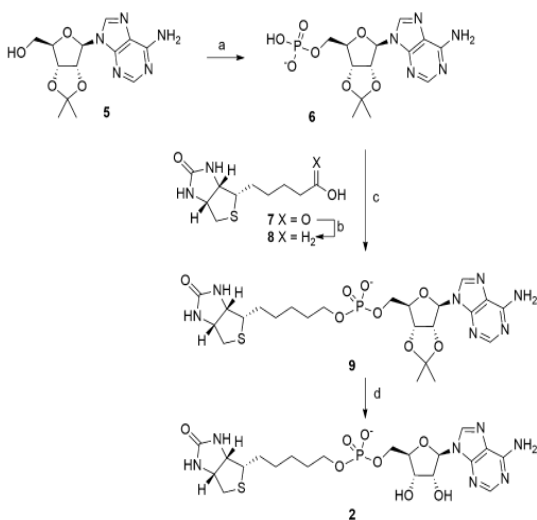


Figure 1. General catalytic mechanism of adenylate forming enzymes (top). Chemical structures are shown for the acyl-AMP intermediate of BPL biotinyl-5'-AMP (1) and its phosphodiester mimic biotinol-5'-AMP (2), acyl-sulfamide biotin adenosine monosulfamide (Bio-AMS) (3), and 1,2,3-triazole (4).

Scheme 1^a

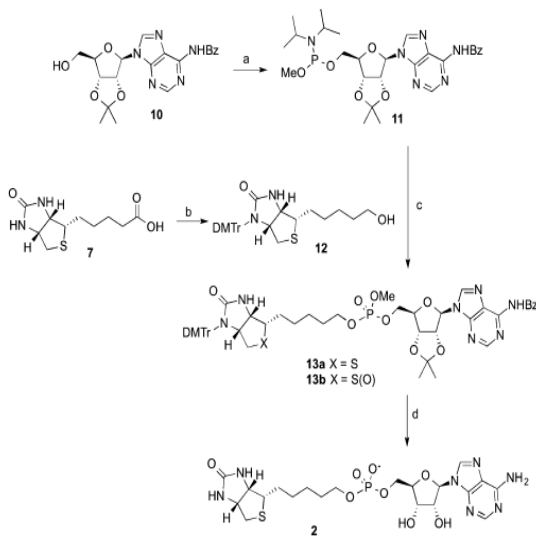


^aReagents and conditions: (a) (i) $POCl_3$, $PO(Et)_3$; (ii) TEAB buffer; (b) (i) $SOCl_2$, MeOH; (ii) $LiAlH_4$, THF; (c) DCC, py; (d) 60% $AcOH_{(aq)}$.

inhibitors, implemented a similar strategy to Scheme 2 for the synthesis of biotinol-5'-AMP 2.²⁵

The alternative "phosphoramidate" synthesis commenced with the conversion of *N*-benzoyl protected adenosine 10 to the corresponding phosphoramidate 11 in 67% yield.²⁷ Biotinol 12 was synthesized as previously reported.²⁸ Specifically, biotin 7 was esterified under acidic conditions to the corresponding methyl ester, followed by selective *N*-tritylation of the ureido ring of biotin methyl ester and a subsequent reduction to give

Scheme 2^a



^aReagents and conditions: (a) $CIP(OMe)N(iPr)_2$, Et_3N , DCM; (b) (i) $SOCl_2$, MeOH; (ii) $DMTrCl$, DCM; (iii) $LiAlH_4$, THF; (c) (i) 5-ETT, MeCN; (ii) $tBuOOH$; (d) (i) 10% TFA, DCM; (ii) NH_3OH , MeOH/ H_2O ; (iii) NaI, H_2O .

biotinol 12. The phosphoramidate 11 was then coupled to biotinol 12 using 5-(ethylthio)-1*H*-tetrazole, with oxidation of the resulting phosphite with *tert*-butyl hydrogen peroxide (TBHP) and immediate quenching with sodium metabisulfite to give phosphotriester 13a in 59%. Attempts at coupling 11 with 12 without the addition of bisulfate gave predominately the overoxidized sulfone analogue 13b, as confirmed by mass spectrometry, see Supporting Information. The formation of 13b was judged to be irreversible, as reduction of 13b to 13a would have resulted in epimerization of the biotin alkyl chain.²⁹ A sequential treatment of phosphotriester 13a with TFA, NH_3OH , and NaI followed by purification of the crude product by reverse phase HPLC gave 2 in >95% purity. This sequence gave biotinol-5'-AMP 2 with an overall 2-fold improvement in yield starting from adenosine 10 compared to the earlier phosphodiester synthesis.

The inhibitory activity of the newly synthesized biotinol-5'-AMP 2 was investigated against a panel of BPLs using an *in vitro* biotinylation assay that measures the incorporation of radiolabeled biotin onto an acceptor protein.^{6,30} The activity of each enzyme was determined in the presence of varying concentrations of biotinol-5'-AMP 2. The apparent inhibition constants (K_i^{app}) were calculated using the Morrison equation for tight binding inhibitors as most of the K_i^{app} values were within 10-fold of the concentration of BPL employed in the assay. Biotinol-5'-AMP 2 inhibited all five clinically relevant microbial BPLs with the greatest potency against *S. aureus* ($K_i^{app} = 18$ nM) and *M. tuberculosis* ($K_i^{app} = 52$ nM). It also inhibited human BPL with a K_i^{app} of 182 nM. Thus, biotinol-5'-AMP 2 is a pan BPL inhibitor, presumably since its structure closely resembles that of the natural reaction intermediate biotinyl-5'-AMP 1, which is common to all BPLs.

It has previously been established that biotin and ATP bind to BPL in an ordered manner, with biotin binding first.^{6,31} This suggests that biotinol-5'-AMP 2 would be a competitive inhibitor against biotin. In support, our published X-ray crystal structures of *S. aureus* BPL in complex with biotin [PDB

3RKY³² and biotinol-5'-AMP 2 [PDB 4DQ2]⁶ demonstrate that both compounds occupy the same binding pocket. The activity of *S. aureus* BPL was measured in the presence of varying concentrations of both inhibitor and biotin in order to define the kinetics of inhibition.³³ Lineweaver–Burk double-reciprocal plots of 1/enzyme velocity versus 1/biotin concentration gave four straight lines that had a common y-intercept (Figure 2). The data demonstrated that increasing

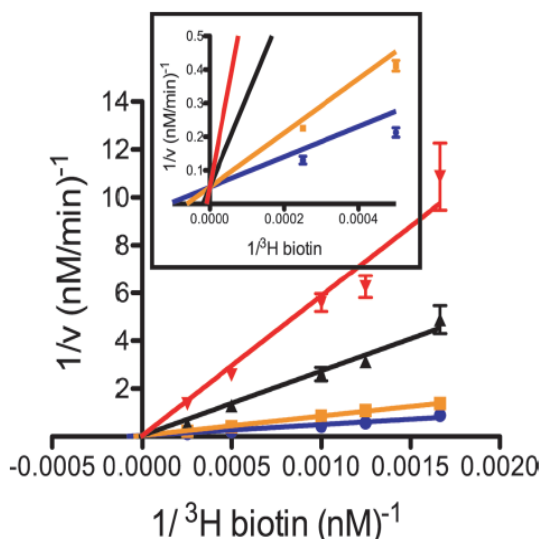


Figure 2. Kinetic analysis of inhibitor binding. *S. aureus* BPL activity was measured in the presence of inhibitor and varying concentrations of biotin. Lineweaver–Burk curves are shown for ³H-biotin. The insert is an expanded view close to the origin showing the curves intersecting the y-axis. The concentrations of 2 employed in the assays were 0 (blue curves), 20 nM (orange curves), 100 nM (black curves), and 200 nM (red curves). Data points are the mean \pm SEM for three replicates.

concentrations of inhibitor were accompanied by increases in the K_M for biotin, while the V_{max} remained unchanged. This supports the proposal that biotinol-5'-AMP 2 is a competitive inhibitor of biotin. Accordingly, the K_i^{app} were extrapolated for each species of BPL using the apparent K_M values for biotin (Table 1).³⁴

Table 1. *In Vitro* Biotinylation Assay Results for Biotin and Inhibition Constants for Biotinol-5'-AMP 2

biotin protein ligase	K_M biotin (μ M)	K_i^{app} biotinol-5'-AMP 2 (nM)
<i>Escherichia coli</i>	0.3	87
<i>Staphylococcus aureus</i>	1.0	18
<i>Klebsiella pneumoniae</i>	2.0	482
<i>Acinetobacter calcoaceticus</i>	0.3	461
<i>Mycobacterium tuberculosis</i>	0.5	52
<i>Homo sapiens</i>	1.1	182

Finally, the antimicrobial activity of biotinol-5'-AMP 2 was assessed against a library of clinically important bacteria using a microdilution broth assay. The resulting minimal inhibitory concentrations (MIC) are shown in Table 2. Encouragingly, biotinol-5'-AMP 2 was effective against staphylococci with minimal inhibitory concentrations varying from 1–8 μ g/mL, but not enterococci nor *E. coli*. The difference in antibacterial activity observed here may be due to differences in compound

Table 2. *In Vitro* Susceptibility Assay of Biotinol-5'-AMP 2 against a Series of Bacterial Strains

bacterium class	strains	resistance	MIC (μ g/mL)
<i>M. tuberculosis</i>	H37Rv		2.5
<i>M. tuberculosis</i>	#37892293		2.5
<i>M. tuberculosis</i>	#3688023		0.5
<i>M. tuberculosis</i>	BCG (SI)	pyrazinamide	resistant
<i>M. tuberculosis</i>	Who-185	rifampicin	2.5
<i>M. tuberculosis</i>	Who-1841	isoniazid	0.5
<i>S. aureus</i> (n = 8)	MSSA		2–4
<i>S. aureus</i> (n = 8)	MRSA	methicillin	2–8
Coagulase negative staphylococci (n = 7)			1–4
<i>Escherichia coli</i>	ATCC 25922		>128
<i>Enterococcus faecalis</i> (n = 3)			>128
<i>Enterococcus faecium</i> (n = 5)			>128
<i>Homo sapiens</i> , HepG2 cell line	HB8065		>200

uptake between the different species. Likewise, *M. tuberculosis* was sensitive to biotinol-5'-AMP 2, including strains resistant to front line antibiotics. In particular, biotinol-5'-AMP inhibited growth of WHO-1841 at 0.5 μ g/mL, a strain resistant to the fatty acid biosynthesis inhibitor isoniazid. The notable exception was the pyrazinamide resistant strain BCG (SI) that was also insensitive to biotinol-5'-AMP 2 for reasons that are not clear. It is noteworthy that, although biotinol-5'-AMP 2 inhibited human BPL *in vitro*, the compound showed no cell cytotoxicity (CC_{50}) against the human liver cell line HepG2 at concentrations as high as 200 μ g/mL, providing a therapeutic index (CC_{50}/MIC) of >25–400-fold, based upon the MICs for *S. aureus* and *M. tuberculosis*, respectively. The observed MIC values of biotinol-5'-AMP 2 against *M. tuberculosis* (0.5–2.5 μ g/mL) are comparable with acyl-AMP mimic bio-AMS 3 (0.1–0.5 μ g/mL).⁵ Interestingly, while both 2 and 3 are active against *M. tuberculosis*, only 2 is cytotoxic over Gram-positive *S. aureus*.

In summary, an improved synthesis of biotinol-5'-AMP 2 and its subsequent biological characterization are reported. The new approach gives an improved yield of 29%. Enzyme inhibition and *in vitro* antibacterial susceptibility assays revealed that biotinol-5'-AMP 2 is a prime candidate for further development as a new class of antimicrobial agent. While this compound is a pan BPL inhibitor, it possesses selective antimicrobial inhibitory activity toward Gram-positive microbes over Gram-negative and importantly human cell lines. Significantly, MIC values between 0.5–2.5 μ g/mL were obtained against resistant strains of *M. tuberculosis*.

■ ASSOCIATED CONTENT

Supporting Information

Biological assays, synthetic procedures, and data for selected compounds. This material is available free of charge via the Internet at <http://pubs.acs.org>.

■ AUTHOR INFORMATION

Corresponding Authors

*Tel: +61 8 8313 6042. E-mail: steven.polyak@adelaide.edu.au.

*Tel: +61 8 8313 5652. E-mail: andrew.abell@adelaide.edu.au.

Present Addresses

[#]School of Medical Sciences (Pharmacology) and Bosch Institute, The University of Sydney, Sydney, New South Wales 2006, Australia.

[∇]CSL Limited, 45 Poplar Road, Parkville, Victoria 3052, Australia.

[○]School of Biomedical Science, Charles Sturt University, Wagga Wagga, New South Wales 2650, Australia.

[◆]Medicinal Chemistry, Monash Institute of Pharmaceutical Sciences, Monash University, Parkville, Victoria 3052, Australia.

Author Contributions

The manuscript was written through contributions of all authors. Medicinal chemistry was performed by W.T. and A.D.A., biochemical assays were performed by A.S.P., B.N., M.Y.Y., T.P.S., and G.W. under the guidance of S.W.P., M.C.J.W., and G.W.B., antibacterial susceptibility assays were performed by R.L., J.M.B., and J.D.T., and cell culture assays were performed by S.W.P.

Funding

This work was supported by the National Health and Medical Research Council of Australia (applications APP1011806 and APP1068885), the Centre for Molecular Pathology, University of Adelaide, and Adelaide Research and Innovation's Commercial Accelerator Scheme. We are grateful to the Carthew family for their financial support of this work. M.C.J.W. is an Australian National Health and Medical Research Council of Australia Senior Research Fellow.

Notes

The authors declare no competing financial interest.

■ ACKNOWLEDGMENTS

We are grateful to the Australian National Fabrication Facility for providing access to analytical HPLC. We also thank Dr. Ivan Bastian for his critical comments on the manuscript.

■ ABBREVIATIONS

BPL, biotin protein ligase; MIC, minimal inhibitory concentration

■ REFERENCES

- (1) Duckworth, B. P.; Nelson, K. M.; Aldrich, C. C. Adenylating enzymes in *Mycobacterium tuberculosis* as drug targets. *Curr. Top. Med. Chem.* 2012, 12 (7), 766–96.
- (2) Schmelz, S.; Naismith, J. H. Adenylate-forming enzymes. *Curr. Opin. Struct. Biol.* 2009, 19 (6), 666–71.
- (3) Kwon, K.; Streaker, E. D.; Beckett, D. Binding specificity and the ligand dissociation process in the E. coli biotin holoenzyme synthetase. *Protein Sci.* 2002, 11 (3), 558–570.
- (4) Brown, P. H.; Beckett, D. Use of binding enthalpy to drive an allosteric transition. *Biochemistry* 2005, 44 (8), 3112–21.
- (5) Duckworth, B. P.; Geders, T. W.; Tiwari, D.; Boshoff, H. I.; Sibbald, P. A.; Barry, C. E., III; Schnappinger, D.; Finzel, B. C.; Aldrich, C. C. Bisubstrate adenylation inhibitors of biotin protein ligase from *Mycobacterium tuberculosis*. *Chem. Biol.* 2011, 18 (11), 1432–1441.
- (6) Soares da Costa, T. P.; Tieu, W.; Yap, M. Y.; Pardini, N. R.; Polyak, S. W.; Sejer Pedersen, D.; Morona, R.; Turnidge, J. D.; Wallace, J. C.; Wilce, M. C.; Booker, G. W.; Abell, A. D. Selective inhibition of biotin protein ligase from *Staphylococcus aureus*. *J. Biol. Chem.* 2012, 287 (21), 17823–32.
- (7) Brown, P. H.; Cronan, J. E.; Grötl, M.; Beckett, D. The biotin repressor: modulation of allostery by corepressor analogs. *J. Mol. Biol.* 2004, 337 (4), 857–869.
- (8) Wood, Z. A.; Weaver, L. H.; Brown, P. H.; Beckett, D.; Matthews, B. W. Co-repressor induced order and biotin repressor dimerization: a case for divergent followed by convergent evolution. *J. Mol. Biol.* 2006, 357 (2), 509–523.
- (9) Tieu, W.; Soares da Costa, T. P.; Yap, M. Y.; Keeling, K. L.; Wilce, M. C. J.; Wallace, J. C.; Booker, G. W.; Polyak, S. W.; Abell, A. D. Optimising in situ click chemistry: the screening and identification of biotin protein ligase inhibitors. *Chem. Sci.* 2013, 4 (9), 3533–3537.
- (10) Tieu, W.; Jarrad, A. M.; Paparella, A. S.; Keeling, K. A.; Soares da Costa, T. P.; Wallace, J. C.; Booker, G. W.; Polyak, S. W.; Abell, A. D. Heterocyclic acyl-phosphate bioisostere-based inhibitors of *Staphylococcus aureus* biotin protein ligase. *Bioorg. Med. Chem. Lett.* 2014, 24, 4689–4693.
- (11) Bottcher, C.; Dennis, E. G.; Booker, G. W.; Polyak, S. W.; Boss, P. K.; Davies, C. A novel tool for studying auxin-metabolism: the inhibition of grapevine indole-3-acetic acid-amido synthetases by a reaction intermediate analogue. *PLoS One* 2012, 7 (5), e37632.
- (12) Lu, X.; Zhou, R.; Sharma, I.; Li, X.; Kumar, G.; Swaminathan, S.; Tonge, P. J.; Tan, D. S. Stable analogues of OSB-AMP: potent inhibitors of MenE, the *o*-succinylbenzoate-CoA synthetase from bacterial menaquinone biosynthesis. *ChemBioChem* 2012, 13 (1), 129–36.
- (13) Somu, R. V.; Boshoff, H.; Qiao, C.; Bennett, E. M.; Barry, C. E., III; Aldrich, C. C. Rationally designed nucleoside antibiotics that inhibit siderophore biosynthesis of *Mycobacterium tuberculosis*. *J. Med. Chem.* 2006, 49 (1), 31–4.
- (14) Qiao, C.; Wilson, D. J.; Bennett, E. M.; Aldrich, C. C. A mechanism-based aryl carrier protein/thiolation domain affinity probe. *J. Am. Chem. Soc.* 2007, 129 (20), 6350–1.
- (15) Xu, Z.; Yin, W.; Martinelli, L. K.; Evans, J.; Chen, J.; Yu, Y.; Wilson, D. J.; Mizrahi, V.; Qiao, C.; Aldrich, C. C. Reaction intermediate analogues as bisubstrate inhibitors of pantothenate synthetase. *Bioorg. Med. Chem.* 2014, 22 (5), 1726–35.
- (16) Yu, X. Y.; Hill, J. M.; Yu, G.; Wang, W.; Kluge, A. F.; Wendler, P.; Gallant, P. Synthesis and structure-activity relationships of a series of novel thiazoles as inhibitors of aminoacyl-tRNA synthetases. *Bioorg. Med. Chem. Lett.* 1999, 9 (3), 375–80.
- (17) Bernier, S.; Dubois, D. Y.; Habegger-Polomat, C.; Gagnon, L. P.; Lapointe, J.; Chenevert, R. Glutamylsulfamoyladenosine and pyroglutamylsulfamoyladenosine are competitive inhibitors of E. coli glutamyl-tRNA synthetase. *J. Enzyme Inhib. Med. Chem.* 2005, 20 (1), 61–7.
- (18) Lun, S.; Guo, H.; Adamson, J.; Cisar, J. S.; Davis, T. D.; Chavadi, S. S.; Warren, J. D.; Quadri, L. E.; Tan, D. S.; Bishai, W. R. Pharmacokinetic and in vivo efficacy studies of the mycobactin biosynthesis inhibitor salicyl-AMS in mice. *Antimicrob. Agents Chemother.* 2013, 57 (10), 5138–40.
- (19) Auld, D. S.; Lovell, S.; Thorne, N.; Lea, W. A.; Maloney, D. J.; Shen, M.; Rai, G.; Battaile, K. P.; Thomas, C. J.; Simeonov, A.; Hanzlik, R. P.; Inglese, J. Molecular basis for the high-affinity binding and stabilization of firefly luciferase by PTC124. *Proc. Natl. Acad. Sci. U.S.A.* 2010, 107 (11), 4878–83.
- (20) Patrone, J. D.; Yao, J.; Scott, N. E.; Dotson, G. D. Selective inhibitors of bacterial phosphopantothenoylecysteine synthetase. *J. Am. Chem. Soc.* 2009, 131 (45), 16340–1.
- (21) Tian, Y.; Suk, D. H.; Cai, F.; Crich, D.; Mesecar, A. D. Bacillus anthracis *o*-succinylbenzoyl-CoA synthetase: reaction kinetics and a novel inhibitor mimicking its reaction intermediate. *Biochemistry* 2008, 47 (47), 12434–47.
- (22) Ciulli, A.; Scott, D. E.; Ando, M.; Reyes, F.; Saldanha, S. A.; Tuck, K. L.; Chirgadzhe, D. Y.; Blundell, T. L.; Abell, C. Inhibition of *Mycobacterium tuberculosis* pantothenate synthetase by analogues of the reaction intermediate. *ChemBioChem* 2008, 9 (16), 2606–11.
- (23) Tuck, K. L.; Saldanha, S. A.; Birch, L. M.; Smith, A. G.; Abell, C. The design and synthesis of inhibitors of pantothenate synthetase. *Org. Biomol. Chem.* 2006, 4 (19), 3598–610.
- (24) Ferreras, J. A.; Ryu, J. S.; Di Lello, F.; Tan, D. S.; Quadri, L. E. Small-molecule inhibition of siderophore biosynthesis in *Mycobacte-*

rium tuberculosis and *Yersinia pestis*. *Nat. Chem. Biol.* 2005, 1 (1), 29–32.

(25) Sittiwong, W.; Cordonier, E. L.; Zempleni, J.; Dussault, P. H. beta-Keto and beta-hydroxyphosphonate analogs of biotin-5'-AMP are inhibitors of holocarboxylase synthetase. *Bioorg. Med. Chem. Lett.* 2014, 24 (24), 5568–71.

(26) Paparella, A. S.; Soares da Costa, T. P.; Yap, M. Y.; Tieu, W.; Wilce, M. C.; Booker, G. W.; Abell, A. D.; Polyak, S. W. Structure guided design of biotin protein ligase inhibitors for antibiotic discovery. *Curr. Top. Med. Chem.* 2014, 14 (1), 4–20.

(27) Desjardins, M.; Garneau, S.; Desgagnés, J.; Lacoste, L.; Yang, F.; Lapointe, J.; Chênevert, R. Glutamyl adenylate analogues are inhibitors of glutamyl-tRNA synthetase. *Bioorg. Chem.* 1998, 26 (1), 1–13.

(28) Alves, A. M.; Holland, D.; Edge, M. D. A chemical method of labelling oligodeoxyribonucleotides with biotin: A single step procedure using a solid phase methodology. *Tetrahedron Lett.* 1989, 30 (23), 3089–3092.

(29) Oh, K. An efficient epimerization of biotin sulfone derivatives to 2-epi-biotin analogs. *Tetrahedron Lett.* 2007, 48 (21), 3685–3688.

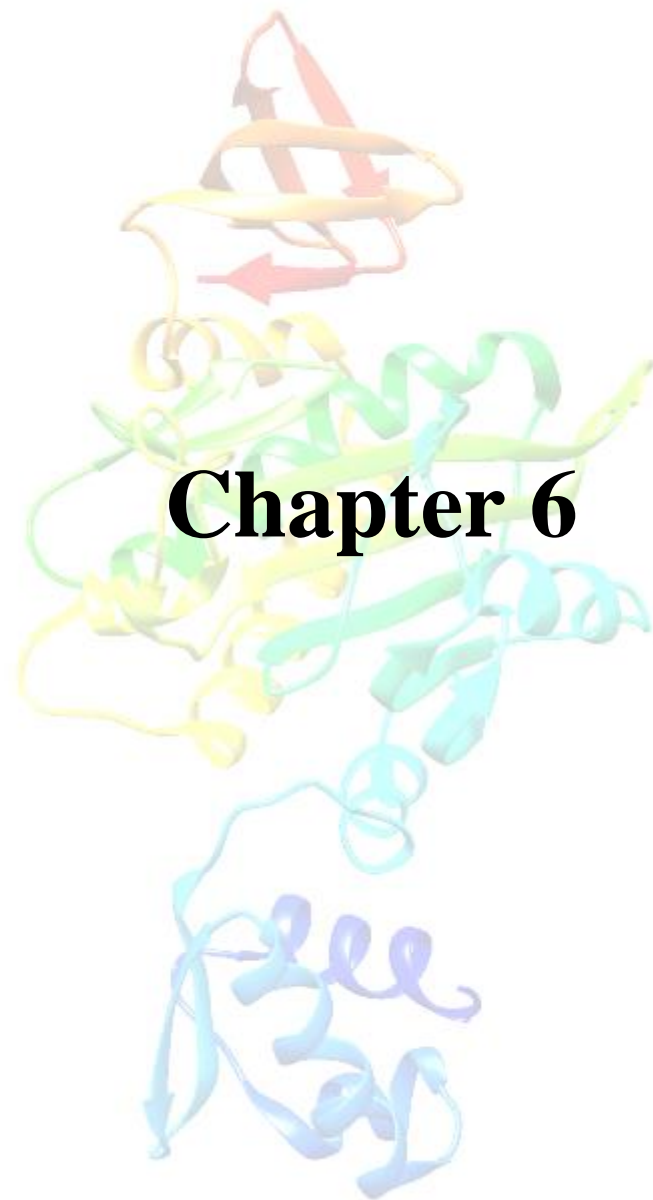
(30) Polyak, S. W.; Chapman-Smith, A.; Brautigan, P. J.; Wallace, J. C. Biotin protein ligase from *Saccharomyces cerevisiae*. The N-terminal domain is required for complete activity. *J. Biol. Chem.* 1999, 274 (46), 32847–54.

(31) Xu, Y.; Beckett, D. Kinetics of biotinyl-5'-adenylate synthesis catalyzed by the *Escherichia coli* repressor of biotin biosynthesis and the stability of the enzyme-product complex. *Biochemistry* 1994, 33 (23), 7354–7360.

(32) Pardini, N. R.; Yap, M. Y.; Traore, D. A.; Polyak, S. W.; Cowieson, N. P.; Abell, A.; Booker, G. W.; Wallace, J. C.; Wilce, J. A.; Wilce, M. C. Structural characterization of *Staphylococcus aureus* biotin protein ligase and interaction partners: an antibiotic target. *Protein Sci.* 2013, 22 (6), 762–73.

(33) Soares da Costa, T. P.; Tieu, W.; Yap, M. Y.; Zvarec, O.; Bell, J. M.; Turnidge, J. D.; Wallace, J. C.; Booker, G. W.; Wilce, M. C.; Abell, A. D.; Polyak, S. W. Biotin analogues with antibacterial activity are potent inhibitors of biotin protein ligase. *ACS Med. Chem. Lett.* 2012, 3 (6), 509–14.

(34) Copeland, R. Tight Binding Inhibition. In *Evaluation of Enzyme Inhibitors in Drug Discovery*, 2nd ed.; Wiley: New York, 2013; pp 245–282.



Statement of Authorship

Title of Paper	A new series of BPL inhibitors to probe the ribose-binding pocket of <i>Staphylococcus aureus</i> biotin protein ligase	
Publication Status	<input type="checkbox"/> Published <input checked="" type="checkbox"/> Accepted for Publication <input type="checkbox"/> Submitted for Publication <input type="checkbox"/> Unpublished and Unsubmitted work written in manuscript style	
Publication Details	Jiage Feng, Ashleigh S. Paparella, William Tieu, David Heim, Sarah Clark, Andrew Hayes, Grant W. Booker, Steven W. Polyak, Andrew D. Abell, <i>ACS Medicinal Chemistry Letters</i> , accepted October 2016	

Principal Author

Name of Principal Author (Candidate)	Ashleigh S. Paparella	
Contribution to the Paper	Expression and purification of SaBPL and HsBPL Performed all <i>in vitro</i> biotinylation assays, and analysis of assay results Co-author on the manuscript.	
Overall percentage (%)	20%	
Certification:	This paper reports on original research I conducted during the period of my Higher Degree by Research candidature and is not subject to any obligations or contractual agreements with a third party that would constrain its inclusion in this thesis. I am the primary co-author of this paper.	
Signature		Date 4/11/16

Co-Author Contributions

By signing the Statement of Authorship, each author certifies that:

- i. the candidate's stated contribution to the publication is accurate (as detailed above);
- ii. permission is granted for the candidate to include the publication in the thesis; and
- iii. the sum of all co-author contributions is equal to 100% less the candidate's stated contribution.

Name of Co-Author	Jiage Feng	
Contribution to the Paper	Performed synthesis and characterization of analogues, docking studies, analysis of data, provided advanced draft of manuscript and subsequent revisions. Is the co-author on the manuscript. Overall contribution: 20%	
Signature		Date 25/10/16

Name of Co-Author	William Tieu	
Contribution to the Paper	Performed synthesis and characterization of compound 12a-c and 12g-i Revised manuscript. Overall contribution: 15%	
Signature		Date 24/10/16

Name of Co-Author	David Heim		
Contribution to the Paper	Performed all antimicrobial susceptibility assays Overall contribution: 5%		
Signature		Date	26/10/2016

Name of Co-Author	Sarah Clark		
Contribution to the Paper	Performed synthesis and characterization of 12j and 12k Overall contribution: 5%		
Signature		Date	26/10/16

Name of Co-Author	Andrew Hayes		
Contribution to the Paper	Performed all cytotoxicity assays in 2 human cell lines Overall contribution: 5%		
Signature		Date	4/11/16

Name of Co-Author	Grant W. Booker		
Contribution to the Paper	Supervised the biological aspects of the project, revised manuscript Overall contribution: 5%		
Signature		Date	19/10/2016

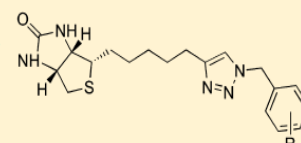
Name of Co-Author	Steven W. Polyak		
Contribution to the Paper	Worked closely with the principal author to write the manuscript. Supervised biological testing Overall contribution: 15%		
Signature		Date	19/10/2016

Name of Co-Author	Andrew D. Abell		
Contribution to the Paper	Supervised all aspects of medicinal chemistry, revised manuscript and is corresponding author. Overall contribution: 15%		
Signature		Date	19/10/2016

New Series of BPL Inhibitors To Probe the Ribose-Binding Pocket of *Staphylococcus aureus* Biotin Protein LigaseJiage Feng,^{†,‡} Ashleigh S. Paparella,[§] William Tieu,^{†,||} David Heim,[§] Sarah Clark,[†] Andrew Hayes,[§] Grant W. Booker,[§] Steven W. Polyak,[§] and Andrew D. Abell^{*,†,‡}[†]Department of Chemistry, [§]Department of Molecular and Cellular Biology, and [‡]Centre for Nanoscale BioPhotonics (CNBP), University of Adelaide, Adelaide, South Australia 5005, Australia

Supporting Information

ABSTRACT: Replacing the labile adenosyl-substituted phosphoanhydride of biotinyl-5'-AMP with a N1-benzyl substituted 1,2,3-triazole gave a new truncated series of inhibitors of *Staphylococcus aureus* biotin protein ligase (SaBPL). The benzyl group presents to the ribose-binding pocket of SaBPL based on *in silico* docking. Halogenated benzyl derivatives (12t, 12u, 12w, and 12x) proved to be the most potent inhibitors of SaBPL. These derivatives inhibited the growth of *S. aureus* ATCC49775 and displayed low cytotoxicity against HepG2 cells.



R	K _i SaBPL (μM)	K _i HsBPL (μM)
12t 3F	0.28 ± 0.02	>10
12u 4F	0.60 ± 0.10	>10
12w 3Cl	0.39 ± 0.04	>10
12x 4Cl	1.10 ± 0.07	>10

KEYWORDS: Enzyme inhibitors, antibiotics, biotin protein ligase, *Staphylococcus aureus*

Biotin protein ligase (BPL) catalyzes the reaction of biotin 1 and ATP 2 to give biotinyl-5'-AMP 3, which then biotinylates and activates essential metabolic enzymes required for fatty acid biosynthesis and gluconeogenesis, specifically acetyl CoA carboxylase and pyruvate carboxylase (Figure 1).^{1–5}

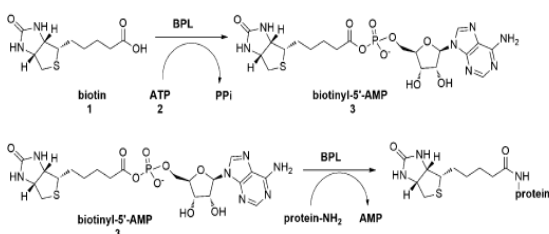


Figure 1. General mechanism of BPL catalyzed biotinylation.

A number of analogues of biotinyl-5'-AMP have recently been reported as inhibitors of BPL as shown in Figure 2. Some of these compounds have potential as antibacterial agents by inhibiting BPL from clinically important pathogens such as *Staphylococcus aureus*,⁶ *Escherichia coli*,^{7,8} and *Mycobacterium tuberculosis*.^{9,10} A range of bioisosteres have been investigated as replacements for the labile phosphoanhydride of biotinyl-5'-AMP 3, including phosphodiester 4,^{11,12} hydroxyphosphonate 5,¹³ ketophosphonate 6,¹³ acylsulfamate 7,¹¹ and sulfonylamide 8¹⁰ (Figure 2). We have also reported biotin triazoles (e.g., 9–11) as a novel class of BPL inhibitor that selectively targets BPL from the clinically important bacterial pathogen *Staphylococcus aureus* over the human homologue.^{3,14,15}

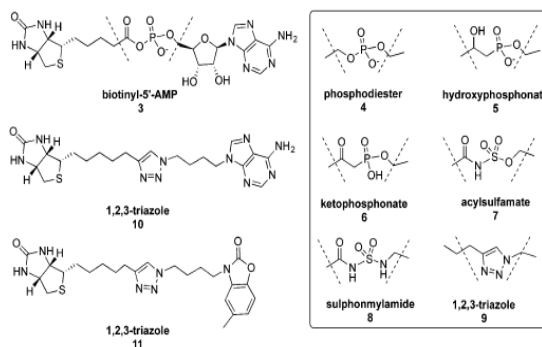


Figure 2. Reported BPL inhibitors, with isosteric replacements for the phosphoanhydride of biotinyl-5'-AMP 3 shown in the box.

Without exception, all isostere-based BPL inhibitors reported to date contain a biotin and an adenine group, or analogue thereof, as discussed above and as shown in Figure 2. These two groups occupy well-defined binding pockets in the enzyme as per biotinyl-5'-AMP 3, as supported by X-ray crystallographic and mutagenesis studies.^{3,16} The ribose group of the triazole series can be removed as in 10, and the adenine can be modified as in 11, which has improved stability and >1000-fold specificity for the BPL from *S. aureus* over the human homologue.³ We now report the first examples of truncated 1,2,3-triazole-based BPL inhibitors with a 1-benzyl substituent

Received: June 26, 2016

Accepted: October 10, 2016

designed to interact with the ribose binding pocket of *S. aureus* BPL (SaBPL), see 12a–y, Figure 3. These derivatives are the

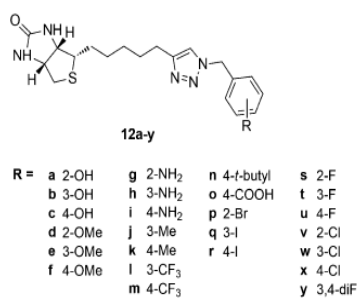


Figure 3. Benzyl-substituted 1,2,3-triazole analogues.

first examples of isostere-based BPL inhibitors lacking an appended adenine or analogue thereof and the associated tether as discussed above. The ribose-binding pocket is composed of amino acids that provide potential hydrogen bonding sites, specifically through the side chains of K187, R122, R125, and R227 as well as the backbone peptide atoms from H126 and S128 (Figure 4a). This series of inhibitors provides an important starting point for further optimization and antibiotic development.

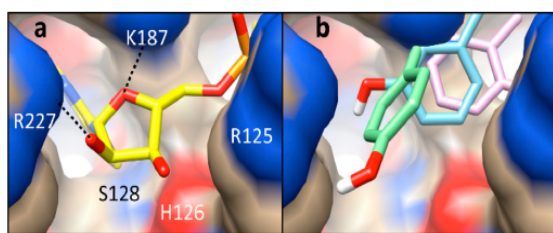


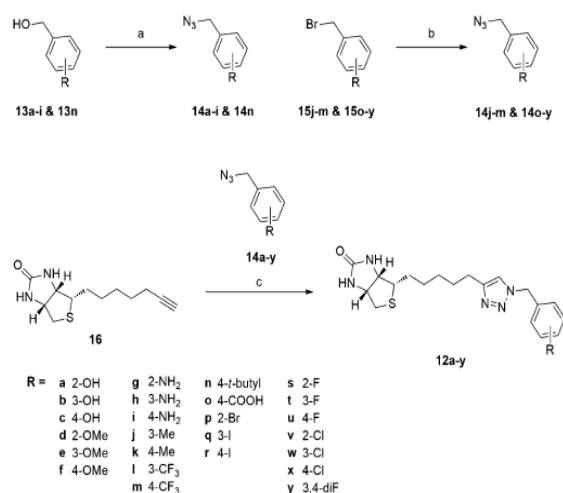
Figure 4. (a) X-ray structure of the SaBPL active site with biotinyl-5'-AMP 3 (yellow) bound PDB ID 3R1R.¹⁰ Amino acids that encompass the ribose-binding pocket are shown. Dashed lines represent hydrogen bonds. (b) *In silico* docking poses for biotin triazole analogues 12a, 12b, and 12c containing a hydroxyl group at C2- (pink), C3- (blue), and C4- (green), respectively.

In silico docking experiments were carried out in order to explore possible binding modes by which this series of benzyl analogues might occupy the active site of SaBPL. Flexible ligand docking was carried out using AutoDockTools (version 1.5.6). The docking protocol was first validated by removing compound 11 from its cocrystal structure with *S. aureus* BPL (PDB 3V7S) and then redocking. This occurred with a high degree of commonality as revealed by superimposition of the docked and crystallized ligands in the active site. We next docked benzylated triazoles 12a–c (Figure 3) into SaBPL. Each of these structures contains a single hydroxyl substituent on the benzyl ring capable of forming a hydrogen bond as per the diol in the ribose of biotinyl-5'-AMP 3. Gratifyingly, the top ranking poses of all three analogues placed the hydroxyl group in the site occupied by the ribose diol of 3 (Figure 4a). Rotation around the alkyl linker connecting the triazole and benzyl moieties produced subtly different poses with regards to the ribose-binding site (Figure 4b). These binding modes minimized steric clashes with the protein and facilitated hydrogen bonding between the alcohol group and R122 for 12a and R227 for 12b and 12c. This data reflects an apparent openness of the solvent exposed pocket and suggests that this

site can accommodate a variety of functional groups as exemplified in the extended series depicted in Figure 3. Synthesis and biological testing of this series provides an opportunity to probe potential interaction with the ribose pocket.

The synthesis of the 1,2,3-triazoles 12a–y was carried out as summarized in Scheme 1. The key benzyl azides 14a–y were

Scheme 1^a



^aConditions and reagents: (a) (i) PPh₃, CCl₄, DMF; (ii) NaN₃, DMF, rt; (b) NaN₃, DMF, rt; (c) Cu₂SO₄ ascorbate, DMSO/H₂O, rt, 12 h (give 12a–y (18%–55%)).

prepared from commercially available benzyl alcohols (13a–i and 13n) and bromides (15j–m and 15o–y). Specifically, commercially available benzyl alcohols 13a–i and 13n were converted directly¹⁷ into the corresponding azides 14a–i and 14n on reaction with triphenylphosphine, in the presence of carbon tetrachloride and sodium azide at ambient temperature. The second series of benzyl azides (14j–m and 14o–y) was prepared from commercially available benzyl bromides 15j–m and 15o–y on reaction with sodium azide in DMF as shown. Huisgen cycloaddition of biotin alkyne 16¹⁸ with each of the benzyl azides 14a–y, in the presence of copper sulfate and sodium ascorbate,³ then gave the desired 1,2,3-triazole 12a–y as shown.

The activity profiles of 1,2,3-triazoles 12a–y were determined using established biochemical and microbiological assay protocols.^{3,19} Compounds displaying inhibitory activity against SaBPL and cytotoxic activity against bacteria, but not mammalian cells, are considered important candidates for further antibiotic development. The *in vitro* potency and selectivity profiles of the 1,2,3-triazoles 12a–y were measured using recombinant BPLs from *S. aureus* and *Homo sapiens*. Here the enzymatic incorporation of radiolabeled biotin onto an acceptor protein was measured in the presence of varying concentrations of each compound with the results shown in Tables 1 and 2. Previous enzymology and X-ray crystallography studies have demonstrated that the biotin triazoles are competitive inhibitors against biotin,^{3,15,16} and as such, inhibitory constants (K_i) were calculated from IC₅₀ values using the known K_M for biotin as previously described.²⁰ The antibacterial activity of the compounds was also determined using *S. aureus* strain ATCC 49775.¹⁸ Growth of the bacteria 20 h post-treatment was measured spectrophotometrically at 600

Table 1. *In Vitro* Biotinylation and Antibacterial Assay Results for Benzyl Triazole Series 1

ID	R	K_i SaBPL (μM)	K_i human BPL (μM)	anti- <i>S. aureus</i> activity ^a
12a	2-OH	>10	>16	–
12b	3-OH	>10	>16	–
12c	4-OH	1.59 \pm 0.08	>16	–
12d	2-OMe	0.53 \pm 0.05	>16	–
12e	3-OMe	1.17 \pm 0.1	>16	–
12f	4-OMe	>10	>16	–
12g	2-NH ₂	1.48 \pm 0.14	>16	+
12h	3-NH ₂	>10	>16	–
12i	4-NH ₂	>10	>16	–
12j	3-Me	0.71 \pm 0.04	>16	+
12k	4-Me	>10	>16	–
12l	3-CF ₃	>10	>16	–
12m	4-CF ₃	>10	>16	–
12n	4-tBu	1.22 \pm 0.07	>16	+
12o	4-COOH	0.67 \pm 0.06	>16	–
12p	2-Br	0.96 \pm 0.13	>16	+
12q	3-I	>10	>16	–
12r	4-I	0.56 \pm 0.06	>16	+

^a+, Optical density of the culture reduced by >40% of nontreated controls. –, compound did not inhibit bacterial growth.

Table 2. *In Vitro* Biotinylation and Antibacterial Assay Results for Benzyl Triazole Series 2

ID	R	K_i SaBPL (μM)	K_i Human BPL (μM)	anti- <i>S. aureus</i> activity ^a	cytotox HepG2 ^b
12s	2-F	>10	>16	–	N/D
12t	3-F	0.28 \pm 0.02	>16	+	>40
12u	4-F	0.6 \pm 0.1	>16	+	>40
12v	2-Cl	>10	>16	–	N/D
12w	3-Cl	0.39 \pm 0.04	>16	+	>40
12x	4-Cl	1.1 \pm 0.07	>16	+	>40
12y	3,4-diF	>10	>16	–	N/D

^a+, optical density of the culture reduced by >40% of nontreated controls. –, compound did not inhibit bacterial growth. ^bCompounds were assayed at 40 $\mu\text{g}/\text{mL}$.

nm. Finally, selected compounds were assessed for potential toxicity using a cytotoxicity assay with cultured mammalian HepG2 cells (ATCC HB-8065).³

The initial series of alcohol analogues 12a–c docked against SaBPL were first assayed against the enzyme (Table 1) with the compound containing a C4 hydroxyl group (12c) showing modest activity ($K_i = 1.59 \mu\text{M}$). Interestingly, the C2 and C3 hydroxylated derivatives (12a and 12b, respectively) were devoid of activity. It thus appears that the ribose pocket is sensitive to the position of the hydroxyl group and more so than predicted by the modeling. This observation is supported on analysis of the results for compounds containing other substituents, although there is little consistency regarding which position is most favored. Specifically, derivatives with a methoxyl group at C2 and C3 were both active (12d, $K_i = 0.53 \mu\text{M}$; 12e, $K_i = 1.1 \mu\text{M}$), while the C4 analogue (12f) was inactive. For an amino substituent, C2 is active (12g, $K_i = 1.49 \mu\text{M}$), while both C3 (12h) and C4 (12i) were inactive. Of the other derivatives initially tested, C3 methyl (12j, $K_i = 0.71 \mu\text{M}$), C4 carboxyl and tertiary butyl (12o, $K_i = 0.67 \mu\text{M}$; 12n, $K_i = 1.1 \mu\text{M}$) were active. The 2-bromo and 4-iodo derivatives 12p and 12r showed good activity against *S. aureus* BPL ($K_i = 0.96$

and $0.56 \mu\text{M}$, respectively), and these compounds provided impetus for the expanded series of halogenated compounds shown in Table 2 and as discussed in detail below. A strongly electron withdrawing trifluoromethyl group at C3 and C4, resulted in compounds (12l and 12m) that were devoid of activity against SaBPL. All of the biotin triazoles tested were inactive against human BPL when 100 μM of compound was included in the assay medium. This is an important finding as it demonstrates that benzyl truncated triazoles retain the selectivity profile (i.e., active against *S. aureus* but not human BPL) of the earlier and more complex triazoles.^{3,15}

The compounds shown in Table 1 were also assayed for antibacterial activity against *S. aureus* ATCC 49775. Compounds were designated as antibacterial if they reduced the optical density of the culture by >40% relative to the nontreated controls (Figure 5). Of the 18 compounds assessed,

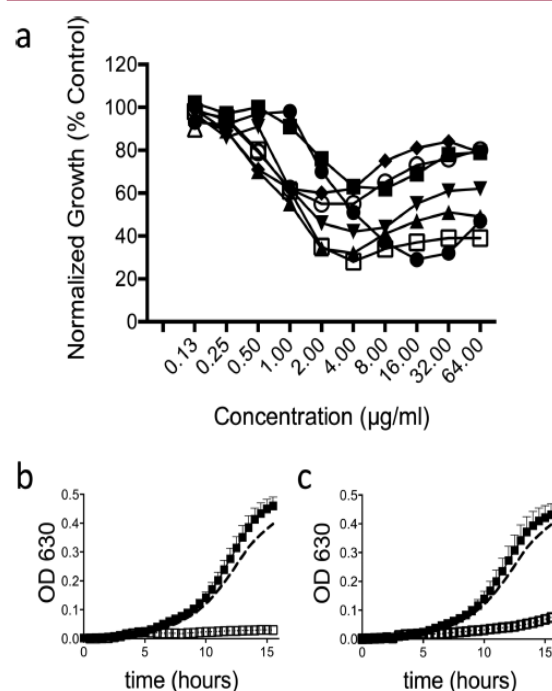


Figure 5. Inhibition of *S. aureus* growth *in vitro*. (a) Compounds 12g (□), 12j (◆), 12p (○), 12r (△), 12t (■), 12u (●), 12w (▼), and 12x (▲) were tested against *S. aureus* strain ATCC 49775. (b,c) Mechanism of action studies for 12g (b) and 12t (c). Growth curves for *S. aureus* RN4220 harboring the plasmid pCN51 (open boxes, negative control) or pCN51-BPL (solid boxes, for recombinant BPL overexpression) are shown. Growth media contained 16 $\mu\text{g}/\text{mL}$ of compound, except, for no treatment controls (dashed line).

only five (those bearing amine, methyl, tertiary butyl, bromo, and iodo substituents, see 12g, 12j, 12n, 12p, and 12r, respectively) were active in the whole cell assays. The fact that these compounds also inhibited SaBPL is consistent with a mechanism of antibacterial action being through the BPL target. It is possible that those BPL inhibitors devoid of whole cell activity, namely, 12c–e, 12g, 12j, and 12p, are unable to penetrate the bacterial membrane, a problem often encountered in antibacterial discovery.²¹

Of the extended halogenated series (12s–x in Table 2) four compounds displayed good activity against SaBPL, see 12t, 12u, 12w, and 12x that had K_i values of 0.28, 0.6, 0.39, and 1.1 μM , respectively. A 3-halo substituent was most favored for

C

DOI: 10.1021/acsmedchemlett.6b00248
ACS Med. Chem. Lett. XXXX, XXX, XXX–XXX

activity as in 12t and 12w. In these cases, the inhibition constants were approximately 2- and 3-fold lower for the 3- vs 4- halogenated analogues, cf. 12t/12u and 12w/12x. A 3-fluoro substituent (12t) provided the most potent compound in this series with a $K_i = 0.28 \mu\text{M}$. The incorporation of a halogen at C2 removed all activity (see 12s and 12v) as did the introduction of a second fluoro substituent as in 12y. Again all active compounds in this series showed excellent selectivity for SaBPL over the human homologue. In addition, 12t, 12u, 12w, and 12x did not show cytotoxicity toward mammalian HepG2 cells at a single concentration of $40 \mu\text{g/mL}$.

Finally, to demonstrate that compounds inhibited protein biotinylation *in vivo*, antibacterial susceptibility assays were performed using a *S. aureus* strain engineered to overexpress the BPL target. Similar approaches to establish the mechanism of action have been employed on *M. tuberculosis*,¹⁰ but not previously for *S. aureus*. Bacteria were grown in media containing $16 \mu\text{g/mL}$ of either 12g (series 1) or 12t (series 2) for 16 h, with the optical density of the culture measured every 30 min. Overexpression of the BPL target abolished the antibacterial activity of both compounds, as *S. aureus* grew at the same rate as nontreated controls (Figure Sb,c). Bacteria harboring the parent cloning vector pCNS1²² that did not express additional BPL, remained highly sensitive to both inhibitors and failed to grow in their presence. Together these data show that the mechanism of action of 12g (from series 1) and 12t (series 2) is clearly via the inhibition of BPL.

The 1-benzyl substituted 1,2,3-triazoles reported here represent a new class of BPL inhibitors that lack the adenine group, or analogue thereof, found in all other isostere-based BPL inhibitors. These compounds have much reduced molecular weight and are relatively easy to prepare. Importantly, the biochemical and microbiological data provide a clear relationship between *in vitro* inhibition of BPL and anti-*S. aureus* activity, with our most potent enzyme inhibitors generally providing our most promising antibacterials (see 12j, 12p, 12r, 12t, 12u, and 12w). In antibiotic drug discovery, this is not always the case as a number of external factors contribute to bioactivity, such as cell permeability and susceptibility to efflux mechanisms and metabolic degradation.

The best lead compound in this new series (12t) with a 3-fluoro substituted benzyl group, has a K_i of 280 nM against SaBPL and demonstrated mechanism of antibacterial activity consistent with the inhibition of protein biotinylation. It is essentially nontoxic to mammalian HepG2 cells and is devoid of activity against human BPL. This compares to the extended 1,2,3-triazole 11 that has K_i of 90 nM against SaBPL. This compound provides clear interactions with both the biotin and adenine pockets of SaBPL and, like the new benzyl series, is essentially inactive against human BPL.³ Our initial SAR data on the new benzyl series provides confidence that further optimization of *in vitro* inhibition will lead to improved antibacterial activity. *In silico* docking supports a binding mechanism in which the benzyl group interacts with the ribose pocket of SaBPL. The compounds reported here provide important new scaffolds for further chemical modification and activity optimization, specifically to interact with the adjacent adenylation site in the enzyme. Such studies are currently underway, particularly the inclusion of extended substituents on the benzyl group and also substitution at C5 of the triazole.

■ ASSOCIATED CONTENT

Supporting Information

The Supporting Information is available free of charge on the ACS Publications website at DOI: 10.1021/acsmedchemlett.6b00248.

Biological assays, synthetic procedures, and data for selected compounds (PDF)

■ AUTHOR INFORMATION

Corresponding Author

*Tel: +61 88 3135652. E-mail: andrew.abell@adelaide.edu.au.

Present Address

^{||}School of Medical Sciences (Pharmacology) and Bosch Institute, The University of Sydney, Sydney, New South Wales 2006, Australia.

Author Contributions

The manuscript was written through contributions of all authors. Medicinal chemistry was performed by J.F., W.T., S.C., and A.D.A., biochemical assays were performed by A.S.P. and S.W.P., antibacterial susceptibility assays were performed by D.H. and A.H. under the guidance of S.W.P. and G.W.B., and cell culture assays were performed by A.H. and S.W.P.

Funding

This work was supported by the National Health and Medical Research Council of Australia (application APP1068885), the Centre for Molecular Pathology, University of Adelaide, and Adelaide Research and Innovation's Commercial Accelerator Scheme. We are grateful to the Wallace and Carthew families for their financial support of this work.

Notes

The authors declare no competing financial interest.

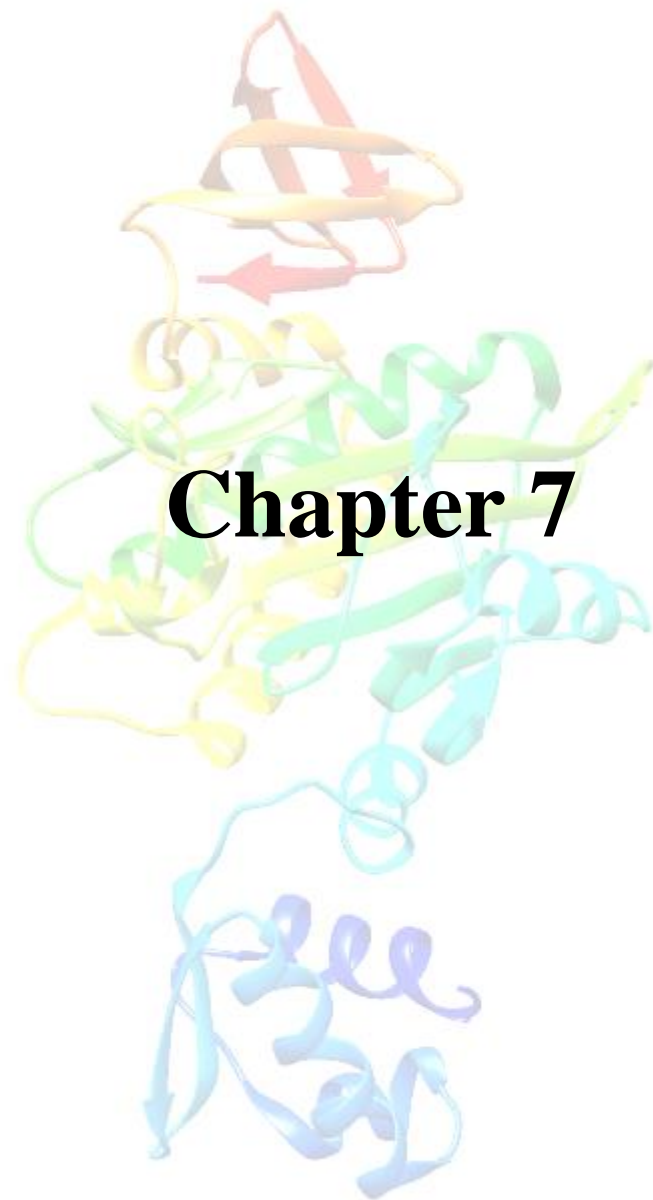
■ ACKNOWLEDGMENTS

We are grateful to the Institute for Photonics and Advanced Sensing (IPAS) for providing access to analytical HPLC and the National Health and Medical Research Council (NHMRC) and Australian Research Council (ARC) for funding. We also thank Dr. Beatriz Blanco Rodriguez for her critical comments on the manuscript.

■ REFERENCES

- (1) Feng, J.; Paparella, A. S.; Booker, G. W.; Polyak, S. W.; Abell, A. D. Biotin Protein Ligase Is a Target for New Antibacterials. *Antibiotics* 2016, 5 (3), 26.
- (2) Duckworth, B. P.; Nelson, K. M.; Aldrich, C. C. Adenylation enzymes in *Mycobacterium tuberculosis* as drug targets. *Curr. Top. Med. Chem.* 2012, 12 (7), 766.
- (3) Soares da Costa, T. P.; Tieu, W.; Yap, M. Y.; Pendini, N. R.; Polyak, S. W.; Sejer Pedersen, D.; Morona, R.; Turnidge, J. D.; Wallace, J. C.; Wilce, M. C.; Booker, G. W.; Abell, A. D. Selective inhibition of biotin protein ligase from *Staphylococcus aureus*. *J. Biol. Chem.* 2012, 287 (21), 17823–32.
- (4) Pendini, N. R.; Bailey, L. M.; Booker, G. W.; Wilce, M. C.; Wallace, J. C.; Polyak, S. W. Microbial biotin protein ligases aid in understanding holocarboxylase synthetase deficiency. *Biochim. Biophys. Acta, Proteins Proteomics* 2008, 1784 (7–8), 973–82.
- (5) Polyak, S.; Abell, A.; Wilce, M.; Zhang, L.; Booker, G. Structure, function and selective inhibition of bacterial acetyl-coa carboxylase. *Appl. Microbiol. Biotechnol.* 2012, 93 (3), 983–992.
- (6) Paparella, A. S.; Soares da Costa, T. P.; Yap, M. Y.; Tieu, W.; Wilce, M. C.; Booker, G. W.; Abell, A. D.; Polyak, S. W. Structure guided design of biotin protein ligase inhibitors for antibiotic discovery. *Curr. Top. Med. Chem.* 2014, 14 (1), 4–20.

- (7) Xu, Y.; Beckett, D. Kinetics of biotinyl-5'-adenylate synthesis catalyzed by the *Escherichia coli* repressor of biotin biosynthesis and the stability of the enzyme-product complex. *Biochemistry* 1994, 33 (23), 7354–7360.
- (8) Brown, P. H.; Beckett, D. Use of binding enthalpy to drive an allosteric transition. *Biochemistry* 2005, 44 (8), 3112–3121.
- (9) Bockman, M. R.; Kalinda, A. S.; Petrelli, R.; De la Mora-Rey, T.; Tiwari, D.; Liu, F.; Dawadi, S.; Nandakumar, M.; Rhee, K. Y.; Schnappinger, D. Targeting *Mycobacterium tuberculosis* Biotin Protein Ligase (MtBPL) with Nucleoside-Based Bisubstrate Adenylation Inhibitors. *J. Med. Chem.* 2015, 58 (18), 7349–7369.
- (10) Duckworth, B. P.; Geders, T. W.; Tiwari, D.; Boshoff, H. I.; Sibbald, P. A.; Barry, C. E., 3rd; Schnappinger, D.; Finzel, B. C.; Aldrich, C. C. Bisubstrate adenylation inhibitors of biotin protein ligase from *Mycobacterium tuberculosis*. *Chem. Biol.* 2011, 18 (11), 1432–41.
- (11) Brown, P. H.; Cronan, J. E.; Grötl, M.; Beckett, D. The biotin repressor: modulation of allostery by corepressor analogs. *J. Mol. Biol.* 2004, 337 (4), 857–869.
- (12) Tieu, W.; Polyak, S. W.; Paparella, A. S.; Yap, M. Y.; Soares da Costa, T. P.; Ng, B.; Wang, G.; Lumb, R.; Bell, J. M.; Turnidge, J. D.; Wilce, M. C.; Booker, G. W.; Abell, A. D. Improved Synthesis of Biotinyl-5'-AMP: Implications for Antibacterial Discovery. *ACS Med. Chem. Lett.* 2015, 6 (2), 216–20.
- (13) Sittiwong, W.; Cordonier, E. L.; Zempleni, J.; Dussault, P. H. beta-Keto and beta-hydroxyphosphonate analogs of biotin-5'-AMP are inhibitors of holocarboxylase synthetase. *Bioorg. Med. Chem. Lett.* 2014, 24 (24), 5568–71.
- (14) Tieu, W.; Jarrad, A. M.; Paparella, A. S.; Keeling, K. A.; Soares da Costa, T. P.; Wallace, J. C.; Booker, G. W.; Polyak, S. W.; Abell, A. D. Heterocyclic acyl-phosphate bioisostere-based inhibitors of *Staphylococcus aureus* biotin protein ligase. *Bioorg. Med. Chem. Lett.* 2014, 24 (19), 4689–93.
- (15) Tieu, W.; Soares da Costa, T. P.; Yap, M. Y.; Keeling, K. L.; Wilce, M. C. J.; Wallace, J. C.; Booker, G. W.; Polyak, S. W.; Abell, A. D. Optimising *in situ* click chemistry: the screening and identification of biotin protein ligase inhibitors. *Chem. Sci.* 2013, 4, 3533–3537.
- (16) Pendini, N. R.; Yap, M. Y.; Polyak, S. W.; Cowieson, N. P.; Abell, A.; Booker, G. W.; Wallace, J. C.; Wilce, J. A.; Wilce, M. C. Structural characterization of *Staphylococcus aureus* biotin protein ligase and interaction partners: An antibiotic target. *Protein Sci.* 2013, 22 (6), 762–73.
- (17) Koziara, A. A Facile, One-Pot Conversion of Primary Alcohols into Amines. *J. Chem. Res. (S)* 1989, No. 9, 296–297.
- (18) Soares da Costa, T. P.; Tieu, W.; Yap, M. Y.; Zvarec, O.; Bell, J. M.; Turnidge, J. D.; Wallace, J. C.; Booker, G. W.; Wilce, M. C.; Abell, A. D.; Polyak, S. W. Biotin analogues with antibacterial activity are potent inhibitors of biotin protein ligase. *ACS Med. Chem. Lett.* 2012, 3 (6), 509–14.
- (19) Polyak, S. W.; Chapman-Smith, A.; Brautigan, P. J.; Wallace, J. C. Biotin Protein Ligase from *Saccharomyces cerevisiae*: The N-terminal domain is required for complete activity. *J. Biol. Chem.* 1999, 274 (46), 32847–32854.
- (20) Cheng, Y.; Prusoff, W. H. Relationship between the inhibition constant (K_i) and the concentration of inhibitor which causes 50% inhibition (IC₅₀) of an enzymatic reaction. *Biochem. Pharmacol.* 1973, 22 (23), 3099–108.
- (21) Tommasi, R.; Brown, D. G.; Walkup, G. K.; Manchester, J. L.; Miller, A. A. ESKAPEing the labyrinth of antibacterial discovery. *Nat. Rev. Drug Discovery* 2015, 14 (8), 529–42.
- (22) Charpentier, E.; Anton, A. L.; Barry, P.; Alfonso, B.; Fang, Y.; Novick, R. P. Novel cassette-based shuttle vector system for gram-positive bacteria. *Appl. Environ. Microbiol.* 2004, 70 (10), 6076–6085.



Statement of Authorship

Title of Paper	Heterocyclic acyl-phosphate bioisostere-based inhibitors of <i>Staphylococcus aureus</i> biotin protein ligase
Publication Status	<input checked="" type="checkbox"/> Published <input type="checkbox"/> Accepted for Publication <input type="checkbox"/> Submitted for Publication <input type="checkbox"/> Unpublished and Unsubmitted work written in manuscript style
Publication Details	William Tieu, Angie M. Jarrad, Ashleigh S. Paparella, Kelly A Keeling, Tatiana P. Soares da Costa, John C. Wallace, Grant W. Booker, Steven W. Po'yak, Andrew D. Abell, 2014, <i>Bioorganic & Medicinal Chemistry Letters</i> , 24, 4689-4693

Candidate Author

Name of Author (Candidate)	Ashleigh S. Paparella
Contribution to the Paper	Performed biochemical assays of 7a-b, 8a-b, 9a-b, 10e and analysis of data.
Overall percentage (%)	5%
Certification:	This paper reports on original research I conducted during the period of my Higher Degree by Research candidature and is not subject to any obligations or contractual agreements with a third party that would constrain its inclusion in this thesis.
Signature	Date 25/10/2016

Co-Author Contributions

By signing the Statement of Authorship, each author certifies that:

- the candidate's stated contribution to the publication is accurate (as detailed above);
- permission is granted for the candidate to include the publication in the thesis; and
- the sum of all co-author contributions is equal to 100% less the candidate's stated contribution.

Name of Co-Author	William Tieu
Contribution to the Paper	Primary role in manuscript preparation. Design of compounds 7a-b, 8a-b, 9a-b and 10e Synthesis and characterization of 5, 7a-b, 8a-b and 9a-b Overall contribution: 22.5%
Signature	Date 24/10/16

Name of Co-Author	Angie M. Jarrad
Contribution to the Paper	Design of compounds 10a-d and 10f-g Synthesis and characterization of 10a-d and 10f-g Antibacterial susceptibility assays of 10a-d and 10f-g Overall contribution: 22.5%
Signature	Date 24 OCT 16

Name of Co-Author	Kelly A. Keeling		
Contribution to the Paper	Synthesis and characterization of 6 and 10d Biochemical assay of 6 Overall contribution: 5%		
Signature		Date	21/10/2016

Name of Co-Author	Tatiana P. Soares da Costa		
Contribution to the Paper	Assisted with biochemical assays Overall contribution: 5%		
Signature		Date	10/10/16

Name of Co-Author	John C. Wallace		
Contribution to the Paper	Provided intellectual discussion Overall contribution: 5%		
Signature		Date	11/10/16

Name of Co-Author	Grant W. Booker		
Contribution to the Paper	Supervised all biological aspects of the project Overall contribution: 5%		
Signature		Date	19/10/2016

Name of Co-Author	Steven W. Polyak		
Contribution to the Paper	Supervised all biological aspects of the project Assisted in proof reading and editing of manuscript. Overall contribution: 15%		
Signature		Date	30/9/2016.

Name of Co-Author	Andrew D. Abell		
Contribution to the Paper	Provided direction in all aspects of synthetic chemistry and is corresponding author on paper. Assisted in proof reading and editing of manuscript Overall contribution: 15%		
Signature		Date	19/10/2016



Contents lists available at ScienceDirect

Bioorganic & Medicinal Chemistry Letters

journal homepage: www.elsevier.com/locate/bmcl

Heterocyclic acyl-phosphate bioisostere-based inhibitors of *Staphylococcus aureus* biotin protein ligase



William Tieu^{a,*}, Angie M. Jarrad^{b,†,§}, Ashleigh S. Paparella^b, Kelly A. Keeling^a,
Tatiana P. Soares da Costa^{b,‡}, John C. Wallace^b, Grant W. Booker^b, Steven W. Polyak^b, Andrew D. Abell^{a,*}

^aSchool of Chemistry and Physics, University of Adelaide, Adelaide, South Australia 5005, Australia

^bSchool of Molecular and Biomedical Science, University of Adelaide, Adelaide, South Australia 5005, Australia

ARTICLE INFO

Article history:

Received 29 May 2014

Revised 7 August 2014

Accepted 11 August 2014

Available online 19 August 2014

Keywords:

Antibiotics

Bioisosteres

Inhibitors

Ligases

Drug design

ABSTRACT

Inhibitors of *Staphylococcus aureus* biotin protein ligase (SaBPL) are generated by replacing the acyl phosphate group of biotinyl-5'-AMP with either a 1,2,3-triazole (see **5/10a/10b**) or a 1,2,4-oxadiazole (see **7**) bioisostere. Importantly, the inhibitors are inactive against the human BPL. The nature of the 5-substituent in the component benzoxazolone of the optimum 1,2,3-triazole series is critical to activity, where this group binds in the ATP binding pocket of the enzyme.

© 2014 Elsevier Ltd. All rights reserved.

Biotin protein ligase (BPL) is an adenylate forming enzyme that catalyses the reaction of biotin and ATP to form an acyl AMP intermediate known as biotinyl-5'-AMP (**1**). This intermediate is then employed in the biotinylation and subsequent activation of acetyl CoA carboxylase; a key metabolic enzyme that is central to membrane biogenesis and, hence, the viability of all organisms.^{1,2} Thus, the inhibition of BPL has been identified as a viable drug target for pathogens resistant to existing chemotherapies.^{3–8} Recent efforts in this area have focused on developing mimics of biotinyl-5'-AMP **1**, where the reactive acyl phosphate group is replaced with a stable bioisosteres^{9–24} but to date, only a handful of acyl phosphate bioisosteres have been reported that mimic biotinyl-5'-AMP.^{5–8} For example, biotinyl-5'-AMP **2** with its phosphodiester bioisostere, is a potent inhibitor of BPL from *Staphylococcus aureus* (SaBPL), *Escherichia coli* and *Homo sapiens* (HsBPL).^{5,24} Importantly, this compound also inhibits the growth of *Staphylococcus aureus* with a minimal inhibitory concentration (MIC) of 8 µg/µL.⁵

Sulfonamide isosteres, as found in **3**, have also been reported to be active against *Mycobacterium tuberculosis* BPL, with no data reported on other BPLs.^{6,7}

We also recently reported a 1,2,3-triazole as an effective bioisostere of the hydrolytically unstable acyl phosphate of **1**, for example, see **4**, Figure 1.⁵ A 1,2,3-triazole heterocycle as in **4** offers significant advantages over other reported acyl phosphate bioisosteres in that it allows for both facile synthesis by Huisgen cycloaddition and also combinatorial in situ approaches to inhibitor discovery and optimization.^{5,25} This work identified 1,2,3-triazole **5** as the most potent ($K_i = 0.09 \pm 0.01$ µM) and selective (>1100 fold in K_i , SaBPL vs HsBPL) inhibitor of SaBPL reported to date.⁵ The triazole **5** inhibits the growth of *S. aureus*, while being devoid of cytotoxicity against cultured human liver cells.⁵ X-ray crystal structures of SaBPL in complex with **5**, in combination with mutagenesis studies, identified a key role for active site amino acids Arg122, Arg125 and Asp180 in selective binding to SaBPL (see Fig. 3). X-ray crystallography also confirmed that the benzoxazolone group of 1,2,3-triazole **5** binds into the ATP pocket of SaBPL thereby functioning as a replacement of the adenine group present in **1–4**.

This paper reports the synthesis of analogues of 1,2,3-triazole **5** and their inhibition against SaBPL and HsBPL. The inverted 1,2,3-triazole **6**, 1,2,4-oxadiazole **7**, 1,2,4-triazole **8** and 1,3,4-oxadiazole **9** heterocycles were compared as possible bioisosteres of the reactive acyl phosphate group of **1** (see Fig. 2). All compounds

* Corresponding authors. Tel.: +61 88 3135360 (W.T.); tel.: +61 88 313 5652; fax: +61 88 303 4358 (A.D.A.).

E-mail addresses: william.tieu@adelaide.edu.au (W. Tieu), andrew.abell@adelaide.edu.au (A.D. Abell).

† These authors contributed equally.

‡ Current address: School of Biomedical Sciences, Charles Sturt University, Boorooma St, Wagga Wagga, New South Wales 2678, Australia.

§ Current address: Institute for Molecular Bioscience, The University of Queensland, Brisbane 4072, Australia.

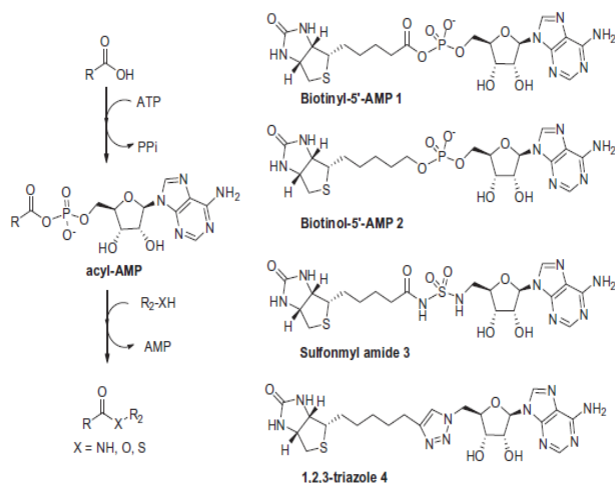


Figure 1. General reaction mechanism of adenylate forming enzymes (left); acyl AMP analogues of biotin protein ligase (right).

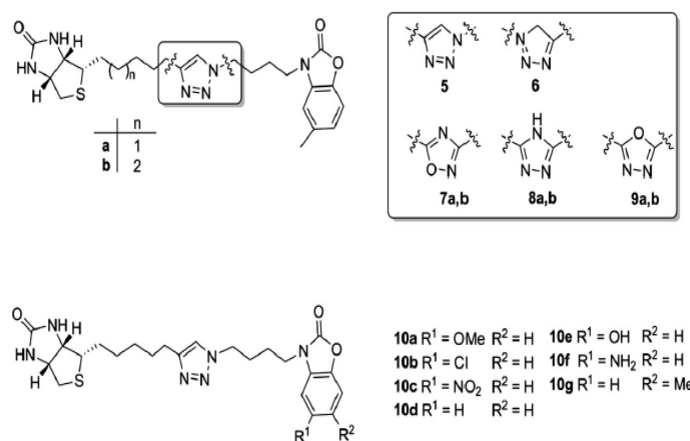


Figure 2. Heterocyclic analogues derived from biotinyl-5'-AMP 1.

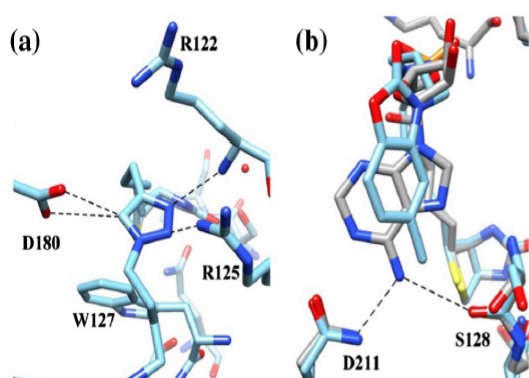


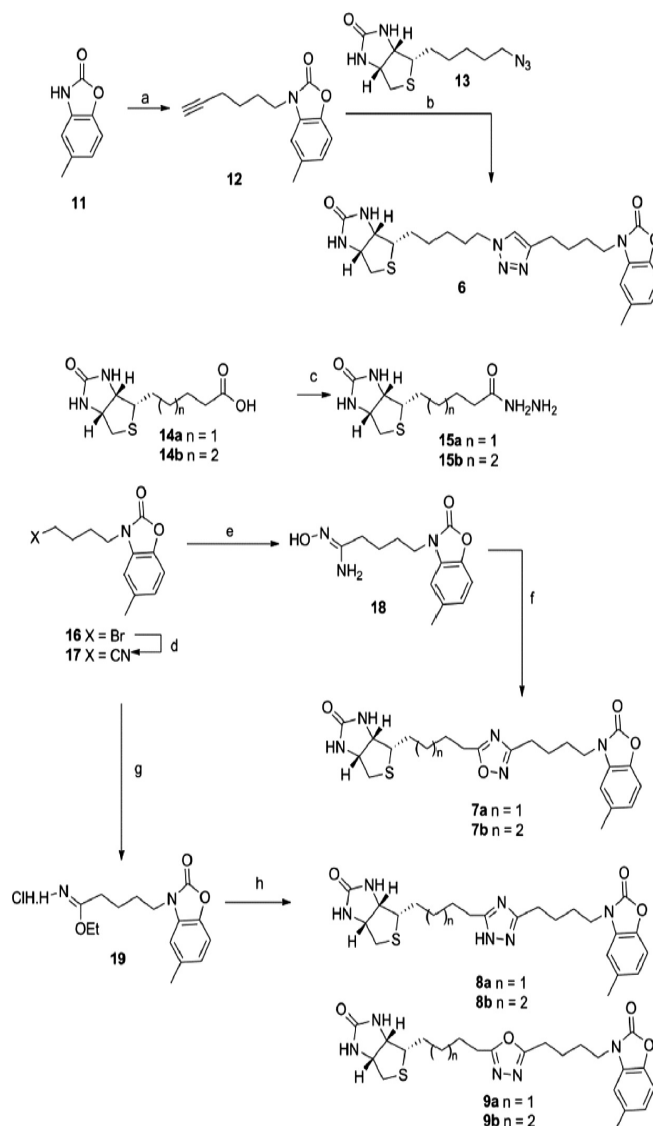
Figure 3. (a) X-ray crystal structure of 5 bound to SaBPL. Interactions between the 1,2,3-triazole ring and residues are highlighted with black dashes. The edge to face pi interaction between 1,2,3-triazole ring and W127 is not shown. (b) An overlay of X-ray crystal structure of biotinyl-5'-AMP 1 and 1,2,3-triazole 5. The hydrogen bonding interactions between amine of 1 and D211 (3.06 Å) and S128 (3.41 Å) are highlighted with black dashes. Methyl substituent of 5 is 4.00 Å and 3.02 Å away from D211 and S128, respectively.

share the benzoxazolone group and optimum tether linkers either side of the bioisostere as found in 5, where a simple methylene-based tether can replace the ribose group of 1 and 4 without

compromising inhibitory activity. A range of substituents on the benzoxazolone group of 5 were also investigated in order to begin to explore interactions with the ATP binding pocket of SaBPL, see compounds 10 Figure 2.

The 1,2,3-triazole 6 was prepared by alkylation of benzoxazolone 11,⁵ followed by copper-catalyzed cycloaddition with biotin azide 13³ in the presence of copper nano powder. Heterocycles 7–9 were each prepared in two steps from a common starting nitrile 17 as shown in Scheme 1. In particular, oxime 18, prepared on reaction of 17 with hydroxylamine, was treated with biotin 14b²⁶ and EDCI with subsequent dehydration under reflux to give 1,2,4-oxadiazole 7b. Conversely, conversion of nitrile 17 to imidic ester 19, followed by microwave reaction with hydrazide 15b in the presence of K₂CO₃, gave 1,2,4-triazole 8b in 32% yield. 1,3,4-Oxadiazole 9b was also isolated from this reaction in 17% yield. Interestingly, reaction of 14 with 19 under acidic conditions (acetic acid) gave solely the 1,3,4-oxadiazole 9b and not the 1,2,4-triazole 8b based on analysis by analytical HPLC and mass spectrometry. Truncated analogues 7a, 8a and 9a were prepared in the same fashion as shown in Scheme 1. The key building blocks 15a,²⁷ 15b and 17 used in these syntheses were prepared as shown in Scheme 1.

The synthesis of the 1,2,3-triazoles 10a–g is summarized in Scheme 2. The key benzoxazolone azides 22a–e were obtained on reacting the respective 2-amino phenol (20a–e) with

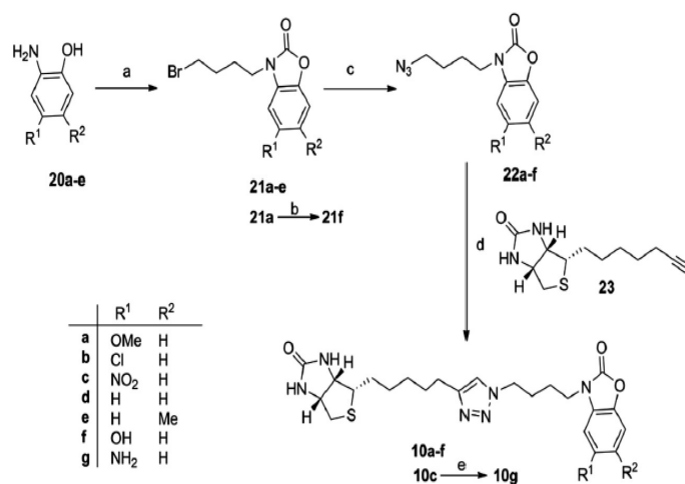


Scheme 1. Reagents and conditions: (a) 5-hexynyl tosylate, K_2CO_3 , DMF; (b) Cu nano powder, MeCN/H₂O; (c) (i) $SOCl_2$, MeOH, (ii) $NH_2NH_2 \cdot H_2O$, Δ ; (d) KCN, DMF; (e) NH_2OH , EtOH, Δ ; (f) (i) **14**, EDCI-HCl, DIPEA, DMF, (ii) PhMe, Δ ; (g) AcCl, EtOH; (h) **15**, K_2CO_3 , 1:1 DMF/PhMe, 150 °C, MW, 2 h (gave **9** (18%) and **8** (32%)) or AcOH, EtOH, Δ , 4 h (gave **9** (21%)).

1,1-carbonyldiimidazole, followed by alkylation with dibromobutane and subsequent conversion of the bromide to azide. Benzoxazolone **22f** was prepared by demethylation of **21a** with NaI in aqueous HBr, followed by treatment with sodium azide. Copper catalyzed cycloaddition of biotin alkyne **23** and benzoxazolone azides **22a–f** in the presence of copper nano powder gave the corresponding 1,2,3-triazole **10a–f**. Reduction of 1,2,3-triazole **10c** with aqueous titanium trichloride gave **10g**.

The complete activity profiles of heterocycles **6–9** and the new derivatives of **5** (i.e., **10a–g**) were determined against SaBPL and HsBPL using an in vitro biotinylation assay^{5,28} that measures the enzymatic incorporation of radiolabelled biotin onto an acceptor protein, see Tables 1 and 2. A 1,2,4-oxadiazole heterocycle as in **7b** provided an effective acyl phosphate bioisostere for the generation of inhibitors of SaBPL (**7b** had a $K_i = 1.2 \pm 0.4 \mu M$). While this compound is somewhat less active than the parent 1,2,3-triazole **5** (K_i of $0.09 \pm 0.01 \mu M$)⁵ it does provide an important new lead for further optimisation. Interestingly, 1,2,3-triazole **6**, 1,3,4-triazole **8b** and 1,3,4-oxadiazole **9b** were all inactive against SaBPL. These

results are somewhat surprising given the close similarities of the constituent heterocycles (i.e., **5** vs **6** and **9b** vs **7b**). We suggest that the relative ability of each heterocycle to hydrogen bond with SaBPL residues Arg125, Asp180 and Lys187 (see Fig. 3a) may account for the observed difference. These three residues undergo significant conformational changes on inhibitor binding and are responsible for creating the tight association between ligand and enzyme.^{3,5,29} Any disruption to these key interactions, by a particular heterocycle, would be expected to significantly impact on binding and hence potency, as in **5** and **6**. In support, we know that certain biotin-based analogues are more effective than others at inducing the conformational change.^{3,29} Specifically, biotin acetylene **23**, the synthetic precursor for **5**, is a more potent inhibitor of SaBPL than is biotin azide **13**, the precursor for **6** (K_i of $0.3 \mu M$ and $>10 \mu M$ respectively).³ Based on this observation alone it is clear that the position of the nitrogen relative to the biotin heterocycle is critical for activity. Whilst 1,2,3-triazole **5** and the 1,2,4-oxadiazole **7b** were active against SaBPL, both were inactive against human BPL (HsBPL). This is an important observation for



Scheme 2. Reagents and conditions: (a) CDI, DCM; Br(CH₂)₄Br, K₂CO₃, DMF; (b) NaI, HBr (aq); (c) NaN₃, DMF; (d) Cu nano powder, MeCN/H₂O; (e) 15% TiCl₃ (aq).

Table 1
Inhibition assay results of 4–12 against SaBPL and HsBPL^{a,b,c}

	Heterocycle	SaBPL K _i (μM)	HsBPL K _i (μM)
5	1,2,3-Triazole	0.09 ± 0.01	NI
6	1,2,3-Triazole ^d	NI	NI
7a	1,2,4-Oxadiazole	NI	NI
7b	1,2,4-Oxadiazole	1.2 ± 0.4	NI
8a	1,2,4-Triazole	NI	NI
8b	1,2,4-Triazole	NI	NI
9a	1,3,4-Oxadiazole	NI	NI
9b	1,3,4-Oxadiazole	NI	NI

^a See Figure 2 for structures and see Supplementary material for procedure.

^b All compounds possessed no inhibition against HsBPL at ≥ 80 μM.

^c NI: No inhibition at concentrations ≥ 80 μM.

^d This heterocycle possesses a different configuration than 5, see Figure 2.

Table 2
Inhibition assay results of 5 and 10a–g against SaBPL and HsBPL^{a,b,c}

	R ₁	R ₂	SaBPL K _i (μM)	HsBPL K _i (μM)
5	Me	H	0.09 ± 0.01	NI
10a	OMe	H	1.87 ± 0.11	NI
10b	Cl	H	0.60 ± 0.05	NI
10c	NO ₂	H	NI	NI
10d	H	H	NI	NI
10e	H	Me	NI	NI
10f	OH	H	NI	NI
10g	NH ₂	H	NI	NI

^a See Figure 2 for structures and see Supplementary material for procedure.

^b All compounds possessed no inhibition against HsBPL at ≥ 80 μM.

^c NI: No inhibition at concentrations ≥ 80 μM.

ongoing development of new antibiotics based on the inhibition of BPL. Finally, the length of the tether between the biotin bicycle and the bioisostere is critical for activity. The corresponding truncated 1,2,4-oxadiazole **7a** (cf. **7b**) was devoid of inhibitory activity against SaBPL.

The results for the second series of compounds revealed that for the best base heterocycle (1,2,3-triazole), both methyl (**5**, K_i = 0.09 ± 0.01 μM) and chloro substituents (**10b**, K_i = 0.60 ± 0.05 μM) were well tolerated at R₁, as was methoxy to a lesser extent (**10a**, K_i = 1.87 ± 0.11 μM) (Table 2). Interestingly, neither a hydroxyl nor amino group were tolerated at R₁ (see **10f** and **10g**), despite molecular modeling suggesting these groups could potentially hydrogen bond with Asn212 and Ser128 residues within the ATP

binding pocket of SaBPL, see Figure 3b.³⁰ The position of the methyl substituent on the 1,2,3-triazole heterocycle is critical, where methyl at the alternative R₂ position gives rise to an inactive compound (see **10e**). Interestingly the unsubstituted derivative (**10d**) is also inactive.

Importantly the two new active 1,2,3-triazoles **10a** and **10b** both displayed bacteriostatic activity against *S. aureus* ATCC 49755 in an antibacterial microdilution broth assay (see Fig. 4). At 8 μg/mL inhibitor concentration, *S. aureus* growth was reduced to 55% for **10a** and 60% for **10b** relative to 58% for **5** and the streptomycin control (MIC = 8 μg/mL). This compares to a value of 24% for biotin acetylene **23**. MIC values could not be obtained for these compounds because of limited solubility at concentrations greater than 64 μg/mL.

In summary, heterocyclic-based bioisosteres of the acyl phosphate of biotinyl-5'-AMP **1** are reported. 1,2,3-Triazole (see **5**, **10a** and **10b**) and 1,2,4-oxadiazole (see **7b**) heterocycles provide potent and selective inhibitors of SaBPL. These heterocycles are, in general, easier to prepare than classic phosphodiester and sulfamylamides bioisosteres and provide improved selectivity for SaBPL over HsBPL. A second series of analogues containing the optimum 1,2,3-triazole isostere, were also prepared, to investigate binding of the terminal benzoxazolone to the ATP binding pocket of SaBPL. A hydrophobic substituent at R₁ on the benzoxazolone

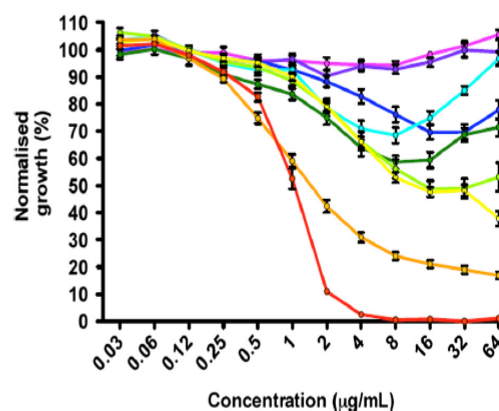


Figure 4. Inhibition of *S. aureus* growth in vitro. Compounds **5** (yellow), **23** (orange), **10a** (lime), **10b** (green), **10c** (fuchsia), **10d** (purple), **10f** (azure), **10g** (blue) and positive control streptomycin (red). See Supplementary data for conditions.

is favored, with chloro being particularly active ($K_i = 0.6 \mu\text{M}$). Work on optimization the 1,2,3-triazoles with a more expansive SAR study and developing these isosteres to other clinically relevant adenylate forming enzyme targets is currently underway.

Acknowledgments

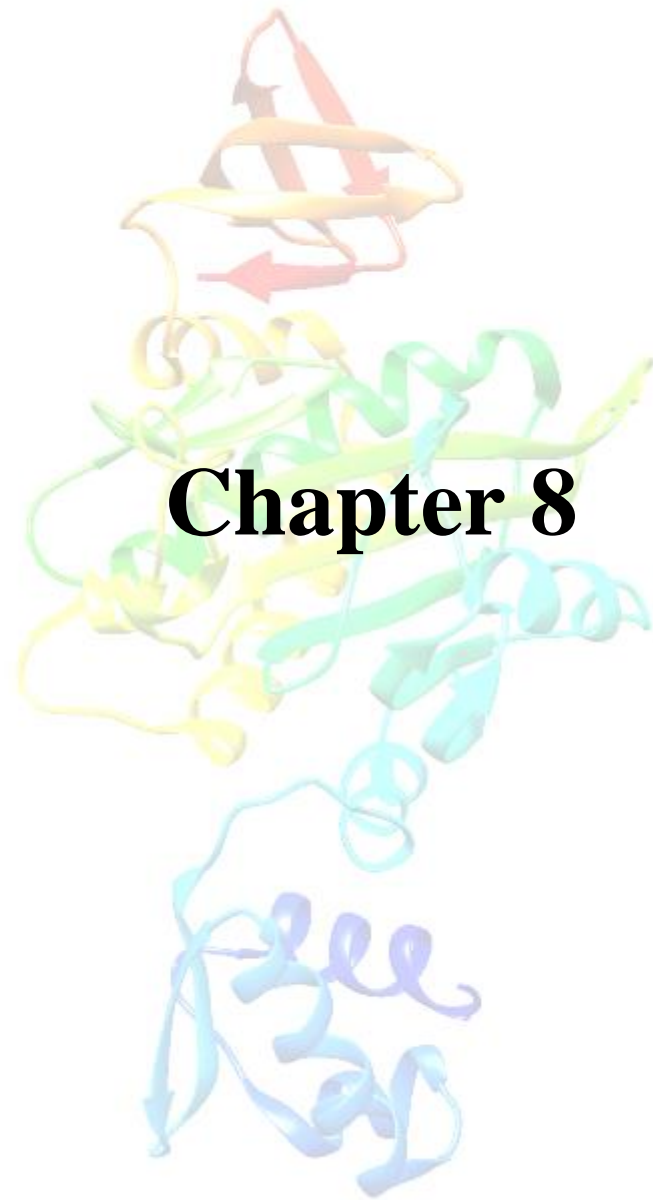
Thank you to Lim Jing Ting Vernise for synthesizing compounds **21e** and **22e**. We are grateful to the National Health and Medical Research Council (NHMRC application APP1011806 and APP1068885) for financial support and to Australian National Fabrication Facility for providing access to analytical HPLC equipment.

Supplementary data

Supplementary data (details on chemical synthesis, enzyme inhibition assay and antimicrobial broth assay) associated with this article can be found, in the online version, at <http://dx.doi.org/10.1016/j.bmcl.2014.08.030>.

References and notes

- Paparella, A. S.; Soares da Costa, T. P.; Yap, M. Y.; Tieu, W.; Wilce, M. C. J.; Booker, G. W.; Abell, A. D.; Polyak, S. W. *Curr. Top. Med. Chem.* **2014**, *14*, 4.
- Polyak, S. W.; Abell, A. D.; Wilce, M. C. J.; Zhang, L.; Booker, G. W. *Appl. Microbiol. Biotechnol.* **2012**, *93*, 983.
- Soares da Costa, T. P.; Tieu, W.; Yap, M. Y.; Zvarec, O.; Bell, J. M.; Turnidge, J. D.; Wallace, J. C.; Booker, G. W.; Wilce, M. C. J.; Abell, A. D.; Polyak, S. W. *ACS Med. Chem. Lett.* **2012**, *3*, 509.
- Payne, D. J.; Gwynn, M. N.; Holmes, D. J.; Pompliano, D. L. *Nat. Rev. Drug Disc.* **2007**, *6*, 29.
- Soares da Costa, T. P.; Tieu, W.; Yap, M. Y.; Pardini, N. R.; Polyak, S. W.; Sejer Pedersen, D.; Morona, R.; Turnidge, J. D.; Wallace, J. C.; Wilce, M. C. J.; Booker, G. W.; Abell, A. D. *J. Biol. Chem.* **2012**, *287*, 17823.
- Duckworth, B. P.; Geders, T. W.; Tiwari, D.; Boshoff, H. I.; Sibbald, P. A.; Barry Iii, C. E.; Schnappinger, D.; Finzel, B. C.; Aldrich, C. C. *Chem. Biol.* **2011**, *18*, 1432.
- Shi, C.; Tiwari, D.; Wilson, D. J.; Seiler, C. L.; Schnappinger, D.; Aldrich, C. C. *ACS Med. Chem. Lett.* **2013**, *4*, 1213.
- Brown, P. H.; Cronan, J. E.; Grötl, M.; Beckett, D. *J. Mol. Biol.* **2004**, *337*, 857.
- Lu, X.; Zhou, R.; Sharma, I.; Li, X.; Kumar, G.; Swaminathan, S.; Tonge, P. J.; Tan, D. S. *ChemBioChem* **2012**, *13*, 129.
- Somu, R. V.; Boshoff, H.; Qiao, C.; Bennett, E. M.; Barry, C. E.; Aldrich, C. C. *J. Med. Chem.* **2005**, *49*, 31.
- Qiao, C.; Wilson, D. J.; Bennett, E. M.; Aldrich, C. C. *J. Am. Chem. Soc.* **2007**, *129*, 6350.
- Yu, X. Y.; Hill, J. M.; Yu, G.; Wang, W.; Kluge, A. F.; Wendler, P.; Gallant, P. *Bioorg. Med. Chem. Lett.* **1999**, *9*, 375.
- Bemier, S.; Akochy, P.-M.; Lapointe, J.; Chênevert, R. *Bioorg. Med. Chem.* **2005**, *13*, 69.
- Auld, D. S.; Lovell, S.; Thorne, N.; Lea, W. A.; Maloney, D. J.; Shen, M.; Rai, G.; Battaile, K. P.; Thomas, C. J.; Simeonov, A.; Hanzlik, R. P.; Ingles, J. *Proc. Natl. Acad. Sci. U.S.A.* **2010**, *107*, 4878.
- Lun, S.; Guo, H.; Adamson, J.; Cisar, J. S.; Davis, T. D.; Chavadi, S. S.; Warren, J. D.; Quadri, L. E. N.; Tan, D. S.; Bishai, W. R. *Antimicrob. Agents Chemother.* **2013**, *57*, 5138.
- Patrone, J. D.; Yao, J.; Scott, N. E.; Dotson, G. D. *J. Am. Chem. Soc.* **2009**, *131*, 16340.
- Tian, Y.; Suk, D.-H.; Cai, F.; Crich, D.; Mesecar, A. D. *Biochemistry* **2008**, *47*, 12434.
- Giulli, A.; Scott, D. E.; Ando, M.; Reyes, F.; Saldanha, S. A.; Tuck, K. L.; Chirgadze, D. Y.; Blundell, T. L.; Abell, C. *ChemBioChem* **2008**, *9*, 2606.
- Tuck, K. L.; Saldanha, S. A.; Birch, L. M.; Smith, A. G.; Abell, C. *Org. Biomol. Chem.* **2006**, *4*, 3598.
- Ferreras, J. A.; Ryu, J.-S.; Di Lello, F.; Tan, D. S.; Quadri, L. E. N. *Nat. Chem. Biol.* **2005**, *1*, 29.
- Schmelz, S.; Naismith, J. H. *Curr. Opin. Struct. Biol.* **2009**, *19*, 666.
- Duckworth, B. P.; Nelson, K. M.; Aldrich, C. C. *Curr. Top. Med. Chem.* **2012**, *12*, 766.
- Vannada, J.; Bennett, E. M.; Wilson, D. J.; Boshoff, H. I.; Barry, C. E.; Aldrich, C. C. *Org. Lett.* **2006**, *8*, 4707.
- Xu, Z.; Yin, W.; Martinelli, L. K.; Evans, J.; Chen, J.; Yu, Y.; Wilson, D. J.; Mizrahi, V.; Qiao, C.; Aldrich, C. C. *Bioorg. Med. Chem.* **2014**, *22*, 1726.
- Tieu, W.; Soares da Costa, T. P.; Yap, M. Y.; Keeling, K. L.; Wilce, M. C. J.; Wallace, J. C.; Booker, G. W.; Polyak, S. W.; Abell, A. D. *Chem. Sci.* **2013**, *4*, 3533.
- Wilbur, D. S.; Chyan, M.-K.; Pathare, P. M.; Hamlin, D. K.; Frownfelter, M. B.; Kegley, B. B. *Bioconjugate Chem.* **2000**, *11*, 569.
- Wilchek, M.; Bayer, E. A. In Meir, W., Edward, A. B., Eds.; *Methods in Enzymology*; Academic Press, 1990; 184, p 123.
- Polyak, S. W.; Chapman-Smith, A.; Brautigan, P. J.; Wallace, J. C. *J. Biol. Chem.* **1999**, *274*, 32847.
- Wood, Z. A.; Weaver, L. H.; Brown, P. H.; Beckett, D. *J. Mol. Biol.* **2006**, *357*, 509.
- See Supporting information.



Statement of Authorship

Title of Paper	Halogenation of biotin protein ligase inhibitors improves antibacterial activity against <i>Staphylococcus aureus</i>
Publication Status	<input type="checkbox"/> Published <input type="checkbox"/> Accepted for Publication <input type="checkbox"/> Submitted for Publication <input checked="" type="checkbox"/> Unpublished and Unsubmitted work written in manuscript style
Publication Details	Ashleigh S. Paparella, Jiage Feng, Andrew Hayes, David Helm, Grant W. Booker, Andrew D. Abell, Steven W. Polyak

Principal Author

Name of Principal Author (Candidate)	Ashleigh S. Paparella		
Contribution to the Paper	Primary role in manuscript preparation Performed <i>in silico</i> Docking of compounds 5a-d Biochemical assay of compounds 4 and 5a-d and analysis of data Surface plasmon resonance experiments of compounds 4 and 5a-c		
Overall percentage (%)	25%		
Certification:	This paper reports on original research I conducted during the period of my Higher Degree by Research candidature and is not subject to any obligations or contractual agreements with a third party that would constrain its inclusion in this thesis. I am a primary author of this paper.		
Signature		Date	11/11/2016

Co-Author Contributions

By signing the Statement of Authorship, each author certifies that:

- the candidate's stated contribution to the publication is accurate (as detailed above);
- permission is granted for the candidate to include the publication in the thesis; and
- the sum of all co-author contributions is equal to 100% less the candidate's stated contribution.

Name of Co-Author	Jiage Feng		
Contribution to the Paper	Design of compounds 5a-d Synthesis and characterization of 5a-d Overall contribution: 15%		
Signature		Date	25/10/16

Name of Co-Author	Andrew Hayes		
Contribution to the Paper	Antimicrobial susceptibility assays of 4 and 5a-d Overall contribution: 5%		
Signature		Date	4/11/16

Name of Co-Author	David Heim		
Contribution to the Paper	Cytotoxicity assays with 5a-c in 1 human cell line Overall contribution: 5%		
Signature		Date	26/10/2016

Name of Co-Author	Grant W. Booker		
Contribution to the Paper	Supervised biological aspects of the project, revised manuscript Overall contribution: 10%		
Signature		Date	19/10/2016

Name of Co-Author	Andrew D. Abell		
Contribution to the Paper	Designed and directed all medicinal chemistry Overall contribution: 20%		
Signature		Date	19/10/2016

Name of Co-Author	Steven W. Polyak		
Contribution to the Paper	Supervised biological aspects of the project. Worked closely with principal author to write the manuscript. Overall contribution: 20%		
Signature		Date	19/10/2016

Halogenation of biotin protein ligase inhibitors improve antibacterial activity against

Staphylococcus aureus

Ashleigh S. Paparella #, Jiage Feng §, Andrew Hayes #, David Heim #, Grant W. Booker #, Andrew D. Abell §, Steven W. Polyak #*

School of Biological Sciences, University of Adelaide, Adelaide, South Australia, 5005, Australia.

§ School of Physical Sciences, University of Adelaide, Adelaide, South Australia, 5005, Australia

*Address correspondence to: Steven W. Polyak, Molecular Life Sciences Building, Department of Molecular and Cellular Biology, University of Adelaide, South Australia, Australia, 5005, Tel: 61-8-8303-5289; Fax: 61-8-8303-4362; E-mail: steven.polyak@adelaide.edu.au

Biotin protein ligase (BPL) represents a promising target for the development of new antibacterials. Chemical analogues of the reaction intermediate produced by BPLs represent a new class of antibiotics. The replacement of the labile phosphoanhydride linker with a non-hydrolysable 1,4-disubstituted-1,2,3-triazole heterocycle has led to the development of potent BPL inhibitors that have excellent selectivity over the human isozyme. However, the antibacterial activity is not potent enough to determine a minimal inhibitory concentration (MIC). In this study we investigated whether halogenation of our lead biotin triazole inhibitor 4 improved cell permeability and antibacterial activity against *Staphylococcus aureus*. The hydrogen on the C5 atom of the triazole heterocycle was targeted for replacement by a halogen atom (I, F, Cl) or a phenyl ring to generate 1,4,5-trisubstituted-1,2,3-triazoles (5a-d). All 4 analogues exhibited sub-micromolar inhibition constants and low micromolar binding affinities against SaBPL, similar to the parent molecule. Importantly the 5-fluoro-1,2,3-triazole had antibacterial activity against *S. aureus* with an MIC of 8 µg/mL this is the first example of a biotin triazole inhibitor where the MIC could be determined. The results from this study highlight that halogenation of BPL inhibitors represent one strategy to improve antibacterial activity against *S. aureus*. These compounds represent promising candidates for further optimization in order to develop BPL antibacterials.

INTRODUCTION:

There is an urgent need to discover new antibiotics to combat antibiotic resistant bacteria [1]. The advent of genome wide DNA sequencing has provided us with a number of potential drug targets that can be exploited for identifying novel antibacterials with new modes of action [2]. One of the major roadblocks associated with target based approaches to antibiotic discovery is the transition of hits with potent *in vitro* activity into bio-actives with whole cell antibacterial activity [2, 3]. The bacterial cell wall and membrane structures present as a formidable barrier that prevents compounds from entering cells and accessing intracellular drug targets. One potential strategy that can improve upon cell permeability is to generate halogenated analogues of a hit molecule [4]. This has been demonstrated with fluoroquinolones, where replacement of C6 with fluorine resulted in an ~100-fold decrease in the minimal inhibitory concentration (MIC)[5, 6]. Similar approaches have also been used to generate phenazine and quinolone scaffolds with biofilm-eradicating activity [7, 8]. One promising target for the development of new antibiotics is the essential enzyme, biotin protein ligase (BPL) [2, 9]. BPL is the sole enzyme responsible for the biotinylation, and subsequent activation, of biotin-dependent enzymes. The clinically important bacterial pathogen *Staphylococcus aureus* possesses two biotin dependent enzymes namely acetyl CoA carboxylase and pyruvate carboxylase, that catalyse key reactions in fatty acid biosynthesis and gluconeogenesis respectively [9]. Protein biotinylation, catalysed by BPL, proceeds through the ligation of biotin **1** and ATP to form biotinyl-5'AMP **2** [9]. A number of chemical analogues of **2** have been investigated as antibacterials that target the BPL from *S. aureus* [10, 11] and other bacteria such as *Escherichia coli* [12-14] and *Mycobacterium tuberculosis* [15, 16]. One such example includes biotinyl-5'AMP **3** (figure 2) that inhibits the growth of *S. aureus* and *M. tuberculosis* with MICs of 2 and 2.5 µg/mL respectively [11].

We have also reported 1,4-disubstituted 1,2,3 triazoles, the biotin triazoles, as a novel class of BPL inhibitor that selectively target the BPL from *S. aureus* over the human homologue [17,

18]. Biotin triazole **4** has been reported as the most potent inhibitor of *S. aureus* BPL (*SaBPL*) with an inhibition constant of 0.09 μM and >1000-fold selectivity over the human homologue [17]. Whilst biotin triazole **4** reduced the growth of *S. aureus* ATCC strain 49775 by 60% with 8 $\mu\text{g/mL}$ in the culture medium, this level of inhibited cell growth was not sufficient to measure a true MIC [10, 17]. Here we report a series of halogenated 1,4,5-trisubstituted biotin triazoles as a new series of *SaBPL* inhibitors with improved antibacterial activity against *S. aureus*, see **5a-d** (figure 2). These derivatives are the first examples of 1,4,5-trisubstituted triazole BPL inhibitors. As a route towards improving the antibacterial activity of lead compound **4** the hydrogen on the C5 atom in the triazole heterocycle was targeted for replacement by iodine, fluorine and chlorine (see compounds **5a-c**). We also synthesized a phenyl substitution, **5d**, to address whether a non-halogenated substitution could improve cell permeability and antibacterial activity.

RESULTS AND DISCUSSION

The molecular mechanism of parent compound **4** binding to *SaBPL* has been determined by X-ray crystallography ([17] PDB 3V7S). This data revealed two key hydrogen bonding interactions between N2 and N3 of the triazole heterocycle with the side chains of R125 and R122 respectively (figure 3a). There is also the potential for hydrogen bonding interactions between the triazole heterocycle and side chains of D180 and K187. *In silico* docking experiments were performed to aid in the design of inhibitors and investigate the possible binding models by which new 1,4,5-trisubstituted triazoles might occupy the active site of the *SaBPL* target. Flexible ligand docking was carried out using AutoDock Vina (1.5.6) [19]. The docking protocol was first validated by removing lead molecule **4** from its co-crystal structure with *SaBPL* (PDB 3V7S) [17] followed by re-docking into the vacated enzyme. The 1,4,5-trisubstituted triazoles **5a-c** were likewise docked into *SaBPL* (figure 3b-d). The *in silico* analysis suggested that the 1,4,5-trisubstituted triazole occupies the same binding pose as 1,4-disubstituted triazole **4**, with rotation about the alkyl chains to best accommodate triazole

heterocycle and maximize binding interactions. The halogen substitutions did not cause steric clashes with the protein that would preclude binding. The predicted binding affinities (supplementary table 1) for **5a-c** were similar, with the phenyl substitution predicted to be the least well tolerated.

The synthesis of the 1,4,5-trisubstituted 1,2,3 triazoles **5a-d** was carried out as summarized in scheme 1 and scheme 2. Synthesis of biotin acetylene **6** which served as the precursor for **7**, was performed as previously described [17]. Synthesis of biotin 1-iodoacetylene **7** was based on conditions reported by Worrell *et al* [20]. Biotin acetylene **6** [17] was treated with 2 equivalents of NMI in the presence of 20% CuI in DMF. Full conversion (>99%) was achieved after 1 hour as judged by ¹H NMR. The reaction mixture was filtered through natural aluminium oxide, washed with MeOH/DCM (1:9) mixture and dried *in vacuo* to give **7** as a pale yellow solid (scheme 1). To prepare **5a**, biotin 1-iodo acetylene **7** was treated with azide **8** [17] in the presence of CuI and stoichiometric quantities of TEA in anhydrous DMF. The resulting 5-iodo-1,2,3-triazole was isolated and purified using flash chromatography to give **5a** in 36% yield (scheme 1)[21].

5-iodo-1,2,3-triazole **5a** was subsequently converted to **5b** and **5c** by halogen exchange based on the optimized conditions reported by Worrell *et al* [22]. **5a** was treated with 5 equivalents of either potassium fluoride or potassium chloride in MeCN/H₂O (1:1) mixture. Vials were placed into the microwave reactor and allowed to stir at 180 °C under 250 psi for 10 minutes. Resulting reaction mixtures were concentrated and purified by flash chromatography to give 5-fluoro-1,2,3-triazole **5b** and 5-chloro-1,2,3-triazole **5c** in 89% and 80% yield respectively (scheme 2). Finally **5d** was prepared by palladium cross coupling reactions via *sp*² arylation of **5a** [23, 24]. 5-iodo-1,2,3-triazole **5a** and phenylboronic acid were coupled in the presence of 1.5 equivalents of potassium carbonate and a catalytic amount of PdCl₂(PPh)₃ in THF at 70 °C for 12 hours to give 5-phenyl-1,2,3-triazole **5d** in 41% yield after purification by flash chromatography (scheme 2).

The complete activity profiles of 1,4,5-tri-substituted triazoles **5a-d** were determined using established biochemical and microbiological assay protocols [17, 25]. The *in vitro* potency and selectivity of triazoles **5a-d** were first measured by enzyme assay and surface plasmon resonance (SPR) using recombinant BPLs from *S. aureus* and *Homo sapiens*. Here, the enzymatic incorporation of radiolabelled biotin onto an acceptor protein was measured in the presence of varying concentrations of inhibitor with the results shown in table 1. Previous enzymology and X-ray crystallography studies have demonstrated that biotin triazole **4** is a competitive inhibitor against biotin **1** [17]. Therefore, inhibition constants (K_i) were calculated from IC_{50} values using the known K_M for biotin as previously described [26]. The biomolecular binding kinetics and equilibrium binding constants (K_D) for each compound were also determined using SPR binding experiments. Varying concentrations of compounds **4** and **5a-c** were separately passed across immobilized *Sa*BPL sensor chip to provide quantitative analysis of the K_D using a steady-state affinity binding model. The antibacterial activity of the compounds was also determined using *S. aureus* strain ATCC 49775, where the growth of bacteria 20 hours post treatment was measured spectrophotometrically at 600 nm [27]. The mechanism of action of 1,4,5-trisubstituted triazoles were also investigated by using a *S. aureus* RN4220 that had been engineered to over-express the BPL target. Finally, selected compounds were assessed for potential toxicity using a cytotoxicity assay with cultured mammalian HepG2 cells (ATCC HB-8065) [17].

1,4,5-trisubstituted 1,2,3 triazoles **5a-d** were first assayed for inhibitory activity against *Sa*BPL (table 1). All compounds in this series had similar inhibitory activity, with the inhibition constants within 4-fold of parent compound **4** ($K_i = 0.23 \mu\text{M}$). The iodinated and the fluorinated analogues **5a** and **5b** were the most potent, with K_i values of $0.41 \mu\text{M}$ and $0.42 \mu\text{M}$, respectively. The chlorinated analogue **5c** proved to be the least potent compound in the series ($K_i = 0.90 \mu\text{M}$). The 5-phenyl-1,2,3-triazole (**5d**) also exhibited sub-micromolar inhibition with a K_i value of $0.78 \mu\text{M}$. This data demonstrated that the active site of *Sa*BPL

can accommodate the halogenated substitutions on the 1,2,3-triazole heterocycle as predicted by the docking. All of the compounds tested were inactive against the human homologue ($K_i > 10 \mu\text{M}$), indicating that substituents added to the C5 atom of the triazole ring, still maintain the reported selectivity observed with **4**.

The kinetics of the interaction between *Sa*BPL and inhibitors were further probed using SPR (table 1). All compounds displayed rapid association and dissociation rates that were unable to be quantified by the SPR software. Consequently a steady state affinity model for binding was employed to determine a K_D . Compound **5a** had the highest affinity for *Sa*BPL ($K_D = 3.8 \mu\text{M}$) with 2.2-fold higher binding affinity compared to parent compound **4** ($K_D = 8.4 \mu\text{M}$). Compound **5b** had a similar potency as **4** ($K_D = 7.1 \mu\text{M}$), whilst compound **5c** was the least potent ($K_D = 10.1 \mu\text{M}$). The binding affinity for **5d** could not be determined due to non-specific binding to the sensor chip surface at high concentrations. There was no significant difference between the binding affinities of **4** and the halogenated analogues, consistent with the *in silico* docking and enzyme assays.

We next directly addressed our hypothesis that halogenation of the triazole would improve whole cell activity by assaying all compounds for antibacterial activity against *S. aureus* ATCC 49755 (figure 5a). The characterized BPL inhibitor, biotinol-5'AMP **3** served as a control. Biotinol-5'AMP inhibited *S. aureus* growth with an MIC of $2 \mu\text{g/mL}$, consistent with previous reports [11]. Parent compound **4** also exhibited dose responsive antibacterial activity, with the greatest affect observed at $2 \mu\text{g/mL}$ where a ~40% reduction in the optical density of the culture was measured. However, an MIC could not be determined. The fluorinated analogue **5b** exhibited the most potent antibacterial activity of all the trisubstituted triazoles, with an MIC of $8 \mu\text{g/mL}$. This is the first example of biotin-triazole inhibitor where an MIC could be determined. The 5-iodo (**5a**) and the 5-chloro (**5c**) analogues, did not exhibit antibacterial activity against *S. aureus*, possibility due to the increase in molecular weight and/or impaired membrane permeability. Interestingly, the 5-phenyl-1,2,3-triazole **5d**

reduced cell growth by >80% at 64 $\mu\text{g}/\text{mL}$. The results from the antibacterial susceptibility assays highlights that fluorination of parent compound **4**, significantly improved the antibacterial activity. To address whether BPL is the target of **5b** in *S. aureus*, antibacterial susceptibility assays were performed using a *S. aureus* strain engineered to over-express the BPL target (figure 5b). Over-expression of BPL reduced the antibacterial activity of **5b** where ~60% growth reduction was observed. Although growth was not fully restored in the presence of the compound, this data does suggest that BPL can bind to **5b** *in vivo*, supporting a mechanism of action through BPL, although there is the possibility of another target. Compound **5b** did exhibit antibacterial activity (MIC 8 $\mu\text{g}/\text{mL}$) against bacteria harbouring the parent cloning vector (pCN51) that did not express additional BPL. Finally, cytotoxicity was assessed using mammalian HepG2 cells at concentrations ranging from 0.625 – 80 $\mu\text{g}/\text{mL}$ for compounds **5a-c** (table 1). None of these compounds showed cytotoxic activity at all concentrations tested.

Fluorination can improve the drug-like properties of lead compounds and, as such, 20% of available drugs are fluorinated [28]. Due to its small size and high electronegativity, the fluorine atom is an attractive modification that can improve the binding affinity, membrane permeability and metabolic stability of lead compounds [29]. In this study **5b** exhibited similar inhibition and binding activities to the *Sa*BPL target as parent compound **4**. Therefore we presumed the improved antibacterial activity is not simply due to an improvement in binding to *Sa*BPL. Importantly, the dissociation rates of **5b** binding to *Sa*BPL were indistinguishable to **4**. Therefore the improved activity is not likely due to high occupancy rates on the BPL target. One explanation for the improved antibacterial activity of **5b** is that the addition of fluorine enhances its membrane permeability. It has been demonstrated that fluorination of drugs improves membrane permeability through enhancements in the free energy of partitioning into the lipid membrane [4]. Another possibility for the improved antibacterial activity of **5b** is that the addition of a carbon-fluorine bond in the molecule

improves upon the metabolic stability inside the bacterial cell, due to the higher energy requirement to hydrolyse a C-F bond compared to its C-H counterpart [30]. The 1,4,5-trisubstituted triazoles reported here represent a new class of BPL inhibitors that exhibit good inhibition and excellent selectivity, but importantly a 5-fluoro-1,2,3 triazole was found to improve upon the antibacterial activity, and is the first example of a triazole inhibitor of *SaBPL*, where an MIC could be determined. Future studies will involve determining the mechanism by which **5b** binds to *SaBPL* via X-ray crystallography and determining the mechanism by which **5b** improves upon the antibacterial activity against *S. aureus*.

REFERENCES

1. Butler, M.S., M.A.T. Blaskovich, and M.A. Cooper, *Antibiotics in the clinical pipeline at the end of 2015*. J Antibiot, 2016.
2. Payne, D.J., et al., *Drugs for bad bugs: confronting the challenges of antibacterial discovery*. Nat Rev Drug Discov, 2007. **6**(1): p. 29-40.
3. Tommasi, R., et al., *ESKAPeIng the labyrinth of antibacterial discovery*. Nat Rev Drug Discov, 2015. **14**(8): p. 529-542.
4. Gerebtzoff, G., et al., *Halogenation of Drugs Enhances Membrane Binding and Permeation*. ChemBioChem, 2004. **5**(5): p. 676-684.
5. Domagala, J.M., *Structure-activity and structure-side-effect relationships for the quinolone antibacterials*. J. Antimicrob Chemother, 1994. **33**(4): p. 685-706.
6. Brighty, K.E. and T.D. Gootz, *The chemistry and biological profile of trovafloxacin*. J. Antimicrob Chemother, 1997. **39**(suppl 2): p. 1-14.
7. Garrison, A.T., et al., *Structure-Activity Relationships of a Diverse Class of Halogenated Phenazines That Targets Persistent, Antibiotic-Tolerant Bacterial Biofilms and Mycobacterium tuberculosis*. J. Med Chem, 2016. **59**(8): p. 3808-3825.
8. Basak, A., et al., *Synthetically Tuning the 2-Position of Halogenated Quinolines: Optimizing Antibacterial and Biofilm Eradication Activities via Alkylation and Reductive Amination Pathways*. Chem. Eu. J., 2016. **22**(27): p. 9181-9189.
9. Paparella, A.S., et al., *Structure guided design of biotin protein ligase inhibitors for antibiotic discovery*. Curr topics med chem, 2014. **14**(1): p. 4-20.
10. Tieu, W., et al., *Heterocyclic acyl-phosphate bioisostere-based inhibitors of Staphylococcus aureus biotin protein ligase*. Bioorg Med Chem Lett, 2014. **24**(19): p. 4689-4693.
11. Tieu, W., et al., *Improved Synthesis of Biotinyl-5'-AMP: Implications for Antibacterial Discovery*. ACS Med Chem Lett, 2015. **6**(2): p. 216-220.
12. Brown, P.H. and D. Beckett, *Use of Binding Enthalpy To Drive an Allosteric Transition*. Biochemistry, 2005. **44**(8): p. 3112-3121.
13. Xu, Y. and D. Beckett, *Kinetics of Biotinyl-5'-adenylate Synthesis Catalyzed by the Escherichia coli Repressor of Biotin Biosynthesis and the Stability of the Enzyme-Product Complex*. Biochemistry, 1994. **33**(23): p. 7354-7360.
14. Xu, Y. and D. Beckett, *[43] Biotinyl-5'-adenylate synthesis catalyzed by Escherichia coli repressor of biotin biosynthesis*, in *Methods in Enzymology*. 1997, Academic Press. p. 405-421.

15. Duckworth, Benjamin P., et al., *Bisubstrate Adenylation Inhibitors of Biotin Protein Ligase from Mycobacterium tuberculosis*. Chem Biol, 2011. **18**(11): p. 1432-1441.
16. Bockman, M.R., et al., *Targeting Mycobacterium tuberculosis Biotin Protein Ligase (MtBPL) with Nucleoside-Based Bisubstrate Adenylation Inhibitors*. J Med Chem, 2015. **58**(18): p. 7349-7369.
17. Soares da Costa, T.P., et al., *Selective inhibition of Biotin Protein Ligase from Staphylococcus aureus*. J Biol Chem, 2012. **287**(21): p. 17823-17832.
18. Tieu, W., et al., *Optimising in situ click chemistry: the screening and identification of biotin protein ligase inhibitors*. Chem Sci, 2013.
19. Trott, O. and A.J. Olson, *AutoDock Vina: Improving the speed and accuracy of docking with a new scoring function, efficient optimization, and multithreading*. J. of Comput Chem, 2010. **31**(2): p. 455-461.
20. Worrell, B.T., S.P. Ellery, and V.V. Fokin, *Copper(I)-Catalyzed Cycloaddition of Bismuth(III) Acetylides with Organic Azides: Synthesis of Stable Triazole Anion Equivalents*. Angew Chem Int Ed, 2013. **52**(49): p. 13037-13041.
21. Hein, J.E., et al., *Copper(I)-Catalyzed Cycloaddition of Organic Azides and 1-Iodoalkynes*. Angew Chem Int Ed, 2009. **48**(43): p. 8018-8021.
22. Worrell, B.T., J.E. Hein, and V.V. Fokin, *Halogen Exchange (Halex) Reaction of 5-Iodo-1,2,3-triazoles: Synthesis and Applications of 5-Fluorotriazoles*. Angew Chem Int Ed, 2012. **51**(47): p. 11791-11794.
23. Deng, J., Y.-M. Wu, and Q.-Y. Chen, *Cross-coupling reaction of iodo-1, 2, 3-triazoles catalyzed by palladium*. Synthesis, 2005. **2005**(16): p. 2730-2738.
24. Suzuki, A., *Recent advances in the cross-coupling reactions of organoboron derivatives with organic electrophiles, 1995–1998*. J. Organomet Chem, 1999. **576**(1–2): p. 147-168.
25. Polyak, S.W., et al., *Biotin Protein Ligase from Saccharomyces cerevisiae : The N-terminal domain is required for complete activity*. J Biol Chem, 1999. **274**(46): p. 32847-32854.
26. Yung-Chi, C. and W.H. Prusoff, *Relationship between the inhibition constant (KI) and the concentration of inhibitor which causes 50 per cent inhibition (I50) of an enzymatic reaction*. Biochem Pharmacol, 1973. **22**(23): p. 3099-3108.
27. Soares da Costa, T.P., et al., *Biotin Analogues with Antibacterial Activity Are Potent Inhibitors of Biotin Protein Ligase*. ACS Med Chem Lett, 2012. **3**(6): p. 509-514.
28. Purser, S., et al., *Fluorine in medicinal chemistry*. Chem Soc Rev, 2008. **37**(2): p. 320-330.

29. Haggmann, W.K., *The Many Roles for Fluorine in Medicinal Chemistry*. J. Med Chem, 2008. **51**(15): p. 4359-4369.
30. Hernandez, M.Z., et al., *Halogen Atoms in the Modern Medicinal Chemistry: Hints for the Drug Design*. Curr Drug Targets, 2010. **11**(3): p. 303-314.

FIGURE LEGENDS

Figure 1. Reaction mechanism of biotin protein ligase

Figure 2. Compounds synthesized in this study

a). Biotinol-5'AMP **3**. b). Parent compound **4**. c). 1,4,5-trisubstituted 1,2,3-triazoles **5a-d**.

Figure 3. Docking studies of 1,4,5-trisubstituted 1,2,3-triazoles with *SaBPL*

a). X-ray crystal structure of **4** (cyan) in complex with *SaBPL* (PDB 3V7S). Amino acids that encompass the triazole binding pocket are shown. Dashed lines represent hydrogen bonds. b). Top ranked *in silico* docking pose for **5a** (blue). c). Top ranked *in silico* docking pose for **5b** (red). d). Top ranked *in silico* docking pose for **5c** (green).

Figure 4. SPR sensograms (left) and concentration vs response plots (right) of compounds **4** and **5a-c** binding to *SaBPL*.

a). SPR sensogram and concentration vs response plot of **4** binding to *SaBPL*. b). SPR sensogram and concentration vs response plot of **5a** binding to *SaBPL*. c). SPR sensogram and concentration vs response plot of **5b** binding to *SaBPL*. d). SPR sensogram and concentration vs response plot of **5c** binding to *SaBPL*. Concentrations of compounds **4** and **5a-c** used were: 0.2 μM (red), 0.4 μM (green), 0.8 μM (blue), 1.6 μM (magenta), 3.1 μM (cyan), 6.3 μM (yellow), 12.5 μM (purple), 25 μM (grey) and 50 μM (orange).

Figure 5. Inhibition of *S. aureus* growth *in vitro*.

a). Compounds **4** (cyan), **5a** (blue), **5b** (red), **5c** (green), **5d** (purple) and biotinol-5'AMP (orange) were tested against *S.aureus* strain ATCC 49775 (n = 3).

b). Compound **5b** was tested for antibacterial susceptibility against *S. aureus* RN4220. *S. aureus* RN4220 harbouring pCN51-BPL (red solid lines) or pCN51 (red dashed lines) are shown (n = 3). Error bars represent standard error of the means (SEM) of data.

LIST OF TABLES:

Table 1. Binding affinities derived from SPR analysis, inhibition and cytotox data for compounds **4** and **5a-d**.

LIST OF SCHEMES:

Scheme 1. Synthesis of biotin 1-iodoacetylene and 5-iodo-1,2,3-triazole **5a**.

Conditions and reagents: (a) CuI, DMF, 1 h, Rt; (b) CuI, DMF, TEA, 12 h, Rt

Scheme 2. Synthesis of **5b-d**, from precursor **5a**.

Conditions and reagents: (a) KX (X=F, X=Cl), MeCN/H₂O (1:1), 180 °C, 10 min, mw; (b) PhB(OH)₂ (1.5 equiv), PdCl₂(PPh)₃ (5 mol%), K₂CO₃ (1.5 equiv), THF, 70 °C, 12 h.

Figure 1.

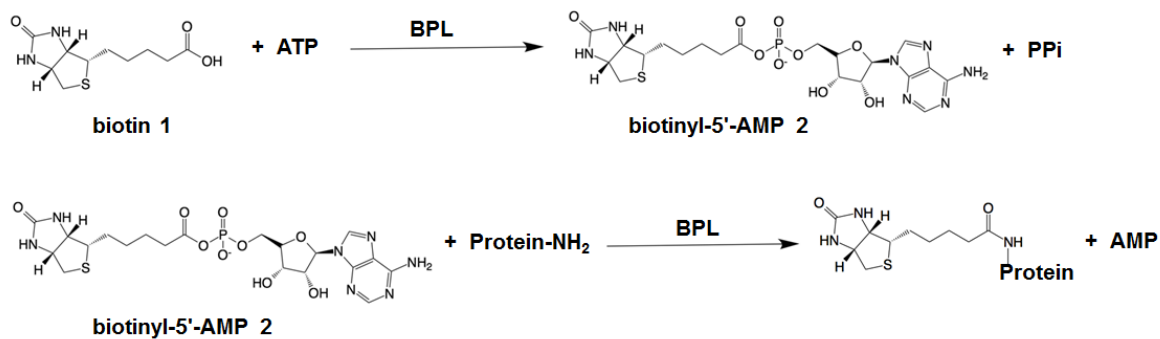


Figure 2.

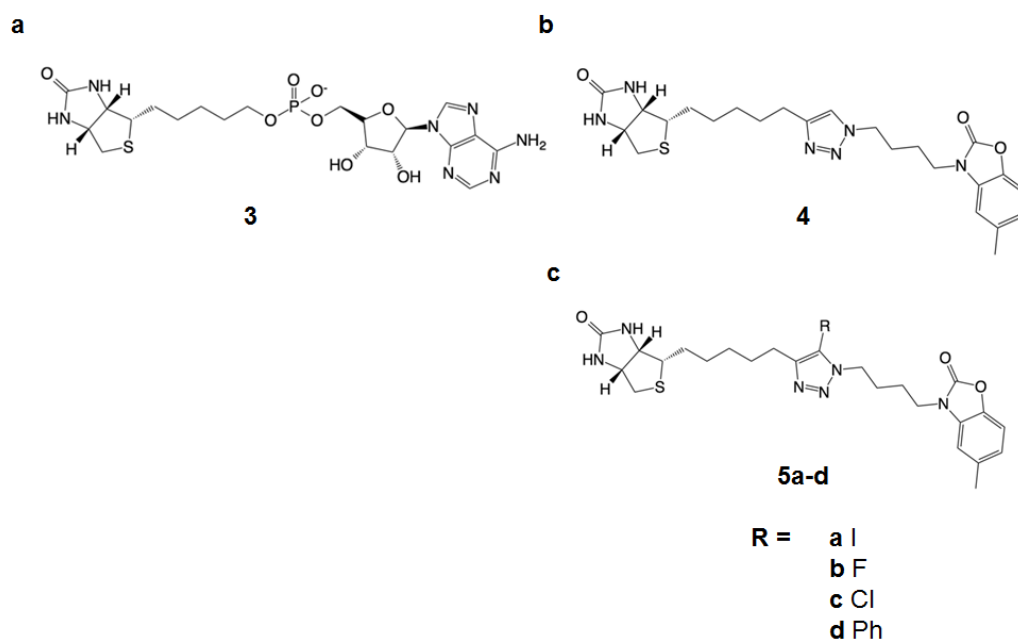


Figure 3.

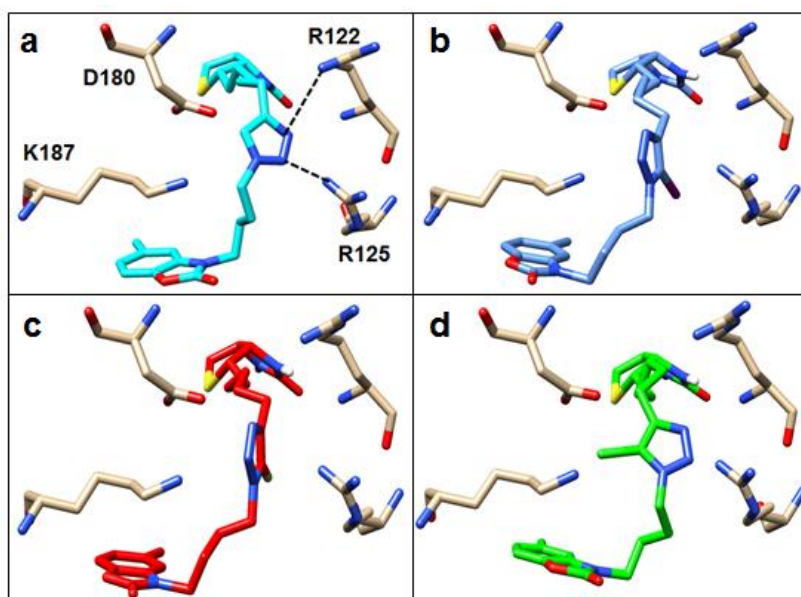


Figure 4.

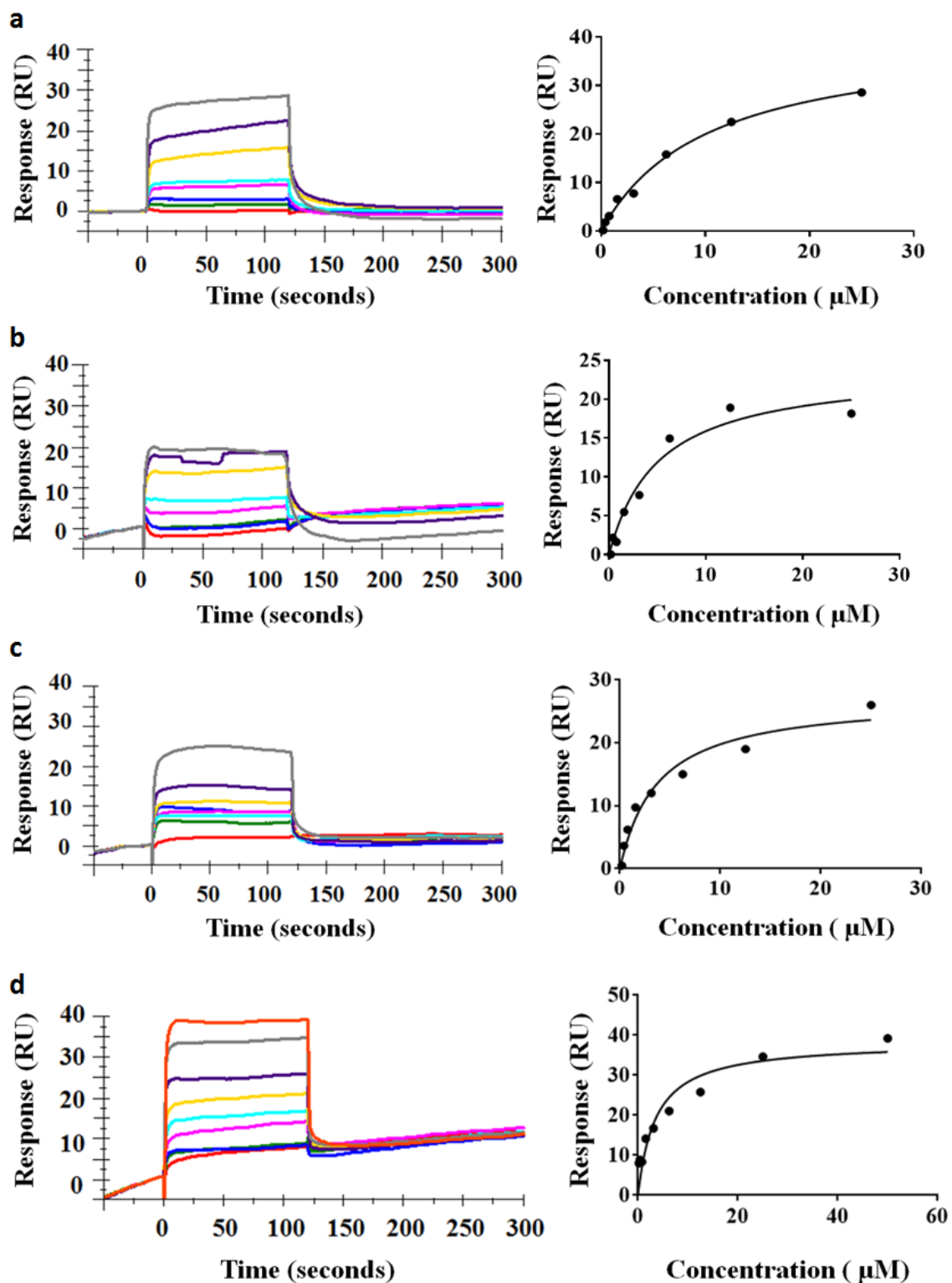


Figure 5.

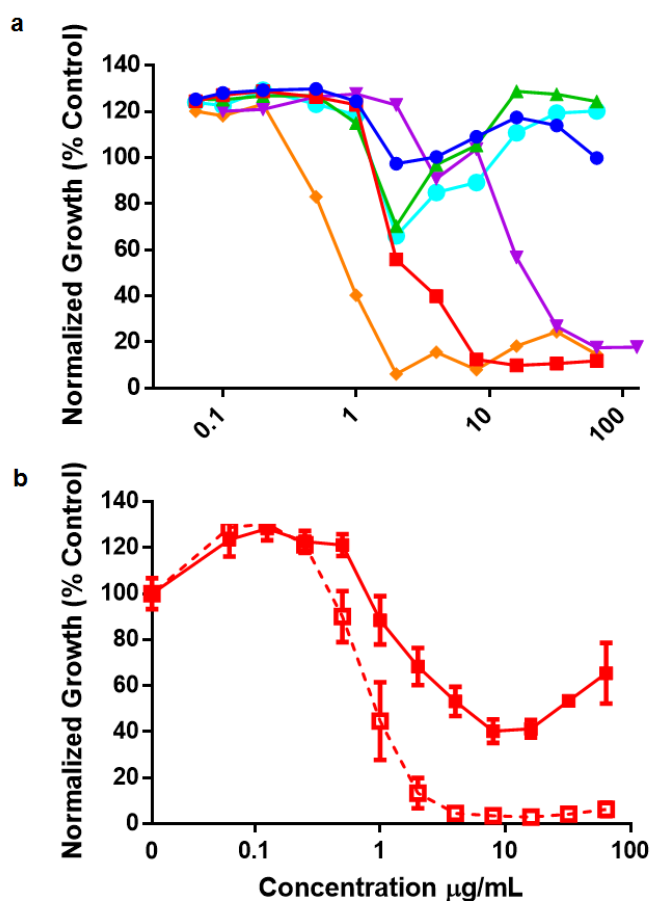


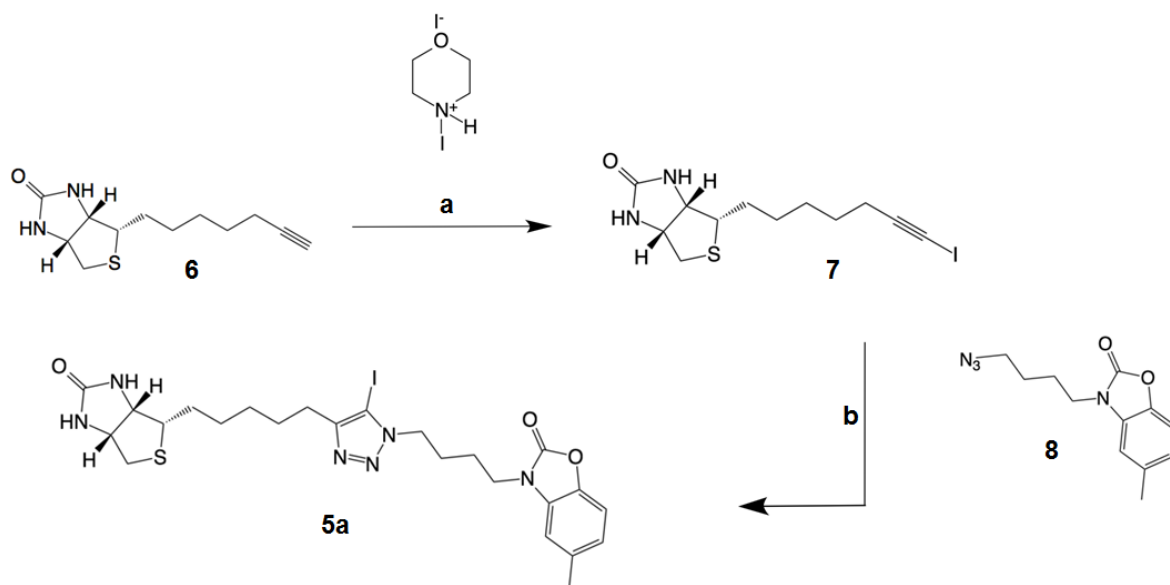
Table 1: Binding affinities derived from SPR analysis, inhibition and cytotox data for compounds **4** and **5a-d**.

ID	R	K_D SaBPL (μM)	K_i SaBPL (μM)	K_i HsBPL (μM)	Cytotox HepG2 (μg/mL)
4	H	8.4 ± 1.0	0.23 ± 0.01	>10	>80
5a	I	3.8 ± 1.5	0.41 ± 0.02	>10	>80
5b	F	7.1 ± 3.4	0.42 ± 0.05	>10	>80
5c	Cl	10.1 ± 1.8	0.9 ± 0.11	>10	>80
5d	Ph	N/D	0.78 ± 0.17	>10	N/D

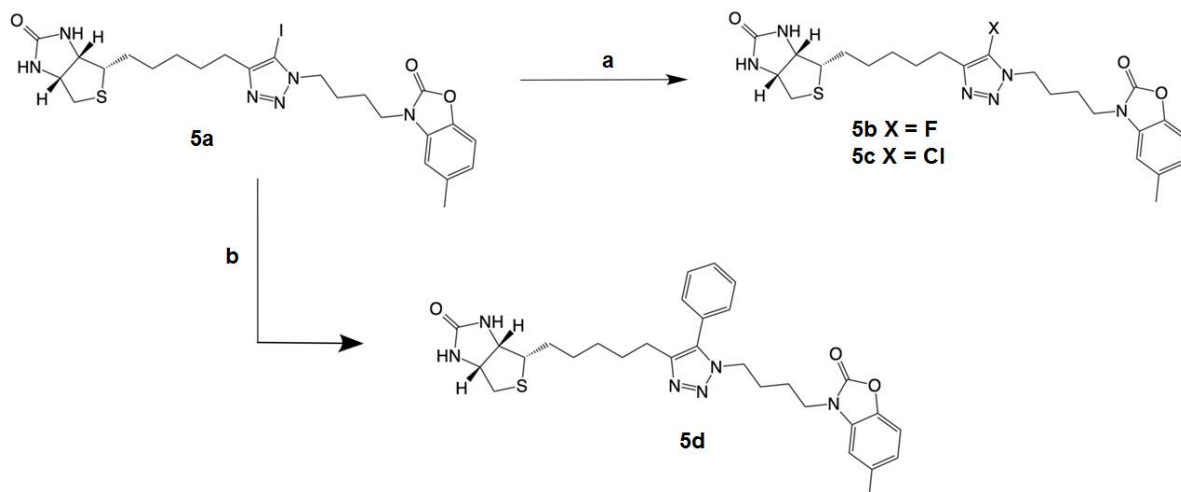
K_D : Represents Dissociation constant

K_i : Represents Inhibition constant

Scheme 1.



Scheme 2.



SUPPLEMENTARY MATERIAL:

Recombinant protein production

The cloning and purification of recombinant BPL from *Staphylococcus aureus* and *Homo sapiens* have been previously described [1, 2].

In vitro biotinylation assays

Quantification of BPL catalysed ³H-biotin incorporation into the biotin domain substrate was performed as previously described [3-5]. A reaction mixture was prepared containing 50 mM Tris HCl pH 8.0, 3 mM ATP, 4.94 μM biotin, 0.06 μM ³H-biotin, 5.5 mM MgCl₂, 100 mM KCl, 0.1 μM DTT and 10 μM biotin domain of *S. aureus* pyruvate carboxylase. To determine inhibitory activity, BPL activity was measured in the presence of varying concentrations of compound. All compounds were dissolved in DMSO and then diluted into the reaction buffer to give a final concentration of 4% DMSO. BPL reaction was initiated by the addition of enzyme to give final concentrations of 6.25 nM for SaBPL and 140 nM for HsBPL. After 10 minutes at 37 °C, 90 μL of stopping buffer (110 mM EDTA and 50 mM Tris HCl pH 8.0) was added to terminate the reaction and a 100 μL aliquot of the reaction mixture was added to the wells of 96-well HTS multiscreen plate containing an Immobilon-P® (Merck Millipore) membrane that had been pre-treated with 50 μL of 70% ethanol. 400 μL of MilliQ-H₂O and followed by 200 μL of TBS. Quantitation of protein-bound radiolabelled biotin was determined by liquid scintillation counting. The IC₅₀ value of each compound was determined from a dose-response curve by varying the concentration of inhibitor under the same enzyme concentration. The data was analysed with GraphPad prism (version 6) using a non-linear fit of log₁₀ [inhibitor] vs. normalized response. The K_i, the absolute inhibition constant for a compound was determined using Eq 1: [6]

Eq 1:

$$K_i = \frac{IC_{50}}{1 + \frac{[S]}{K_M}}$$

Where [S] is the substrate concentration ([biotin] = 5 μ M) and K_M is the affinity of the enzyme for biotin (*S.aureus* BPL = 1 μ M, [3], and *H. sapiens* BPL = 1 μ M [2]).

Surface Plasmon Resonance

SPR was performed using a BiacoreTM S200 instrument (GE healthcare). *S. aureus* BPL was immobilised on a CM5 sensor chip by standard amine coupling chemistry. The carboxymethyl groups on the chip were activated by the addition *N*-ethyl-*N'*-(3-diethylamino-propyl) carbodiimide and *N*-hydroxysuccinimide. BPL (120 μ g/mL) in 10 mM sodium acetate buffer (pH 5.8) was coupled onto the surface, and 50 mM Tris pH 8.0 was injected to block any unreacted sites. Typically, 7,000 resonance units of BPL were immobilised on the sensor chip. One channel was left blank which was subtracted from the sample channel to allow analysis methods to distinguish between actual and non-specific binding. Experiments were conducted at 25 °C with a running buffer containing 10 mM HEPES pH 7.4, 150 mM NaCl, 0.005% surfactant p20 and 5% (v/v) DMSO. For compounds that were poorly water soluble, samples were initially dissolved in DMSO and diluted in running buffer so that the final concentration of DMSO was 5%. To correct for variations in DMSO concentration during the preparation of these compounds, a solvent correction curve was included in the analysis by preparing a series of test solutions between 4.5% and 5.8% DMSO. Binding experiments were performed by injecting the analyte solutions into the instrument across the sensor surface of all flow cells at a flow rate of 30 μ L/min with a contact time of 120 seconds followed by a dissociation time of 300 seconds. Zero concentration samples were used as blanks. The time-dependent binding curves of all flow cells were monitored simultaneously. The results of compounds **5a-d** showed fast on and off rates outside the range of kinetic quantification, so

K_D values were determined by transforming time-dependent binding curves into an affinity-steady state 1:1 model using Biacore™ S200 evaluation software (GE healthcare).

Antibacterial Activity Evaluation

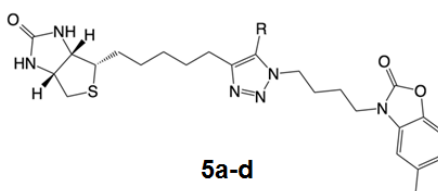
Antibacterial activity was determined by a microdilution broth method as recommended by the CLSI (Clinical and Laboratory Standards Institute, Document M07-A8, 2009, Wayne, Pa.) using cation-adjusted Mueller-Hinton broth (trek Diagnostics Systems, U.K.). Compounds were dissolved in DMSO. Serial two-fold dilutions of each compound were made using DMSO as the diluent. Trays were inoculated with 5×10^4 CFU of each strain in a volume of 100 μ L (final concentration of DMSO was 3.2 % (v/v)), and incubated at 35 °C for 16-20 hours. Growth of the bacterium was quantified by measuring the absorbance at 620 nm.

Assay of cytotoxicity

Mammalian HepG2 cells were suspended in Dulbecco-modified Eagle's medium containing 10% fetal bovine serum, and then seeded in 96-well tissue culture plates at either 5 000, 10 000 or 20 000 cells per well. After 24 hours, cells were treated with varying concentrations of the test compound such that the DMSO concentration was consistent at 2 % (v/v) in all wells. After treatment for 24 or 48 hours, WST-1 cell proliferation reagent (Roche) was added to each well and incubated for 0.5 hours at 37 °C. The WST-1 assay quantitatively monitors the metabolic activity of cells by measuring the hydrolysis of the WST-1 reagent, the products of which are detectable at absorbance 450 nm.

Docking studies

Docking experiments were performed using AutoDock vina (version 1.5.6) and the binding affinities were predicted [7]. All molecules were drawn using ACD/Chemsketch and the 3D structure was optimized, before loading into UCSF Chimera (version 1.5). Protein for docking was taken from RCSB protein data bank: *Staphylococcus aureus*, 3V7S [3]. The original bound ligand and all water molecules were removed from the original protein data bank file. Compounds **4** and **5a-d** were docked into the active site of *S. aureus* BPL as defined by Grid Box coordinates (x = 52.8, y = 20.94, z = 22.55), size (x = 18, y = 20, z = 22) and spacing set to 1 Å. Final docked conformations were ranked by binding energy and the top 3 conformations (as shown by table below) were selected to compare and overlay with the original bound ligand.



- R =**
- a** I (SaBPL: $K_i = 0.41 \mu\text{M} \pm 0.02 \mu\text{M}$)
 - b** F (SaBPL: $K_i = 0.42 \mu\text{M} \pm 0.05 \mu\text{M}$)
 - c** Cl (SaBPL: $K_i = 0.9 \mu\text{M} \pm 0.11 \mu\text{M}$)
 - d** Ph (SaBPL: $K_i = 0.78 \mu\text{M} \pm 0.17 \mu\text{M}$)

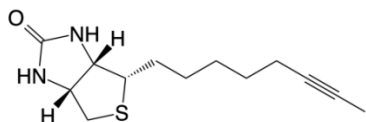
Supplementary table 1: Predicted binding affinities of compounds **4** and **5a-d**

	R	Lowest binding energy (kcal/mol)	2 nd binding energy (kcal/mol)	Lowest binding energy	3 rd binding energy (kcal/mol)	Lowest binding energy
4	5-H	-11.1	-10.9		-9.8	
5a	5-I	-11.3	-10.4		-8.4	
5b	5- F	-11.6	-11.3		-10.8	
5c	5-Cl	-11.5	-10.9		-9.2	
5d	5-Ph	-8.5	-8.4		-8.3	

Synthetic Chemistry methods

All reagents were obtained from commercial sources and are of reagent grade or as specified. Solvents were also obtained from commercial sources, except for anhydrous THF, anhydrous DCM and anhydrous DMF which were dried over solvent purifier (PS-Micro, Innovative Technology, USA). Reactions were monitored by TLC using precoated plates (silica gel 60 F254, 250 μm , Merck, Darmstadt, Germany), spots were visualised under ultraviolet light at 254 nm and with either sulphuric acid-vanillin spray, potassium permanganate dip or Hanessian's stain. Column chromatography was performed with silica gel (40-63 μm 60 \AA , Davisil, Grace, Germany). HPLC was performed on HP Series 1100 with Phenomenex Gemini C18 5 μM (250 x 4.60 mm) for Analytical HPLC and Phenomenex Luna C18 10 μM (50 x 10.00 mm) for Semi-preparative HPLC. Microwave reactions were performed on a CEM Discovery SP with external IR temperature monitoring. Reactions were stirred for 5 min in a sealed container at ambient temperature, followed by 5 min stirring with increased microwave power until the prescribed temperature was reached. Both power and pressure were kept variable. ^1H and ^{13}C NMR spectra were recorded on a Varian Inova 500 MHz or a Varian Inova 600 MHz. Chemical shifts are given in ppm (δ) relative to the residue signals, which in the case of DMSO- d_6 were 2.55 ppm for ^1H and 39.55 ppm for ^{13}C , CDCl_3 were 7.26 ppm for ^1H and 77.23 ppm for ^{13}C and D_2O was 4.79 for ^1H . Structural assignment was confirmed with COSY, ROESY, HMQC and HMBC. Mixtures of isomers are designated A and B in NMR spectra without individual assignment. Partial integrals are also reported for each isomer. High-resolution mass spectra (HRMS) were recorded on an Agilent 6230 time of flight (TOF) liquid chromatography mass spectra (LC/MS) ($\Delta < 5$ ppm).

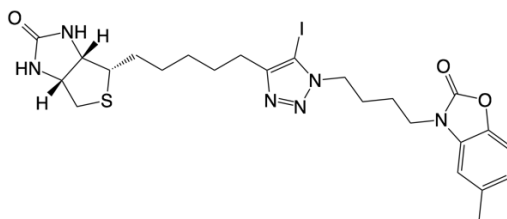
(3aS,4S,6aR)-4-(7-iodohept-6-yn-1-yl)tetrahydro-1H-thieno[3,4-d]imidazol-2(3H)-one 7



To a solution of biotin acetylene **6** (100 mg, 0.42 mmol) in dry DMF (5 ml) was added CuI (5 mg, 0.08 mmol) and N-iodomorpholine (143 mg, 0.42 mmol). The reaction mixture was stirred at ambient temperature for 3 h, after which a fine white precipitate had formed. The suspension was filtered through a pad of natural alumina, which was further washed with 10% MeOH in DCM (3 x 20 ml). The combined organics were concentrated in vacuo and purified by flash chromatography on silica eluting with 10% MeOH in DCM to give a yellow solid. ¹H NMR of purified compound confirmed the presence of the target compound **7** as a yellow solid (145 mg, 95%) > 98% by ¹H NMR.

¹H NMR (500 MHz, DMSO-d₆): δ 6.42 (1H, bs, C(O)NH), 6.34 (1H, s, C(O)NH), 4.294.31 (1H, m, NHCH), 4.11-4.14 (1H, m, NHCH), 3.08-3.10 (1H, m, SCH), 2.80-2.83 (1H, m, SCHa), 2.53-2.59 (3H, m, SCHb, CH₂C≡C-I), 1.43-1.65 (4H, m, 2 x CH₂), 1.27-1.39 (4H, m, 2 x CH₂); ¹³C NMR (125 MHz, DMSO-d₆): δ 165.8, 122.2, 79.8, 64.2, 62.3, 58.6, 52.8, 31.5, 31.3, 31.4, 30.9 HPLC Rt = 16.9 min.

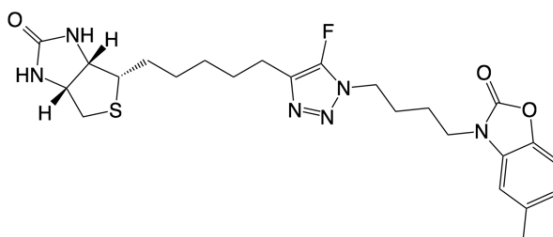
3-(4-(5-iodo-4-(5-((3a*S*,4*S*,6a*R*)-2-oxohexahydro-1*H*-thieno[3,4-*d*]imidazol-4-yl)pentyl)-1*H*-1,2,3-triazol-1-yl)butyl)-5-methylbenzo[*d*]oxazol-2(3*H*)-one 5a



To a solution of 1-iodoalkyne **7** (20 mg, 0.06 mmol) and azide (14 mg, 0.06 mmol) in dry DMF (1 ml per 10 mg of 1-iodoalkyne) was added CuI (0.05 equiv) and TEA (2.0 equiv) and the mixture was stirred at ambient temperature for 12 h. The volatiles were removed under reduced pressure and the resulting residue was purified by column chromatography on silica gel, and was purified by flash chromatography on silica eluting with 5% MeOH in DCM to give a yellowish solid (12 mg, 36%).

¹H NMR (500 MHz; CDCl₃): δ 7.08 (1H, d, J = 8.1 Hz, ArH), 6.90-6.92 (1H, m, ArH), 6.78 (1H, m, ArH), 5.08 (1H, bs, NH), 4.86 (1H, bs, NH), 4.50-4.53 (1H, m, NHCH), 4.42 (2H, t, J = 6.9 Hz, ArNtriCH₂), 4.30-4.33 (1H, m, NHCH), 3.84 (2H, t, J = 6.9 Hz, NCH₂), 3.143.19 (1H, m, SCH), 2.93 (1H, dd, J = 5.0, 12.8 Hz, SCHa), 2.74 (1H, d, J = 12.8 Hz, SCHb), 2.64 (2H, d, J = 7.5 Hz, ArTriCH₂), 2.40 (3H, s, ArCH₃), 1.97-2.02 (2H, m, CH₂), 1.791.84 (2H, m, CH₂), 1.64-1.72 (4H, m, 2 x CH₂), 1.38-1.49 (4H, m, 2 x CH₂); ¹³C NMR (125 MHz; CDCl₃): δ 162.8, 154.9, 151.8, 140.7, 134.0, 130.8, 122.9, 109.7, 108.8, 61.9, 60.1, 55.5, 49.7, 41.3, 40.6, 28.9, 28.6, 28.6, 28.4, 26.6, 25.8, 24.5, 21.5, HRMS calcd. for (M + H) C₂₄H₃₂N₆O₃S, requires 611.1301, found 611.1298 HPLC Rt = 17.0 min

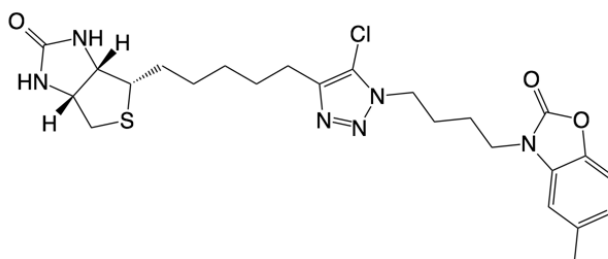
3-(4-(5-fluoro-4-(5-((3a*S*,4*S*,6a*R*)-2-oxohexahydro-1*H*-thieno[3,4-*d*]imidazol-4-yl)pentyl)-1*H*-1,2,3-triazol-1-yl)butyl)-5-methylbenzo[*d*]oxazol-2(3*H*)-one 5b



To a 5 ml round-bottomed microwave vial was added a solution of 5-iodo-1,2,3-triazole **5a** (15 mg, 0.03 mmol) in acetonitrile (1 ml per 100 mg of triazole) and de-ionised water (1 ml per 100 mg of triazole) and potassium fluoride (7 mg, 0.12 mmol). The vial was placed into the microwave reactor set at a pressure of 250 psi and heated at 180 oC for 10 min. After the vial was cooled to room temperature, the mixture was concentrated in vacuo and the residue was purified by column by flash chromatography on silica eluting with 5% MeOH in DCM to yield 5-fluoro-triazole **5b** as an off white solid (11 mg, 89%).

¹H NMR (500 MHz; CDCl₃): δ 7.08 (1H, d, J = 8.1 Hz, ArH), 6.90-6.92 (1H, m, ArH), 6.76-6.77 (1H, m, ArH), 5.06 (1H, bs, NH), 4.82 (1H, bs, NH), 4.49-4.52 (1H, m, NHCH), 4.30-4.33 (1H, m, NHCH), 4.27 (2H, t, J = 6.9 Hz, ArNtriCH₂), 3.85 (2H, t, J = 6.9 Hz, NCH₂), 3.14-3.17 (1H, m, SCH), 2.92 (1H, dd, J = 5.0, 12.8 Hz, SCH_a), 2.73 (1H, d, J = 12.8 Hz, SCH_b), 2.62 (2H, d, J = 7.5 Hz, ArCtriCH₂), 2.40 (3H, s, ArCH₃), 1.96-2.02 (2H, m, CH₂), 1.79-1.85 (2H, m, CH₂), 1.63-1.70 (4H, m, 2 x CH₂), 1.37-1.48 (4H, m, 2 x CH₂); ¹³C NMR (125 MHz; CDCl₃): δ 162.8, 154.9, 140.7, 134.0, 130.7, 122.9, 110.0, 109.7, 108.7, 61.9, 60.0, 55.5, 46.1, 41.2, 40.5, 28.9, 28.6, 28.6, 28.0, 26.2, 24.7, 23.4, 21.5, HRMS calcd. for (M + H⁺) C₂₄H₃₂FN₆O₃S, requires 503.2241, found 503.2220 HPLC Rt = 16.7 min

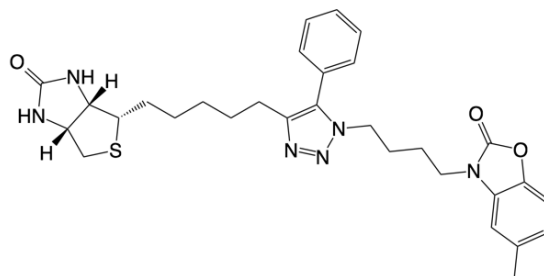
3-(4-(5-chloro-4-(5-((3a*S*,4*S*,6a*R*)-2-oxohexahydro-1*H*-thieno[3,4-*d*]imidazol-4-yl)pentyl)-1*H*-1,2,3-triazol-1-yl)butyl)-5-methylbenzo[*d*]oxazol-2(3*H*)-one 5c



To a 5 ml round-bottomed microwave vial was added a solution of 5-iodo-1,2,3-triazole **5a** (15 mg, 0.03 mmol) in acetonitrile (1 ml per 100 mg of triazole) and de-ionised water (1 ml per 100 mg of triazole) and potassium chloride (9 mg, 0.12 mmol). The vial was placed into the microwave reactor set at a pressure of 250 psi and heated at 180 oC for 10 min. After the vial was cooled to room temperature, the mixture was concentrated in vacuo and was purified by flash chromatography on silica eluting with 5% MeOH in DCM to yield 5-chloro-triazole as an off white solid (10 mg, 80%).

¹H NMR (500 MHz; CDCl₃): δ 7.03 (1H, m, ArH), 6.97-6.99 (1H, m, ArH), 6.83 (1H, d, J = 8.1 Hz, ArH), 5.39 (1H, bs, NH), 5.08 (1H, bs, NH), 4.49-4.51 (1H, m, NHCH), 4.35 (2H, t, J = 6.9 Hz, ArNtriCH₂), 4.29-4.32 (1H, m, NHCH), 3.84 (2H, t, J = 6.9 Hz, NCH₂), 3.133.17 (1H, m, SCH), 2.91 (1H, dd, J = 5.0, 12.8 Hz, SCHa), 2.72 (1H, d, J = 12.8 Hz, SCHb), 2.62 (2H, t, J = 7.5 Hz, ArCtriCH₂), 2.38 (3H, s, ArCH₃), 1.95-2.01 (2H, m, CH₂), 1.77-1.83 (2H, m, CH₂), 1.63-1.73 (4H, m, 2 x CH₂), 1.36-1.47 (4H, m, 2 x CH₂); ¹³C NMR (125 MHz; CDCl₃): δ 163.1, 154.8, 143.6, 142.8, 132.7, 128.4, 124.3, 122.2, 110.8, 107.8, 62.0, 60.1, 55.6, 47.3, 41.3, 40.5, 28.9, 28.6, 28.5, 28.0, 26.2, 24.6, 24.3, 21.4; HRMS calcd. for (M + H⁺) C₂₄H₃₂ClN₆O₃S, requires 519.1945, found 519.1909 HPLC Rt = 17.1 min

5-methyl-3-(4-(4-(5-((3a*S*,4*S*,6a*R*)-2-oxohexahydro-1*H*-thieno[3,4-*d*]imidazol-4-yl)pentyl)-5-phenyl-1*H*-1,2,3-triazol-1-yl)butyl)benzo[*d*]oxazol-2(3*H*)-one 5d

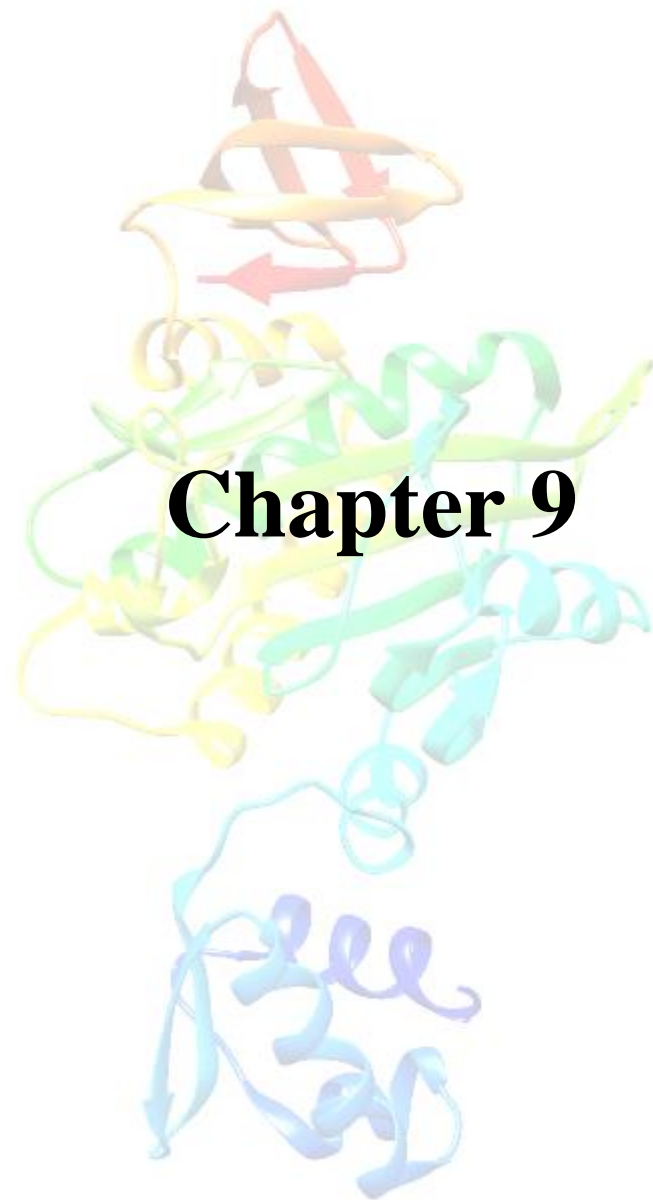


To a solution of 5-iodo-triazole **5a** (75 mg, 0.13 mmol) in dry THF (5 ml) was added K₂CO₃ (52 mg, 0.38 mmol), followed by adding phenylboronic acid (15 mg, 0.13 mmol) and PdCl₂(PPh₃)₃ (8 mg, 5 mol %). The reaction mixture was stirred at 70 °C for 12 h, after which the solvent was removed in vacuo and purified by flash chromatography on silica eluting with 5% MeOH in DCM to give the target compound **5d** as a yellowish solid (30 mg, 41%).

¹H NMR (500 MHz; CDCl₃): δ 7.44-7.47 (3H, m, 3 x ArBnH), 7.17-7.19 (2H, m, 2 x ArBnH), 7.00-7.01 (1H, m, ArH), 6.94-6.96 (1H, m, ArH), 6.77 (1H, d, J = 7.9 Hz, ArH), 5.86 (1H, bs, C(O)NH), 5.52 (1H, bs, C(O)NH), 4.45-4.49 (1H, m, NHCH), 4.24-4.27 (3H, m, NHCH, ArNtriCH₂), 3.70 (2H, t, J = 6.9 Hz, NCH₂), 3.06-3.10 (1H, m, SCH), 2.84-2.88 (1H, m, SCHa), 2.70 (1H, dd, J = 5.1, 12.8 Hz, SCHb), 2.56 (2H, dt, J = 1.5, 7.3 Hz, ArCtriCH₂), 2.37 (3H, s, ArCH₃), 1.73-1.79 (2H, m, CH₂), 1.56-1.69 (6H, m, 3x CH₂), 1.28-1.38 (4H, m, 2 x CH₂); ¹³C NMR (125 MHz; CDCl₃): δ 166.2, 157.3, 148.3, 145.4, 136.8, 135.3, 132.1, 132.0, 131.9, 131.1, 130.1, 126.9, 113.4, 110.5, 64.7, 62.8, 58.5, 50.1, 44.0, 43.2, 31.8, 31.7, 31.3, 31.1, 29.4, 27.5, 27.2, 24.1. HRMS calcd. for (M + H⁺) C₃₀H₃₇N₆O₃S, requires 561.2648, found 561.2640 HPLC Rt = 17.4 min

REFERENCES

1. Pendini, N., et al., *Purification, crystallization and preliminary crystallographic analysis of biotin protein ligase from Staphylococcus aureus*. Acta crystallographica. Section F, Structural biology and crystallization communications, 2008. **64**(Pt 6): p. 520-523.
2. Mayende, L., et al., *A novel molecular mechanism to explain biotin-unresponsive holocarboxylase synthetase deficiency*. Journal of Molecular Medicine, 2012. **90**(1): p. 81-88.
3. Soares da Costa, T.P., et al., *Selective inhibition of Biotin Protein Ligase from Staphylococcus aureus*. Journal of Biological Chemistry, 2012. **287**(21): p. 17823-17832.
4. Soares da Costa, T.P., et al., *Biotin Analogues with Antibacterial Activity Are Potent Inhibitors of Biotin Protein Ligase*. ACS Medicinal Chemistry Letters, 2012. **3**(6): p. 509-514.
5. Chapman-Smith, A., et al., *Molecular recognition in a post-translational modification of exceptional specificity. Mutants of the biotinylated domain of acetyl-CoA carboxylase defective in recognition by biotin protein ligase*. The Journal of biological chemistry, 1999. **274**(3): p. 1449-1457.
6. Yung-Chi, C. and W.H. Prusoff, *Relationship between the inhibition constant (KI) and the concentration of inhibitor which causes 50 per cent inhibition (I50) of an enzymatic reaction*. Biochemical Pharmacology, 1973. **22**(23): p. 3099-3108.
7. Trott, O. and A.J. Olson, *AutoDock Vina: Improving the speed and accuracy of docking with a new scoring function, efficient optimization, and multithreading*. Journal of Computational Chemistry, 2010. **31**(2): p. 455-461.



Statement of Authorship

Title of Paper	A template guided approach to generating cell permeable inhibitors of <i>Staphylococcus aureus</i> biotin protein ligase
Publication Status	<input type="checkbox"/> Published <input type="checkbox"/> Accepted for Publication <input type="checkbox"/> Submitted for Publication <input checked="" type="checkbox"/> Unpublished and Unsubmitted work written in manuscript style
Publication Details	Ashleigh S. Paparella, Jiage Feng, Beatriz Blanco-Rodriguez, Zikai Feng, Andrew Hayes, Warida Phetsang, Mark AT. Blaskovich, Matthew A. Cooper, Grant W. Booker, Andrew D. Abel, Steven W. Polyak

Principal Author

Name of Principal Author (Candidate)	Ashleigh S. Paparella		
Contribution to the Paper	Primary role in manuscript preparation Expression and purification of all BPLs Performed <i>in situ</i> click chemistry reactions Biological testing of compound 3 against <i>MtBPL</i> and <i>AcBPL</i> and compound 12 against <i>SaBPL</i> , <i>MtBPL</i> , <i>AcBPL</i> and <i>KpBPL</i>		
Overall percentage (%)	20%		
Certification:	This paper reports on original research I conducted during the period of my Higher Degree by Research candidature and is not subject to any obligations or contractual agreements with a third party that would constrain its inclusion in this thesis. I am a primary author of this paper.		
Signature		Date	26/10/2016

Co-Author Contributions

By signing the Statement of Authorship, each author certifies that:

- the candidate's stated contribution to the publication is accurate (as detailed above);
- permission is granted for the candidate to include the publication in the thesis; and
- the sum of all co-author contributions is equal to 100% less the candidate's stated contribution.

Name of Co-Author	Jiage Feng		
Contribution to the Paper	Analysis of <i>in situ</i> generated products using LC/HRMS Synthesis and characterization of compounds 1-4 Overall contribution: 15%		
Signature		Date	26/10/16

Name of Co-Author	Beatriz Blanco-Rodriguez		
Contribution to the Paper	Synthesis and characterization of compounds 12 and 13 Revised manuscript Overall contribution: 10%		
Signature		Date	24-10-2016

Name of Co-Author	Zikai Feng		
Contribution to the Paper	Biological testing of compound 3 against KpBPL Overall contribution: 5%		
Signature		Date	24 Oct 2016

Name of Co-Author	Andrew Hayes		
Contribution to the Paper	Antimicrobial susceptibility assay of compound 10 Overall contribution: 5%		
Signature		Date	4/11/16

Name of Co-Author	Mark AT Blaskovich		
Contribution to the Paper	Design and synthesis of azide functionalised NBD and DMACA fluorophores, conducted at University of Queensland. Overall contribution: 5%		
Signature		Date	Nov 1 2016

Name of Co-Author	Matthew A Cooper		
Contribution to the Paper	Provided azide functionalised NDB and DMACA fluorophores Overall contribution: 5%		
Signature		Date	Nov 1 2016

Name of Co-Author	Grant W. Booker		
Contribution to the Paper	Supervised biological aspects of the project, revised manuscript Overall contribution: 5%		
Signature		Date	19/10/2016

Name of Co-Author	Andrew D. Abell		
Contribution to the Paper	Supervised all aspects of medicinal chemistry, conducted at University of Adelaide, Overall contribution: 15%		
Signature		Date	19/10/2016

Name of Co-Author	Wanida Phetsang		
Contribution to the Paper	Synthesis and characterization of NBD and DMACA azides conducted at University of Queensland. Performed SR-SIM fluorescent imaging of compounds 12 and 13 Overall contribution: 5%		
Signature		Date	Nov/2016

Name of Co-Author	Steven W. Polyak		
Contribution to the Paper	Supervised biological aspects of project Worked closely with principal author to write the manuscript Overall contribution: 10%		
Signature		Date	19/10/2016

A template guided approach to generating cell permeable inhibitors of *Staphylococcus aureus* biotin protein ligase

Ashleigh S. Paparella #, Jiage Feng §, Beatriz Blanco-Rodriguez §, Zikai Feng #, Wanida Phetsang ‡, Mark AT. Blaskovich ‡, Matthew A. Cooper ‡, Grant W. Booker #, Andrew D. Abell § and Steven W. Polyak #*

School of Biological Sciences, University of Adelaide, South Australia, 5055, Australia.

§ School of Physical Sciences, University of Adelaide, South Australia, 5005, Australia.

‡ Institute for Molecular Bioscience, The University of Queensland, Brisbane, Queensland, 4072, Australia.

*Address correspondence to: Steven W. Polyak, Molecular Life Sciences Building, Department of Molecular and Cellular Biology, University of Adelaide, South Australia, Australia, 5005, Tel: 61-8-8303-5289; Fax: 61-8-8303-4362; E-mail: steven.polyak@adelaide.edu.au

The essential enzyme, biotin protein ligase (BPL) represents a novel target for the development of new antibiotics. We have previously reported 1,4-disubstituted 1,2,3-triazole inhibitors of the BPL from *Staphylococcus aureus* that were generated using *in situ* click chemistry. In this work, we have used wildtype SaBPL to catalyse the synthesis of 1,4-triazole 3. We have also adopted this approach to other BPLs from clinically relevant bacteria. The 1,4-disubstituted triazole inhibitors exhibit antibacterial activity against *S. aureus*, however, the mechanism of uptake is yet to be determined. To facilitate mechanism-of-uptake studies we synthesized azide-functionalized analogues of two fluorophores and tested them for chemical ligation to biotin acetylene 1 using BPL as a catalyst. 1,4-triazole 12 was generated by SaBPL *in situ* and contains a nitrobenzofurazan (NDB) fluorophore and exhibited inhibitory activity against SaBPL ($K_i = 1.4 \mu\text{M}$). Finally, compound 12 was imaged within *S. aureus* using SR-SIM fluorescence microscopy, indicating that this fluorescent probe can be used to gain insight into the mechanism of uptake of BPL inhibitors in *S. aureus*.

INTRODUCTION

There is a well-documented need to develop new antibiotics to treat the growing number of antibiotic resistant bacteria [1]. Two important hurdles that must be overcome during early stage drug discovery are 1) the need to identify the *in vivo* mechanism of action and 2) to identify mechanisms by which the compound penetrates the bacterial cell [2, 3]. Small molecules that help to investigate these issues are welcome tools in drug discovery programs [4-6]. One emerging target for the development of new antibiotics is the essential metabolic enzyme, biotin protein ligase (BPL) [7]. BPL catalyses protein biotinylation through the formation of the adenylated reaction intermediate from its substrates biotin and ATP to form biotinyl-5'AMP [7] (scheme1). Non-hydrolysable analogues of biotinyl-5'AMP have been reported that are inhibitors of the BPLs from *Escherichia coli* [8, 9], *S. aureus* [7, 10-12], and *Mycobacterium tuberculosis* [13, 14]. Of particular interest is the replacement of the hydrolysable phosphoanhydride linker, present in biotinyl-5'AMP with a more stable 1,4-disubstituted 1,2,3-triazole [15, 16]. Synthesis of the 1,2,3-triazole linker proceeds via the Huisgen cycloaddition reaction between an acetylene and an azide [17]. In special cases this reaction can be catalysed by an enzyme [16, 18-23], in a process known as *in situ* click chemistry. This is a useful approach for identifying enzyme inhibitors as the target enzyme is able to select out and synthesize its own optimized inhibitors from libraries of acetylene and azide containing small molecules [18]. We have previously reported that the BPL from *S. aureus* (*Sa*BPL) can catalyse the formation of the 1,2,3-triazole from biotin acetylene **1** and an azide precursor **2** (scheme 1)[16]. Here analysis of the products was performed using HPLC. One of the limitations associated with *in situ* click chemistry is the production of tight-binding inhibitors. Tight-binding inhibitors often remain associated within the enzyme's active site, thereby preventing further rounds of catalysis [16, 20, 21]. To overcome this problem we reported the use of a 'leaky' mutant *Sa*BPL-R122G to enhance the turnover rate for the cycloaddition reaction [16]. Mutations equivalent to R122G in other BPLs has been

shown to reduce affinity for ATP binding and compromise enzyme activity [24]. To adapt this technology to BPLs from other clinically important bacterial pathogens it was important to develop an alternative detection method with higher sensitivity than analytical HPLC to analyse *in situ* generated products without the need for BPL mutants. To improve product detection we employed liquid chromatography coupled to high resolution electrospray mass spectrometry (LC/HRMS) to analyse *in situ* generated products catalysed by the BPLs from *S. aureus*, *M. tuberculosis*, *Klebsiella pneumoniae* and *Acinetobacter calcoaceticus*. LC/HRMS allows precise identification of individual products using a combination of retention time and high resolution molecular mass [20]. We also used this approach to screen for biotinylated compounds that can be used as fluorescent probes to investigate the *in vivo* mechanism of uptake of BPL inhibitors. To identify such probes we synthesized azide-functionalized analogues of two fluorophores for chemical ligation to biotin acetylene **1** using BPL as a catalyst. Here *Sa*BPL catalysed the formation of 1,4-triazole **12**, containing an nitrobenzofurazan (NBD) fluorophore. Compound **12** was found to inhibited activity of *Sa*BPL, consistent with its mechanism of action through the BPL target. Finally, SR-SIM fluorescent imaging of *S. aureus* and *Escherichia coli* revealed the former compound **12** was permeant for *S. aureus* but not *E. coli*. This newly generated fluorescent probe will be used to further investigate the mechanism of uptake of BPL inhibitors in *S. aureus*.

RESULTS AND DISCUSSION

As mentioned above, our previous study used a mutant *Sa*BPL as a template to catalyse the Huisgen cycloaddition of biotin acetylene **1** and azide **2**, with analytical HPLC as the detection method (scheme 1). The use of analytical HPLC did not permit the resolution of regioisomers (1,4 vs 1,5). Therefore, we turned to LC/HRMS to analyse the products. 1,4-triazole **3** and 1,5-triazole **4** were separately prepared using CuAAC and RuAAC catalysed reactions from biotin acetylene **1** and azide **2** (scheme 1) respectively. The retention times of the purified standards were analysed by LC/HRMS using positive mode with selective ion

monitoring of triazoles **3** and **4** ($M+H^+ = 471.2398$ Da) (figure 1). LC/HRMS analysis revealed baseline separation of the two isomers with a 1 minute difference in the retention times of 1,4-triazole **3** (7.2 min) and 1,5-triazole **4** (8.2 min) (figures 1a and 1b respectively). We next repeated the Huisgen cycloaddition of biotin acetylene **1** and azide **2** using wildtype *Sa*BPL as the catalyst. Here, *Sa*BPL catalysed the formation of the triazole product (figure 1c). The retention time of the *in situ* formed triazole (7.2 min) corresponded with that of the CuAAC prepared standard confirming that *Sa*BPL selectively forms 1,4-triazole **3**. Triazole **3** was not formed in the absence of BPL (figure 1d), and neither isomer was produced by using bovine serum albumin as a non-specific protein (figure 1e), indicating that this reaction is truly template guided.

Encouraged by the successful *in situ* click chemistry experiments with *Sa*BPL, we next turned our attention to expanding the panel of BPL enzymes that could be employed in *in situ* experiments. Recombinant BPL enzymes from *M. tuberculosis* (*Mt*BPL), *K. pneumoniae* (*Kp*BPL) and *A. calcoaceticus* (*Ac*BPL) were tested as templates for Huisgen cycloaddition of biotin acetylene **1** and azide **2** (figure 1). LC/HRMS analysis confirmed formation of triazole **3** by *Mt*BPL and to a lesser extent *Kp*BPL (figure 1f and 1g). In all cases the retention times of the *in situ* generated triazole products were consistent with the formation of 1,4-triazole **3**. In contrast there was no detectable formation of triazole **3** by *Ac*BPL. CuAAC prepared triazole **3** was also tested for inhibitory activity of *Mt*BPL, *Kp*BPL and *Ac*BPL using an *in vitro* biotinylation assay that measures the incorporation of biotin onto an acceptor protein. Triazole **3** was active against *Mt*BPL ($K_i = 0.57 \pm 0.08$ μ M) and exhibited similar potency to *Sa*BPL ($K_i = 0.66 \pm 0.05$ μ M) [16]. Consistent with the *in situ* experiment above triazole **3** was inactive against *Ac*BPL ($K_i > 10$ μ M). Triazole **3** was also inactive against *Kp*BPL. This is consistent with the LC/HRMS analysis as triazole **3** was only formed weakly by *Kp*BPL. These results demonstrate that the *in situ* click chemistry approach can potentially be used to identify triazole inhibitors of other BPL enzymes, including *Mt*BPL.

In early stage antibacterial discovery, it is important to elucidate the mechanism of entry into the bacterial cell [2, 3]. Therefore, compounds that can be used as probes to understand these mechanisms are useful research tools. To identify such probes two fluorophores were functionalized with an azide substituent namely, nitrobenzofurazan (NBD) (Sigma-Aldrich) and 7-(dimethylamino)-coumarin-4-acetic acid (DMACA) [25, 26]. This yielded **7** and **11** respectively (scheme 2). Both fluorophores have previously been acetylene-functionalized and successfully ligated via Huisgen cycloaddition to azide-functionalized analogues of linezolid and trimethoprim for imaging within Gram-positive bacteria [4, 27]. Azides **7** and **11** were tested for chemical ligation to biotin acetylene **1** using *Sa*BPL, *Mt*BPL, *Kp*BPL or *Ac*BPL as a catalyst to potentially form triazoles **12** and **13** (scheme 3). A series of 12 binary *in situ* click chemistry reactions were incubated at 37 °C for 2 days, potentially giving rise to 24 products. LC/HRMS analysis revealed only one product formed by *Sa*BPL, triazole **12** (figure 2a). Encouragingly, there was no triazole product detected in the absence of BPL nor in the presence of bovine serum albumin (data not shown). To confirm the regioselectivity of the *in situ* triazole, 1,4-triazole **12** was prepared using CuAAC before biochemical and microbiological assays were pursued.

First 1,4-triazole **12** was synthesized and purified as described in schemes 2 and 3. LC/HRMS analysis was employed to compare the retention times of both the *in situ* and CuAAC prepared triazole **12**. The LC/HRMS analysis revealed that *in situ* generated triazole **12** had the same retention time as CuAAC prepared triazole **12**, consistent with *Sa*BPL producing the 1,4 regioisomer as expected. We also synthesized 1,4-triazole **13** as described in schemes 2 and 3 to use in biochemical and microbiological assays as a control compound which was not formed in the *in situ* click chemistry experiments.

1,4-triazole **12** was next tested for inhibitory activity against *Sa*BPL using an *in vitro* biotinylation assay. Previous enzymology and X-ray crystallography studies have demonstrated that triazole inhibitors are competitive inhibitors against biotin [15, 16, 28] and

as such the inhibition constant was calculated from the IC_{50} value using the known K_M for biotin as previously described [29]. 1,4-triazole **12** exhibited inhibitory activity against *Sa*BPL ($K_i = 1.4 \pm 0.1 \mu\text{M}$). Consistent with the *in situ* click chemistry reactions 1,4, triazole **12** was not active against *Mt*BPL, *Kp*BPL or *Ac*BPL ($K_i > 10 \mu\text{M}$) Interestingly, 1,4-triazole **13** also inhibited *Sa*BPL ($K_i = 5.0 \pm 0.7 \mu\text{M}$) although it was at least 3-fold less potent than compound **12**. This data could suggest that azide **11** requires the biotin moiety to anchor the DMACA fluorophore into the ATP binding pocket of *Sa*BPL.

To demonstrate the utility of 1,4-triazoles **12** and **13** as tools to probe the mechanism of uptake, compounds **12** and **13** were imaged with Gram-positive and Gram-negative bacteria using SR-SIM fluorescence microscopy. Compounds **12** and **13** were incubated with either *S. aureus* ATCC 25923 or *E. coli* ATCC 25922 and cells were co-stained with fluorescent dyes selective for the bacterial membrane (FM4-64FX) and nucleic acid (Hoechst 3342 for **12** or SYTO 21 for **13**) (figure 3). The staining pattern of compound **12** with *S. aureus* demonstrated that the compound was predominantly detected within the bacterial cytoplasm. Single cell analysis suggested a small amount of material also associated with the inside layer of the bacterial membrane (figure 4a). The staining pattern of compound **12** with *E. coli* was with consistent the compound co-localizing with the membrane stain and not penetrating into the cytoplasm (figure 3). However, single cell analysis showed some fluorescence within the cell (figure 4b). In sharp contrast weak staining with compound **13** was observed with *S. aureus* but not with *E. coli* (figure 3). This data is consistent with our previous studies which show BPL inhibitors are active against *S. aureus* but not *E. coli* [11]. Together this data demonstrates that compound **12** can be used as a fluorescent probe to gain insight into the mechanism of uptake of BPL inhibitors in *S. aureus*. Current studies will focus on competitive uptake studies using fluorescent **12** and other BPL inhibitors to address the specific mechanism of uptake for this class of anti-*Staph* agents. Compound **12** could also be used to investigate the membrane permeability of BPL inhibitors. A recent study involved

using spinning disc confocal microscopy (SDCM) to study passive transport of small molecules containing an NBD fluorophore into liposomes [30]. Compound **12** represents a promising candidate for such membrane permeation studies.

CONCLUSIONS

The results from this study have shown that the *in situ* click chemistry reaction between biotin acetylene **1** and azide **2** can be catalysed by wildtype *Sa*BPL using LC/HRMS analysis. LC/HRMS analysis also demonstrated that the enzyme generates the 1,4-triazole **3** over the 1,5-triazole **4**. We have also shown that *Sa*BPL can catalyse the Huisgen cycloaddition of biotin acetylene **1** and an azide functionalized analogue of the fluorophore NBD. This *in situ* generated triazole, compound **12**, was a potent inhibitor *Sa*BPL and SR-SIM fluorescence microscopy demonstrated the utility of **12** for staining. This fluorescent probe will now be used to help gain insight into the mechanism of uptake and action of BPL inhibitors in *S. aureus*, enabling the development of BPL antibacterials. Finally, we have also shown that *Mt*BPL can be used to catalyse the Huisgen cycloaddition of biotin acetylene **1** and azide **2**. The *in situ* generated triazole **3** exhibited sub-micromolar inhibition against *Mt*BPL and exhibits similar potency to *Sa*BPL, highlighting that *in situ* click chemistry could be used to identify potent inhibitors of *Mt*BPL. This *in situ* approach to developing cell permeant BPL inhibitors could also be adapted to other clinically important bacteria, such as *M. tuberculosis*.

REFERENCES

1. Tommasi, R., et al., *ESKAPeIng the labyrinth of antibacterial discovery*. Nat Rev Drug Discov, 2015. **14**(8): p. 529-542.
2. Silver, L.L., *Challenges of Antibacterial Discovery*. Clin Microbiol Rev, 2011. **24**(1): p. 71-109.
3. Lewis, K., *Antibiotics: Recover the lost art of drug discovery*. Nature, 2012. **485**(7399): p. 439-440.
4. Phetsang, W., et al., *An azido-oxazolidinone antibiotic for live bacterial cell imaging and generation of antibiotic variants*. Bioorg Med Chem, 2014. **22**(16): p. 4490-4498.
5. Jefferson, K.K., D.A. Goldmann, and G.B. Pier, *Use of Confocal Microscopy To Analyze the Rate of Vancomycin Penetration through Staphylococcus aureus Biofilms*. Antimicrob Agents Chemother, 2005. **49**(6): p. 2467-2473.
6. Tran, T.T., et al., *Daptomycin-Resistant Enterococcus faecalis Diverts the Antibiotic Molecule from the Division Septum and Remodels Cell Membrane Phospholipids*. mBio, 2013. **4**(4).
7. Paparella, A.S., et al., *Structure guided design of biotin protein ligase inhibitors for antibiotic discovery*. Curr topics med chem, 2014. **14**(1): p. 4-20.
8. Brown, P.H. and D. Beckett, *Use of Binding Enthalpy To Drive an Allosteric Transition*. Biochemistry, 2005. **44**(8): p. 3112-3121.
9. Xu, Y. and D. Beckett, *Kinetics of Biotinyl-5'-adenylate Synthesis Catalyzed by the Escherichia coli Repressor of Biotin Biosynthesis and the Stability of the Enzyme-Product Complex*. Biochemistry, 1994. **33**(23): p. 7354-7360.
10. Tieu, W., et al., *Heterocyclic acyl-phosphate bioisostere-based inhibitors of Staphylococcus aureus biotin protein ligase*. Bioorg Med Chem Lett, 2014. **24**(19): p. 4689-4693.
11. Tieu, W., et al., *Improved Synthesis of Biotinyl-5'-AMP: Implications for Antibacterial Discovery*. ACS Med Chem Lett, 2015. **6**(2): p. 216-220.
12. Soares da Costa, T.P., et al., *Biotin Analogues with Antibacterial Activity Are Potent Inhibitors of Biotin Protein Ligase*. ACS Med Chem Lett, 2012. **3**(6): p. 509-514.
13. Duckworth, Benjamin P., et al., *Bisubstrate Adenylation Inhibitors of Biotin Protein Ligase from Mycobacterium tuberculosis*. Chem Biol, 2011. **18**(11): p. 1432-1441.

14. Bockman, M.R., et al., *Targeting Mycobacterium tuberculosis Biotin Protein Ligase (MtBPL) with Nucleoside-Based Bisubstrate Adenylation Inhibitors*. J Med Chem, 2015. **58**(18): p. 7349-7369.
15. Soares da Costa, T.P., et al., *Selective inhibition of Biotin Protein Ligase from Staphylococcus aureus*. J Biol Chem, 2012. **287**(21): p. 17823-17832.
16. Tieu, W., et al., *Optimising in situ click chemistry: the screening and identification of biotin protein ligase inhibitors*. Chem Sci, 2013.
17. Kolb, H.C., M.G. Finn, and K.B. Sharpless, *Click Chemistry: Diverse Chemical Function from a Few Good Reactions*. Angew Chem Int Ed, 2001. **40**(11): p. 2004-2021.
18. Sharpless, K.B.M., R., *In situ click chemistry: a powerful means for lead discovery*. Expert Opin Drug Discov, 2006. **1**(6): p. 525-538.
19. Whiting, M., et al., *Inhibitors of HIV-1 Protease by Using In Situ Click Chemistry*. Angew Chem Int Ed, 2006. **45**(9): p. 1435-1439.
20. Manetsch, R., et al., *In Situ Click Chemistry: Enzyme Inhibitors Made to Their Own Specifications*. J. Am Chem Soc, 2004. **126**(40): p. 12809-12818.
21. Krasiński, A., et al., *In Situ Selection of Lead Compounds by Click Chemistry: Target-Guided Optimization of Acetylcholinesterase Inhibitors*. J. Am Chem Soc, 2005. **127**(18): p. 6686-6692.
22. Millward, S.W., et al., *Iterative in Situ Click Chemistry Assembles a Branched Capture Agent and Allosteric Inhibitor for Akt1*. J. Am Chem Soc, 2011. **133**(45): p. 18280-18288.
23. Mocharla, V.P., et al., *In Situ Click Chemistry: Enzyme-Generated Inhibitors of Carbonic Anhydrase II*. Angew Chem Int Ed, 2005. **44**(1): p. 116-120.
24. Tron, C.M., et al., *Structural and Functional Studies of the Biotin Protein Ligase from Aquifex aeolicus Reveal a Critical Role for a Conserved Residue in Target Specificity*. J. Mol Biol, 2009. **387**(1): p. 129-146.
25. Portonovo, P., et al., *First Total Synthesis of a Fluorescent Didemnin*. Tetrahedron, 2000. **56**(23): p. 3687-3690.
26. Alexander, M.D., et al., *A Central Strategy for Converting Natural Products into Fluorescent Probes*. ChemBioChem, 2006. **7**(3): p. 409-416.
27. Phetsang, W., et al., *Fluorescent Trimethoprim Conjugate Probes To Assess Drug Accumulation in Wild Type and Mutant Escherichia coli*. ACS Infect Dis, 2016. **2**(10): p. 688-701.

28. Pendini, N.R., et al., *Structural characterization of Staphylococcus aureus biotin protein ligase and interaction partners: An antibiotic target*. Prot sci, 2013. **22**(6): p. 762-773.
29. Yung-Chi, C. and W.H. Prusoff, *Relationship between the inhibition constant (KI) and the concentration of inhibitor which causes 50 per cent inhibition (I50) of an enzymatic reaction*. Biochem Pharmacol, 1973. **22**(23): p. 3099-3108.
30. Li S, H.P., Malmstadt N. , *Confocal Imaging to Quantify Passive Transport across Biomimetic Lipid Membranes*. Anal Chem, 2010. **82**(18): p. 7766 - 7771.

FIGURE LEGENDS

Figure 1. LC/HRMS traces of *in situ* generated and reference triazoles, with selective ion monitoring for triazoles **3** and **4** ($M+H^+ = 471.2398$ Da).

a). 1,4-triazole **3** prepared by CuAAC. b). 1,5-triazole **4** prepared by RuAAC. c). Triazole **3** from *in situ* reaction of **1** and **2** in the presence of SaBPL. d). *In situ* reaction of **1** and **2** in the absence of BPL. e). *In situ* reaction of **1** and **2** in the presence of bovine serum albumin. f). *In situ* reaction of **1** and **2** in the presence of MtBPL. g). *In situ* reaction of **1** and **2** in the presence of KpBPL.

Figure 2. LC/HRMS traces of *in situ* generated triazole **12** at selective ion monitoring ($M + H^+ = 502.1979$ Da).

a). *In situ* generated triazole **12** in the presence of SaBPL. b). 1,4-triazole **12** prepared by CuAAC.

Figure 3

Staining of *S. aureus* ATCC 25923 and *E. coli* ATCC 25922 with compounds **12** and **13**. Bacterial membrane was stained with FM4-64F and nucleic acid was stained with Hoechst 33342 for **12** or SYTO 21 for **13**. Bars represent 1 μ m.

Figure 4

Single cell staining analysis of compound **12**, FM4-64F (bacterial membrane) and Hoechst 33342 (nucleic acid).

a). Single cell staining analysis of *S. aureus* ATCC 25923. b). Single cell staining analysis of *E. coli* ATCC 25922.

LIST OF SCHEMES

Scheme 1. BPL catalysed reaction of biotin and ATP (top) and synthesis of 1,4-triazole **3** by BPL and CUAAC and 1,5-triazole **4** by RuAAC from biotin acetylene **1** and azide **2** (bottom).

a). Cu nanopowder, 2:1 AcCN/H₂O, 12 h , sonication, 35 °C. b). Cp*Ru(PPh₃)₂Cl, 1:1 DMF/THF, 12 h, 35 °C.

Scheme 2. Synthesis of azide-functionalized fluorophores **7** (top) and **11** (bottom).

a). BrCH₂CH₂CH₂NH₂·HBr, MeOH, 0°C, 1h, 0°C to 35°C, 12 h. b). NaN₃, DMF, 35°C, 12 h. c). CO(CH₂CO₂Et)₂, ZnCl₂, EtOH, Δ, 17h. d). BrCH₂CH₂CH₂NH₂·HCl, DMAP, EDC·HCl, DCM, 35°C, 12h e). NaN₃, DMF, 35°C, 12 h.

Scheme 3. Synthesis of 1,4-triazoles **12** and **13** from biotin acetylene **1** and azides **7** and **11**.

Figure 1

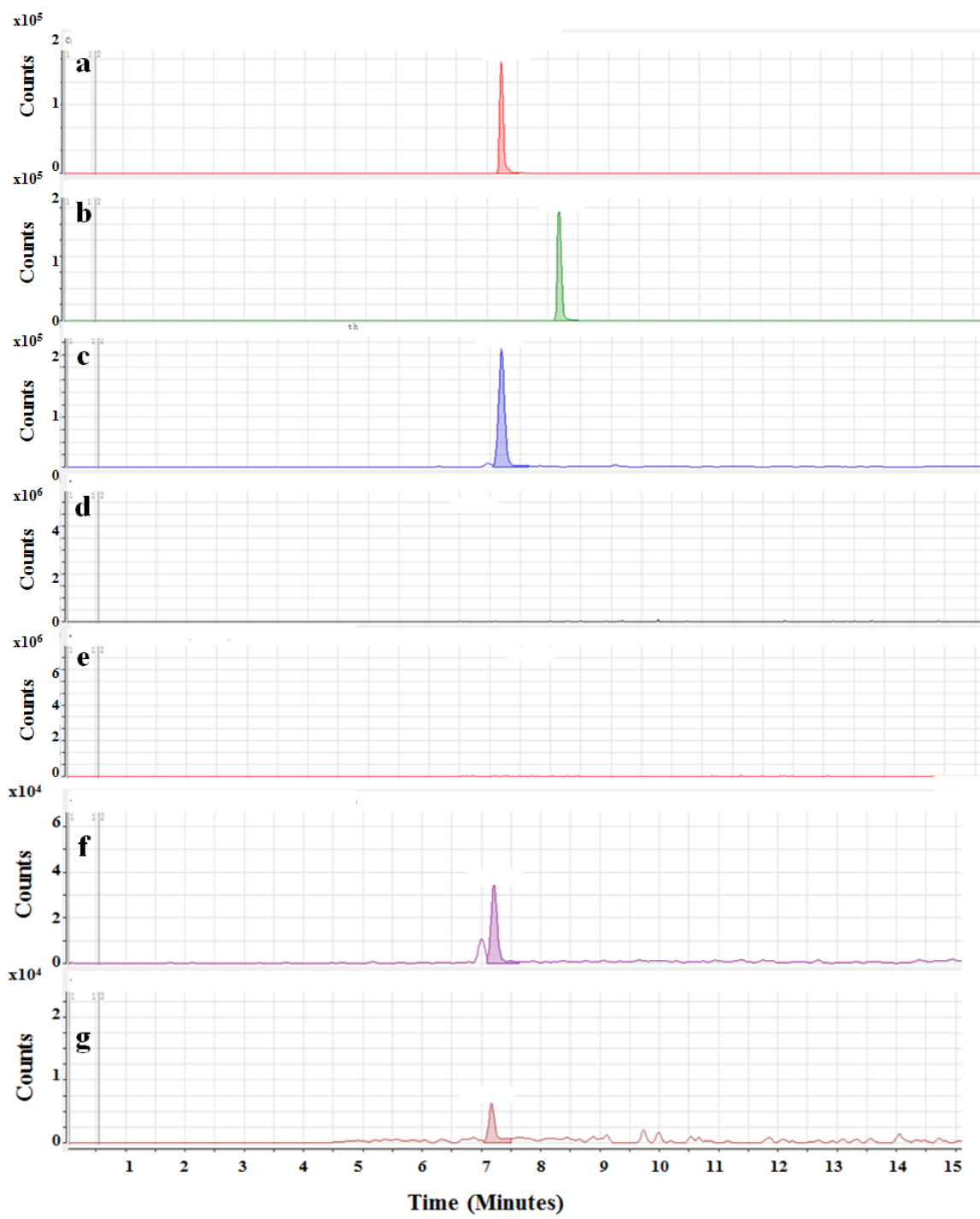


Figure 2

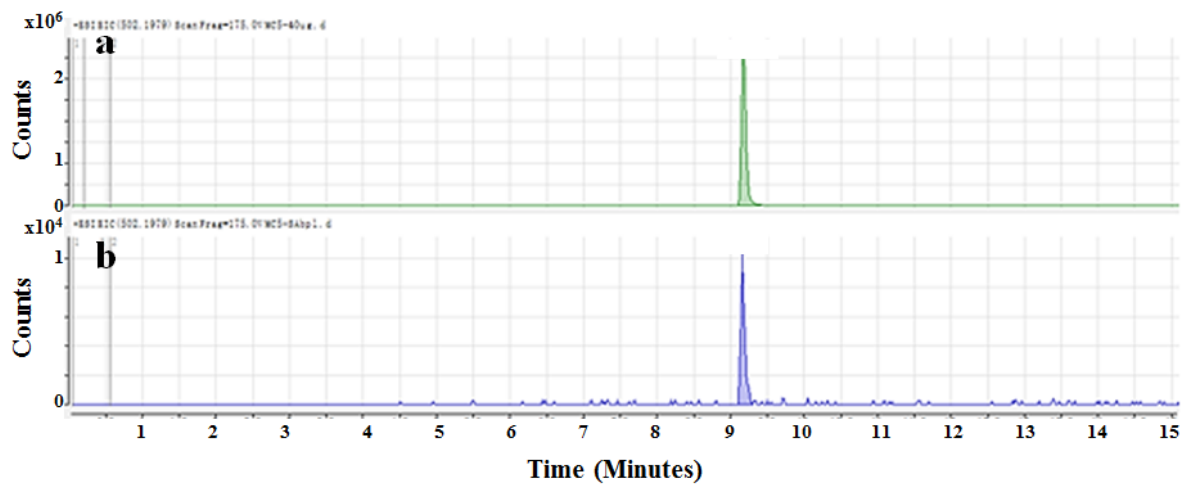


Figure 3

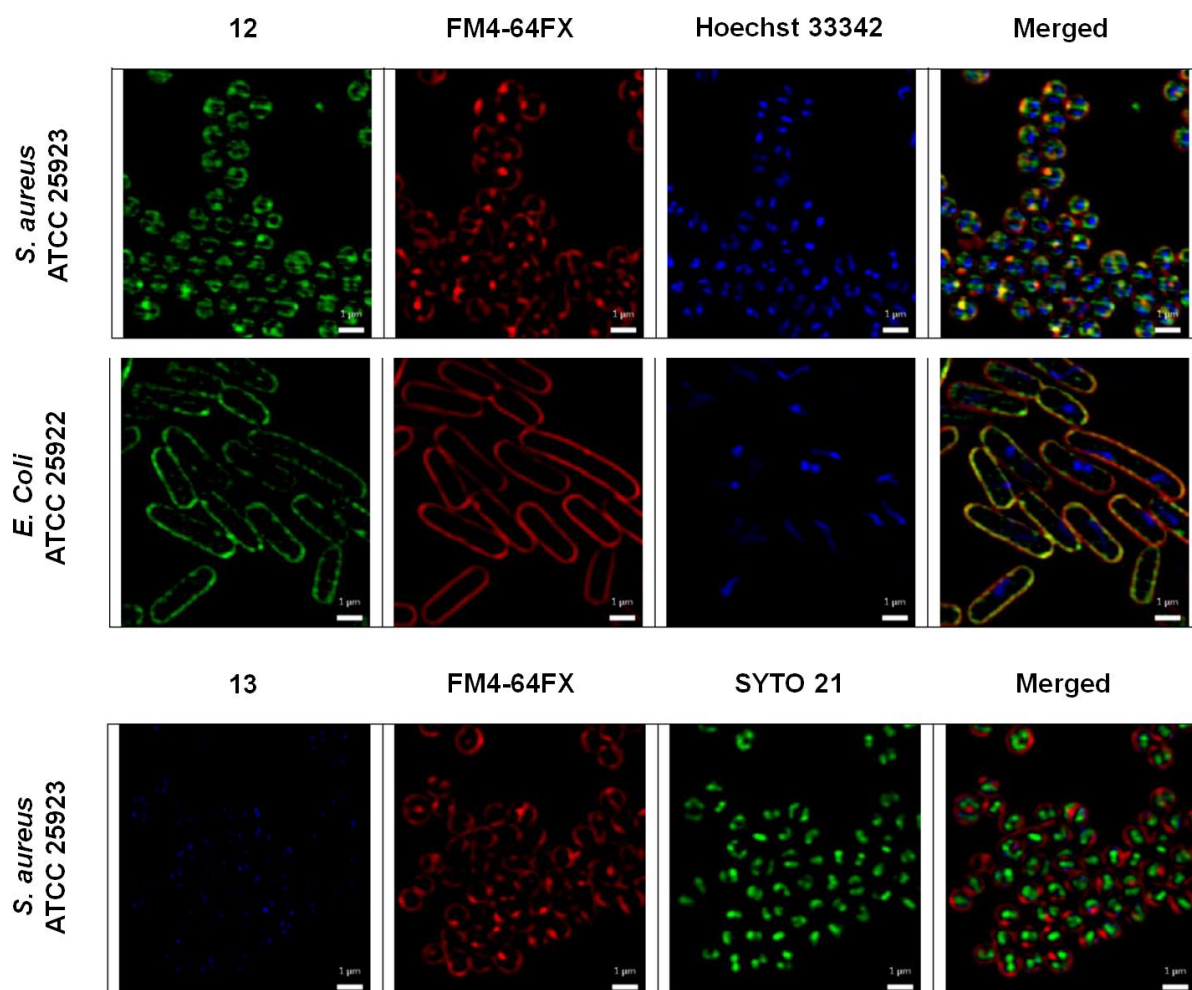
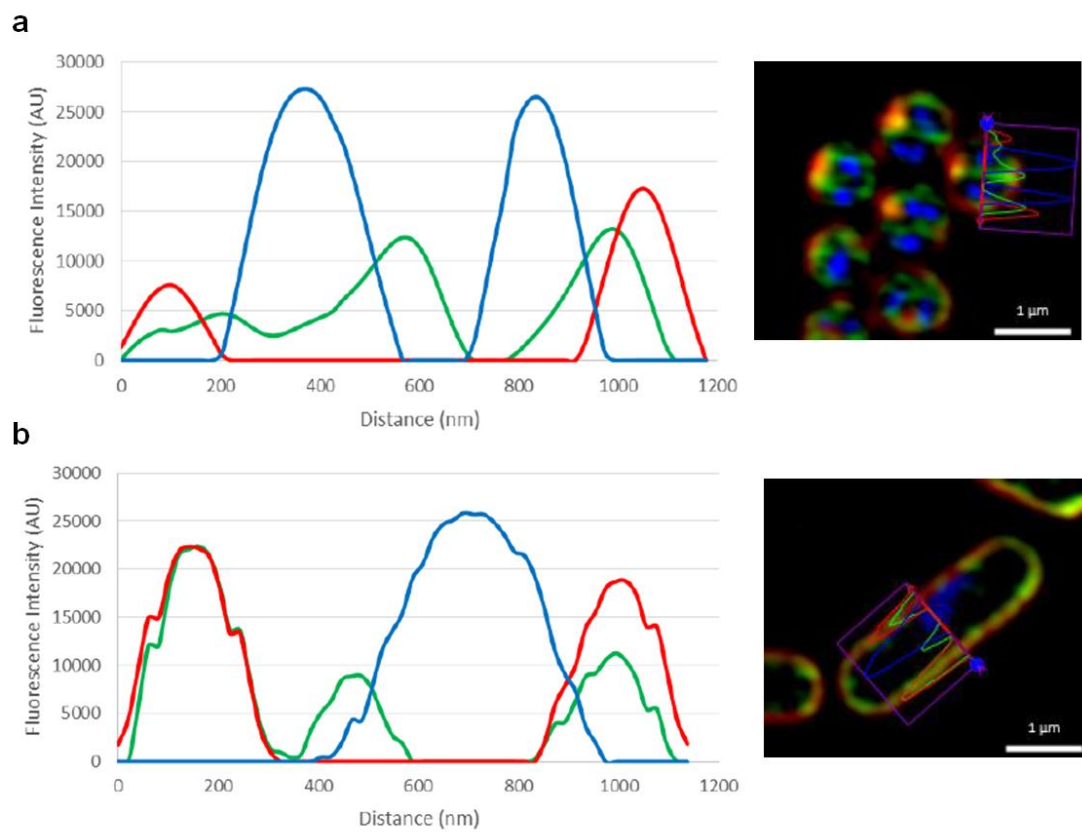
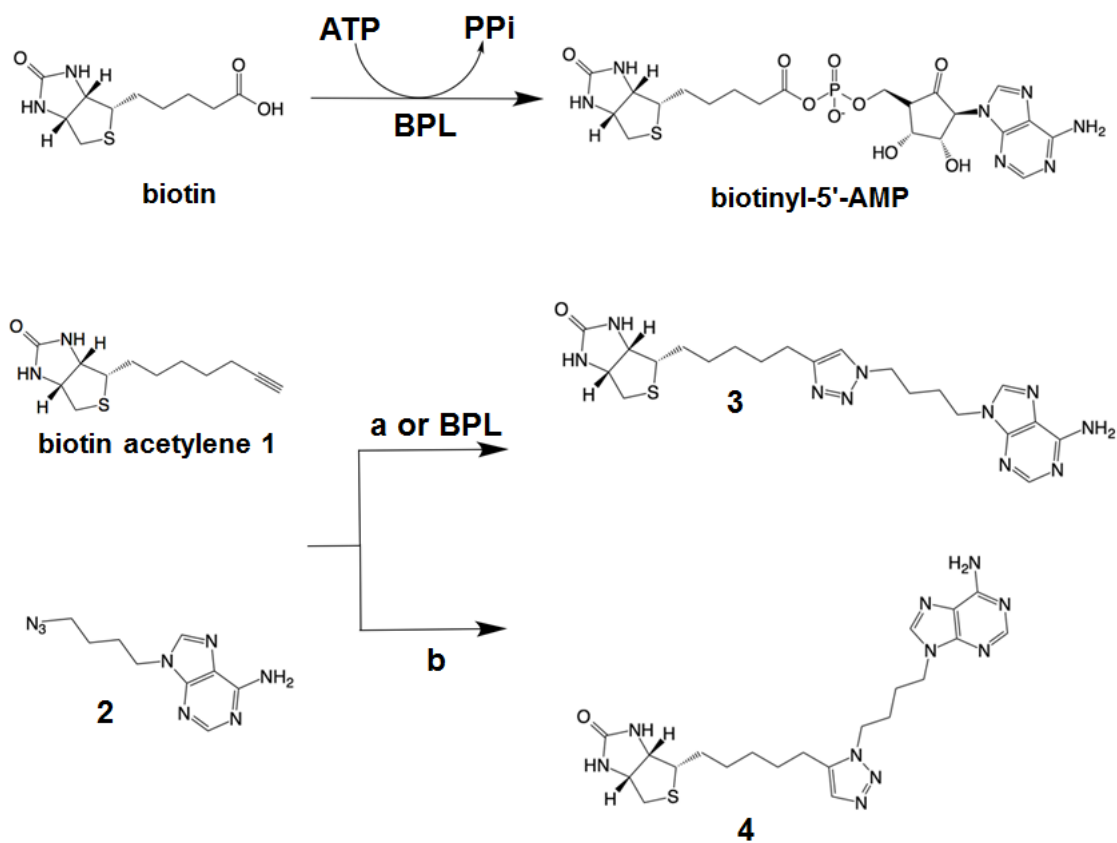


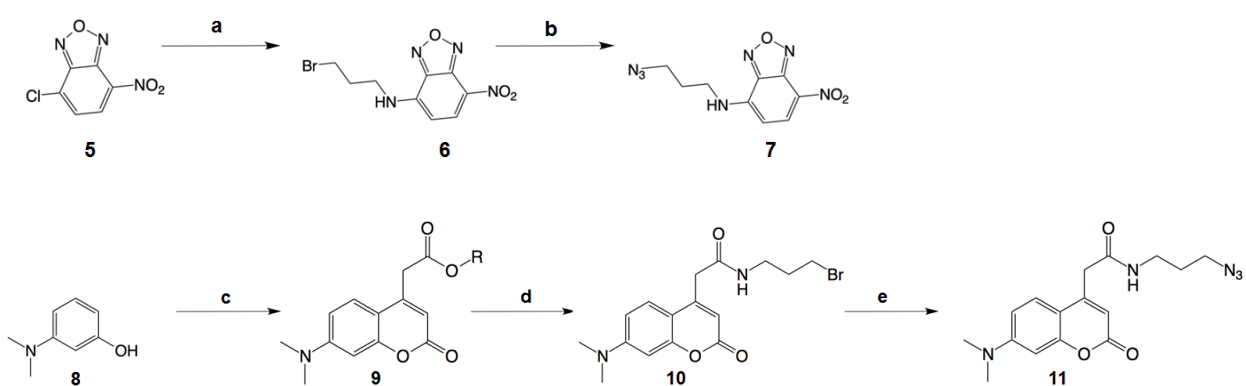
Figure 4



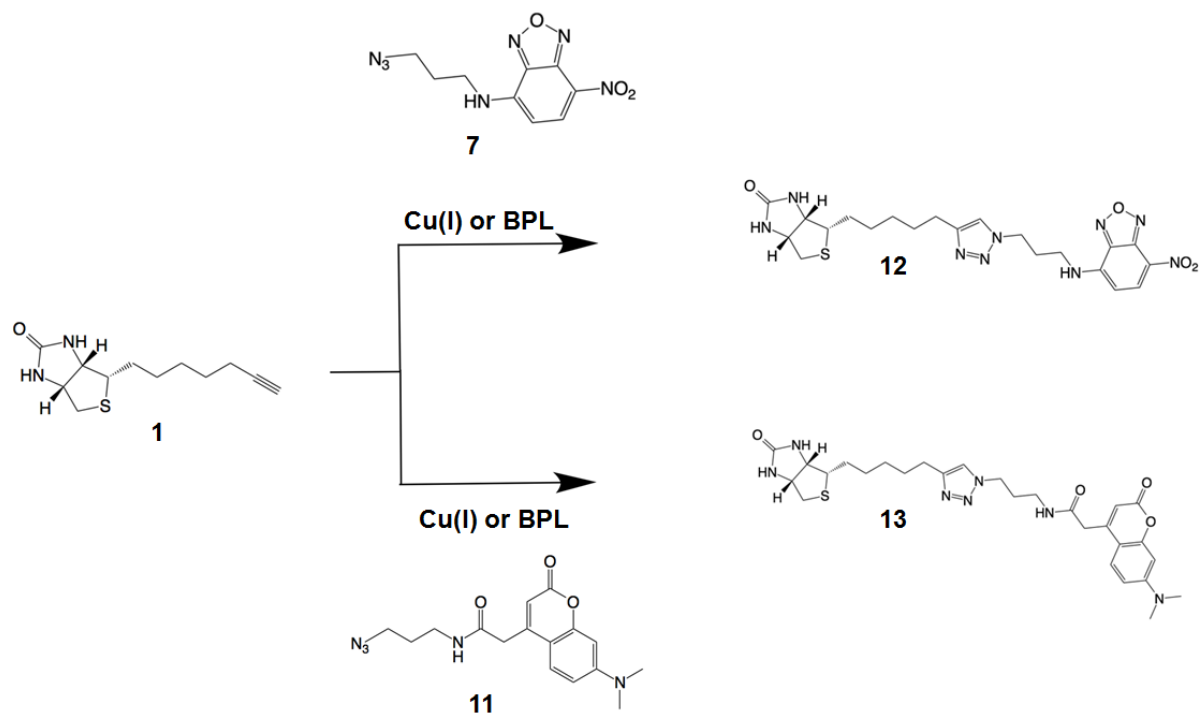
Scheme 1



Scheme 2



Scheme 3.



SUPPLEMENTARY MATERIAL

LC/MS analysis of *in situ* reactions

Aliquots of each reaction (50 μL) were diluted with a stock solution of 0.1% TFA in acetonitrile (50 μL). Samples of the diluted reaction mixtures (10 μL) were separately injected into the LC/MS system, and the analytes were fractionated using the Poroshell 120 EC-C18 reverse phase column (dimensions 2.1 mm x 50 mm), using eluents (0.1% TFA in water) and B (0.08% TFA in acetonitrile) at a flow rate of 0.3 mL/min. The gradient increased from 2% acetonitrile to 100% acetonitrile wash for 5 min. The mass spectroscopy detector was tuned to the positive mode with selective ion monitoring of the target molecule. The presence of the *in situ* product was identified by retention time and molecular weight ($\Delta < 5$ ppm).

***In situ* click experiment 1**

The stock solutions of biotin acetylene **1** and azide **2** were separately prepared by dissolving in a mixture 10% DMSO in Milli-Q water to give a concentration of 2.5 mM for each compound. The *in situ* click reaction mixture was then prepared by adding these solutions to PBS (137 mM NaCl, 2.7 mM KCl, 8 mM Na_2HPO_4 , 1.46 mM KH_2PO_4 , pH 7.4) to give final concentration of 500 μM for each component (final DMSO concentration 4% (v/v)). SaBPL was then added to the mixture to give a final concentration of 2 μM . Control samples were prepared in parallel using either PBS or BSA (final concentration 2 μM) in place of SaBPL. All 3 reaction mixtures were incubated at 37 $^\circ\text{C}$ for 48 hours. Each reaction was analysed using LC/HRMS (as described above) with selective ion monitoring of the target triazole ($\text{M}+\text{H}^+ = 471.2398$ Da). The regioselectivity of cycloaddition products were identified by comparison of its retention time with the authentic samples of 1,4-triazole **3** and 1,5-triazole **4**, which were prepared through CuAAC and RuAAC respectively.

In situ click experiment 2

The *in situ* click reaction was performed essentially as described above in experiment 1 except each reaction contained either 1) *MtBPL*, 2) *KpBPL*, or 3) *AcBPL* in place of *SaBPL*. The control samples were also prepared in parallel using either PBS or BSA (final concentration 2 μM), in place of BPL enzymes. All 6 sample mixtures were incubated at 37 $^{\circ}\text{C}$ for 48 hours. Each reaction was analysed using LC/HRMS with selective ion monitoring of the target triazole ($\text{M}+\text{H}^{+} = 471.2398 \text{ Da}$). The regioselectivity of the cycloaddition products were identified by comparison of its retention time with the authentic samples of 1,4-triazole **3** and 1,5 triazole **4**, which were prepared through CuAAC and RuAAC respectively.

In situ click experiment 3

The *in situ* click library screening was performed between the biotin acetylene **1** (final concentration 500 μM) and one of the azides **7** and **11** (final concentration 500 μM each). The individual reaction mixture was treated in parallel with either *SaBPL*, *MtBPL*, *KpBPL*, *AcBPL*, BSA or no enzyme to give total 12 samples, which were incubated at 37 $^{\circ}\text{C}$ for 48 hours. Each sample was analysed using LC/HRMS by electrospray ionisation with positive selected-ion monitoring tuned to molecular masses of target triazoles. The cycloaddition product of 1,4-triazole **12** was identified by comparison of its retention time with that determined from analysis of the copper-catalysed reaction and by its molecular weight ($\text{M}+\text{H}^{+} = 502.1979 \text{ Da}$).

Protein expression and purification:

The cloning, expression and purification of *SaBPL* [1], *MtBPL* [2], *KpBPL* (ref biotinol paper) and *AcBPL* (biotinol paper) have been previously described.

In vitro Biotinylation assays

Quantification of BPL catalysed ^3H -biotin incorporation into the biotin domain substrate was performed as previously described [3, 4]. A reaction was prepared containing 50 mM Tris HCl pH 8.0, 3 mM ATP, 4.94 μM biotin, 0.06 μM ^3H -biotin, 5.5 mM MgCl_2 , 100 mM KCl, 0.1 μM DTT and 10 μM biotin domain of *S. aureus* pyruvate carboxylase. To determine inhibitory activity, BPL activity was measured in the presence of varying concentrations of compound. All compounds were dissolved in DMSO and then diluted into the reaction buffer to give a final concentration of 4% DMSO. BPL reaction was initiated by the addition of enzyme to give final concentrations of 6.25 nM for *Sa*BPL, 20 nM for *Mt*BPL, 100 nM for *Kp*BPL and 10 nM for *Ac*BPL. After 10 minutes at 37 °C, 90 μL of stopping buffer (110 mM EDTA and 50 mM Tris HCl pH 8.0) was added to terminate the reaction and 100 μL aliquot of the reaction mixture was added to the wells of a 96-well HTS multiscreen plate containing an Immobilon-P® (Merck Millipore) membrane that had been pre-treated with 50 μL of 70% ethanol, 400 μL of MilliQ- H_2O followed by 200 μL of TBS. Quantitation of protein-bound radiolabelled biotin was determined by liquid scintillation counting. The IC_{50} value of each compound was determined from a dose-response curve by varying the concentration of inhibitor under the same enzyme concentration. The data was analysed with GraphPad Prism (version 6) using a non-linear fit of \log_{10} [inhibitor] vs. normalized response. The K_i , the absolute inhibition constant for a compound was determined using Eq 1: [5]

$$K_i = \frac{IC_{50}}{1 + \frac{[S]}{K_M}}$$

Where [S] is the substrate concentration ([biotin] = 5 μM) and K_M is the affinity of the enzyme for biotin (*S.aureus* BPL = 1 μM , [3], and *H. sapiens* BPL = 1 μM [3]).

Bacterial SR-SIM fluorescence microscopy of compound 12

SIM was performed using the Zeiss Elyra PS.1 SIM/STORM microscope (green channel: laser HR Diode 488-100, filter BP495-550 + LP750; red channel: laser HR DPSS 561-100, filter BP570-620 + LP750; blue channel: laser HR Diode 405-50, filter BP420-480 + LP750). Images were analyzed with ZEN2012. VectaShield H1000 (Abacus ALS Cat.-No.: VEH1000) was used as a mounting media. Cover slip glasses (Zeiss/Schott, 18 mm × 18 mm, No.1.5H) were used to prepare samples. Hank's Balanced Salt Solution (HBSS) without phenol red, CaCl₂, and MgSO₄ (Sigma Aldrich Cat.-No.: H6648) was used for bacterial staining. Fluorescent dyes FM4-64FX (Life Technologies, Australia Cat.-No.: F34653), Hoechst 33342 (Life Technologies, Australia Cat.-No.: H21492), and SYTO 21 (Life Technologies, Australia Cat.-No.: S7556) were used for membrane staining and DNA staining, respectively.

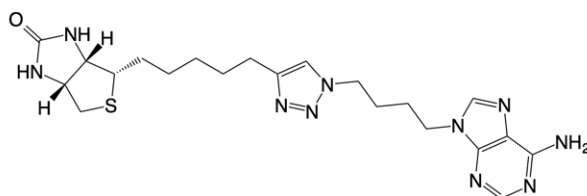
S. aureus (ATCC 25923) and *E. coli* (ATCC 25922) were cultured in LB at 37 °C overnight. A sample of each culture was then diluted 50-fold in LB and incubated at 37 °C for 1.5-2 h. 1 mL of the resultant mid-log phase cultures were transferred to an Eppendorf tube and centrifuged. Bacteria were washed once with HBSS, then suspended in 20 µL of HBSS. 2 µL of this suspended bacteria solution was dropped onto a cover slip, spread and dried. An ice-cold solution (200 µL) of **12** or **13** (64 µg/mL in HBSS) was then added to the bacteria, left for 1 hour on ice, and then washed once with ice-cold HBSS. An ice-cold solution (200 µL) of Hoechst 33342 (10 µg/mL in HBSS) or Syto 21 (5 µM in HBSS) was then dropped onto the bacteria, left for 5 min on ice for *S. aureus* and 10 min for *E. coli*, then drained. This was followed by adding an ice-cold solution (200 µL) of FM4-64FX (5 µg/mL in HBSS) onto the bacteria, left for 2 min on ice for *S. aureus* and 5 min for *E. coli* and then washed once with ice-cold HBSS. The bacteria were fixed with 4% paraformaldehyde 10 min for *S. aureus* on

ice and 20 min for *E. coli* on ice, followed by mounting on slides using VectaShield H1000 as a mounting media.

Synthetic Chemistry methods

All reagents were obtained from commercial sources and are of reagent grade or as specified. Solvents were also obtained from commercial sources, except for anhydrous THF, anhydrous DCM and anhydrous DMF which were dried over solvent purifier (PS-Micro, Innovative Technology, USA). Reactions were monitored by TLC using precoated plates (silica gel 60 F254, 250 μm , Merck, Darmstadt, Germany), spots were visualised under ultraviolet light at 254 nm and with either sulphuric acid-vanillin spray, potassium permanganate dip or Hanessian's stain. Column chromatography was performed with silica gel (40-63 μm 60 \AA , Davisil, Grace, Germany). HPLC was performed on HP Series 1100 with Phenomenex Gemini C18 5 μM (250 x 4.60 mm) for Analytical HPLC and Phenomenex Luna C18 10 μM (50 x 10.00 mm) for Semi-preparative HPLC. Microwave reactions were performed on a CEM Discovery SP with external IR temperature monitoring. Reactions were stirred for 5 min in a sealed container at ambient temperature, followed by 5 min stirring with increased microwave power until the prescribed temperature was reached. Both power and pressure were kept variable. ^1H and ^{13}C NMR spectra were recorded on a Varian Inova 500 MHz or a Varian Inova 600 MHz. Chemical shifts are given in ppm (δ) relative to the residue signals, which in the case of DMSO- d_6 were 2.55 ppm for ^1H and 39.55 ppm for ^{13}C , CDCl_3 were 7.26 ppm for ^1H and 77.23 ppm for ^{13}C and D_2O was 4.79 for ^1H . Structural assignment was confirmed with COSY, ROESY, HMQC and HMBC. Mixtures of isomers are designated A and B in NMR spectra without individual assignment. Partial integrals are also reported for each isomer. High-resolution mass spectra (HRMS) were recorded on an Agilent 6230 time of flight (TOF) liquid chromatography mass spectra (LC/MS) ($\Delta < 5$ ppm).

Preparation of (3aS,6aR)-4-[5-[1-[4-(6-aminopurin-9-yl)butyl]triazol-4-yl]pentyl]-1,3,3a,4,6,6a-hexahydrothieno[3,4-d]imidazol-2-one 3



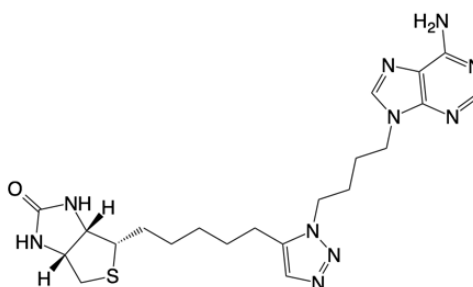
Biotin acetylene **1** (31 mg, 0.13 mmol) was reacted with alkyl adenine **2** (36 mg, 0.14 mmol) and Cu nanopowder (2 mg, 0.026 mmol) using 'general CuAAC'. The crude material was purified by flash chromatography on silica eluting with 8% methanol in dichloromethane to give a crystalline white solid (46 mg, 73%).

$^1\text{H NMR}$ (600 MHz; DMSO- d_6): δ 8.12 (1H, s, ArH), 8.11 (1H, s, ArH), 7.86 (1H, s, Ar^{tri}H), 7.20 (2H, bs, ArNH₂), 6.52 (1H, bs, C(O)NH), 6.40 (1H, bs, C(O)NH), 4.34-4.38 (3H, m, ArN^{tri}CH₂, NHCH), 4.34-4.38 (3H, m, Ar^{ad}CH₂, NHCH), 3.12-3.16 (m, 1H, SCH), 3.12-3.16 (1H, dd, $J = 4.8, 12$ Hz, SCH_a), 2.59-2.64 (3H, m, SCH_b, ArC^{tri}CH₂), 1.76-1.80 (4H, m, 2 x CH₂), 1.28-1.67 (8H, m, 4 x CH₂);

$^{13}\text{C NMR}$ (150 MHz; DMSO- d_6): 162.8, 156.0, 152.4, 149.5, 146.8, 140.8, 121.8, 118.7, 61.2, 59.2, 55.6, 48.5, 42.2, 40.0, 28.8, 28.6, 28.5, 28.3, 27.0, 26.7, 25.1;

LC/HRMS calcd. for (M + H) C₂₁H₃₁N₁₀OS: requires 471.2398, found 471.2392; $R_t = 7.17$ min.

Preparation of (3a*S*,4*S*,6a*R*)-4-[5-[1-[4-(6-aminopurin-9-yl)butyl]triazol-4-yl]pentyl]-1,3,3a,4,6,6a-hexahydrothieno[3,4-*d*]imidazol-2-one 4



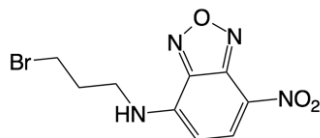
Biotin acetylene **1** (41 mg, 0.17 mmol) was reacted with alkyl adenine **2** (47 mg, 0.19 mmol) and Cp**Ru*(PPh₃)₂Cl (27 mg, 0.034 mmol) using 'general RuAAC'. The crude material was purified by flash chromatography on silica eluting with 7% methanol in dichloromethane to give a white solid (46 mg, 55%).

¹H NMR (600 MHz; 1% CD₃OD, CDCl₃): δ 8.20 (1H, s, ArH), 7.76 (1H, s, ArH), 7.37 (1H, s, Ar^{tri}H), 6.14 (1H, bs, C(O)NH), 5.58 (1H, bs, C(O)NH), 4.47 (1H, dd, *J* = 4.8, 7.8 Hz, NHCH), 4.13-4.29 (5H, m, ArCH₂, ArN^{tri}CH₂, NHCH), 3.08-3.12 (1H, m, SCH), 2.88 (1H, dd, *J* = 5.4, 12.9 Hz, SCH_b), 2.69 (1H, d, *J* = 12.9 Hz, SCH_a), 1.81-1.89 (2H, m, ArC^{tri}CH₂), 1.26-1.68 (10H, m, 5 x CH₂);

¹³C NMR (150 MHz; DMSO-*d*⁶): 163.9, 155.6, 152.6, 149.4, 140.1, 137.1, 131.7, 118.8, 72.2, 62.0, 59.9, 46.7, 43.0, 40.3, 29.0, 28.7, 28.5, 27.8, 27.0, 26.7, 22.8;

LC/HRMS calcd. for (M + H) C₂₁H₃₁N₁₀OS: requires 471.2398, found 471.2395; R_t = 8.19 min.

***N*-(3-bromopropyl)-7-nitrobenzo[*c*][1,2,5]oxadiazol-4-amine 6**



To a stirring solution of 3-bromopropylamine hydrobromide (175 mg, 1.0 mmol) in ice-cold MeOH (2 mL) was added NBD-Cl (200 mg, 1.0 mmol) in MeOH (8 mL) dropwise over 1 h. The reaction was gradually allowed to warm to room temperature and stir at that temperature overnight. The mixture was partitioned between water and dichloromethane. The organic phase was separated and the aqueous phase was extracted with dichloromethane (x3). The organics were combined, dried over magnesium sulphate, filtrated and concentrated under reduced pressure. The crude material was purified by flash chromatography on silica eluting with 5% methanol in dichloromethane to give as yellow solid (96 mg, 32%).

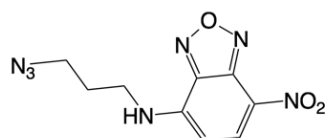
¹H NMR (500 MHz, CDCl₃) δ 8.47 (d, *J* = 8.7 Hz, 1H, ArH), 6.78 (s, 1H, NH), 6.30 (d, *J* = 8.7 Hz, 1H, ArH), 3.79 (dd, *J* = 13.0, 6.5 Hz, 2H, CH₂), 3.59 (t, *J* = 6.1 Hz, 2H, CH₂) and 2.54 2.29 (m, 2H, CH₂) ppm

¹³C NMR (125 MHz, CDCl₃) δ 144.3, 144.1, 143.9, 136.8, 123.8, 99.1, 42.4, 31.0 and 30.2.

HRMS calcd. for (M + Na⁺) C₉H₉BrN₄NaO₃: 322.9756, found 322.9748

HPLC R_t = 18.11 min.

N*-(3-azidopropyl)-7-nitrobenzo[*c*][1,2,5]oxadiazol-4-amine **7*



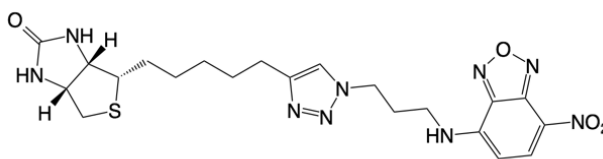
Bromide **6** (96 mg, 0.32 mmol) was reacted with sodium azide (24 mg, 0.37 mmol) in DMF and purified by flash chromatography on silica eluting with 30% EtOAc in hexane to yield a yellowish oil (62 mg, 76%).

¹H NMR (500 MHz, CDCl₃) δ 8.43 (d, *J* = 8.7 Hz, 1H, ArH), 6.93 (br s, 1H, NH), 6.22 (d, *J* = 8.7 Hz, 1H, ArH), 3.67 (dd, *J* = 12.2, 6.0 Hz, 2H, CH₂), 3.57 (t, *J* = 6.2 Hz, 2H, CH₂) and 2.12-2.04 (m, 2H, CH₂).

¹³C NMR (125 MHz, CDCl₃) δ 144.3, 144.2, 143.9, 136.8, 123.6, 98.9, 49.1, 41.7, 27.7.

HRMS calcd. for (M + H) C₉H₉BrN₄NaO₃: 322.9756, found 322.9748

(3a*S*,4*S*,6a*R*)-4-(5-(1-(3-((7-nitrobenzo[*c*][1,2,5]oxadiazol-4-yl)amino)propyl)-1*H*-1,2,3-triazol-4-yl)pentyl)tetrahydro-1*H*-thieno[3,4-*d*]imidazol-2(3*H*)-one 12



Biotin alkyne **1** (50 mg, 0.21 mmol) was reacted with azide **7** (62 mg, 0.19 mmol) and Cu nanopowder (2 mg, 0.026 mmol) using General Procedure G1. The crude material was purified by flash chromatography on silica gel eluting with 3% MeOH in DCM to give a crystalline white solid (40 mg, 38%).

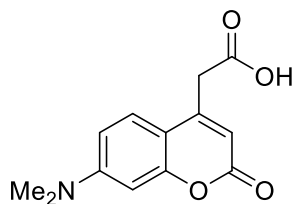
¹H NMR: (500 MHz, DMSO-*d*₆) δ 9.49 (s, 1H, NH), 8.49 (d, *J* = 8.8 Hz, 1H, ArH), 7.86 (s, 1H, ArH), 6.42 (s, 1H, NH), 6.36 (s, 1H, NH), 6.35 (d, *J* = 7.5 Hz, 1H, ArH), 4.44 (t, *J* = 6.9 Hz, 2H, CH₂), 4.35-4.27 (m, 1H, NHCH), 4.19-4.09 (m, 1H, NHCH), 3.56-3.43 (m, 2H, CH₂), 3.08 (m, 1H, SCH), 2.81 (dd, *J* = 12.4, 5.1 Hz, 1H, SCH_a), 2.57 (d, 2H, *J* = 12.4 Hz, SCH_b), 2.57 (m, 2H, CH₂), 2.24 (p, *J* = 6.9 Hz, 2H, CH₂), 1.65-1.51 (m, 3H, CH₂+CHH), 1.49-1.41 (m, 1H, CHH), 1.35 (m, 4H, 2xCH₂).

¹³C NMR: (125 MHz, DMSO-*d*₆) δ 162.9, 147.1, 125.1, 144.5, 144.2, 137.9, 122.0, 121.0, 99.3, 79.2, 61.2, 59.3, 55.6, 47.0, 28.9, 28.7, 28.5, 28.3, 25.0.

HRMS: calcd for C₂₁H₂₈N₉O₄S (M+H⁺): 502.1985, found 502.1979;

HPLC: R_t = 14.98 min.

7-Dimethylaminocoumarin-4-acetic acid **9**

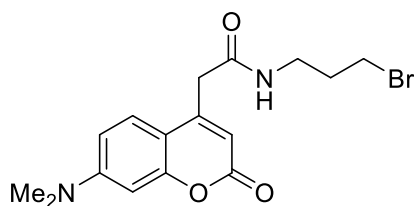


M-Dimethylaminophenol (500 mg, 3.7 mmol), diethyl 1,3-acetonedicarboxylate (0.73 mL, 4 mmol, 1.1 equiv.) and ZnCl₂ (595 mg, 4.4 mmol, 1.2 eq) were dissolved in absolute ethanol (2 mL). The reaction mixture was heated at reflux (100 °C) for 15 h. The reaction mixture was cooled to room temperature and the solvent was removed under reduced pressure. The crude material was purified by flash chromatography on silica eluting with 5% methanol in dichloromethane to give a colourless oil that was treated with 2 M LiOH aq (2.3 mL, 4.57 mmol, 2 eq) in THF for 2 h. Water was added and the aqueous phase was extracted with ethyl acetate (x3). The aqueous layer was acidified to pH 2 with 2 M HCl aq and the precipitate formed was filtered and air dried to give the title compound as a yellow solid (450 mg, 50 %, over two steps).

¹H NMR (500 MHz, MeOD): 7.70 (d, *J* = 9 Hz, 1H, Coum-H), 7.14 (dd, *J* = 9, 3 Hz, 1H, Coum-H), 7.05 (d, *J* = 3 Hz, 1H, Coum-H), 6.26 (s, 1H, Coum-H) and 3.86 (s, 2H, CH₂) and 3.19 (s, 6H, N(CH₃)₂) ppm.

¹³C NMR (125 MHz, MeOD): 172.6, 163.0, 156.5, 151.5, 151.0, 127.80, 114.0, 113.56, 103.7, 88.52, 43.01 and 38.33 ppm.

***N*-(3-bromopropyl)-2-(7-(dimethylamino)-2-oxo-2H-chromen-4-yl)acetamide 10**



To a solution of 7-Dimethylaminocoumarin-4-acetic acid (450 mg, 1.8 mmol) and 3-bromopropylamine hydrobromide (350 mg, 2 mmol, 1.1 eq) in 9 mL of anhydrous dichloromethane were added EDC·HCl (414 mg, 2.2 mmol, 1.2 eq) and DMAP (44 mg, 0.36 mmol, 0.2 eq) at 0 °C. The mixture was allowed to warm to room temperature for overnight. After the reaction was completed it was diluted with water and washed with water and brine, dried over magnesium sulphate and concentrated under reduced pressure. The crude material was purified by flash chromatography on silica eluting with 20 % ethyl acetate in dichloromethane to give the title compound as yellow solid (70 mg, 10%).

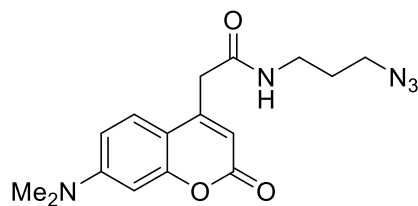
¹H NMR (500 MHz, CDCl₃) δ 7.48 (d, *J* = 9.0 Hz, 1H, ArH), 6.61 (dd, *J* = 9.0, 2.5 Hz, 1H, ArH), 6.44 (d, *J* = 2.5 Hz, 1H, ArH), 6.27 (br s, 1H, NH), 6.04 (s, 1H, CH), 3.63 (s, 2H, CH₂CO), 3.37 (q, *J* = 6.5 Hz, 2H, CH₂), 3.31 (t, *J* = 6.6 Hz, 2H, CH₂), 3.04 (s, 3H, (CH₃)₃) and 2.06–2.00 (m, 2H, CH₂) ppm.

¹³C NMR (125 MHz, CDCl₃) δ 168.4 (C), 162.0 (C), 156.1 (C), 153.3 (C), 149.9 (C), 125.8 (CH), 110.5 (C), 109.4 (CH), 108.3 (CH), 98.3 (CH), 41.0 (CH₂), 40.2 (3xCH₃), 38.7 (CH₂), 32.1 (CH₂) and 30.8 (CH₂) ppm.

MS HRMS (ESI) calculated for C₁₆H₂₀BrN₂O₃: 367.0657/369.0637; found, 367.0688/369.0669.

Analytical HPLC: Sample was dissolved in methanol (1 mg/ml) and eluted with solvent A: 0.1% TFA in MilliQ water and solvent B: 0.08% TFA in MeCN on a phenomenex Luna 5 μm C18 (2) 100 Å (250 x 4.60 mm), flow rate = 1 ml/min, gradient 0–100% of solvent B over 15 min, with UV detection at 360 nm. Retention time 16.40 min. Purity 100%.

***N*-(3-azidopropyl)-2-(7-(dimethylamino)-2-oxo-2H-chromen-4-yl)acetamide 11**



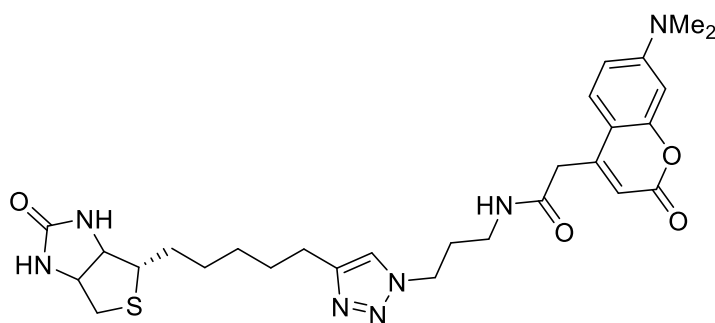
Bromide **10** (96 mg, 0.32 mmol) was reacted with sodium azide (24 mg, 0.37 mmol) according to general procedure **J2** and purified by flash chromatography on silica eluting with 30% EtOAc in hexane to yield a yellowish oil (30 mg, 41%).

¹H NMR (500 MHz, CDCl₃) δ 7.46 (d, *J* = 9.0 Hz, 1H, ArH), 6.62 (dd, *J* = 9.0, 2.5 Hz, 1H, ArH), 6.51 (d, *J* = 2.5 Hz, 1H, ArH), 6.03 (s, 1H, ArH), 5.85 (br s, 1H, NH), 3.63 (s, 2H, CH₂CO), 3.31 (q, *J* = 6.4 Hz, 2H, CH₂), 3.25 (t, *J* = 6.6 Hz, 2H, CH₂), 3.06 (s, 6H, N(CH₃)₂) and 1.71 (p, *J* = 6.6 Hz, 2H, CH₂N₃) ppm.

¹³C NMR (125 MHz, CDCl₃) δ 168.1 (C), 161.8 (C), 156.3 (C), 153.4 (C), 149.6 (C), 125.7 (CH), 110.6 (CH), 109.4 (CH), 108.2 (C), 98.4 (CH), 49.5 (CH₂), 41.1 (CH₂), 40.3 (2xCH₃), 37.8 (CH₂) and 28.7 (CH₂) ppm.

MS HRMS (ESI) calcd for C₁₆H₂₀N₅O₃ (M-H⁺): 330.1566, found 330.1557.

2-(7-(dimethylamino)-2-oxo-2H-chromen-4-yl)-N-(3-(4-(5-((4S)-2-oxohexahydro-1H-thieno[3,4-d]imidazol-4-yl)pentyl)-1H-1,2,3-triazol-1-yl)propyl)acetamide 13



Biotin alkyne **1** (50 mg, 0.21 mmol) was reacted with azide **11** (62 mg, 0.19 mmol) and Cu nanopowder (2 mg, 0.026 mmol) using 'general CuAAC'. The crude material was purified by flash chromatography on silica gel eluting with 3% MeOH in DCM to give a crystalline white solid (54 mg, 45%).

¹H NMR (500 MHz, DMSO-*d*₆) δ 8.28 (t, *J* = 5.5 Hz, 1H, NH), 7.79 (s, 1H, ArH), 7.54 (d, *J* = 9.0 Hz, 1H,), 6.72 (dd, *J* = 9.0, 2.5 Hz, 1H, ArH), 6.54 (d, *J* = 2.5 Hz, 1H, ArH), 6.43 (s, *J* = 13.9 Hz, 1H, NHCH), 6.35 (s, 1H, NHCH), 6.00 (s, 1H, CH), 4.32–4.26 (m, 3H, CH₂+NHCH), 4.13 (m, 1H, NHCH), 3.61 (s, 2H, CH₂), 3.13–3.04 (m, 3H, CH₂+SCH), 3.01 (s, 6H, 2xCH₃), 2.81 (dd, *J* = 12.4, 5.1 Hz, 1H, SCHa), 2.59 (m, 2H, CH₂), 2.57 (d, *J* = 8.1 Hz, 1H, SCHb), 1.94 (p, *J* = 6.9 Hz, 2H, CH₂), 1.66–1.52 (m, 3H, CH₂+CHH), 1.45 (m, 1H, CHH) and 1.35 (m, 4H, 2xCH₂) ppm.

¹³C NMR (125 MHz, DMSO-*d*₆) δ 168.0 (C), 162.7 (C), 160.7 (C), 155.4 (C), 152.8 (C), 151.1 (C), 146.8 (C), 125.9 (CH), 121.7 (CH), 109.4 (CH), 109.0 (C), 108.2 (CH), 97.5 (CH), 61.1 (CH), 59.2 (CH), 55.5 (CH), 46.9 (CH₂), 39.8 (CH₂), 39.7 (2xCH₃), 38.8 (CH₂), 36.1 (CH₂), 29.8 (CH₂), 28.8 (CH₂), 28.6 (CH₂), 28.4 (CH₂), 28.2 (CH₂) and 25.0 (CH₂) ppm.

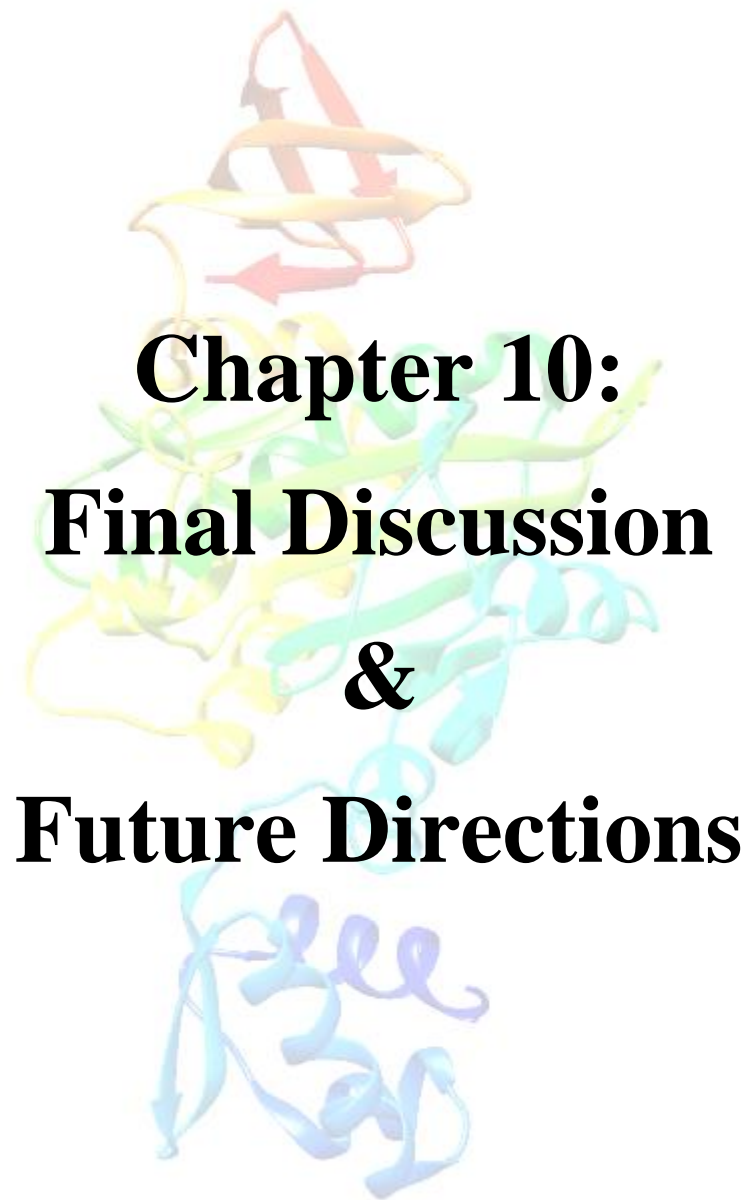
MS HRMS (ESI) calcd for C₂₈H₃₈N₇O₄S (M-H⁺): 568.2700, found 568.2733.

IR (ATR) ν: 3223 (N-H), 2924 (=C-H), 1979 (N=N), 1694 and 1613 (C=O) and 1252 (N-C) cm⁻¹.

Analytical HPLC: Sample was dissolved in methanol (1 mg/ml) and eluted with solvent A: 0.1% TFA in MilliQ water and solvent B: 0.08% TFA in MeCN on a phenomenex Luna 5 μM C18 (2) 100 Å (250 x 4.60 mm), flow rate = 1 ml/min, gradient 0–100% of solvent B over 15 min, with UV detection at 360 nm. Retention time 14.31 min. Purity 100%.

References:

1. Pendini, N.R., et al., *Purification, crystallization and preliminary crystallographic analysis of biotin protein ligase from Staphylococcus aureus*. Acta Crystallographica Section F, 2008. **64**(6): p. 520-523.
2. Tieu, W., et al., *Improved Synthesis of Biotinol-5'-AMP: Implications for Antibacterial Discovery*. ACS Medicinal Chemistry Letters, 2015. **6**(2): p. 216-220.
3. Soares da Costa, T.P., et al., *Selective inhibition of Biotin Protein Ligase from Staphylococcus aureus*. Journal of Biological Chemistry, 2012. **287**(21): p. 17823-17832.
4. Soares da Costa, T.P., et al., *Biotin Analogues with Antibacterial Activity Are Potent Inhibitors of Biotin Protein Ligase*. ACS Medicinal Chemistry Letters, 2012. **3**(6): p. 509-514.
5. Cheng, Y. and W.H. Prusoff, *Relationship between the inhibition constant (K_I) and the concentration of inhibitor which causes 50 per cent inhibition (I₅₀) of an enzymatic reaction*. Biochem Pharmacol, 1973. **22**(23): p. 3099-108.



**Chapter 10:
Final Discussion
&
Future Directions**

10.1 Final discussions and future directions

10.1.1 Key findings

Non-hydrolysable analogues of the BPL reaction intermediate **1** (figure 10.1a) have been demonstrated to be excellent inhibitors with potential as new antibacterials [1-8]. In this thesis several synthesized analogues of **1** were characterized for their biochemical and microbiological properties that will enable the development of new BPL antibacterials. The first generation analogue, biotinol-5'AMP **2** (figure 10.1b)(Chapter 5) [3] was a potent inhibitor of *Sa*BPL ($K_i = 18$ nM) and *Mt*BPL ($K_i = 52$ nM). Importantly, it exhibited antibacterial activity against both antibiotic sensitive and resistant strains of *S. aureus* (MIC 2 – 8 $\mu\text{g/mL}$) and *M. tuberculosis* (MIC 0.5 – 2.5 $\mu\text{g/mL}$) [3]. This data provided proof of concept that BPL inhibitors can serve as antibacterials against drug resistant strains of bacteria that are becoming more prevalent and difficult to treat in both healthcare settings and the wider community.

A second generation of inhibitors, the biotin triazoles, were also investigated [1, 4, 5, 9, 10]. The most potent exemplar, BPL068 **3** (figure 10.1c) served as the lead compound for this project. Compound **3** is the most potent inhibitor of *Sa*BPL ($K_i = 230$ nM) from the biotin triazole class, exhibits >1000 fold selectivity for *Sa*BPL and shows no cytotoxicity against cultured mammalian HepG2 cells [1]. However, the antibacterial activity of **3** was not potent enough to determine a MIC [1, 2]. To improve antibacterial activity two approaches to inhibitor optimization were pursued.

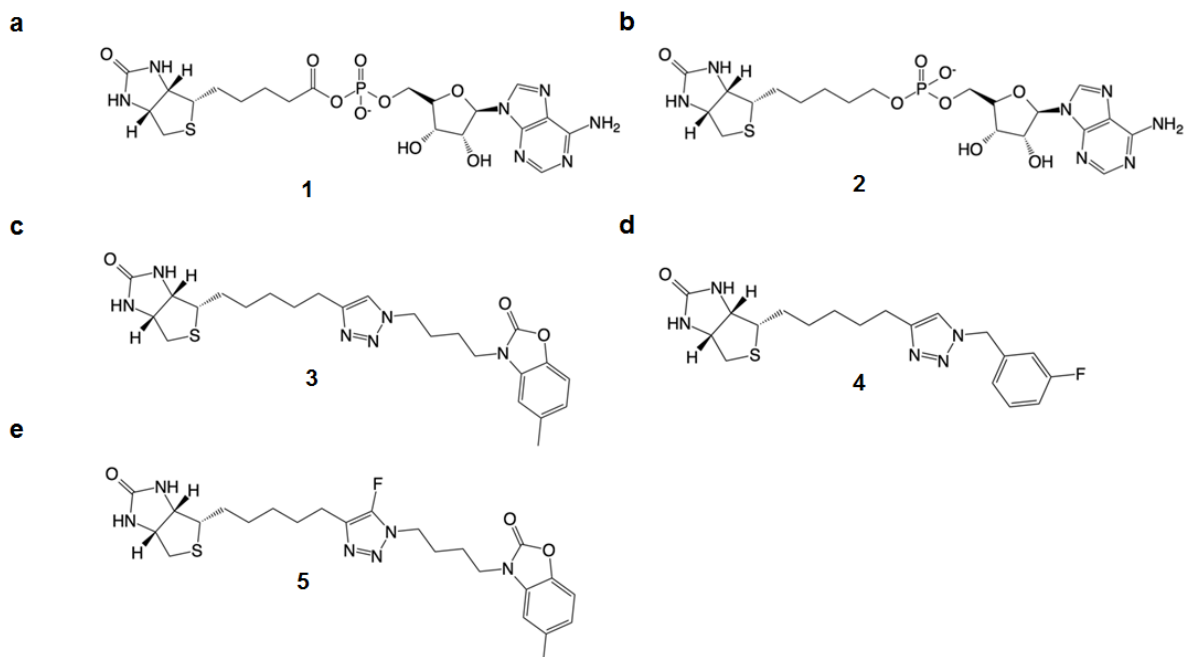


Figure 10.1 Key inhibitors identified in this study

The first approach that was investigated to improve the potency and antibacterial activity of biotin triazole inhibitors was to generate a series of small more ‘drug-like’ molecules. The molecular weight of small molecule drugs can impact on the oral bioavailability. In Lipinski’s landmark study, molecular weight was one key physicochemical property that was identified as impacting oral bioavailability and cell permeability with <500 being optimal [11]. In chapter 6 a series of biotin triazoles with 1-benzyl substituents, with an average molecular weight of <500 were synthesized and represent the first example of reaction intermediate **1** analogues that lack an appended adenine or benzoxalone moiety. The most potent exemplar contained a fluorine **4** ($K_i = 280$ nM) at position 3 of the benzyl ring (figure 10.1d). Encouragingly, compound **4** exhibits similar potency to compound **3** and exhibits modest antibacterial activity against *S. aureus*. Recent work in our laboratory, in collaboration with Prof. Andrew Abell in the Department of Chemistry at the University of Adelaide, has looked at designing a modified benzyl series in which the C5 atom of the triazole heterocycle has been replaced by either a fluorine or an iodine atom to make 1,4,5-trisubstituted triazoles.

Studies are currently underway to investigate whether these compounds have improved antibacterial activity against *S. aureus*.

The second approach investigated to improve the potency and antibacterial activity of BPL inhibitors, was to modify the 1,2,3-triazole heterocycle. In chapter 8, a series of 1,4,5-trisubstituted-1,2,3-triazoles were synthesized to investigate whether halogenation of compound **3** improved antibacterial activity. In this study compound **5** (figure 10.1e) exhibited antibacterial activity against *S. aureus* ATCC 49775, where it had an MIC of 8 µg/mL. X-ray crystallography studies are currently underway in collaboration with Prof. Matthew Wilce at Monash University to determine the molecular mechanism of binding. Enzyme inhibition and surface plasmon resonance binding assays demonstrated that compound **5** exhibited similar potency and binding affinity compared to compound **3**. Therefore it is unlikely that the additional fluorine atom will make extra interactions with SaBPL. Compound **5** is the first example of a biotin triazole inhibitor for which an MIC could be reported. Fluorination of compounds represents one strategy to impart favourable properties to a lead molecule including improved binding affinity, membrane permeability and metabolic stability [12-16]. One study looked at quantifying the effect of halogenation on membrane permeability. Here, halogenated drugs through either the addition of a chlorine atom or a tri-fluoromethyl group were characterized using surface activity measurements to yield the lipid-water partition coefficient and permeability coefficient (measurements of membrane permeability) [17]. Both the addition of chlorine and a tri-fluoromethyl group improved both measurements in the order of $H < Cl < CF_3$ [17]. Such studies could be pursued with compound **5** to determine whether it has enhanced membrane permeability in comparison to compound **3**.

10.1.2 Investigating mechanism of uptake of BPL inhibitors

In chapter 9, an *in situ* click chemistry approach was used to identify cell permeant compounds that could be employed in mechanism-of-uptake studies. Here, compound **6** was generated *in situ* by SaBPL from biotin acetylene and an azide-functionalized nitrobenzofurazan (NBD) fluorophore (figure 10.2). SR-SIM fluorescence microscopy demonstrated that the staining pattern of compound **6** was consistent with the compound being located in the cytoplasm in *S. aureus*, where it could co-localize with the BPL target. The mechanism of uptake for new antibacterials should be defined during early stage drug discovery. This is valuable information as certain properties can be incorporated into small molecule inhibitors to enhance uptake. One of the main uptake mechanisms for compounds that bind intracellular targets, such as BPL, is through passive diffusion across the lipid bilayer into the bacterial cytoplasm. [18]. An alternative way for BPL inhibitors containing a biotinyl moiety to enter *S. aureus* is by active transport through the biotin transporter BioY (described below). Compound **6** could be employed to investigate whether BPL inhibitors passively diffuse across a lipid bilayer, using liposomes. One such study involved using spinning disc confocal microscopy (SDCM) of giant unilamellar vesicles (liposomes) to investigate passive transport of small molecules [19]. These molecules consisted of polyethylene glycol chains of various lengths attached to an NBD fluorophore [19]. Confocal microscopy imaging studies could also be employed to investigate where BPL inhibitors localize in *S. aureus*. Such studies have been performed with the glycopeptide antibiotic, vancomycin [20, 21]. The location of BPL inhibitors in *S. aureus* could be used to help gain insight into the mechanism of action *in vivo*.

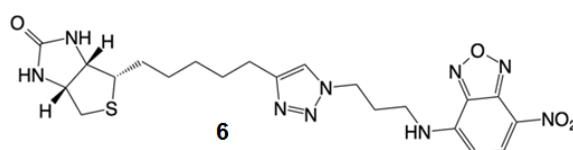


Figure 10.2: SaBPL inhibitor containing NBD fluorophore

The BioY transporter is a part of the energy coupling factor (ECF) family of vitamin transporters that uses ATP hydrolysis to move solutes across the bacterial cell membrane [22]. A fluorescence polarization assay that measures binding of biotin to the *S. aureus* BioY protein complex recombinantly expressed on the cell surface of *E. coli* has been developed in our laboratory [23]. This assay showed that both biotin acetylene and the lead molecule BPL068 **3** could compete with a fluorescently labelled biotin reagent to bind to BioY with equivalent affinity as biotin [23]. Whilst this data suggests that the biotin triazoles can bind to BioY, it does not address whether these compounds are actively transported into *S. aureus*. We have recently purchased a transposon based *S. aureus bioY* null mutant (NE1541, Bei Resources), that will be employed in further mechanism of uptake studies. Here, the MIC of BPL inhibitors will be compared for the *bioY* knockout and its parent strain. If NE1541 is resistant to the compounds, this would provide strong evidence to implicate the BioY transporter complex in inhibitor uptake. If BPL inhibitors are found to enter *S. aureus* predominantly through the SaBioY transporter complex, then the fluorescence polarization assay described above could be used in conjunction with antimicrobial susceptibility assays to identify compounds with enhanced antibacterial activity. One such experiment could investigate the binding affinity of compound **5** compared to BPL068 **3** to determine whether high binding affinity to SaBioY correlates with better antibacterial activity. By incorporating chemical properties that result in a better binding affinity to BioY, BPL with lower MICs could be developed.

10.1.3 Investigating the mechanism of action of BPL inhibitors

One of the hurdles that must be overcome during early stage antibacterial discovery is to determine the mechanism of action of inhibitors *in vivo* [24, 25]. This is important information as it is necessary to confirm that the observed antibacterial effect is due to inhibition of the expected biological target. It is also important to determine whether there are any off target effects and whether this could raise any potential mechanisms of host toxicity [24].

In chapters 6 and 8, *S. aureus* RN4220 was employed to generate a BPL over-expression strain to aid in mechanism of action studies (Mr A. Hayes, School of Biological Sciences, University of Adelaide). When *SaBPL* was over-expressed, the MIC was elevated, this is consistent with compounds binding to the *SaBPL* target *in vivo* [5]. Although over-expression studies can aid in supporting the mechanism of action of an inhibitor, it is not definitive proof that inhibition of the candidate enzyme is the cause of the antibacterial effect [24]. It only demonstrates that the inhibitor can bind to the target enzyme *in vivo* [24].

Another well accepted method to determine the mechanism of action of an antibacterial *in vivo* is through target alteration [24]. This can be performed by evolving resistance of a bacterial strain to a compound through serial passage with sub-optimal concentrations of that compound, thus raising the MIC until a resistance phenotype is observed. The genome of the bacterial strain can then be sequenced to identify mutations associated with the resistance phenotype. If mutations map to the gene encoding the candidate enzyme, this is strong evidence that the candidate gene is responsible for the antibacterial effect [24]. This approach has also been recently attempted in our laboratory. To facilitate these studies we have identified another inhibitor which is extremely potent against *SaBPL* ($K_i = 0.4$ nM), has ~5000-fold selectivity for *SaBPL* over the human homologue, does not show any cytotoxicity against cultured mammalian liver and kidney cells and, importantly, has an MIC for *S. aureus* ATCC 49775 of < 1 $\mu\text{g}/\text{mL}$. This *SaBPL* inhibitor, termed, BPL199, does not contain a

triazole heterocycle that is reported in this thesis (S. Poylak, personal communication). BPL199 was used to evolve resistance in 7 *S. aureus* strains. The genome of each was sequenced and amongst the mutations identified was a loss of function of pyruvate carboxylase (one of two biotin-dependent enzymes in *S. aureus*) and a single missense mutation in *SaBPL*. Here, Asp 200 has been mutated to glutamic acid (D200E). *SaBPL* is a multi-functional class II BPL that is both a biotin ligase and a transcriptional repressor (as described in chapter 2). Comparative genomics analysis predict that *SaBPL* regulates three target promoters, namely the *bioO* operon which encodes the genes involved in biotin biosynthesis, the *bioY* gene encoding the biotin transporter protein BioY and finally the *yhfS-yhfT* genes which are predicted to encode 2 putative fatty acid ligases [26]. When all available biotin-dependent enzymes have been modified by BPL, *SaBPL* dimerizes and the reaction intermediate acts a co-repressor to facilitate repression of all 3 target genes [9, 26-30]. Recent work in our laboratory performed by Ms J. Satiaputra has confirmed that biotin represses all 3 BPL target genes through quantitative PCR (qPCR) studies on *S. aureus in vivo* and using a LacZ reporter system constructed in *E. coli*. Finally, BPL199 was also used in the qPCR experiments to define its role as a co-repressor. BPL199 did indeed act as a co-repressor and downregulate *bioD* (biotin biosynthesis) and *bioY* transcripts (J. Satiaputra, personal communication). Asp 200 is located in the dimerization interface of *SaBPL*. Studies in our laboratory have shown that *SaBPL* D200E mutant (described above) behaves as a monomer in solution and exhibits a weaker binding affinity to the target operator sequences (Mr. A Hayes, personal communication). This result demonstrates that D200E *SaBPL* mutant may exhibit weak repression of the target promoters *in vivo*. As a consequence the genes involved in biotin synthesis and biotin transport may no longer be repressed, hence biotin can out-compete the inhibitor for the BPL active site. As *SaBPL* is the master regulator protein of all biotin-mediated events in *S. aureus* it is important to not only design BPL inhibitors that stop protein biotinylation but also induce dimerization, thereby affecting both functions of BPL.

All of these studies help to further define the mechanisms of action and uptake of BPL inhibitors.

10.1.4 Pharmacological properties of BPL inhibitors in pre-clinical candidates

The aim of this project is to identify BPL inhibitors that could be developed into pre-clinical candidates. Therefore an investigation into the pharmacological properties of our compounds is important. One common reason for the high attrition rate seen in antibacterial discovery is poor bioavailability in serum [31]. Antibiotics need to have a free concentration in serum that is above the MIC in order to be efficacious. This pharmacological parameter is often higher for antibiotics than drugs for other therapeutic areas [31]. Serum binding proteins are often problematic for antibiotics. If the percentage of antibiotic bound to serum is too high the free drug concentration may be reduced to concentrations below the MIC, thereby reducing efficacy [31, 32]. Testing BPL inhibitors for serum protein binding early on can remove high protein binding compounds before they are progressed to animal models. This can be performed using dialysis experiments, where the drug is incubated with serum proteins within a dialysis membrane. Any drug that does not bind to the serum proteins can pass through the dialysis membrane due to its small molecular weight [33]. The concentration of the unbound drug that has passed through the dialysis membrane can be determined using LC/MS [33]. Other approaches also include the use of HTS-multiscreen plates to separate the unbound drug from serum proteins after incubation. Antimicrobial susceptibility assays can also be performed in the presence of serum to see if the MIC of a compound is altered significantly [32]. These experiments employed to measure serum binding levels should be used to predict the efficacy of BPL inhibitors in an animal model, enabling the development of pre-clinical candidates.

The stability of compounds in serum is another pharmacological parameter that should be tested early on. One enzyme present in human serum that could potentially hydrolyse BPL inhibitors is biotinidase [34, 35]. Mammals cannot synthesize their own biotin and rely on

biotin uptake through the SMVT transporter or by recycling biotin that has been attached to biotin-dependent enzymes through the action of biotinidase [36]. Recently published work investigated molecules functionalized with biotin that could potentially be used for pre-targeted therapeutic and medical imaging technologies. By introducing a biotin triazole linker into the compound, resistance to biotinidase hydrolysis was far greater than for ester and amide linkers [37]. This is an important discovery as it highlights that biotin triazoles with good antibacterial efficacy are stable in human serum.

10.1.5 Addressing the challenges of antibacterial discovery

The two main approaches employed by large pharmaceutical companies to identify new antibiotics are target based screening of compound libraries for binding to a protein target or phenotypic screening for whole cell activity against bacteria [38, 39]. Both approaches have advantages and disadvantages when it comes to antibacterial discovery. In target based screening approaches, compounds that bind to and/or inhibit the protein target can be quickly and cheaply identified. The many small molecules that have been curated in corporate compound collections are often designed around Lipinski's rule of 5 [11, 38]. In target based screening, many targets often have low hit rates against the hydrophilic molecules in the compound collection. Therefore hydrophobic molecules, which are commonly at a higher proportion in compound libraries than hydrophilic molecules are often identified, which could lead to high serum binding and therefore poor bio-availability [31, 40]. It is also often difficult to develop these inhibitors into bio-actives with whole cell antibacterial activity [39]. In contrast, whole cell screening identifies compounds with antibacterial activity, which is an advantage over target based screening approaches. Many of the antibiotics in clinical use were discovered by this approach. Hence, it is not uncommon to identify previously discovered classes of antibiotics, making it difficult to identify novel chemical scaffolds [24, 41]. Most antibiotics have been discovered from cultivable soil microorganisms. However, there are many more species of bacteria that cannot be cultivated under laboratory conditions. These

microorganisms represent an important source of new antibiotics and therefore it is important to develop new technologies to culture such organisms [42]. The iChip, is one device that has been developed to isolate and grow uncultivable bacteria in their natural environment [43]. This approach was used to identify a new antibiotic, teixobactin, which inhibits cell wall synthesis in Gram-positive bacteria [44, 45]. Novel technologies such as this will be important to continue bioprospecting the natural world for new classes of antibiotics. As mentioned in chapter 1, BPL was identified as a potential antibiotic target by both GlaxoSmith Kline [38] and Astrazeneca [39] and was the subject of high-throughput screening campaigns, with no hits being identified by either company. We have employed a structure based drug design approach to identify inhibitors of BPL. To facilitate BPL antibacterial development it is important to screen rationally designed compounds that bind to and/or inhibit BPL in conjunction with antimicrobial susceptibility assays. This approach utilizes the advantages of both target based and phenotypic screening approaches that are employed by large pharmaceutical companies. Therefore compounds that exhibit good potency and antibacterial activity are identified, enabling BPL antibacterial development.

Many small molecules that have been curated in corporate compound collections are often designed to follow Lipinski's rule of 5 [11, 38]. However, studies have shown that antibacterials do not generally abide by Lipinski's rules [24, 40, 46, 47]. Antibiotics tend to be more polar than drugs for other therapeutic areas [47]. There are also differences observed in the chemical properties of antibiotics that target Gram-positive versus Gram-negative bacteria [47]. Gram-positive bio-actives generally have a higher molecular weight and are more polar compared to corporate compound libraries. Antibiotics that target Gram-negative bacteria are even more polar than those that are only active on Gram-positive bacteria and have a size limit of ~600 Da, presumably to pass through outer membrane porins [24, 46, 47]. Antibiotics that enter Gram-negative organisms also tend to be charged at physiological pH. To enter Gram-negative bacteria, molecules need to be charged to cross the outer membrane,

but also need to be able to cross the inner membrane (hydrophobic) in order to access intracellular targets [46]. Fluoroquinolones active against both Gram-positive and Gram-negative organisms are zwitterionic which is believed to contribute to their ability to permeate through the outer membrane of Gram-negative organisms and also permeate the gut endothelial layer [46]. These compounds successfully address the requirements for entry into Gram-negative organisms. This information is useful to generate a set of 'rules' that can be employed to incorporate useful chemical properties into newly discovered inhibitors to enhance antibacterial activity against both Gram-positive and Gram-negative bacteria. Currently, these rules are not well understood for antibiotics.

Development of resistance limits the useful lifetime of an antibiotic in the clinic. There have only been 5 new classes of antibiotics introduced for clinical use since the year 2000, and of particular concern none of these can be used to treat Gram-negative bacteria [48]. In order to develop new classes of antibiotics it is important to look at the properties of successful antibiotics used in systemic monotherapy. Antibiotics that are used in systemic monotherapy commonly have multiple targets and, therefore, a low occurrence of high-level resistance through single step mutation of their targets [49-51]. Some examples of these antibiotics include the β -lactams and fluoroquinolone classes. β -lactam containing antibiotics act through inhibition of at least two penicillin binding proteins and fluoroquinolones act through inhibition of two DNA topoisomerases [49, 50]. Antibiotics that target single enzymes are all subject to high-level resistance from a single step mutation in the target enzyme. Some examples include rifampin, which targets RNA polymerase, and novobiocin, which targets the B subunit of DNA gyrase [49, 50]. These drugs are not used in standard systemic monotherapy but are used in combination with other drugs [49]. Using two antibiotics that have single targets in combination with each other gives the advantage of having multiple targets in the bacterium thereby slowing development of resistance. This combination therapy approach may be an avenue to progress BPL antibacterials to pre-clinical development.

Another strategy to improve and/or broaden the spectrum of antibacterials is to make hybrid antibiotics [49]. Here, two separate pharmacophores from different established antibiotic classes are covalently attached by a linker [51]. One such antibiotic pursued by Roche (Ro 23-9424) is a β -lactam-fluoroquinolone hybrid [52]. This compound exhibited a broader spectrum of antibacterial activity against bacteria that were resistant to either one or both of the compounds [52-54]. However, this compound had a relatively short half-life in human phase I trials, likely due to chemical and enzymatic instability [49]. Another example is an oxazolidinone-fluoroquinolone hybrid developed by Morphochem (now Biovertis) [55]. This hybrid approach is one solution to overcoming multi-drug resistance, however more work needs to be done to improve stability in serum. We have recently used *in situ* click chemistry to ‘click’ azide-functionalized analogues of established antibiotic classes to biotin acetylene to identify SaBPL inhibitors that could be used as hybrid antibiotics. Compound **7** (Figure 10.3) was identified in an *in situ* click chemistry experiment and contains the biotin triazole pharmacophore with an appended quinolonyl group belonging to the fluoroquinolone class of antibiotics. Further studies will involve investigating the spectrum of antibacterial activity. This approach could be continued using either rational design of compounds to link to the biotin triazole or through using *in situ* click chemistry.

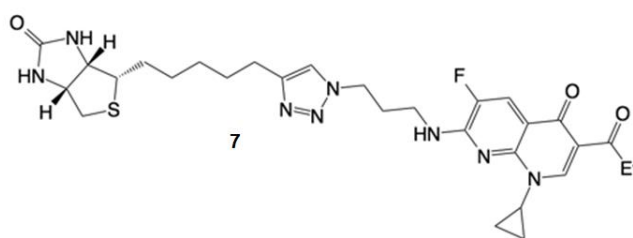


Figure 10.3: Biotin triazole – fluoroquinolone hybrid molecule

Finally, the use of nanoparticles has been gaining attention to improve drug delivery. This approach has been investigated to enhance the antibacterial activity and/or extend the spectrum of activity of inhibitors [56]. Nanoparticles allow for targeted delivery of antibacterials, improved solubility, improved half-life and can be used to deliver

combinations of drugs [57, 58]. Recently, mesoporous silica nanoparticles were used to extend the spectrum of antibacterial activity of histidine kinase autophosphorylation inhibitors in Gram-negative bacteria [58]. Here, the MIC of the inhibitor encapsulated in the nanoparticle was significantly reduced in comparison to the free drug, where no antibacterial activity could be observed against Gram-negative pathogens [58]. Another study involved encapsulating gentamicin, a protein synthesis inhibitor, into polymeric nanoparticles for potential use in osteomyelitis treatment [59]. Here, gentamicin encapsulated nanoparticles exhibited antibacterial activity against both *S. aureus* and *Staphylococcus epidermidis in vitro* [59]. This approach could be adapted to improve the antibacterial activity of BPL inhibitors as well as other antibacterials in early stage development.

10.2 Conclusions

There is an urgent need to develop new antibiotics to combat the growing rise in antibiotic resistant bacteria. The biotin-triazoles represent a new class of antibiotics to target the essential metabolic enzyme BPL. In this project multiple SAR series have been designed and characterized to identify BPL inhibitors with improved potency and antibacterial activity. Here we identified 1,4,5-trisubstituted triazoles that exhibited improved antibacterial activity against *S. aureus*. We have also developed new fluorescent probes that will be important in facilitating mechanism of uptake and action studies, which are necessary requirements for a pre-clinical candidate. All the work presented in this thesis will be valuable in optimizing BPL inhibitors as potential pre-clinical candidates to target the superbug *Staphylococcus aureus*.

10.3 References

1. Soares da Costa, T.P., et al., *Selective inhibition of Biotin Protein Ligase from Staphylococcus aureus*. J. Biol Chem, 2012. **287**(21): p. 17823-17832.
2. Tieu, W., et al., *Heterocyclic acyl-phosphate bioisostere-based inhibitors of Staphylococcus aureus biotin protein ligase*. Bioorg Med Chem Lett, 2014. **24**(19): p. 4689-4693.
3. Brown, P.H and D. Beckett, *The Biotin Repressor: Modulation of Allostery by Corepressor Analogs*. J Mol Biol, 2004. **337**(4): p. 857-869
4. Tieu, W., et al., *Optimising in situ click chemistry: the screening and identification of biotin protein ligase inhibitors*. Chem Sci, 2013. **4**: p. 3533-3537
5. Feng, J., et al., *New Series of BPL Inhibitors to Probe the Ribose-Binding Pocket of Staphylococcus aureus Biotin Protein Ligase*. ACS Medicinal Chemistry Letters, 2016.
6. Duckworth, Benjamin P., et al., *Bisubstrate Adenylation Inhibitors of Biotin Protein Ligase from Mycobacterium tuberculosis*. Chem. Biol, 2011. **18**(11): p. 1432-1441.
7. Shi, C., et al., *Bisubstrate Inhibitors of Biotin Protein Ligase in Mycobacterium tuberculosis Resistant to Cyclonucleoside Formation*. ACS Med Chem Lett, 2013. **4**(12): p. 1213-1217.
8. Bockman, M.R., et al., *Targeting Mycobacterium tuberculosis Biotin Protein Ligase (MtBPL) with Nucleoside-Based Bisubstrate Adenylation Inhibitors*. J Med Chem, 2015. **58**(18): p. 7349-7369.
9. Paparella, A.S., et al., *Structure guided design of biotin protein ligase inhibitors for antibiotic discovery*. Curr Top Med Chem, 2014. **14**(1): p. 4-20.
10. Feng, J., et al., *Biotin Protein Ligase Is a Target for New Antibacterials*. Antibiotics, 2016. **5**(3): p. 26.
11. Lipinski, C.A., et al., *Experimental and computational approaches to estimate solubility and permeability in drug discovery and development settings I*. Adv Drug Del Rev, 2001. **46**(1-3): p. 3-26.
12. B Kevin Park, a. Neil R Kitteringham, and P.M. O'Neill, *Metabolism of Fluorine-containing drugs*. Annu Rev Pharmacol and Toxicol, 2001. **41**(1): p. 443-470.
13. Hagmann, W.K., *The Many Roles for Fluorine in Medicinal Chemistry*. J Med Chem, 2008. **51**(15): p. 4359-4369.
14. Kirk, K.L., *Fluorine in medicinal chemistry: Recent therapeutic applications of fluorinated small molecules*. J Fluorine Chem, 2006. **127**(8): p. 1013-1029.

15. Purser, S., et al., *Fluorine in medicinal chemistry*. Chem Soc Rev, 2008. **37**(2): p. 320-330.
16. Vulpetti, A. and C. Dalvit, *Fluorine local environment: from screening to drug design*. Drug Discov Today, 2012. **17**(15–16): p. 890-897.
17. Gerebtzoff, G., et al., *Halogenation of Drugs Enhances Membrane Binding and Permeation*. ChemBioChem, 2004. **5**(5): p. 676-684.
18. Sugano, K., et al., *Coexistence of passive and carrier-mediated processes in drug transport*. Nat Rev Drug Discov, 2010. **9**(8): p. 597-614.
19. Li, S., P. Hu, and N. Malmstadt, *Confocal Imaging to Quantify Passive Transport across Biomimetic Lipid Membranes*. Anal Chem, 2010. **82**(18): p. 7766-7771.
20. Daniel, R.A. and J. Errington, *Control of Cell Morphogenesis in Bacteria: Two Distinct Ways to Make a Rod-Shaped Cell*. Cell, 2003. **113**(6): p. 767-776.
21. Tiyanont, K., et al., *Imaging peptidoglycan biosynthesis in Bacillus subtilis with fluorescent antibiotics*. PNAS, 2006. **103**(29): p. 11033-11038.
22. Hebbeln, P., et al., *Biotin uptake in prokaryotes by solute transporters with an optional ATP-binding cassette-containing module*. PNAS, 2007. **104**(8): p. 2909-2914.
23. Azhar, A., *Structure-function relationships of the biotin transporters from Staphylococcus aureus*, in *Department of Molecular and Cellular Biology* 2015, University of Adelaide.
24. Silver, L.L., *Challenges of Antibacterial Discovery*. Clin Microbiol Rev, 2011. **24**(1): p. 71-109.
25. Lewis, K., *Antibiotics: Recover the lost art of drug discovery*. Nature, 2012. **485**(7399): p. 439-440.
26. Rodionov, D.A., A.A. Mironov, and M.S. Gelfand, *Conservation of the Biotin Regulon and the BirA Regulatory Signal in Eubacteria and Archaea*. Genome Research, 2002. **12**(10): p. 1507-1516.
27. J. Satiaputra, K.E.S., G.W. Booker, S.W. Polyak, *Mechanisms of biotin-regulated gene expression in microbes*. Synth Sys Biotechnol 2016.
28. Soares da Costa, T.P., et al., *Dual roles of F123 in protein homodimerization and inhibitor binding to biotin protein ligase from Staphylococcus aureus*. Mol Microbiol, 2014. **91**(1): p. 110-120.
29. Pardini, N., et al., *Structural characterization of Staphylococcus aureus biotin protein ligase and interaction partners: an antibiotic target*. Prot sci , 2013. **22**(6): p. 762-773.

30. Henke, S.K. and J.E. Cronan, *The Staphylococcus aureus group II biotin protein ligase BirA is an effective regulator of biotin operon transcription and requires the DNA binding domain for full enzymatic activity*. Mol Microbiol, 2016
31. Gwynn, M.N., et al., *Challenges of antibacterial discovery revisited*. Ann. N. Y. Acad Sci, 2010. **1213**(1): p. 5-19.
32. Zeitlinger, M.A., et al., *Protein Binding: Do We Ever Learn?* Antimicrob Agents Chemother, 2011. **55**(7): p. 3067-3074.
33. Kaplan, N., et al., *In vitro activity (MICs and rate of kill) of AFN-1252, a novel FabI inhibitor, in the presence of serum and in combination with other antibiotics*. J Chemother, 2013. **25**(1): p. 18-25.
34. Oizumi, J. and K. Hayakawa, *Enkephalin hydrolysis by human serum biotinidase*. Biochim et Biophys Acta (BBA) - General Subjects, 1991. **1074**(3): p. 433-438.
35. Nilsson, L. and B. Kågedal, *Co-purification of human serum lipoamidase and biotinidase: evidence that the two enzyme activities are due to the same enzyme protein*. Biochemical Journal, 1993. **291**(2): p. 545-551.
36. Zempleni, J., *Uptake, Localization and Non-Carboxylase roles of Biotin*. Annu Rev Nutr, 2005. **25**(1): p. 175-196.
37. Germeroth, A.I., et al., *Triazole biotin: a tight-binding biotinidase-resistant conjugate*. Org. Biomol. Chem, 2013. **11**(44): p. 7700-7704.
38. Payne, D.J., et al., *Drugs for bad bugs: confronting the challenges of antibacterial discovery*. Nat Rev Drug Discov, 2007. **6**(1): p. 29-40.
39. Tommasi, R., et al., *ESKAPEing the labyrinth of antibacterial discovery*. Nat Rev Drug Discov, 2015. **14**(8): p. 529-542.
40. Brown, D.G., et al., *Trends and Exceptions of Physical Properties on Antibacterial Activity for Gram-Positive and Gram-Negative Pathogens*. J Med Chem, 2014. **57**(23): p. 10144-10161.
41. Fischbach, M.A. and C.T. Walsh, *Antibiotics for Emerging Pathogens*. Science, 2009. **325**(5944): p. 1089-1093.
42. Kaeberlein, T., et al., *Isolatin "Uncultivable" Microorganisms in Pure Culture in a Simulate Natural Environment*. Science, 2002. **296**: p. 1127-1129.
43. Nichols, D., et al., *Use of ichip for high-throughput in situ cultivation of "Uncultivable" microbial species*. Appl environ microbiol, 2010. **76**(8): p. 2445-2450.
44. Ling, L.L., et al., *A new antibiotic kills pathogen without detectable resistance*. Nature, 2015. **517**: p. 455-459.

45. Homma, T., et al., *Dual targeting of cell wall precursors by teixobactin leads to cell lysis*. Antimicrob agents chemother, 2016. pii: AAC. 0150-16.
46. Silver, L.L., *A Gestalt approach to Gram-negative entry*. Bioorg Med Chem, 2016. pii. S0968-0896(16)30467-9. doi: 10.1016/j.bmc,2016.06.044.
47. O'Shea, R. and H.E. Moser, *Physicochemical Properties of Antibacterial Compounds: Implications for Drug Discovery*. J Med Chem, 2008. **51**(10): p. 2871-2878.
48. Butler, M.S., M.A.T. Blaskovich, and M.A. Cooper, *Antibiotics in the clinical pipeline at the end of 2015*. J Antibiot, 2016.
49. Silver, L.L., *Multi-targeting by monotherapeutic antibacterials*. Nat Rev Drug Discov, 2007. **6**(1): p. 41-55.
50. Silver, L.L., *Appropriate Targets for Antibacterial Drugs*. Cold Spring Harbor Perspectives in Medicine, 2016.
51. Brötz-Oesterhelt, H. and N.A. Brunner, *How many modes of action should an antibiotic have?* Curr Opin Pharmacol, 2008. **8**(5): p. 564-573.
52. Pace, J., et al., *Escherichia coli resistant to cephalosporins and quinolones is still susceptible to cephalosporin-quinolone ester RO 23-9424*. Antimicrob agents chemother, 1991. **35**(5): p. 910-915.
53. Pfaller, M.A., et al., *RO 23-9424 a new cephalosporin 3'-quinolone: in vitro antimicrobial activity and tentative disc diffusion interpretive criteria*. J Antimicrob chemother, 1993. **31**(1): p. 81-88.
54. Georgopapadakou N.A. and Bertasso, A., *Mechanisms of action of cephalosporin 3'quinolone esters, carbamates and tertiary amines in Escherichia coli*. Antimicrob agents and chemother, 1993. **37**(3): p. 559-565.
55. Hubschwerlen C., et al., *Structure-activity relationship in the oxalidinone-quinolone hybrid series: influence of the central spacer on the antibacterial activity and the mode of action*. Bioorg Med Chem Lett, 2003. **13**(23): p. 4229-4233.
56. Petros, R.A and J.M. DeSimone, *Strategies in the design of nanoparticles for therapeutic applications*. Nat Rev Drug Discov, 2010. **9**(8): p. 615-627.
57. Gao, W., et al., *Nanoparticle approaches against bacterial infections*. Wiley Interdisciplinary Reviews: Nanomedicine and Nanobiotechnology, 2014. **6**(6): p. 532-547.
58. Velikova, N., et al., *Broadening the antibacterial spectrum of histidine kinase autophosphorylation inhibitors via the use of ε-poly-L-lysine capped mesoporous silica-based nanoparticles*. Nanomedicine 2016. pii: S1549-9634(16)30163-0. doi: 10.1016/j.nano.2016.09.011.

59. Posadowska, U., et al., *Gentamicin loaded PLGA nanoparticles as local drug delivery system for the osteomyelitis treatment*. Acta of Bioengineering & Biomechanics, 2015. **17**(3): p. 41-48.